Mathematical modelling of hypoxia and temperature signalling pathways in lifespan.

Suhayl Mulla

Doctor of Philosophy

Aston University

March 2019

Aston University

Mathematical modelling of hypoxia and temperature signalling pathways in lifespan.

Suhayl Mulla

Doctor of Philosophy

2019

Thesis Summary

A crucial step towards our understanding of ageing is the identification and characterisation of lifespan modifiers. Currently, investigations into lifespan modifiers use the non-parametric Kaplan-Meier estimator and the log-rank statistical test. Few studies employ parametric modelling to investigate lifespan modifiers and those that do use models which demonstrate monophasic lifespan. Recent studies have identified two phases of lifespan in *C. elegans* which cannot currently be modelled by monophasic parametric models. The aim of this research was to develop a biphasic parametric model (Bilogistic model) capable of modelling biphasic lifespan in *C. elegans*. The Bilogistic model has 5 parameters: the *f* parameter defines the proportion of lifespan in the early phase and late phase, and two death rates (k_1 & k_2) and two time phases (t_1 & t_2) for the early and late phases. The Bilogistic model was applied to lifespan data from flies, bees and mice to identify and quantify parameters. Two predictive models (chronological and biological) which used the Bilogistic model were developed and applied to temperature interventions in both wild type and *trpa-1(ok999)* mutants. Critical time points of interventions were identified, and indicated times at which the effects of intervention were lost. Also observed was that early lifespan conditions are important in determining the overall lifespan. The relationship between the HIF-1 (hypoxia) and TRPA-1 (temperature) signalling pathways were investigated in *C. elegans* mutants at different temperatures and oxygen concentrations. A relationship whereby TRPA-1 signals to HIF-1 was identified in mammalian cells but was not found to be applicable to *C. elegans*. In conclusion, a novel Bilogistic model has been developed and used to investigate the role of the TRPA-1 and HIF-1 pathways in *C. elegans* lifespan. However further work is required to fully understand the interaction between these pathways and how they act to regulate lifespan.

Key words: *C. elegans*, Lifespan, Parametric modelling, Temperature, Hypoxia

Acknowledgments

Firstly I would like thank my supervisors at Aston University, Dr Alex Cheong, Dr Michael Stich and Dr Zita Balklava for providing me with the opportunity to do this PhD.

I would like to thank Alex for his continuous guidance, encouragement and support throughout my PhD. I would also like to express my gratitude to Michael for all his advice particularly for his expertise in mathematics. I am also grateful to Zita for the valuable assistance in the lab and for helping me with all of my worm work.

Thank you to my placement students Adele Ludlam and Tajlima Miah for all of their assistance in the lab during their placement year.

I would like to thank the past and present friends and colleagues at Aston for the support, help and laughs throughout my PhD.

Finally a huge thank you to my friends and family, in particular thank you to my parents for all of their support over the years and for the encouragement to keep going until the end.

Thank you everyone.

Table of Contents

List of Abbreviations

AHA-1	Aryl hydrocarbon receptor nuclear translocator homolog
AGE-1	Ageing alteration 1
AITC	allyl-isothiocynate
AMP	Adenosine Monophosphate
AMPK	5’ AMP activated protein kinase
ANOVA	Analysis of Variance
ATP	Adenosine Triphosphate
Avg	Average
bp	Base pair
C. elegans	Caenorhabditis elegans
CGC	Caenorhabditis Genetics Center
cGMP	Cyclic guanosine monophosphate
DAF-2	Abnormal dauer formation 2
DAF-9	Abnormal dauer formation 9
DAF-12	Abnormal dauer formation 12
DAF-16	Abnormal dauer formation 16
DMEM	Dulbecco’s modified Eagle media
DMOG	Dimethyloxalylglycine
DMSO	Dimethyl sulfoxide
DNA	Deoxyribonucleic acid
D/R	Dose-response

List of Abbreviations (Continued…)

E. coli	Escherichia coli
EDTA	Ethylenediaminetetraacetic acid
EGL-9	Egg-laying defective protein 9 / Hypoxia inducible factor prolyl hydroxylase
ER	Endoplasmic reticulum
ERCC8	Excision repair cross-complementation group 8
FBS	Foetal bovine serum
FOXO	Forkhead Box O
FuDR	5-Fluoro-2'-deoxyuridine
GCY-8	Receptor type guanylyl cyclase gcy-8
GCY-18	Receptor type guanylyl cyclase gcy-18
GCY-23	Receptor type guanylyl cyclase gcy-23
GCY-31	Soluble guanylate cyclase gcy-31
GCY-33	Soluble guanylate cyclase gcy-33
GCY-35	Soluble guanylate cyclase gcy-35
GCY-36	Soluble guanylate cyclase gcy-36
HCF-1	Host cell factor 1
HEPES	4-(2-hydroxyethyl)-1-piperazineethanesulfonic acid
HIF-1	Hypoxia-inducible factor-1
HIF-1α	Hypoxia-inducible factor-1 alpha
HIF-1β	Aryl hydrocarbon receptor nuclear translocator

List of Abbreviations (Continued…)

HIF-2α	Endothelial PAS domain-containing protein 1
HIF-3α	Hypoxia-inducible factor-3 alpha
HRE	HIF response element
HSF-1	Heat shock factor 1
Hsp16-1	Heat Shock Protein 16.1
Hsp16-2	Heat Shock Protein 16.2
IGF-1	Insulin-like growth factor 1
IIS	Insulin/Insulin-like growth factor signalling
ITP	Interventions Testing Program
JNK	c-Jun N-terminal kinase
LB	Lysogeny broth
L1	Larval stage 1
L2	Larval stage 2
L3	Larval stage 3
L4	Larval stage 4
mRNA	Messenger RNA
mTOR	Mechanistic target of rapamycin
NAD	Nicotinamide adenine dinucleotide
NADH	Nicotinamide adenine dinucleotide reduced
NF-κb	Nuclear factor kappa-light-chain-enhancer of activated B cells
NGM	Nematode Growth Media

List of Abbreviations (Continued…)

NIA	National Institute for Aging
N2	*C. elegans* wild type isolate Bristol strain variant
PBS	Phosphate buffered saline
PHD	Prolyl hydroxylase
PKC-2	Protein kinase C-like 2
RMSE	Root mean square error
RNA	Ribonucleic acid
RNAi	RNA interference
ROS	Reactive oxygen species
RPMI	Roswell Park Memorial Institute
SEM	Standard error of the mean
SGK-1	Serine/threonine protein kinase sgk-1
sGC	Soluble guanylyl cyclase
shsps	Small heat shock proteins
SIRT1	Sirtuin 1
Sir2.1	NAD-dependent protein deacetylase sir-2.1
SMK-1	SMEK (Dictyostelium suppressor of MEK null) homolog)
SOD1	Superoxide dismutase
TAX-2	abnormal chemotaxis 2/ cyclin nucleotide gated channel 2
TAX-4	abnormal chemotaxis 4/ cyclin nucleotide gated channel 4
TOR	Target of rapamycin

List of Abbreviations (Continued…)

TRPA-1	Transient receptor potential cation channel subfamily A member 1
TRPA-2	Transient receptor potential cation channel subfamily A member 2
TRPC	Transient receptor potential cation channel subfamily C
TRPM	Transient receptor potential cation channel subfamily M
TRPV3	Transient receptor potential cation channel subfamily V member 3
UPR	Unfolded protein response
UV	Ultraviolet
VEGF	Vascular endothelial growth factor
VHL	von Hippel-Lindau disease tumour suppressor
w^{dah}	White dahomey
WRN	Werner syndrome RecQ like helicase
WT	Wild type
2PM	2-parameter model
5PM	5-parameter model

List of Figures

List of Figures (Continued…)

List of Figures (Continued…)

List of Figures (Continued…)

List of Tables

List of Equations

Chapter 1.0: General introduction

1.1 Ageing and its implications

Ageing is an intricate process involving complex genetic networks and molecular pathways, which is further influenced by environmental factors. It is broadly defined as the intrinsic deterioration of function with age (Flatt, 2012, Mansfeld et al., 2015). Ageing is additionally considered to be one of the greatest risk factors for many diseases including neurodegenerative diseases, cardiovascular diseases, metabolic syndrome and cancer (Niccoli and Partridge, 2012, Dillin et al., 2014). In most organisms, as chronological age progresses, mortality increases (and survival decreases) with higher mortality rates later on in life. Evolutionarily, it is suggested that this is due to natural selection being unable to play a role in removing deleterious genes causing it to be more common in populations which then results in ageing (Medawar, 1952). It has also been suggested that pleiotropic genes which are beneficial earlier in life and are required to maintain fitness lead to ageing as the genetic pleiotropy results in detrimental consequences later in life by displaying itself as ageing (Williams, 1957). However, this explanation is incomplete as ageing is an adaptive process, in which the rate of ageing can alter over time under different circumstances (Lenart and Bienertova-Vaska, 2017).

Although numerous genes and genetic pathways have been identified to play a role in the ageing process, a single master controller of ageing has not been identified and is unlikely to be identified (Bonsall, 2006). It is more likely that a number of different contributors collectively determine the ageing process with input from various environmental factors (or lifestyle choices).

To measure ageing and to understand how the ageing process can be altered, the survival or mortality of a population is commonly studied. Due to the difficulty in longitudinal ageing studies of humans, animal models are often used to understand which mechanisms are involved in the ageing process. In particular, mice, flies and worms are used to study survival and mortality (Mitchell et al., 2015). Survival under different conditions can then be analysed to identify how manipulation of the factors which contribute to the ageing process affects survival.

1.2 *C. elegans* as a model organism

C. elegans is a non-parasitic free-living nematode first described in 1900 by Émile Maupas who discovered it in the soil in Algeria (Maupas, 1900, Blaxter, 2011). Since then it has been used as a model organism for a range of different research purposes from investigating molecular mechanisms to studying behaviour. Most notably it was established by Sydney Brenner since 1963 who used it to study development and neurobiology at a molecular level. It is also important in investigating the role and interactions of single proteins within a whole organism and allows for identification of phenotypic changes. (Corsi et al., 2015).

C. elegans are normally found in the soil, in compost heaps or in other bacteria rich environments and are not specific to a single geographical location as they have been found globally (Felix and Braendle, 2010, Andersen et al., 2012). In the laboratory, they are cultured either on solid agar or in liquid culture. In both cases they feed upon a bacterial food source with the most common being the *Escherichia coli* (*E. coli*) OP50 strain (Corsi et al., 2015). They are transparent and grow up to approximately 1mm in length and so are easy to visualise under a stereo microscope. They can also be cheaply cultivated in the laboratory without requiring too much space or maintenance.

1.2.1 *C. elegans* physiology

C. elegans have 2 sexes: hermaphrodites and males. Males are a lot rarer than hermaphrodites, with 1 male for every 1000 hermaphrodites. Sex determination is based on the autosome to allosome ratio: hermaphrodites have 5 autosome pairs and a pair of the X allosome, whereas males have a single X allosome (Corsi et al., 2015, Hillier et al., 2005). Although males have one less chromosome, they have been found to have more somatic cells (1031) compared to the hermaphrodites (959). However, the adult hermaphrodites tend to grow to a larger size compared to the males (Corsi et al., 2015, Wood, 1988). The lineage of all cells in both hermaphrodites and males have been identified and shows that the worm is comprised of a few tissue types and organ systems such as the mouth, pharynx, intestine, cuticle, nervous system, musculature, and sex specific gonads. They do not have a circulatory or respiratory system but instead rely upon gas diffusion to the tissue and use their muscles

which run the length of the body to propel itself to crawl either forward or backwards. Males have a single testis, vas deferens, and a tail with spicules for mating, while hermaphrodites have two ovaries, an oviduct, a spermatheca, a vulva and a uterus (Corsi et al., 2015, Wood, 1988, Sulston and Horvitz, 1977, Kimble and Hirsh, 1979). Hermaphrodites have 302 neurons and males have 385 neurons which control worm movement, the response to sensory (mechanical, chemical and thermal) stimuli, and also feeding, mating and egg laying (Corsi et al., 2015, Sammut et al., 2015).

1.2.2 *C. elegans* life cycle

C. elegans worms typically have a 3-day lifecycle (generation time) from being laid as an egg to becoming a fully developed egg laying adult (hermaphrodite). Development starts with fertilisation of the oocyte and continues after hatching as it progresses through the larval stages into adulthood (Figure 1.1). There are 4 larval stages, L1 through to L4, the L1 stage occurs when the egg hatches and is approximately 14 hours post fertilisation. The L1 stage worm then undergoes cell division and moults into the L2 stage. Moulting is the generation of a new cuticle under the old one, and occurs additionally three more times, once between each larval stage, until it becomes an adult. Somatic cell division comes to an end at the adult stage, and 12 hours after the final moult process hermaphrodites are capable of egg laying. Egg laying lasts for approximately 4 days in which 300 fertilised eggs are laid. At that point the sperm produced in the hermaphrodite becomes a limiting factor for fertilisation. However, if males also fertilise the hermaphrodite, up to 1000 fertilised eggs can be laid. If fertilised by males it increases the likelihood of male presence in the progeny with approximately 50% of the population becoming males (Anderson et al., 2010, Corsi et al., 2015).

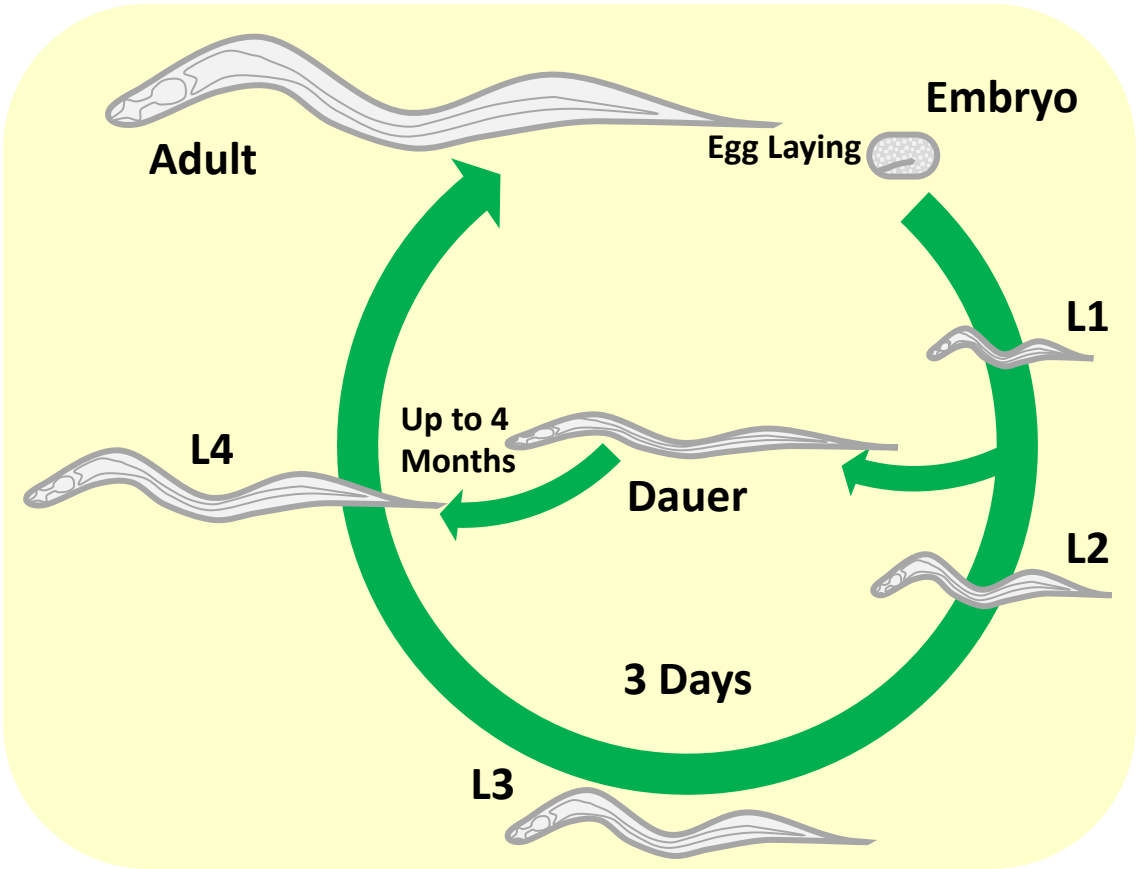

Figure 1.1: Lifecycle of C. elegans

In 1998, the *C. elegans* worm became the first multicellular organism to have its entire genome sequenced. It has a 100Mb genome sequence which is structured in to the 6 chromosome pairs (5 autosomes and 1 allosome), which is 30 times smaller than the human genome size. So far, 20,215 protein coding genes have been identified in the *C. elegans* from a total number of 48,447 genes (WS268, 2019), compared to the human genome which currently has an estimated 19,940 protein coding genes and 58,721 total genes (GENCODE Version 29, 2019). This indicates, that on a genetic level, worms are similar to humans, with an estimated 60-80% of genes in worms having a homologous gene in humans and approximately 40% of human disease genes have a homologue in *C. elegans* (Culetto and Sattelle, 2000, Kaletta and Hengartner, 2006).

1.2.3 *C. elegans* lifespan

The wild type (N2) worm has an average lifespan of 18 days at 20°C, which can be extended or shortened under different environmental conditions (Klass, 1977). Additionally, genetic mutations can alter its lifespan (Friedman and Johnson, 1988). *C. elegans* can also show other

ways of extending their lifespan, for example by diet. The most common change to diet is by calorie restriction, which has been shown to extend lifespan in many different organisms (Houthoofd et al., 2005, Weindruch et al., 1986). Additionally, in the absence of food, worms which are in the L1 stage are able to undergo developmental arrest until food is reintroduced (Johnson et al., 1984). Similarly, worms can enter an alternative lifecycle dependent on environmental conditions by developing into dauer larvae. Under optimal conditions, L1 and L2 larvae continue development into the L3 larval stage. However, under stress conditions, they develop into the alternative dauer larval stage. This is an arrested state which can be due to a number of factors but is often due to a change in environment such as starvation, crowding or high temperatures. Once worms enter the dauer stage, they have the potential to survive for many months. However, if returned to regular conditions, they continue into the L4 and adult stages with a normal lifespan (Riddle et al., 1997, Hu, 2007). As the dauer stage is able to indefinitely extend lifespan, it is important to understand how this occurs and if these mechanisms are interconnected with the adult worms' ability to extend lifespan. Although larval arrest and dauer formation do extend the lifespan of *C. elegans,* it is important to note that the changes to lifespan are based on adult (post L4 stage) worms.

1.3 Factors of ageing and their role in *C. elegans*

C. elegans is an excellent model organism for many different research areas, but in particular it is well established for research into ageing. This is often conducted by the generation of a synchronous population of worms and measuring the changes in lifespan (or healthspan) under different experimental conditions. This provides understanding of the different factors influencing ageing by promoting a phenotype which changes lifespan and altering the level of ageing-related deterioration in the worm. Thus, many factors have been implicated in why ageing occurs and from this many theories of ageing have been developed and investigated in multiple organisms (Figure 1.2).

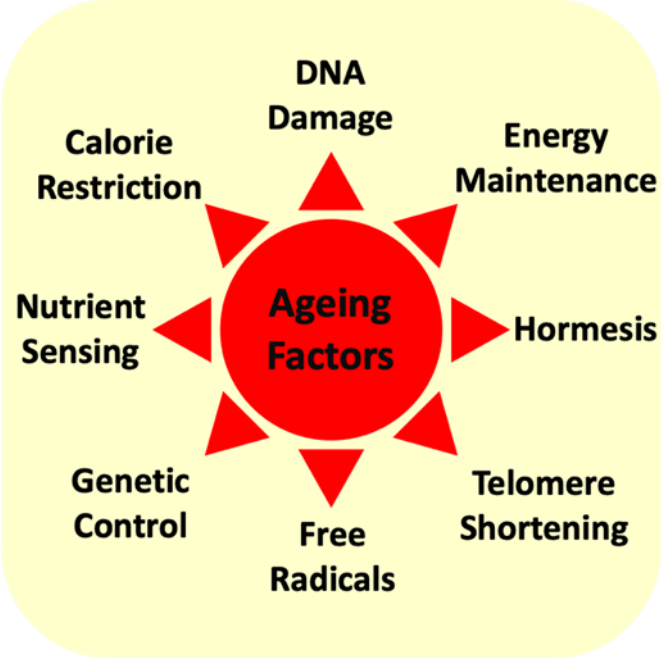

Figure 1.2: Factors involved in ageing

1.3.1 Calorie restriction

Calorie restriction is the act of restricting nutrients from dietary intake without malnutrition. It is one of the most common non-genetic interventions used to alter lifespan. It has a highly conserved effect as it has been replicated in many species including *C. elegans*, yeast, rodents and primates (Jiang et al., 2000, McCay et al., 1935, Weindruch et al., 1986, Bodkin et al., 2003, Mattison et al., 2017). Calorie restriction was first identified in 1935 when it was demonstrated that a 40% reduction in calorie intake extended the lifespan of rats (McCay et al., 1935).

Additionally, in *C. elegans*, bacterial food source is important in regulating lifespan. For example it has been shown that feeding worms different strains (OP50 vs HB101) of *E. coli* results in differences in lifespan (So et al., 2011). Furthermore, there are also differences between live or dead bacteria used for food as killing bacteria by UV treatment results in an increased lifespan (Gems and Riddle, 2000).

The mechanism through which calorie restriction acts to extend lifespan is not yet completely understood, although a number of theories have been suggested. One of which proposes oxidative stress and redox imbalance which leads to the generation of reactive oxygen species

(ROS) resulting in DNA damage. The damage from oxidative stress by can be prevented by regenerating anti-oxidants (Ungvari et al., 2008, Sohal and Weindruch, 1996). Calorie restriction can also induce sirtuins, particularly SIRT1, which is known for its regulation of energy metabolism and endocrine signalling pathways as well as the stress response. Sirtuins are also linked to redox state as its activation is dependent upon the NAD^+/NADH levels (Cohen et al., 2004, Ungvari et al., 2008). One such example of the beneficial effects of calorie restriction affecting redox state is found in the reduction of oxidative stress and additional inflammation protection by release of nitric oxide in the vasculature (Ungvari et al., 2008). Calorie restriction can also affect the insulin signalling pathway and may be one of the pathways by which lifespan is extended. The insulin signalling pathway is particularly important in regulation of lifespan of many different species, and in *C. elegans* is the prominent DAF-16 pathway (Argentino et al., 2005, Kenyon, 2010). Additionally, calorie restriction has been shown to reduce core body temperature, which in turn may act to extend lifespan as seen in *C. elegans* and also in mice (Duffy et al., 1990, Redman et al., 2008). Hormesis may also explain the beneficial effects of calorie restriction as the moderate stress may elicit a protective response which in turn promotes improved health and lifespan. The effect of hormesis has also been shown to act upon mitochondrial redox balance by restriction of calories causing mitochondrial stress, which in turn induces stress defence mechanisms (Ristow and Schmeisser, 2011, Ristow and Schmeisser, 2014). It is likely that many of these mechanisms are interrelated and act together to extend lifespan during calorie restriction.

1.3.2 DNA damage theory of ageing

It is thought that the ageing process is a result of damage to cellular components and DNA. DNA holds the genetic code for life and disruption or damage to this genetic code has a number of consequences i.e. ageing. DNA can be mutated which results in a change in base pairs sequence or it can be damaged either chemically or physically leading to structural change of the DNA double helix (Gensler and Bernstein, 1981). Deficiencies in DNA damage repair pathways can lead to the accumulation of DNA damages leading to ageing by cellular senescence or apoptosis. This suggests that increased longevity/protection from ageing is

proportional to the DNA repair pathway activity; and this has been seen in *C. elegans* as more damage or reduced capability to repair damage results in a shortened lifespan (Hyun et al., 2008). This is supported by progeroid syndromes (e.g. Werner syndrome, Cockayne syndrome and trichothiodystrophy) which are due to mutations in DNA repair proteins and pathways e.g. ERCC8, WRN helicase, Transcription factor II Human subunits (Kulkarni and Wilson, 2008). DNA damage can be caused by either internal or external sources such as ROS or UV radiation. The theory suggests that when nuclear DNA is damaged by internal or external sources, it is unable to be repaired by the normal DNA repair mechanisms. This may lead to the accumulation of damaged DNA leading to further mutations, changes in transcription or gene expression and also apoptosis which inevitably leads to the disruption of cellular function or tissue homeostasis which affects functionality of the organism (Wang et al., 2016, Freitas and de Magalhaes, 2011).

1.3.3 The free radical theory of ageing

The free radical theory of ageing is based upon the idea that ageing is due to the production of free radicals during cellular metabolic process (Harman, 2006, Harman, 1956). The production of free radicals (ROS generated in the mitochondria) leads to accumulation of damage over time, particularly as the free radicals are able to react with DNA, proteins and lipid molecules leading them to cause damage to other molecules or to become dysfunctional and affect cellular processes (Wickens, 2001). This free radical production is due to dysfunctional mitochondria which generate more free radicals which leads to further deterioration of the mitochondria which then affects other cellular processes leading to an exacerbated ageing phenotype (López-Otín et al., 2013).

The damage caused by free radicals can be prevented by enzymatic or non-enzymatic defence mechanisms such as anti-oxidants or enzymes like superoxide dismutases (e.g. SOD1). It is thought that these defensive mechanisms tend to show declining activity with age, which leads to a greater imbalance of ROS and antioxidants leading to increased damage, thus increasing oxidative stress (Wickens, 2001).

This theory is also linked with the rate of living theory which states that an organism's metabolic rate and lifespan are inversely proportional. The free radical theory helps to explain this as a higher metabolic rate would mean more free radicals produced resulting in more damage and therefore an increased rate of ageing and a shorter lifespan (Harman, 1956).

It has been shown that in *C. elegans* there is a correlation between oxidative stress and ageing which supports the idea that ageing is due to oxidative stress (Vanfleteren, 1993). Conversely studies have shown that increased levels of ROS can actually extend lifespan (Ewald et al., 2017).

1.3.4 Energy Maintenance Theory of Ageing

More recently a novel theory of ageing based upon mitochondrial function has been proposed, linking multiple theories of ageing (Chaudhari and Kipreos, 2018). It is based upon the idea that survival in older animals is promoted by maintaining energy levels which is improved in long and fused mitochondria and suggested to generate fewer ROS. However, as the overall effect of ROS on lifespan is still unclear, more work is required to determine the mechanism of action. Additionally, it is suggested that during calorie restriction there is reduced insulin signalling which leads to DAF-16 promoting mitochondrial fusion and also an increase in glycolysis. This study concludes that the maintenance of ATP levels or higher ATP levels correlates with an increased lifespan (Chaudhari and Kipreos, 2018).

1.3.5 Genetic control of ageing

In *C. elegans,* a number of genes have been identified which regulate the lifespan of the worm. In 1988, the *age-1* gene was the first to be identified as a regulator of ageing as the *age-1 (hx546)* mutant leads to an average increase in lifespan of 40% suggesting that the normal function of this *age-1* gene leads to promotion of the signals activating the ageing process (Friedman and Johnson, 1988).

Following on, many more genes have been found to alter the ageing process. The most important from them is the FOXO family orthologue DAF-16, which is part of the evolutionarily conserved insulin and IGF-1 signalling (IIS) pathway and fits into the calorie restriction theory

of ageing. Normally IIS signalling occurs when insulin-like peptides activate the DAF-2 (IGF-1) receptor resulting in a phosphorylation cascade leading to the phosphorylation and deactivation of DAF-16 which leads to a reduction in lifespan due to inactivation of cell protective factors. Further supporting this theory is that *C. elegans daf-2* mutants have been shown to have an extended lifespan compared to wild type worms, due to the inability to deactivate DAF-16, thus promoting activity of cell protective factors such as anti-oxidants and heat-shock proteins (Sun et al., 2017).

In addition to these genes, a number of other genes (for example *hif-1* and *trpa-1*) have been identified to influence the lifespan and ageing of worms to varying degrees of change, which will later be discussed in their response to environmental change (Section 1.4 and 1.5).

1.3.6 Hormesis

Hormesis is the application of mild stressors to organisms to elicit long term beneficial effects. It has therefore become an important area in the ageing field as these mild stressors have been shown to lead to improved biological function and possibly anti-ageing properties. The most common methods of hormesis used in ageing are calorie restriction and heat shock. However, the mechanisms by which hormesis extends lifespan are not believed to be universal but rather act by mechanisms dependent on the stressor. It has also been shown that the IIS pathway plays a major role in hormetic lifespan extension (Cypser et al., 2006). Linked to this is the unfolded protein response (UPR) and endoplasmic reticulum (ER) stress. It activates cellular mechanisms to alleviate stress in the ER. It has been shown that activation of the UPR (ER) has a reduced function with age. It is also seen that in *C. elegans* the lifespan extension via the reduction in IIS signalling requires components which make up the UPR. Additionally the decline in function of the UPR contributes to the ageing process, yet it is not clear how the UPR and ER exactly change with age (Taylor, 2016).

1.3.7 Other nutrient sensors

The ability to detect nutrients and the rate of living theory are linked by another major protein; AMP-activated protein kinase (AMPK). In the ageing process AMPK acts to regulate energy

metabolism and cellular homeostasis (Onken and Driscoll, 2010). AMPK is of interest due to its highly diverse and central role being a part of many key signalling pathways such as rapamycin (mTOR), sirtuins, and the IIS pathway (Salminen and Kaarniranta, 2012). AMPK is thought to be linked with the ageing process due to its activation by metformin resulting in extended lifespan in multiple organisms (Onken and Driscoll, 2010, Salminen and Kaarniranta, 2012). Additionally, it is thought that AMPK function is impaired with age as it loses its ability to detect AMP and leads to a reduction in mitochondrial biogenesis and function, again linked to ageing (Reznick et al., 2007). Additionally, the mTOR pathway is also linked to AMPK which is important as mTOR activity decreases with increased lifespan. AMPK is also linked to sirtuins whereby increased expression/activation of sirtuins/Sir2.1 has been shown to extend lifespan, possibly by DNA repair to improve the ageing phenotype (Salminen and Kaarniranta, 2012).

1.3.8 Telomere length and loss

Telomeres have been suggested to act as biomarkers of ageing as it is thought that they shorten with age. Although DNA damage accumulates with age it is well known that specifically the telomeres which cap chromosomes are shortened with age. It is thought that this is due to oxidative stress resulting in DNA damage (Mather et al., 2011). Correlation has been shown between telomere length and age as people who live longer tend to have longer telomeres than those who have a shorter lifespan. However it is unknown whether the shortening of telomeres is a cause or effect of ageing (Shammas, 2011). In *C. elegans,* it has been shown that this may not be the case as telomere length in *C. elegans* was independent of longevity (Raices et al., 2005).

1.4 Temperature and Lifespan

1.4.1 Rate of living theory

Temperature is a known regulator of lifespan, and it has been well documented that reducing temperature extends lifespan in many different homeothermic and poikilothermic organisms. Further to this raising the temperature results in a reduction in lifespan (Conti, 2008). In flies

the temperature is a direct regulator of lifespan and in mice, changes to core body temperature also influences lifespan (Conti, 2008, Loeb and Northrop, 1916).

In *C. elegans,* as in other organisms, the physiological mechanism of how changing the temperature affects lifespan is not yet completely understood. One distinguished theory is that at lower temperatures there is a reduction in rates of chemical reactions, this is known as the rate of living theory (Pearl, 1928, Shaw and Bercaw, 1962)

This also links with Arrhenius's theory, where the temperature is proposed to determine rates of reactions which can be calculated alongside activation energies (Arrhenius, 1889). The Arrhenius equation has been applied to testing of equipment where temperature is used to stress equipment to see how long it will last, (i.e. time to failure tests). Arrhenius's law states that for every 10°C increase in temperature, the rate of reaction doubles (Shaw and Bercaw, 1962, Arrhenius, 1889).

1.4.2 Genetic thermoregulation, AFD neuron and Heatshock proteins

As it is not entirely understood how temperature changes leads to a physiological mechanism which reduces lifespan a genetic approach has become the common method to investigate the potential pathways that are involved in temperature-based lifespan modifications. It has been seen that genetics play an active role in controlling lifespan, however this is still not well understood as different studies suggest a plethora of different factors which differentially regulate lifespan (Miller et al., 2017).

Miller reviewed the impact of different culture temperatures on a number of mutant worms and found that there are a substantial number of genes which play a role in temperature dependent lifespan extension. She then suggested that lifespan extension simply cannot be explained by changes in thermodynamic reaction kinetics (Miller et al., 2017). This study went on to suggest a few genes which are affected by temperature, such as *cep-1* and *rsks-1* which has a varying lifespan at lower and higher temperatures indicating temperature dependent activation (Miller et al., 2017).

Another mechanism which has been investigated is the thermosensory AFD neuron which responds thermotaxically to temperatures within a normal range (15°C-25°C). Inactivation of the AFD neuron via ablation or mutation leads to loss of this thermotaxic ability (Lee and Kenyon, 2009). Although it is still not fully understood how AFD acts to increase lifespan, it is thought that this thermotaxis ability involves cyclic guanosine monophosphate (cGMP) -gated ion channels TAX-2 and TAX-4 and guanylate cyclases GCY-8, GCY-18 and GCY-23. Temperature changes lead to a Ca^{2+} current which signals to PKC-2 resulting in a phosphorylation cascade signalling to the DAF-9 transcription factor and the steroid signalling pathway which ultimately leads to inhibition of DAF-12 resulting in anti-ageing properties. However once ablated, this instead leads to DAF-12 activation and ageing. DAF-12 is the thyroid hormone receptor beta orthologue which normally is involved in lipid oxidation to support reproduction and growth (Lee and Kenyon, 2009, Land and Rubin, 2017, Mori and Sasakura, 2009, Ramot et al., 2008, Wang et al., 2015). The effect this thermosensory neuron has on lifespan is only effective at higher (25°C) temperatures as there is no consequence of ablation at lower (15°C) temperatures (Lee and Kenyon, 2009). Heat shock proteins are also important in the lifespan of *C. elegans*, with an increase during transient exposure to high temperatures at a young age leading to longevity (Morley and Morimoto, 2004). Heat shock proteins act as molecular chaperones responding to heat shock and other stressors. They ensure proteostasis by assisting protein folding and assembly to prevent damage and aggregation of proteins which occurs due to high temperatures. In *C. elegans* temperatures above 26°C enable a heat shock response whereby the *hsp16-1* reporter expression increases with small increases in temperature (Zevian and Yanowitz, 2014, Dawe et al., 2006).

1.4.3 TRPA-1 and thermoregulation of lifespan

Another prominent protein which has been suggested to be required for cold dependent lifespan extension is the cold/pain sensor transient receptor potential ankyrin 1 (TRPA-1, also known as ANKTM1) (Xiao et al., 2013). This somatosensory voltage dependent TRPA-1 non-selective Ca^{2+} cation channel is the only TRPA protein expressed in humans, worms, flies and other mammals (Figure 1.3). However, in *C. elegans* there is also an uncharacterised TRPA-

2 protein, which does not have sequence homology related to TRPA channels in humans, rodents or flies (Kindt et al., 2007).

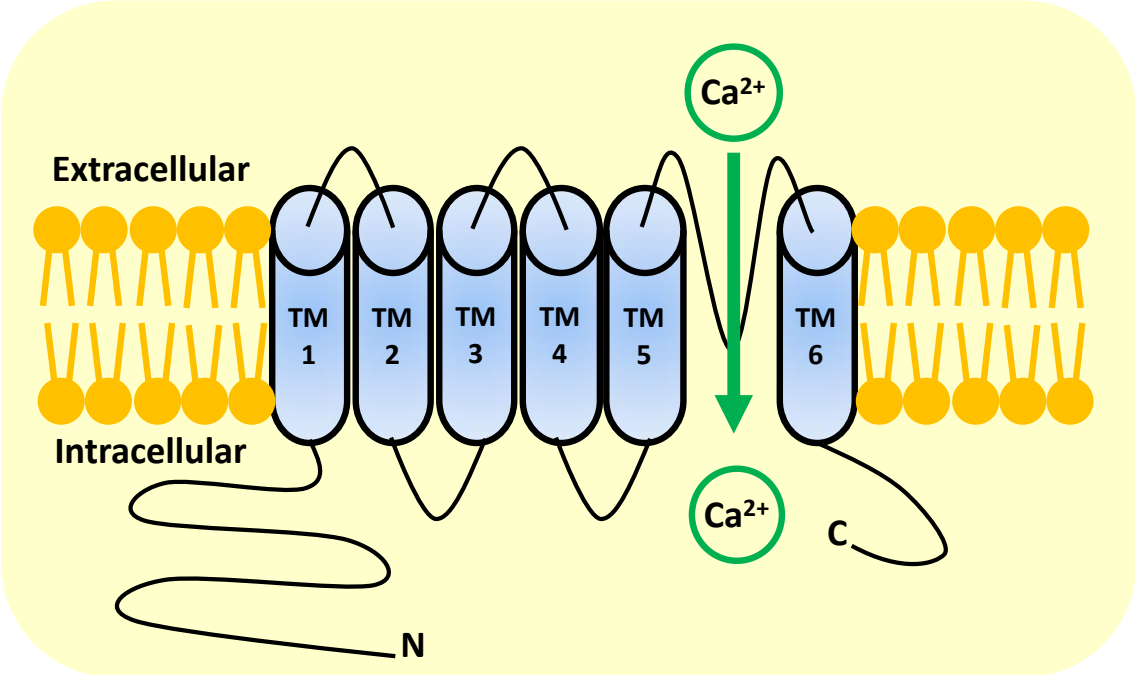

Figure 1.3: The TRPA-1 ion channel which allows Ca^{2+} entry into the cell.

TRPA-1 in *C. elegans* is expressed in many different tissues types including sensory neurons, epithelial cells, muscle tissue and tissue which makes up the excretory system (Kindt et al., 2007, Xiao et al., 2013). Temperature-regulated activation of TRPA-1 is contested as to whether it is activated by heat or cold. Additionally, differences between species and if indeed cold is the activator of the TRPA-1 channel is disputed (Chen et al., 2013, Chen, 2015).

The lifespan regulatory function of TRPA-1 requires downstream regulators and it is unsurprising that it acts via the master lifespan regulator DAF-16. TRPA-1 allows Ca^{2+} ions into the cell which is thought to activate the calcium-sensitive kinase PKC-2 which then phosphorylates the kinase SGK-1 (amongst other effectors and transcription factors) found upstream of DAF-16 and promotes nuclear DAF-16 localisation (Figure 1.4; (Xiao et al., 2013).

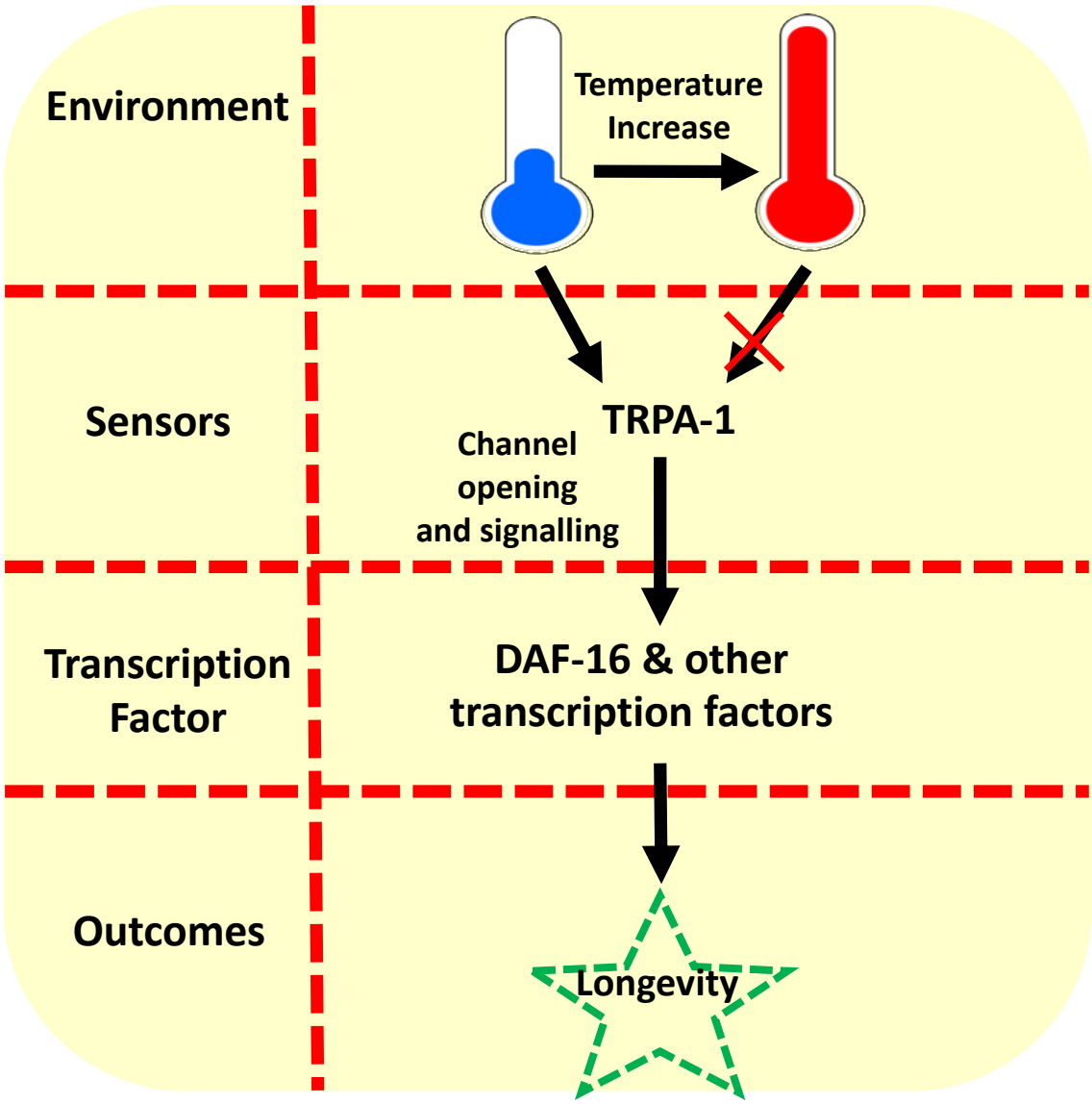

Figure 1.4: Cold dependent temperature activation of TRPA-1 signalling to DAF-16 and other transcription factors resulting in longevity.

Additionally, it has been found that temperature differentially regulates lifespan of adult and larval worms, as the cold stimuli in larval worms reduces overall lifespan but in adult worms it increases lifespan (Xiao et al., 2013). The opposite is also seen at higher temperatures as larval worms which have been grown at higher temperatures have a longer lifespan but once they reach adulthood if they are continually grown at the high temperature then it results in a reduced lifespan. However, if they are shifted to a lower temperature upon reaching adulthood then an increase in lifespan is seen (Xiao et al., 2013, Henderson et al., 2018).

In addition to cold activation and cold-regulated lifespan extension in *C. elegans,* the TRPA-1 channel has a mechanosensory role in foraging and nocioception (Kindt et al., 2007). It also has a role in oxygen sensing as it is regulated by oxygen-sensitive prolyl hydroxylases (PHDs). During the inflammatory response it is controlled by HIF-1α which binds to the *TRPA1* gene therefore controlling cytokine release from inflammatory synoviocytes (Hatano et al., 2012).

Finally, TRPA-1 can be activated by many different chemical compounds such as electrophilic compounds like hydrogen peroxide or allyl-isothiocynate (AITC) and also non-electrophilic compounds such as the essential oil carvacrol found in oregano and thyme plants or cannabidiol, suggesting links to the cannabinoid signalling pathways (Skerratt, 2017).

1.4.4 DAF-16 and longevity

DAF-16 is a transcription factor which has been comprehensively implicated with ageing and longevity in *C. elegans*. It is the single orthologue of the Forkhead Box O (FOXO) family of proteins, therefore acting as a central mediator in many signalling pathways (Lin et al., 1997, Sun et al., 2017). The most common pathway which has been associated with the DAF-16 pathway is the IIS pathway which as previously mentioned (section 1.3.5) is involved in glucose uptake providing energy to cells for growth and reproduction. The IIS pathway also plays a major role in longevity via calorie restriction. Other than this the DAF-16 pathway is involved in many other cellular stress signalling pathways. The mTOR pathway, AMPK pathway, JNK pathway, sirtuin signalling pathway and also germline signalling pathway are all dependent on DAF-16 activity to function. Additionally DAF-16 regulation occurs by a plethora of alternative mechanisms, such as co-factors, (Heat shock factor 1 (HSF-1), HCF-1 SMK-1) as well as post translational regulators such as acetylases, phosphatases and ubiquitinases which play roles in dauer formation, apoptosis, lipogenesis, reproduction and development, anabolism and catabolism and cell cycle signalling and arrest, as well as signalling to protect from stress factors such as oxidative stress, heat stress and stress from food deprivation (Sun et al., 2017, Yen et al., 2011). Many of these pathways contribute to longevity and healthy ageing.

Overall DAF-16 has approximately 3000 gene targets, making its role very complex (Tepper et al., 2013). Further complicating its role are the different isoforms of the *daf-16* gene with 8

in total varying, from *daf-16a* to *daf-16h*. These different isoforms share sequence similarity but may have varying importance depending on their role for instance in longevity or in dauer formation (Sun et al., 2017, Kwon et al., 2010, Yen et al., 2011, Lin et al., 2001). DAF-16 shuttles between the cytoplasm and nucleus of the cell where it binds to the DAF-16 binding element (5'-TTGTTTAC-'3). It is expressed in tissue including, muscle, neurons intestines and pharynx and is expressed during all phases of developmental lifecycle stages and adulthood throughout the *C. elegans* lifespan (Lin et al., 2001, Sun et al., 2017).

It is proposed that temperature can influence DAF-16 signalling, via the temperature sensitive TRPA-1 cation channel which allows Ca^{2+} entry into the cell activating a signalling cascade which activates DAF-16.

The other major players which respond to temperature with DAF-16 are the heat shock proteins. HSF-1 is a transcription factor which regulates heat shock protein transcription which go on to interact with DAF-16 and it is thought that together they extend lifespan. A reduction in HSF-1 activity promotes onset of the ageing phenotype whereas over expression of HSF-1 leads to DAF-16 dependent lifespan extension. It is thought that HSF-1 and DAF-16 act together to target 4 genes of the small heat shock proteins (shsps) (Hesp et al., 2015). However, further details on this mechanism is still under investigation (Yen et al., 2011).

Overall it is still not widely understood how temperature mechanistically acts to alter lifespan. Although a number of viable mechanisms have been identified, it is likely that these mechanisms all act to alter lifespan, but function complementarily to one another or under different conditions for example, under varying temperature conditions, or at different time points during the worm's lifespan. Therefore, it is important to further characterise how the signal to and from DAF-16 is transduced and what specific gene targets are activated to alter lifespan, with perhaps each mechanism providing a small synergistic contribution to lifespan extension.

1.5 Oxygen and ageing

1.5.1 Oxygen and organisms

Oxygen plays a major role in regulating the lifespan and ageing process of all organisms. Without oxygen we would be unable to survive and yet it is also responsible for cellular damage which leads to the ageing phenotype according to the free radical ageing theory (Harman, 1956). All multicellular organisms (except *Loricifera*) require oxygen for survival as none are able to survive in anoxia (Danovaro et al., 2010).

Many lifespan studies have been conducted in varying oxygen levels in a range of organisms. Mammals (including rodents) and drosophila which have been exposed to hyperoxia have a reduced lifespan but in *C. elegans* there is no negative effect of this high oxygen exposure (Rascón and Harrison, 2010, Jamieson, 1989). Conversely, low oxygen levels or (physiological) hypoxia have been shown to have varying effects. For example, in drosophila some studies report that hypoxia results in lifespan extension while in others, a reduction is reported (Rascón and Harrison, 2010, Vigne and Frelin, 2006).

Human cell culture studies have shown that culturing fibroblasts (human diploid WI-38) at low oxygen levels (10%) leads to an increase in replicative lifespan as opposed to the higher concentration of oxygen which led to damage of cells and loss of viability (Packer and Fuehr, 1977).

1.5.2 Hypoxia in *C. elegans*

Since 1993, it has been reported that hypoxia extends the lifespan of *C. elegans* although there is some variability in this finding, particularly due to the varied methodology of the studies (Honda et al., 1993). Many studies do not maintain worms in hypoxia throughout the entirety of their lifespan, as some studies remove them from hypoxic conditions daily in order to measure lifespan. Some pass gas over the culture plates contained within a small chamber and one study even uses a plastic bag containing an oxygen scavenger to sequester oxygen, although measuring how much oxygen is remaining is difficult to assess. Additionally, studies in hypoxia are also dependent on their definition of hypoxia, as some define hypoxia as 1%

oxygen, whereas others define it as 0.5% or even as low as 0.1% (Leiser et al., 2013, Honda et al., 1993, Mehta et al., 2009, Kitazume et al., 2018, Fawcett et al., 2012, Liu and Cai, 2013). Regardless of methodologies, it is generally reported that a reduction in oxygen levels normally results in an increase in lifespan (Honda et al., 1993, Leiser et al., 2013, Mehta et al., 2009, Liu and Cai, 2013).

1.5.3 Neuronal response to oxygen

C. elegans respond to changing oxygen levels by the BAG and URX, AQR and PQR sensory neurons. High oxygen levels are detected by the URX, AQR and PQR neurons and low oxygen levels are detected by BAG neurons (Liu and Cai, 2013). At the molecular level, soluble guanylyl cyclases (sGCs) expressed on the neurons act to sense gas by binding to the gaseous ligand such as oxygen. The sGCs are differentially expressed in the different neurons. In BAG neurons, the sGCs expressed are GCY-31 and GCY-33 which detect a decrease in oxygen and signal via cGMP/Ca^{2+} signalling resulting in TAX-2 depolarisation and play a role in regulating lifespan. GCY-33 is also expressed in URX, AQR and PQR neurons in addition to GCY-35 and GCY-36 which detect increases in oxygen levels and again signal via cGMP (Liu and Cai, 2013, Zimmer et al., 2009, Gray et al., 2004, Chang et al., 2006, Cheung et al., 2004, Rogers et al., 2006). These sGCs in the BAG and URX neurons play a complementary role in balancing the action of one another in lifespan regulation. BAG neurons play an inhibitory role which acts to prevent the pro-longevity effect of low oxygen conditions and the URX neuron also plays an inhibitory role to prevent the anti-longevity effect of high oxygen levels. Additionally it is believed that the action of BAG and URX neurons with sGCs is independent to other pathways which respond to oxygen changes (Liu and Cai, 2013, Coates and de Bono, 2002).

1.5.4 HIF-1 signalling in hypoxia

Another important signalling pathway involved in oxygen sensing is the HIF-1 signalling pathway. Hypoxia inducible factor (HIF) is a highly conserved transcription factor which responds to low oxygen levels. In humans, HIF is a heterodimer which is made up of an α and a β subunit (Wang et al., 1995). Three HIF-α subunits have currently been identified, (HIF-1α,

HIF-2α and HIF-3α) which when translocated to the nucleus form heterodimers with HIF-β (Aryl hydrocarbon receptor nuclear translocator) which is constitutively expressed in the nucleus. HIF-1α is expressed in most tissue types although it has greater expression in the heart and kidneys. The three HIF-α subunits have different functions (Tian et al., 1997, Wang et al., 1995, Gu et al., 2018). HIF-1α has been studied extensively and when active generally acts to target metabolic processes to adapt to hypoxia and increase oxygen delivery. This occurs when the HIF-1 heterodimer binds to the DNA sequence known as the HIF-1 response element (HRE; 5'-TACGTG-'3) which is on the promoter of a number of genes such as vascular endothelial growth factor (VEGF), glucose transporters and erythropoietin (Shen et al., 2005, Semenza, 2009). Additionally, it plays a role in cancer and embryo development where it acts to promote tumour angiogenesis and placental vascularisation (Semenza, 2009). Similarly, HIF-1 is known to play a protective role in ischemia reperfusion disease (Howell and Tennant, 2014).

HIF-2α has been shown to have a similar mechanism of action to HIF-1α and acts to promote genes expression such as VEGF (Ratcliffe, 2007). Additional studies have found a protective role in heart failure and in embryonic development by maintaining catecholamine homeostasis (Brown et al., 2009, Giaccia, 2013).

HIF-3α function is not as well understood as the other two subunits. Studies suggests that HIF-3α has more of a regulatory role and targets a number of genes, some of which overlap with HIF-1α targets (Zhang et al., 2014). One known function is that it acts to repress angiogenic factors (Kobayashi et al., 2015).

HIF is regulated by oxygen. In the presence of oxygen HIF is hydroxylated by PHDs on proline residues. This in turn leads to ubiquitination by the Von-Hippel-Lindau protein (pVHL) E3 ubiquitin ligase which targets it for proteasomal degradation. In low oxygen conditions HIF is stabilised as oxygen inhibits the PHDs which in turn allows HIFα to be translocated to the nucleus to regulate gene expression (Tanimoto et al., 2000).

1.5.5 HIF in *C. elegans*

In *C. elegans,* there is only one single HIF-α orthologue (HIF-1) and one single HIF-β orthologue (AHA-1) which dimerise to control gene expression. Just as in humans the HIF-1 regulatory pathway is evolutionarily conserved as HIF-1 is degraded in the presence of oxygen by action from the prolyl hydroxylase (EGL-9) and the E3 ligase VHL-1 (Figure 1.5; (Pitt et al., 2014, Jiang et al., 2001). It is located on chromosome V and has a number of gene targets in response to hypoxia. These gene targets affect cellular metabolism, dauer formation and apoptosis. HIF-1 is also involved in regulating a number of signalling pathways: for example HIF-1 regulates the mRNA levels of EGL-9, thus leading potentially to a negative feedback loop (Shen et al., 2005, Jiang et al., 2001).

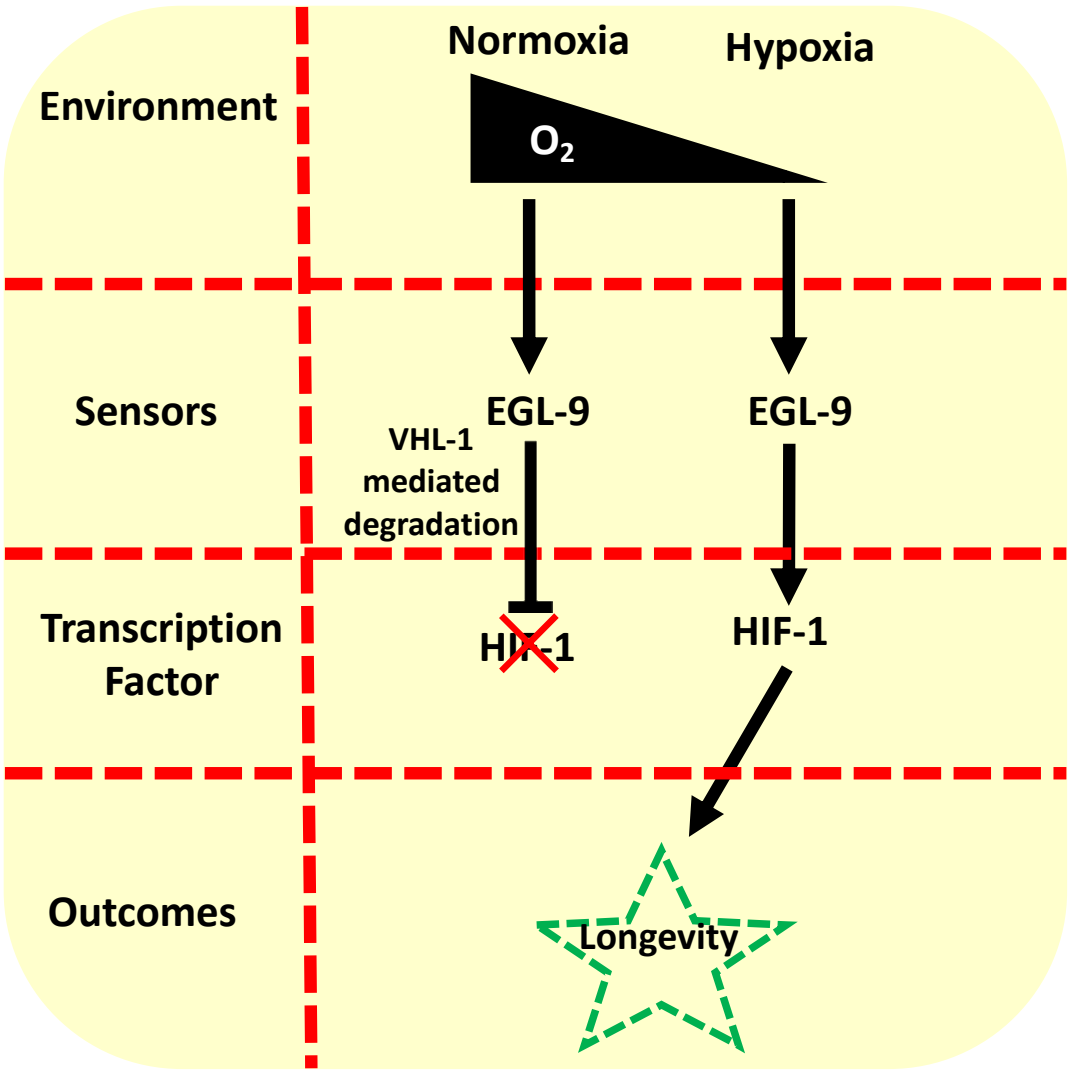

Figure 1.5: Hypoxia prevents EGL-9 mediated HIF-1 degradation which can act to promote lifespan signalling factors.

1.5.6 Lifespan and HIF-1

Another major role of HIF-1 in *C. elegans* is its role in lifespan and ageing. As mentioned previously (section 1.5.2), hypoxia acts to extend lifespan. HIF-1 has been extensively investigated to identify its role in lifespan changes. Stabilisation of HIF-1 via knockdown of VHL-1 or EGL-9 results in an increase in lifespan. Loss of VHL-1 protein also results in improvements in other biomarkers of ageing including reduction of autofluorescence. The same study concluded that the VHL-EGL-HIF pathway acts distinctly from the IIS pathway to extend lifespan. Mutation to *vhl-1* and *egl-9* show similar lifespan extensions whereas *hif-1* deletion shows no difference in lifespan (Mehta et al., 2009). Conversely, further studies showed that *hif-1* deletion in *C. elegans* increases lifespan although the methodology in this study was different (Zhang et al., 2009). HIF-1 also shows temperature sensitivity as at higher temperatures loss of *hif-1* extends lifespan but this is not observed at low temperatures (Leiser et al., 2011). Additionally, *hif-1* overexpression has been shown to extend lifespan however this is dose dependent (Zhang et al., 2009). Furthermore, it has been reported that HIF-1 is required for lifespan extension in response to hypoxia and that DAF-16 is also required for this lifespan extension (Leiser et al., 2013). It is not yet clear whether the two pathways are linked but other studies have shown that in mammalian cells, the DAF-16 orthologue FOXO3a is a target of HIF-1α (Bakker et al., 2007).

DAF-16/FOXO is a shared target of both TRPA-1 and HIF-1, however in addition to this, TRPA-1 and HIF-1 show many different links to one another in multiple different organisms. Chemically induced hypoxia i.e. treatment with desferroxamine or dimethyloxalylglycine leads to HIF-1α activation and also results in increased *TRPA1* mRNA levels. Additionally, in the same study HIF-1α has been shown to bind to a number of HRE motif sites on the *TRPA1* gene resulting in increased expression and induction of TRPA-1 ion channels, which in turn leads to increases in cellular Ca^{2+} (Hatano et al., 2012). Further linking these two pathways is the proposal that TRPA-1 is a sensor for oxygen and is sensitised (to pain) in hypoxic conditions and is also regulated by PHDs in a similar manner to how HIF is regulated (So et al., 2016). As previously mentioned HIF-1 responds to temperature changes, indicating that

both of these temperature and hypoxia signalling pathways are tightly linked. Therefore, these oxygen and temperature signalling pathways would be ideal to further investigate lifespan changes in *C. elegans* as a measure of ageing in response to environmental changes including both temperature and oxygen.

1.6 Measures of ageing

1.6.1 Lifespan and chronological age as a measure of ageing

Lifespan or chronological age has commonly been used as a surrogate measurement for the ageing process (Klass, 1977). This is due to the correlation between the ageing phenotype and increased age even though the two are in fact distinct (Bansal et al., 2015). Lifespan is clearly defined as a measurement of an organism's survival as time passes. This simple definition makes it easy to measure and conduct by simple survival assays and can be conducted on a range of organisms so relative comparisons can be made. Although extremely easy to conduct, there are positive and negative qualities of lifespan in its ability to act as a measure of ageing. The chronological age of an individual is an accurate measurement of its lifespan. However, its ability to act as a measure of the ageing process is less accurate primarily due to the many variations between individuals. Population studies and measuring the average lifespan of a population to generate survival curves are generally considered to be more useful and more accurate measures of ageing. However, the methodology of conducting lifespan assays is also important as differences in methodology can yield different results. Factors to consider is population size, frequency of measurement and number of replicates.

1.6.2 Biological age as an alternative measure of ageing

An alternative measure of the ageing process is biological age. Unlike chronological age which measures the time passed since birth, biological age is calculated from measurements of multiple different parameters which act as biomarkers of how an organism's body (tissues, organs and systems) is functioning. Changes in the characteristic biomarkers are measured as bodily function deteriorates over time. Higher levels of biomarkers which characterise greater deterioration of bodily function result in a higher biological age. Therefore, biological

age as a whole is a closer measure of the health or wellness of an individual which normally deteriorates in the ageing process. As there is no single direct measurement of biological age but a range of substitute measurements, it is difficult to get consistent and comparable measure of biological age. Example of biomarkers can be either lifestyle factors (such as weight, blood pressure, breathing tests, amount of exercise and food intake) or biomedical factors (such as genetic makeup, immunoglobulin G structure or telomere length or DNA methylation). These biomarkers can be investigated individually or collectively in a population to give a measure of biological age. However, in different organisms there are different biomarkers of biological age and also multiple different markers for the same bodily functions making it difficult to draw comparisons. Additionally, these single tests show high levels of inter- and intra- individual variability, making it difficult to extrapolate from a population, particularly when investigating treatments or interventions (Levine et al., 2018, Kato et al., 2006).

1.6.3 Healthspan

Linked to biological age is healthspan which does not have a single universally accepted definition. Many studies measure a few biomarkers which correspond to good health but then conclude that it affects healthspan as a whole (Bansal et al., 2015). One definition is that healthspan is a measure of the disease free or healthy time period of an individual's lifespan, although another definition is the average length of healthy life (Kaeberlein, 2018, Crimmins, 2015). Therefore, before healthspan can be widely used as a surrogate measure of ageing, standardised measures must be implemented. Like biological age, healthspan is characterised by a number of measures which identify whether an individual is in a healthy state. Similarly, many studies measure different biomarkers of healthspan as it is difficult to measure all of them given that there is no finite number of biomarkers. This also makes it difficult to standardise a measurement of healthspan (Bansal et al., 2015). As previously mentioned, the average lifespan and (life expectancy) in humans has increased over time, but healthspan has not increased at the same rate (Olshansky, 2018). In particular during later lifespan, a number of chronic late onset diseases have become prevalent in the elderly. These include diseases

such as dementia, diabetes or cancer. Additionally, healthspan can be affected by a number of diseases and even though one measure shows a positive health outcome others may not. Thus overall healthspan is currently more difficult to improve than lifespan. Many studies have initiated setting out parameters which are used to measure healthspan and which are relevant to humans (Bansal et al., 2015, Xia et al., 2017, Lara et al., 2015, Burkle et al., 2015). In *C. elegans,* conflicting results have been reported as it has been shown that healthspan and lifespan are not proportional to one another yet coincidentally (or not) improvements to healthspan result in an increase in lifespan (Richardson et al., 2016, Rollins et al., 2017).

1.6.4 Frailty Index

Another alternative measure of ageing linked to healthspan is the frailty index which determines the health status of an individual from an index of health biomarkers (Searle et al., 2008). Specifically, for each biomarker, the number of individuals in a health deficit are calculated and thus healthy and frail proportions of a population are generated. Therefore, in many studies, the frailty index is used as a measure for biological age. Similarly, the whole population rather than an individual can be investigated and, by conducting lifespan studies, a frailty measurement can be made (Rockwood et al., 2017, Goggins et al., 2005). Mouse models to study frailty have become more widespread, with many studies investigating a range of parameters and physiological changes in relation to frailty, which in turn provides the opportunity to translate applicable findings to humans (Kane et al., 2016).

1.6.5 Applying frailty index to mortality

Lifespan studies are able to provide data at various time points in which there is a proportion of the population that is in deficit (dead) and the remaining population which is alive and not in deficit. Multiple groups have studied this assumption, with all groups concluding that the frailty index in humans and mice is predictive of mortality (Rockwood et al., 2017, Kojima et al., 2018). Although it is a simple assumption, it can be assumed from lifespan data that at lower survival proportions the population is frailer and therefore has a higher biological age.

1.7 Measurement of lifespan

1.7.1 Traditional lifespan assay methods

Lifespan assays are a key method for studying biological and physiological processes such as ageing and stress resistance which affect longevity in organisms including flies, mice or worms. Although ageing and lifespan are separate concepts they are linked to one another. Due to the short lifespan, genetic simplicity and straightforward methodology *C. elegans* lifespan assays are an ideal method to measure ageing. Lifespan measurement is a property of an ageing population which is done by the documentation of each worms' lifespan in the studied population.

Lifespan assays involve measurement of the consequence of ageing which uses death as an endpoint. In a population a start point is needed, often birth or first day of adulthood, and the number of individuals which are alive, and dead are measured at regular intervals. This is commonly shown as proportions of alive vs dead over time.

C. elegans lifespan can be measured in many different ways which further complicates the comparison of results among different studies. The most common difference is conducting lifespan assays on either solid medium or in a liquid culture.

Lifespan assays on solid medium use Nematode Growth Media (NGM) agar plates typically seeded with bacteria (e.g. *E. coli* OP50) as a food source. Other food sources can be used such as *E. coli* HB101 or HT115, which are often used to introduce RNAi for gene knockdown in *C. elegans* (Amrit et al., 2014).

Conventionally, these survival assays are conducted manually, using a microscope and a worm pick to count and record alive, dead and censored worms manually. A synchronised young adult (L4) population is selected, which is then counted at regular intervals, typically daily or every other day.

1.7.2 Digital lifespan assays

Additionally, worm lifespan can be measured digitally using flatbed scanners. In this thesis the term "digital" lifespan measurement includes both automated and semi-automated lifespan

measurement systems. There are many setups that have been produced for digital lifespan measurement. The *C. elegans* 'lifespan machine' is a well characterised system which uses a Linux server and a custom-built image analysis software to automate lifespan measurement by taking scans at regular intervals (~15 minutes) and compares differences between images (Stroustrup et al., 2013).

Another automated system is the 'Wormscan' system which requires the user to take subsequent images which are analysed for differences by the image processing software Fiji (Mathew et al., 2012).

Both manual lifespan assays and digital lifespan assays have their benefits and drawbacks. For example, the automated systems require less user contact and can be higher throughput on a larger scale compared to manual counting. However, as dead worm detection is based on image parameters the exact time of death may be difficult to determine. Thus, it may result in less accurate survival curves compared to manual counting which can accurately determine whether a worm is dead or alive. However, frequency of counting also affects the determination of death; most manual counting assays record worms on a daily basis with some studies using a less frequent measurement time points, whereas the automated counting can record lifespan at up to 15-minute intervals giving a much higher resolution of the generated survival curve. In automated systems there is also minimal user contact resulting in less extraneous variables which may affect worm lifespan and potential biases from the user. However, other factors such as the heat and light from the scanners are known factors which may affect lifespan and must be taken into consideration (De Magalhaes Filho et al., 2018).

Liquid cultures of *C. elegans* is an alternative method for growth and to conduct lifespan assays. The worms are grown in a S-Basal medium and are placed on a platform shaker which provides sufficient oxygenation to the worms for proper growth (Amrit et al., 2014). In the lifespan measurement in liquid culture, worms which do not respond to shaking are classified as dead. Additionally, there is a 'wormfarm' automated lifespan system which is able to measure lifespan of worms in a liquid culture (Xian et al., 2013).

1.8 Lifespan analysis

1.8.1 Kaplan-Meier estimator and other non-parametric models

The most common method for analysis of population survival is the non-parametric Kaplan-Meier estimator (Goel et al., 2010). Also known as the product limit estimator, it is defined as the probability of survival in a given length of time at specific measured time points (Kaplan and Meier, 1958, Goel et al., 2010). Not only can the Kaplan-Meier estimator be used to calculate lifespan but it has a number of applications which require measurement of time to an event, for example disease onset in patients or drug treatment comparisons (Collett, 2015). From the Kaplan-Meier estimator a number of useful quantities can be obtained. Thus it calculates the probability of an event (death) occurring at given time points and can also take into account censored individuals. Additionally a median survival time is calculated, which is the time point when 50% death of the original population occurs (Goel et al., 2010). From the Kaplan-Meier estimator it is also possible to calculate a survival function and from this, the hazard function, which is the probability that an individual will survive beyond a given time point and the probability that an individual will die at a given time point (Collett, 2015). The most common method for comparison of Kaplan-Meier curves is the log-rank test which statistically tests the null hypothesis that there is no statistically significant difference between the two populations in the probability of death at a given time point (Goel et al., 2010). However, by using the Kaplan-Meier estimator to measure lifespan data, the different experimental realisations cannot be collated with one another, and as a result differences between realisations are often overlooked particularly as each curve can only be compared with a single other curve. Additionally, by coupling it with the log-rank test the only output obtained is whether there is a difference between the two curves but there is no indication as to when differences in lifespan may occur. Thus, the Kaplan-Meier coupled to the log-rank test is an insufficient methodology for examining lifespan data in detail.

Another non-parametric test is the Kolmogorov-Smirnov test. It is able to quantify differences between two samples by comparing the two distributions against the null hypothesis that the

two samples come from the same distribution. It does this by comparing empirical cumulative distributions, in this case observed lifespan distributions (Massey, 1951).

Other models which can be used to fit survival data can be semi-parametric or parametric, which assume a distribution of the experimental data. One example of a semi-parametric model is the Cox proportional hazards model which estimates the effect of a known covariate (continuous variable) upon a hazard which is relative to the baseline hazard (hazard function when all covariates are set to 0). The Cox model allows relative comparison of multiple covariates and is commonly used in clinical investigations as its use is restrictive in situations where hazards are not proportional. This model is a semi-parametric as the baseline hazard function is not assumed but remains unspecified (Cox, 1972, Bradburn et al., 2003, Bugnard et al., 1994).

The accelerated failure time model is an alternative parametric model to the proportional hazards model and uses a Weibull or exponential distribution to compare two populations. It defines the difference between the curves by a multiplicative parameter as the curves are either shifted to the left or right from one another (Bradburn et al., 2003, Swindell, 2009).

1.8.2 Parametric modelling

As an alternative to the non-parametric and semi-parametric models, parametric models can be used to fit lifespan curves. Unlike non-parametric and semi-parametric models, the parametric models have finite parameter values expressed by mathematical equations. A number of parametric models of cumulative distribution functions have been developed which allow fitting to lifespan curves and other time series data. The majority of survival models are sigmoidal in shape with an exponential decrease. The parametric models are useful for modelling lifespan as the number of parameters can be adjusted depending on the type of survival data. However, the chosen parametric model must fit data sets as they assume a baseline hazard to estimate parameters. It is therefore important that parametric functions are accurate so to gain reliable conclusions, as inappropriate models would not yield reliable results (Dätwyler and Stucki, 2011). The most renowned model is the Gompertz model which was originally applied to the law of mortality itself based upon the hazard (of death) which

increases exponentially as time passes (Gompertz, 1825). Life tables of mortality is commonly used to investigate the number of deaths in populations over time and are often attributed to specific causes. The Gompertz model was originally developed to approximate life tables and has been further developed by the addition of an extra parameter into the Gompertz-Makeham function (Makeham, 1860).

Another popular model is the Weibull model, which has the mortality/failure rate proportional to the power function of time (Weibull, 1951). The Weibull model is used as the baseline hazard of the proportional Cox model and accelerated failure time models (Bradburn et al., 2003, Cox, 1972). Variation of these models have since been developed with varied fitting powers. The majority of models which are used to fit survival data have two parameters which follow a monophasic decrease. A number of other models with a varied number of parameters have since been developed and applied to many biological time-to-event data sets in survival of animals, bacterial cultures of growth or inactivation and tumour growth. (Vanfleteren et al., 1998, Xiong et al., 1999, Marusic, 1996, Wilson, 1994). Additionally, these sigmoidal curves are applied in engineering to failure rates of components to investigate for how long they will function as intended.

1.9 Two phases of *C. elegans* lifespan

C. elegans is a model organism in which their survival is modelled. Its lifespan is commonly modelled by Gompertz or Weibull models. However, recent studies have shown that even isogenic populations of *C. elegans* grown in similar conditions have variations in lifespan which can be due to a number of intrinsic factors including mutations, modifications and random changes to processes which may have cumulative effects upon lifespan of individuals (Kirkwood et al., 2005). For example Hsp16-2 shows a large variation in expression levels which has been linked with variations in survival (Rea et al., 2005). Another study has also introduced the idea of subpopulations of short-lived and long-lived individuals, with physiological differences in movement, autofluorescence and tissue integrity. Compared to long-lived worms, short-lived worms have greater autofluorescence, lower tissue integrity and move less. Additionally, a correlation is seen between longer lifespan and smaller body size

and fewer eggs laid. The study concludes that short-lived individuals die earlier but still appear to be healthy while the longer lived individuals undergo physiological decline early on but continue to spend the rest of their long lifespan with reduced function (Zhang et al., 2016). Another study uses post mortem analysis and identify two causes of death. Thus the population is split into two subpopulations based on differences in pharyngeal pathologies and are termed big 'P' and small 'p' which correspond to early deaths and late deaths. They conclude that the 'P' deaths are due to a pharyngeal infection and subsequently damaged due to high pharyngeal pumping rates (Zhao et al., 2017). Finally, an additional study which investigates maximal movement velocity of worms as a measure of healthspan indicate that worms can be split into two subpopulations; those with a high movement velocity and those with a low movement velocity and the study shows that there is a distinct differences in lifespan between these two groups (Hahm et al., 2015). These studies provide compelling evidence that there are two phases of lifespan in *C. elegans* and therefore modelling lifespan data with the commonly used monophasic parametric models is unsuitable for lifespan analysis.

1.10 Thesis justification, hypothesis and aims

Lifespan in *C. elegans* is observed to occur in two phases with the early phase death of short-lived individuals and the late phase death of long-lived individuals. Current parametric models used to analyse lifespan follow monophasic survival and therefore would be unable to reliably model two phase (biphasic) lifespan. Temperature and oxygen changes are important environmental modifiers which control lifespan of *C. elegans* signalling via TRPA-1 and HIF-1 signalling pathways respectively. Mathematical modelling of lifespan of TRPA-1 and HIF-1 signalling pathway factors allows further investigation of the role played by the two signalling pathways and will provide insight into the interaction between the two pathways.

We hypothesise that a parametric biphasic lifespan model would be a more accurate model for fitting lifespan data of *C. elegans* compared to commonly used existing models. Using this model would allow further investigation to changes in lifespan under different temperatures and oxygen conditions and by using mutant animals to identify the specific roles played by these factors in influencing lifespan. This will also lead to better understanding of signalling

between HIF-1 and TRPA-1 and how it affects lifespan. Furthermore, using this model will allow different data realisations to be collated with one another providing a more comprehensive method of analysis.

The aim of this thesis is to use mathematical modelling techniques to investigate how TRPA-1 and HIF-1 signalling regulate lifespan. More specific objectives are:

- To generate a novel mathematical model capable of modelling biphasic lifespan data and to confirm that *C. elegans* lifespan can be biphasic. To compare this model with existing models using goodness of fit testing. To identify the versatility of this model by applying it to a range of conditions and species to identify lifespan differences.
- To generate predictive models which can predict the effect of intervention on lifespan. Verify the accuracy of the predictive models by comparing predictions to experimental lifespan data. To identify critical intervention time points at which lifespan has significantly changed or can no longer be changed.
- To use the parametric model to determine the relationship between TRPA-1 and HIF-1 signalling in relation to temperature and oxygen changes and to determine the effects upon lifespan in *C. elegans*. To identify signalling between the TRPA-1 and HIF-1 pathways in mammalian cells and to identify if signalling is consistent in *C. elegans*.

Chapter 2.0: Materials and Methods

2.1 Materials

All materials were purchased from Sigma-Aldrich Company (Dorset, UK) unless otherwise stated. Plasticware for cell and worm culture was purchased from Thermo Fisher Scientific (Loughborough, UK) and VWR International (Lutterworth, UK).

2.2 *C. elegans* experiments

2.2.1 Strains growth and maintenance

The *C. elegans* strains N2 (wild isolate), and *daf-16(mu86)* (10980 bp deletion), *hif-1(ia4)* (1231 bp deletion), *trpa-1(ok999)* (1334 bp deletion), *egl-9(sa307)* (243 bp deletion) and *egl-9(n586)* (base substitution) were acquired from the Caenorhabditis Genetics Center (CGC), University of Minnesota. All strains were cultured on solid nematode growth media (NGM) agar (Table 2.1).

Table 2.1: Recipe for making NGM agar.

Reagents	**For 100ml of dH_2O**
Agar	1.7g
NaCl	0.3g
Peptone	0.25g
Autoclave	
1M $CaCl_2$	100µl
1M $MgSO_4$	100µl
1M KPO_4	2.5ml
Cholesterol (5mg/ml in Ethanol)	100µl
Nystatin (10mg/ml in DMSO) (N6261)	100µl
FuDR (150mM)	33µl (lifespan assay plates only)

10ml of NGM agar was poured into each 55mm plate and allowed to solidify and dry at room temperature overnight. Once dry, NGM plates were seeded with 200µl of *Escherichia Coli* (*E. coli*) OP50 strain (CGC) and *E. coli* was allowed to dry on the plate at room temperature. OP50

cultures were seeded from a single colony grown in LB broth overnight at 37°C in a shaking incubator. *C. elegans* strains were maintained in an incubator (RLSD01502; LabCold) at 20°C unless stated otherwise. Strains were viewed using a stereomicroscope (Motic SMZ-171T) and were handled using a flame sterilised platinum worm pick (#59-AWP; WormStuff, Genesee Scientific).

2.2.2 *C. elegans* lifespan assays

NGM plates used for lifespan assays were additionally supplemented with 50μM (33μl of 150mM in 100ml of NGM agar) of 5-Fluoro-2'-deoxyuridine (FuDR; F10705-1.0; Melford Laboratories) to prevent growth of unwanted offspring. Lifespan assays were conducted on a population of synchronised worms. Adult worms (containing eggs) were placed into a drop (~10μl) of alkaline hypochlorite solution (250μl of dH_2O, 230μl of sodium hypochlorite and 30μl of 10M NaOH) on the NGM plate. The solution killed the worms, causing eggs to be released. Hatching occurs simultaneously resulting in a synchronised population. Offspring were grown and at least 50 L4 stage worms were transferred onto new NGM plates containing FuDR for lifespan assays. Worms were transferred onto new plates weekly but more frequently if the seeded OP50 had become depleted, if plates had any unwanted bacterial or fungal contamination or showed desiccation. Day 0 is considered as the first day of adulthood and time points for events (death or censorship) were marked almost daily (Figure 2.1). Total number of dead and censored worms and total number of trials for all experiments in chapters 3.0, 4.0 and 5.0 is shown in Appendix 8.1 (Table 8.1a, 8.1b and 8.1c respectively).

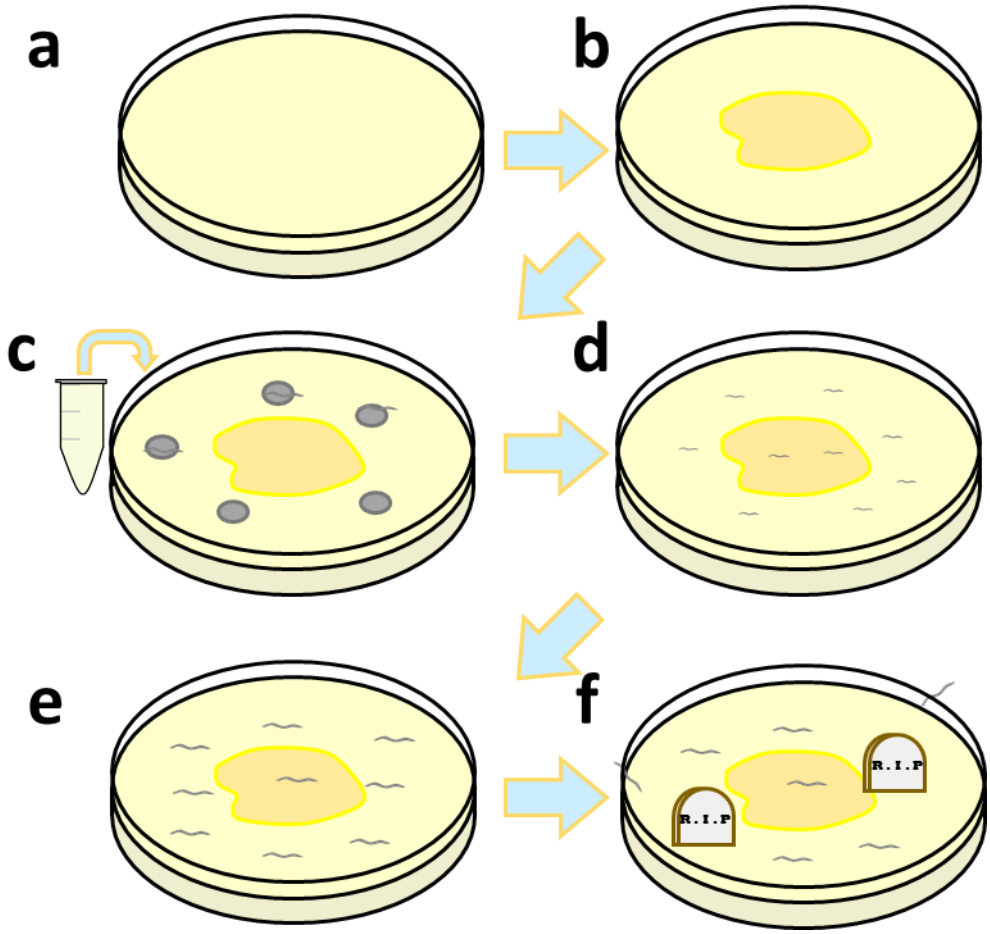

Figure 2.1: Workflow for setting up a lifespan assay, **(a)** NGM agar plates are made and **(b)** seeded with *E. coli*. **(c)** Droplets of alkaline hypochlorite solution is spotted onto the plate and adult worms containing eggs are placed in the solution to release the eggs. **(d)** This generates a synchronised population which can then be **(e)** transferred onto an experimental (treatment) plate and lifespan can be **(f)** measured as alive, dead or censored.

Worms were classified into 3 categories at each measured time point: alive, dead or censored. They were classified as alive if any movement is observed. If no movement is observed the agar surrounding the worm is tapped with the sterile worm pick. If still no movement is observed, then the head of the worm is gently tapped with the worm pick to elicit a physical response. If after this there is still no response the worms are classified as dead and are removed from the plate. Worms can also be classified as censored from the experiment if a final time of death is unable to be determined. Censorship of worms occurs if worms do not naturally die from old age. Some examples where censorship would occur are internal hatching of eggs (bagging), bacterial or fungal contamination, vulval protrusion and rupturing or death

due to worms crawling off of the agar. Although worms are censored from lifespan experiments they are still included for statistical analyses.

2.2.3 *C. elegans* lifespan assays from digital recording

Flatbed photo scanners were used for some lifespan assays where manual counting assays could not be conducted (for example in hypoxic environments). Use of flatbed scanners to conduct automated lifespan measurements such as with the 'automated wormscan' (Mathew et al., 2012) and 'the *C. elegans* lifespan machine' (Stroustrup et al., 2013) inspired the use of flatbed photo scanners for acquisition of photos. The Epson Perfection V800 Photo Scanner was used to scan the agar plates (up to 12 at a time) at least twice daily to generate high resolution images of all plates (Figure 2.2). Once images were acquired the individual plates were analysed manually by comparing images taken. If worms had moved position then they were classified as alive, had they not moved they were classified as dead. Additionally, missing worms (crawled off the plate) were classified as censored along with worms which were seen to have had internal hatching of eggs (bagging), bacterial or fungal contamination, vulval protrusion and rupturing.

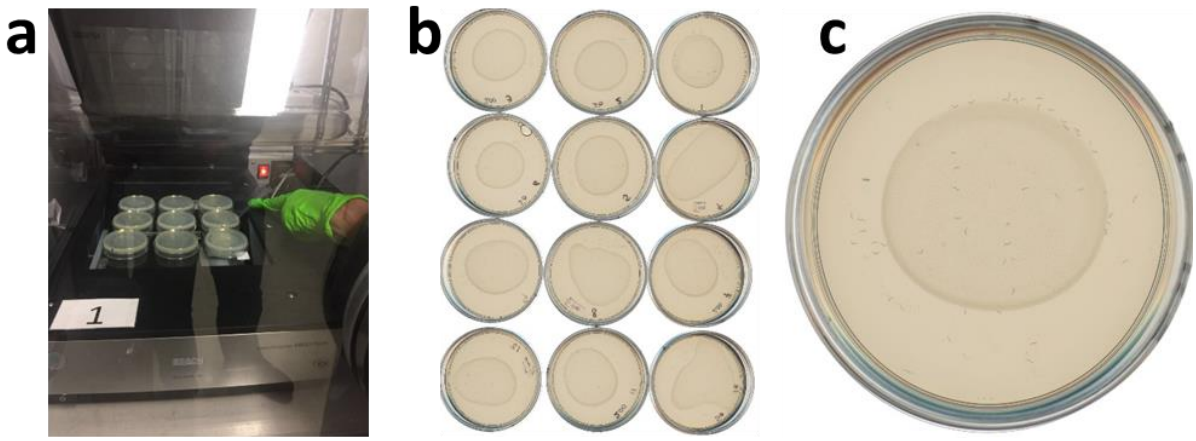

Figure 2.2: Digital lifespan recording. **(a)** Loading plates onto scanners. **(b)** Representative scan of 12 plates. **(c)** Representative scan of a single plate zoomed in.

2.2.4 *C. elegans* treatments

2.2.4.1 Temperature Intervention

In temperature intervention studies, *C. elegans* (L4 stage) were incubated at an initial temperature (either 15°C or 25°C) for a certain time period of their lifetime and then incubated at the alternative temperature (25°C or 15°C) for the remaining length of their lifetime. *C. elegans* N2 and *trpa-1(ok999)* strains were used in switching experiments. Temperature switching was conducted by transferring worms between incubators pre-set at either 15°C or 25°C.

2.2.4.2 Pharmacological Intervention

Pharmacological intervention was used to influence lifespan of *C. elegans* to identify how drugs affect the lifespan of worms, specific populations and parameters. In these studies, the pharmacological intervention occurred from day 0 (synchronised worms at L4 stage) for the entire adult lifetime, until death.

2.2.4.2.1 Carvacrol

Carvacrol (Figure 2.3; 282197) is a monoterpene phenol found in Oregano and other aromatic plants and is known to have antibacterial properties (Xu et al., 2006). However, it also acts as an activator of human TRPA1 and TRPV3 ion channels. It has previously been shown to allow Ca^{2+} ion entry into cells. Carvacrol (0mM, 50mM, 200mM and 500mM; Solvent: DMSO; Control) was added to melted NGM agar before pouring into 55mm plates culture plate.

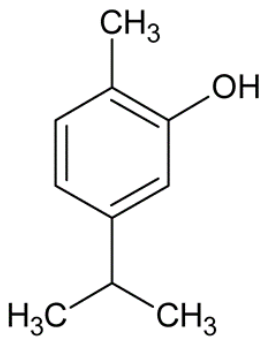

Figure 2.3: Molecular structure of carvacrol

2.2.4.3 Hypoxia

C. elegans (L4) were exposed to hypoxia (1% O_2, 99% N_2) by placing them inside the hypoxia O_2 Control InVitro Glove Box (Coy Laboratories). Temperature was regulated using a climate control system in the room to an average temperature of 20°C. As previously mentioned (section 2.2.3), a flatbed photo scanner (EPSON V800) was used to take images of worms in the hypoxia chamber to generate survival curves.

2.3 *Drosophila* lifespan assay

Control w^{Dah} was derived by backcrossing w^{1118} into the outbred wild type *Dahomey* background. The *dfoxo*Δ flies were previously described (Slack et al., 2011). Flies were raised and maintained on standard sugar/yeast medium (Bass et al., 2007). Lifespan experiments were conducted at 25°C on a 12:12 hours light/dark cycle at constant humidity. Flies were reared at standard density, allowed to mate for 24 h, sorted by sex, and then transferred to experimental vials at a density of ten flies per vial. Approximately 100 flies were used per experimental replicate. Flies were transferred to fresh vials three times a week, and deaths were scored during transferral. Drosophila experiments were conducted by Cathy Slack at Aston University, UK.

2.4 Honey bee lifespan assay

Lifespan data of caged and hived (free flying) bees originated from two independent studies (Woyciechowski and Moron, 2009, Kuszewska et al., In preparation). One part of newly emerged workers from each colony was placed in a wood-frame cage (51-100 bees) kept in an incubator (34-36°C). The bees were provided with a small piece of honeycomb and 50% sucrose solution and water *ad libitum*. The cages were checked every day and dead bees were counted. The second part of newly emerged workers (59 - 100 bees) were marked individually on the thorax and returned to their native colonies. The colonies were checked daily (depending on weather conditions) and the alive bees were counted every 3-4 days (Kuszewska et al., In preparation). Honey bee experiments were conducted by Karolina Kuszewska and Michał Woyciechowski at Jagiellonian University, Poland.

2.5 Rapamycin effect on mouse lifespan

Published data for rapamycin intervention in the mouse was kindly provided by the National Institute on Aging (NIA) Interventions Testing Program (ITP) (Miller et al., 2014). Rapamycin concentration used was 42ppm (42mg rapamycin per kg of food).

2.6 Survival curve analysis

From the survival data generated by measuring alive, dead and censored worms Kaplan-Meier survival curves were constructed by inputting events at measured time points into GraphPad Prism 7.0 (GraphPad Software). Time points were inputted as days and events are encoded as per the software's input requirements with death encoded as 1 and censorship as 0. Survival proportions at each time point was calculated by the software. A log-rank (Mantel-Cox) test was conducted to statistically compare differences between two curves.

2.6.1 Average lifespan and Median Survival

Average lifespan was calculated by finding the average time of death for a population (sum of when worms die divided by the total number of worms that die). Average lifespan can be calculated for a whole population for their entire lifespan or for the worms remaining post treatment. This is equal to the integral of the survival curve. The median survival of a population is the time point at which 50% of a population is remaining.

2.6.2 Curve fitting

Non-linear regression models which were based on logistic functions were used to fit curves to the survival proportions. The MATLAB (MathWorks) Curve fitting toolbox (R2016a, v9.0.0.370719) and sfit objects were used to fit data using a non-linear least squared fit method (Trust-Region algorithm) to estimate parameters. When fitting the survival data, other settings were kept to default: Robust=Off, DiffMinChange=0.00000001, DiffMaxChange=0.1, MaxFunEvals=600, MaxIter=400, TolFun=0.000001, TolX=0.000001.

2.6.3 Novel 5-parameter Bilogistic model and reduced versions

A number of models were used to fit survival data. A novel 5-parameter Bilogistic model was constructed to be able to fit both biphasic and monophasic data (Equation 1). The *f* parameter

splits the curve into two phases giving a weighting to each phase. The two phases correspond to an early phase and late phase of death. There are two death rates (deaths per day), k_1 and k_2 (one for each phase), and two time parameters, t_1 and t_2, representing the median survival for each phase (Figure 2.4). 3 variants of the Bilogistic model were also constructed to reduce the model to 4 parameters: 1) the two death rates were the same ($k_1 = k_2$); 2) the two phases had equal weight ($f = 0.5$); 3) only one phase existed ($f = 0$). Additionally, the model was further reduced to 3 parameters with there being 2 variants: 1) where the two phases had equal weighting and the two death rates were the same ($f = 0.5$ & $k_1 = k_2$); 2) where the weighting between the two phases was fixed to an average of previously calculated *f*'s for the realisations used and the two death rates were the same (f = average & $k_1 = k_2$). The terms in the numerator ensure that for $t = 0$ the pre-factor of the function is N_0, which is typically rescaled in each experiment to be 100%.

The first derivative of the 5-parameter model is proportional to the hazard for each population over time (Equation 2).

$$N(t) = N_0 \left[f \frac{1 + e^{-k_1 t_1}}{1 + e^{k_1 (t - t_1)}} + (1 - f) \frac{1 + e^{-k_2 t_2}}{1 + e^{k_2 (t - t_2)}} \right]$$

Equation 1: Bilogistic 5-parameter model.

$$\frac{dN}{dt} = N_0 \left[\frac{f k_1 (e^{-k_1 t_1} + 1) e^{k_1 (t - t_1)}}{(1 + e^{k_1 (t - t_1)})^2} + \frac{(1 - f) k_2 (e^{-k_2 t_2} + 1) e^{k_2 (t - t_2)}}{(1 + e^{k_2 (t - t_2)})^2} \right]$$

Equation 2: First derivative of the Bilogistic model.

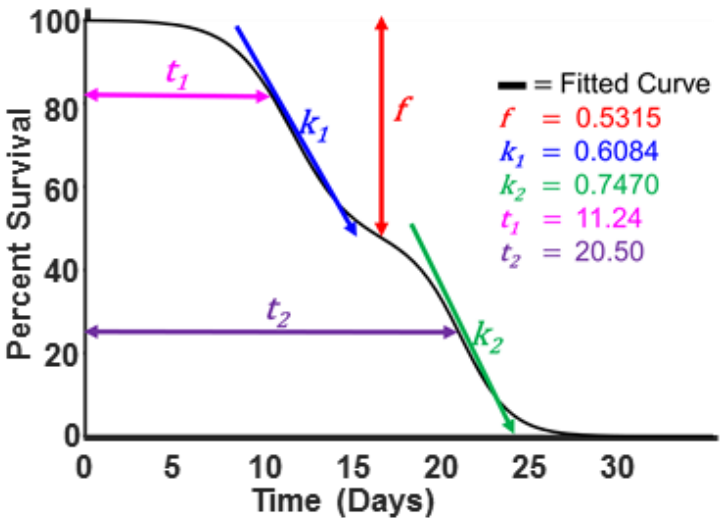

Figure 2.4: Example of curve fitting and parameter (f, k_1, k_2, t_1, t_2) estimation for a survival curve using our Bilogistic model

2.6.4 Other sigmoidal models

The six other models which have been previously been used to characterise survival data were: Whiting-Buchanan Model (Equation 3; (Whiting and Buchanan, 1993)), Gompertz-Makeham (Equation 4; (Makeham, 1860, Gompertz, 1825) Logistic Model (Equation 5; (Pletcher et al., 2000)), Wilson's 2-parameter Model (Equation 6; (Wilson, 1994)), Weibull Model (Equation 7; (Weibull, 1951)) and Gompertz Model (Equation 8; (Gompertz, 1825)). For all models containing an f parameter it is bound between 0 and 1. Additionally, both death rates (k_i) and time parameters (t_i) were bound to being positive values and the t_1 value was always lower than t_2.

$$N(t) = N_0\left[f\frac{1+e^{-k_1 t_{lag}}}{1+e^{k_1(t-t_{lag})}} + (1-f)\frac{1+e^{-k_2 t_{lag}}}{1+e^{k_2(t-t_{lag})}}\right]$$

Equation 3: Whiting-Buchanan Model

$$N(t) = N_0(e^{-ct-\frac{a}{b}(e^{(bt)}-1)})$$

Equation 4: Gompertz-Makeham Model

$$N(t) = \frac{N_0}{1+e^{\frac{t-t_{lag}}{k}}}$$

Equation 5: Logistic Model

$$N(t) = \frac{N_0}{1 + \left(\frac{t}{t_{lag}}\right)^k}$$

Equation 6: Wilson Model

$$N(t) = N_0 \left(e^{-(at)^b}\right)$$

Equation 7: Weibull Model

$$N(t) = N_0 \left(e^{-\frac{a}{b}(e^{(bt)}-1)}\right)$$

Equation 8: Gompertz Model

2.6.5 Curve fitting statistical analysis

After parameters were obtained statistical analysis was conducted. GraphPad Prism was used to perform an ordinary two-way Analysis of Variance (ANOVA), with all groups compared to one another (non-repeated measure). After average lifetime values were obtained statistical analysis was conducted. GraphPad Prism was used to perform an ordinary one-way Analysis of Variance (ANOVA), with all groups compared to one another (non-repeated measure). In conjunction to this ANOVA, Tukey's multiple comparison test was also conducted. Statistical *p*-values $p<0.05$, $p<0.01$, $p<0.001$ and $p<0.0001$ shows a statistically significant difference between groups and is indicated in the figures.

2.7 Goodness of Fit and model comparison

2.7.1 Root Mean Square Error

The root mean square error (RMSE) was used for the goodness of fit statistical analysis of the different models using MATLAB (MathWorks, R2016a, v9.0.0.370719). It represents the model performance accuracy taking in to account the number of data points and parameters and applying a penalty to models with higher parameters so that simplest model with the best fit is shown. Fitted models with lower RMSE values indicate a better fit. The statistical significance between two groups was examined using two-way analysis of variance (ANOVA) followed by Tukey's multiple comparison tests using GraphPad Prism. Statistical *p*-values $p<0.05$, $p<0.01$,

$p<0.001$ and $p<0.0001$ shows a statistically significant difference between groups and is indicated in the figures.

2.7.2 Residual Analysis

Another method used to analyse goodness of fit of the models was to look at residuals. Residual differences between experimental lifespan data points and fitted model curves were calculated for each data set. Residual differences for each experimental realisation in a single data set was collated into one set which then underwent a data binning procedure to smooth the data. Data bin sizes were considered and grouped based upon the species, number of experimental realisations, number of residual data points per day and total length of lifespan; in *C. elegans*, the data bin sizes were 2, 3 and 4 days. Residual plots which show the smallest residual error without universal deviations throughout the lifespan indicate best overall fit.

2.8 Cell culture

Mammalian cell culture experiments were conducted to support whole organism experiments to investigate specific mechanisms of signalling between hypoxia and temperature pathways. Using *in vitro* studies in conjunction with *in vivo* studies, allows for comparison and identification of pathways which are organism specific and those which are conserved.

2.8.1 Plasmid cloning

Plasmid constructs used are pHRE-MP-GLuc HIF responsive plasmid DNA (Cavadas and Cheong, 2014) and pcDNA3.1/neo(+)-human TRPA1 plasmid DNA kindly provided as a gift from Katsuhiko Muraki at Aichi Gakuin University, Japan (Hatano et al., 2012). Plasmid constructs were transformed into α-Select Bronze Competent Cells (BIO-85025; Bioline Reagents) using the heat shock method. 1ng of plasmid construct was mixed with 50μl α-Select Bronze Competent Cells and stored on ice for 30 minutes. This was then transferred to 42°C for 50 seconds and placed on ice for 2 minutes. 100μl of LB was added to the plasmid-cell mix and incubated at 37°C for one hour with shaking. The culture was spread onto a LB agar plate supplemented with 100μg/ml of Ampicillin (A9518) and incubated at 37°C overnight. The following day single colonies were identified and selected. Selected colonies were used

to inoculate LB (w/ 100μg Ampicillin) and incubated overnight at 37°C with shaking. Plasmid DNA was purified using the Pureyield Plasmid Midiprep System (A2492; Promega) using vacuum DNA purification and elution by centrifugation as per the standard protocol. DNA concentration was quantified using the NanoDrop spectrophotometer (Thermo Fisher Scientific).

2.8.2 Mammalian Cell Growth and Maintenance

All cell culture methods were carried out in a Microflow class II advanced biological safety cabinet (Bioquell) with aseptic technique to ensure sterile conditions.

2.8.2.1 HEK-293 cell culture

Human embryonic kidney cells (HEK-293) are a human cell line derived from an aborted foetus in 1977 containing a transformed sheared adenovirus 5 (Graham et al., 1977). It is widely used due to its ease of growth and transfection capability.

HEK-293 cells were cultured in 75cm^2 flasks with Dulbecco's modified Eagle Medium (1x DMEM) with 4.5g/l of D-Glucose, 4mM L-glutamine and 1mM Pyruvate (41966-029; Gibco Life Technologies). It was additionally supplemented with 10% Foetal Bovine Serum (FBS; 10500-064; Gibco Life Technologies) and 5% Penicillin-Streptomycin (P4333).

When adherent HEK-293 cells reached 70-80% confluence they were passaged using Trypsin-EDTA 10x solution (T4174) and re-seeded into new flasks at the desired concentration. Growth media was replaced every 72 hours until cells required further passage. Cells were maintained in a CO_2 incubator at 37°C in an atmosphere of 5% CO_2/ 95% air.

2.8.2.2 HepG2 cell culture

HepG2 is a human liver hepatocellular carcinoma isolated from a 15 year old Caucasian male (Aden et al., 1980).

HepG2 cells were cultured in 75cm^2 flasks with RPMI-1640 with 1mM (0.3g/l) L-glutamine and Sodium Bicarbonate (2g/L) (R8758). It was additionally supplemented with 10% Foetal Bovine Serum (FBS) and 5% Penicillin-Streptomycin. When adherent HepG2 cells reached 70-80%

confluence they were passaged using Trypsin-EDTA 10x solution and re-seeded into new flasks at the desired concentration. Growth media was replaced every 72 hours until cells required further passage. Cell were maintained in a CO_2 incubator at 37°C in an atmosphere of 5% CO_2/ 95% air.

2.8.3 Seeding of mammalian cells

Cells were detached from the flask using Trypsin-EDTA 10x solution and suspended in DMEM and then counted using a haemocytometer. 50, 000 cells were seeded in a 24 well plate with 500µl of media. Cells were incubated at 37°C in 5% CO_2/ 95% air for 24 hours to allow for cell adherence to the well and proliferation.

2.8.4 Transient Transfection

A calcium phosphate co-precipitation methodology (Chen, 2012) was used for transient transfection of cells.

Two solutions were prepared prior to the transfection, solution A and solution B (Table 2.2).

Table 2.2: Recipe for Calcium Phosphate Co-precipitation solutions A and B.

Solution	**Description**	**Typical volume for 24 well plate**
Solution A	2M $CaCl_2$ (12.2µl per 1-5µg of plasmid DNA; filter sterilised) Plasmid DNA (200ng per well) dH_2O	12.2µl 2400ng Make up to 120µl
Solution B	2X HEPES buffered Saline (HBS) (50mM HEPES (H-3375), 280mM NaCl, 1.5mM Na_2HPO_4 dissolved in H_2O; pH 7.0, filter sterilised)	120 µl

Solution A was added to solution B whilst mixing and was incubated for 10 minutes at room temperature. After incubation 10μl of the total solution was added to cells in each well. Cells were incubated at 37°C in 5% CO_2/95% air for 48 hours.

2.8.5 Treatments

24 hours post transfection, the 500μl of growth media was replaced with fresh media and then treated using a number of different conditions. Treatment of cells usually lasted 24 hours.

2.8.5.1 Hypoxia

Cells were exposed to hypoxic conditions (1% O_2, 94% N_2, 5% CO_2) in a hypoxia O_2 Control InVitro Glove Box (Coy laboratories) and growth media used in treatments was pre-exposed to hypoxia for at least 16 hours before application to cells.

2.8.5.2 Carvacrol

A dose response treatment with carvacrol was also conducted to show the effect of increasing carvacrol concentration on HIF using doses at 5μM, 20μM, 50μM, 200μM and 500μM.

2.9 Gaussia Luciferase assay

Gaussia luciferase acts as a secreted bioluminescent reporter which is then able to quantify the genetic plasmid construct (Figure 2.5) (Cavadas and Cheong, 2014). The pHRE-MP-GLuc HIF plasmid construct was used by which HIF activity was measured. 10μl of conditioned media was collected 24 hours post-treatment and transferred into an opaque 96-well plate. 2.5mM coelenterazine (#303; Nanolight) was diluted in PBS to 100μM. 50μl of 100μM coelenterazine was added to aliquoted media in each well and was read on a SpectraMax Gemini EM Microplate Reader (Molecular Devices) at the ambient temperature. The SoftMax Pro Software (v5.0) was used to configure the plate reading settings: Top read, Luminescence, Emission: Lm1 461nm, Reads/Well: 6.

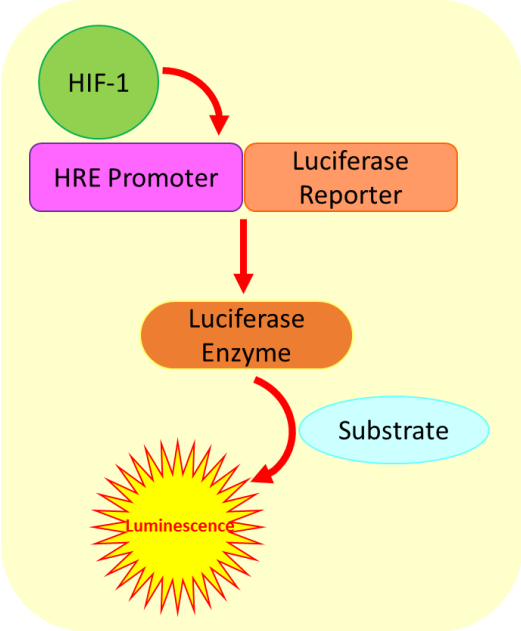

Figure 2.5: Mechanism by Gaussia Luciferase acts as a reporter for HIF activity. The luciferase enzyme is encoded and secreted after HIF binds the HRE promoter. Coelenterazine acts as a substrate which the luciferase enzyme catalyses to produce luminescence.

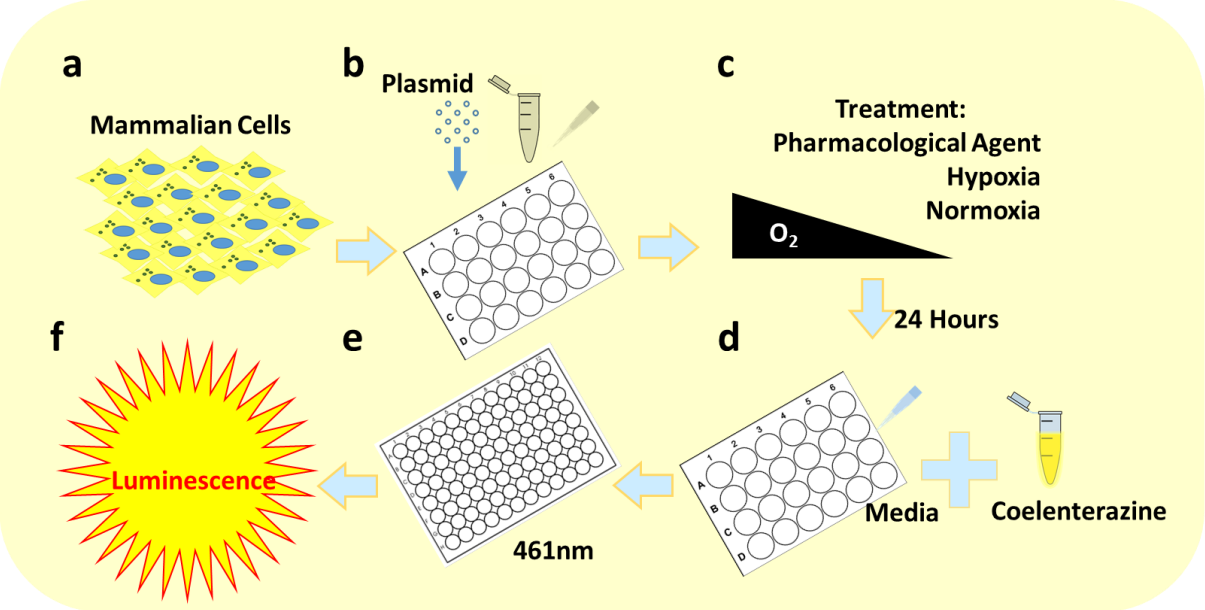

Figure 2.6: Workflow of the Gaussia Luciferase assay. **(a)** Mammalian cells are seeded, **(b)** transfected and **(c)** treated **(d)** media is collected and **(e)** the substrate coelenterazine is added to a 96-well plate and **(f)** luminescence was measured on a plate reader.

2.9.1 Statistical Analysis

Average (relative) luminescence for individual treatments in the Gaussia Luciferase assay was calculated (±SEM) using GraphPad. An Ordinary One-Way ANOVA with Tukey's multiple comparisons test was used to compare individual treatments in the Gaussia Luciferase assay. Statistical *p*-values $p<0.05$, $p<0.01$, $p<0.001$ and $p<0.0001$ shows a statistically significant difference between groups and is indicated in the figures.

Chapter 3.0: Biphasic lifespan dynamics in multiple organisms

3.1 Preface

Ageing research has focused on identifying lifespan modifiers, but a major challenge lies in understanding and appropriately interpreting their effects. The shape of the survival curve reveals crucial information on the mechanism of action. In this chapter, a novel Bilogistic model is introduced to describe and quantify lifespan data which can be applied to a range of standard animal models. The novel Bilogistic model provides a better fit to the experimental data than existing models such as the Gompertz-Makeham model and reveals the existence of two distinct sub-populations corresponding to two phases in the survival pattern in worms, flies, bees and mice. The model parameters account for the death rates for short-lived and long-lived subpopulations, enabling statistical analysis of intra- and inter-group variance. Thus, the Bilogistic model can provide a rational statistical analysis of lifespan modifiers such as temperature, daf-16/FOXO mutation and rapamycin, on each phase, and establishes that biphasic survival dynamics is widespread across different organisms.

3.2 Introduction

Today, many societies face the challenge of a rapidly ageing population with associated health problems and an increase in healthcare expenses. A crucial step towards our understanding of ageing is the identification and characterisation of lifespan modifiers in animal models such as worms, flies or mice. Common lifespan modifiers which have been investigated are temperature (Klass, 1977), diet (Colman et al., 2014), pharmacological interventions (Miller et al., 2014) and genetic pathways (Kenyon et al., 1993).

The most common method for testing a potential lifespan modifier is to carry out lifespan assays and use the non-parametric Kaplan-Meier estimator to determine lifespan and probability of survival in a given length of time (Goel et al., 2010). The Kaplan-Meier estimator is often coupled with the log-rank statistical test, which tests the null hypothesis that there is no statistically significant difference between the control and test group (Goel et al., 2010). This allows qualitative comparison between the two groups (i.e. tests if the two groups are different), but it is not possible to statistically compare experimental or biological replicates. Crucially, as it is only a significance test comparing two curves, it is unable to identify where differences may occur. Survival curves can be one of three types (Type 1, 2 and 3). Type-1 curves have lower mortality early on and greater mortality in later life. Type-2 curves show a consistent mortality throughout the lifespan. Type-3 curves show greater mortality early in life and lower mortality later on in life (Deevey, 1947).

An alternative is to perform parametric modelling of the data by fitting a mathematical function to the survival curve. Common distributions for lifespan data are the logistic and exponential distributions (Lawless, 2014). Two-parameter sigmoidal functions such as the logistic (Pletcher et al., 2000), Weibull (Weibull, 1951) or Gompertz (Gompertz, 1825) models fit lifespan data. Simple logistic functions often have a death rate and time lag parameters, or parameters which define the shape and scale of the curve. With these logistic functions it is possible to fit data points which follow a typical sigmoidal shape where there is a shoulder, an exponential but monotonic decrease and then a tailing (Lawless, 2014, Xiong et al., 1999). However, these models often do not adequately fit all experimental data, as it has been previously shown that

not all lifespan curves show a simple monotonic decrease. For example, in *C. elegans* lifespan, it has recently been shown that there are short lived and long-lived worms which make up the population therefore reinforcing the fact that lifespan curves are likely to show small differences in death rates and time points within the survival curve resulting in shapes which are different to the standard monotonic decrease. (Zhang et al., 2016, Zhao et al., 2017). As is often done in parametric modelling by fitting the common logistic curves such as Gompertz and Weibull, there is an over-smoothing of the curves which leads to unintentionally discarding features which make up the lifespan curve. Therefore, to prevent this over-smoothing of experimental data, a novel parametric model is required, which is able to better model many different variations of survival curves whether they show a monotonic or biphasic decrease in lifespan and whether the rate of change is high or low or time lags are different at different points in the survival curve.

3.2.1 Aims and Objectives

This chapter aims to:

1) Introduce a novel parametric model which describes and distinguishes two phases within the survival curve of a population, each with its own death rate and median survival.
2) Examine differences between existing models and how well they fit experimental data and show that this novel model provides a significantly better fit of experimental data compared to the other existing models.
3) Show that this novel model can be applied to fit a variety of different animal models, suggesting that a biphasic dynamism in the lifespan can be a general property of ageing populations.
4) Explore how this model can statistically compare experimental data and replicates to quantitatively measure the effects of lifespan modifiers from experimental replicates to reveal new features in the survival curve.

3.3 Materials and Methods

3.3.1 *C. elegans* lifespan assay

The *C. elegans* strains N2 (wild isolate), and *daf-16*(*mu86*) were acquired from the Caenorhabditis Genetics Center (CGC), University of Minnesota. All strains were maintained on solid nematode growth media (NGM) plates at 20°C unless stated otherwise and supplemented with nystatin (10 µg/ml) and seeded with *E. coli* OP50 strain.

NGM plates used for lifespan assays were supplemented with 5-fluoro-2'-deoxyuridine (FuDR) (50µM) to prevent growth of unwanted offspring. Lifespan assays were conducted on a population of worms synchronised by alkaline hypocholorite treatment. Once synchronised, 50 L4 stage worms were transferred onto fresh NGM FuDR plates for the start of the experiment. Worms were transferred onto fresh plates weekly, but more frequently if the seeded OP50 was depleted or in cases of unwanted bacterial or fungal contamination. Day 0 is considered as the first day of adulthood and time points for events (death or censorship) were marked almost daily. Worms were classified into 3 categories at each time point: alive, dead or censored. DR

3.3.2 Drosophila lifespan assay

Control w^{Dah} was derived by backcrossing w^{1118} into the outbred wild type *Dahomey* background. The *dfoxo*Δ flies were previously described (Slack et al., 2011). Flies were raised and maintained on standard sugar/yeast medium (Bass et al., 2007). Lifespan experiments were conducted at 25°C on a 12:12 hours light/dark cycle at constant humidity. Flies were reared at standard density, allowed to mate for 24 h, sorted by sex, and then transferred to experimental vials at a density of ten flies per vial. Approximately 100 flies were used per experimental replicate. Flies were transferred to fresh vials three times a week, and deaths were scored during transferral.

3.3.4 Honey bee lifespan assay

Lifespan data of caged and hived (free flying) bees originated from two independent studies (Woyciechowski and Moron, 2009, Kuszewska et al., In preparation). One part of newly emerged workers from each colony was placed in a wood-frame cage (51-100 bees) kept in

an incubator (34 - 36°C). The bees were provided with a small piece of honeycomb and 50% sucrose solution and water ad libitum. The cages were checked every day and dead bees were counted. The second part of newly emerged workers (59-100 bees) were marked individually on the thorax and returned to their native colonies. The colonies were checked every day or every 3-4 day (depending on weather conditions) and the alive bees were counted (Kuszewska et al., In preparation).

3.3.5 Rapamycin effect on mouse lifespan

Data from the rapamycin intervention in the mouse was kindly provided by the National Institute on Ageing (NIA) Interventions Testing Program (ITP) (Miller et al., 2014). Rapamycin concentration used was 42ppm (42mg rapamycin per kg of food).

3.3.6 Survival curve analysis

Kaplan-Meier survival curves were constructed by inputting events occurring at given time points into GraphPad Prism 7. Survival proportions at each time point were calculated and a log-rank (Mantel-Cox) test was conducted to statistically compare differences between two curves.

3.3.7 Lifespan models

A novel Bilogistic model with 5 parameters capable of fitting biphasic data was constructed (Equation 1). The f parameter splits the curve into two phases giving a weighting to each phase. There are two death rates k_1 and k_2 and two time parameters t_1 and t_2, representing the median survival for each phase. Simpler variants of this model with fewer parameters were also constructed where the two death rates were the same ($k_1 = k_2$), the two phases had equal weight ($f = 0.5$), or there existed only one phase ($f = 0$). The terms in the numerator make sure that for $t = 0$ the pre-factor of the function is N_0, which is typically rescaled in each experiment to be 100%. The first derivative of the Bilogistic 5-parameter model is proportional to the hazard for each subpopulation over time (Equation 2).

$$N(t) = N_0\left[f\frac{1+e^{-k_1 t_1}}{1+e^{k_1(t-t_1)}} + (1-f)\frac{1+e^{-k_2 t_2}}{1+e^{k_2(t-t_2)}}\right]$$

Equation 1: Bilogistic 5-parameter model

$$\frac{dN}{dt} = N_0\left[\frac{fk_1(e^{-k_1 t_1}+1)e^{k_1(t-t_1)}}{(1+e^{k_1(t-t_1)})^2} + \frac{(1-f)k_2(e^{-k_2 t_2}+1)e^{k_2(t-t_2)}}{(1+e^{k_2(t-t_2)})^2}\right]$$

Equation 2: First derivative of the Bilogistic model

The six other models which have been previously been used to characterise survival data were: Whiting-Buchanan Model (Equation 3; (Whiting and Buchanan, 1993)), Gompertz-Makeham (Equation 4; (Makeham, 1860, Gompertz, 1825) Logistic Model (Equation 5; (Pletcher et al., 2000)), Wilsons' 2-parameter Model (Equation 6; (Wilson, 1994)), Weibull Model (Equation 7; (Weibull, 1951)) and Gompertz Model (Equation 8; (Gompertz, 1825)).

$$N(t) = N_0\left[f\frac{1+e^{-k_1 t_{lag}}}{1+e^{k_1(t-t_{lag})}} + (1-f)\frac{1+e^{-k_2 t_{lag}}}{1+e^{k_2(t-t_{lag})}}\right]$$

Equation 3: Whiting-Buchanan Model

$$N(t) = N_0(e^{-ct-\frac{a}{b}(e^{(bt)}-1)})$$

Equation 4: Gompertz-Makeham Model

$$N(t) = \frac{N_0}{1+e^{\frac{t-t_{lag}}{k}}}$$

Equation 5: Logistic Model

$$N(t) = \frac{N_0}{1+\left(\frac{t}{t_{lag}}\right)^k}$$

Equation 6: Wilson Model

$$N(t) = N_0\left(e^{-(at)^b}\right)$$

Equation 7: Weibull Model

$$N(t) = N_0\left(e^{-\frac{a}{b}(e^{(bt)}-1)}\right)$$

Equation 8: Gompertz Model

The MATLAB (MathWorks) curve fitting toolbox (R2016a, v9.0.0.370719) was used to fit data using a non-linear least squared fit method (Trust-Region algorithm) to estimate parameters.

All models can be used in common statistical analysis packages, such as GraphPad Prism 7 for curve fitting (nonlinear regression), parameter estimation and goodness-of-fit tests including residual analysis and RMSE.

3.3.8 Residual analysis

Residual analysis was conducted to identify how well each model fits experimental data points for each data set. This method is an indicator of goodness of fit and allows for the comparison of the different models. Residual differences for each experimental realisation in a single data set was collated into a single set. This data was smoothed by a data binning procedure. Data bin sizes was dependent on the species, number of experimental realisations, number of residual data points per day and total length of lifespan. Residual plots which show the smallest errors or deviations throughout the lifespan indicate the best overall fit.

3.3.9 Root mean square error

The root mean square error (RMSE) was used for the goodness of fit statistical analysis of the different models using MATLAB (MathWorks, R2016a, v9.0.0.370719). It represents the model performance and lower values of RMSE indicate better fit. The statistical significance between two groups was examined using two-way analysis of variance (ANOVA) followed by Tukey's multiple comparison tests using GraphPad Prism 7. Statistical p-values $p<0.05$, $p<0.01$, $p<0.001$ and $p<0.0001$ shows a statistically significant difference between groups and is indicated in the figures.

3.4 Results

3.4.1 Modelling the effect of temperature on *C. elegans*

The nematode worm *C. elegans* is a commonly used organism for studying lifespan. As previously described (section 1.4), cooler temperatures extend the lifespan of the worm and hotter temperatures shorten it (Klass, 1977). In this study, the lifespan curves in response to four temperatures (15°C - 30°C; Figure 3.1a) were used to model the effect of temperature on *C. elegans* survival. A novel Bilogistic model (Equation 1) was constructed to fit biphasic lifespan curves which was observed from the experimental data (Figure 3.1a). The parameters of this Bilogistic model are as follows: the *f* value (which denotes the weighting or proportion of the two phases), the death rates k_1 and k_2 and median survival times t_1 and t_2 for each of the phases (Figure 2.4). The Bilogistic model was used to fit the lifespan data points (Figure 3.1b) and visually, it was able to capture both monophasic and biphasic dynamics of all of the lifespan curves.

The first derivative of the fitted curves is proportional to the hazard of death for each of the phases over time (Equation 2). The phases represent a short-lived (1st phase) and a long-lived subpopulation (2nd phase). Increasing the temperature increased the hazard of both phases (Figure 3.1c, d). Changes to parameters due to temperatures were also investigated. Increasing temperature did not affect the proportion of each phase (the *f* value; Figure 3.1e) but showed a significantly reduced the median survival of both phases (t_1 and t_2; Figure 3.1f). Furthermore, the significant difference between t_1 and t_2 at 15°C and 20°C revealed the two distinct phases. With higher temperatures an increase in the rate of death in the 2nd phase although not statistically significant was seen, i.e. the long-lived subgroup died faster (k_2; Figure 3.1g) and the larger number of deaths in the 1st phase masked the 2nd phase, resulting in overlapping phases (Figure 3.1c, d, f, g). In such cases the separation of phases has to be interpreted with caution.

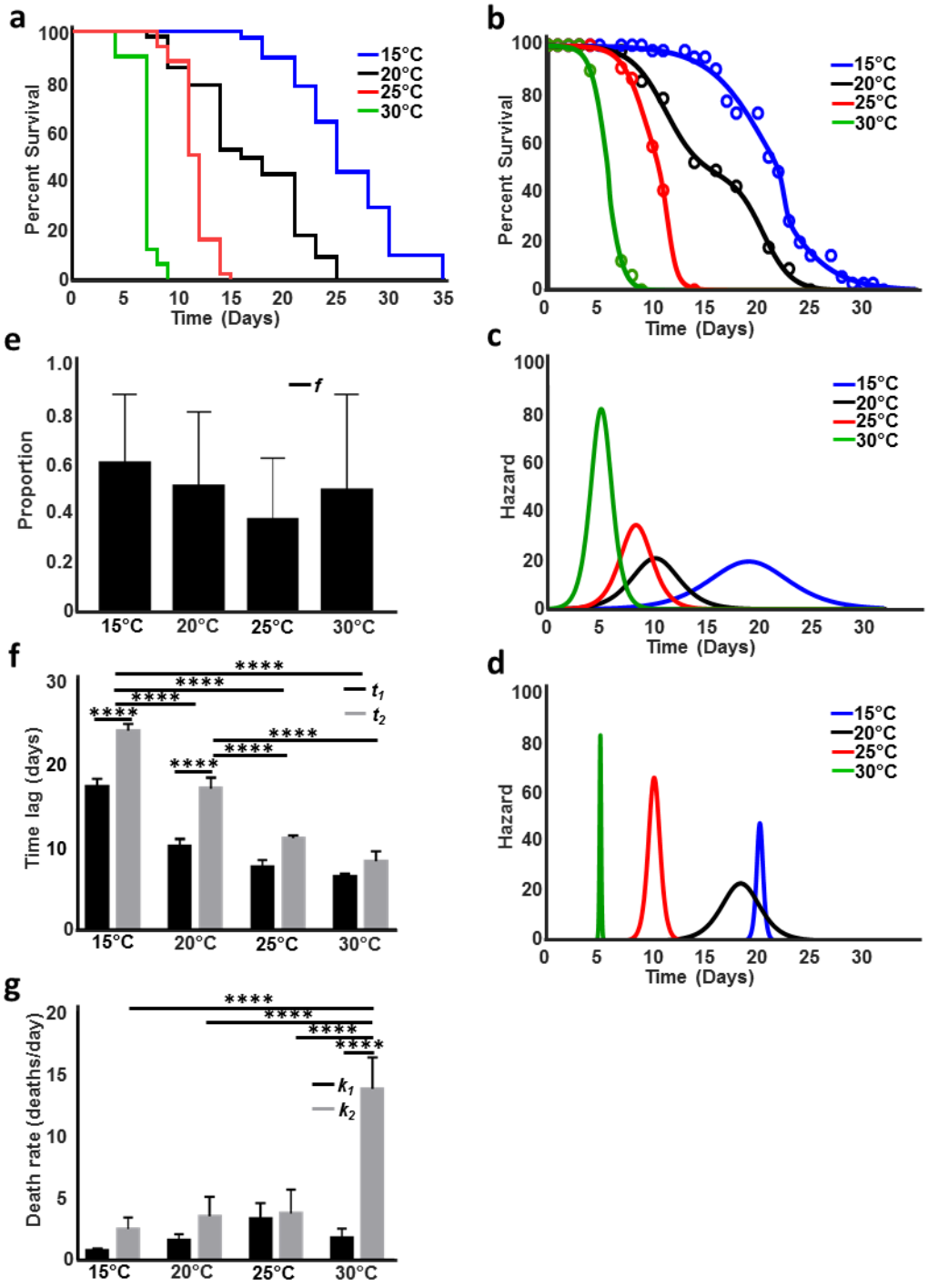

Figure 3.1: *C. elegans* lifespan displays biphasic dynamics. **(a)** Representative lifespan of control N2 worms maintained at different temperatures (15°C, 20°C, 25°C and 30°C). **(b)** Curves fitted to the data shown in **a**. **(c, d)** Comparison of 1st (**c**) and 2nd (**d**) phases of lifespan curves of N2 worms maintained at different temperatures. The phases were obtained from 1st order differentiation of fitted lifespan curves. **(e-g)** Quantification of parameters estimated for lifespan curves of N2 worms maintained at 15°C (n=20), 20°C (n=15), 25°C (n=14) and 30°C (n=3). Data is shown as mean ± SEM. **** p<0.0001.

Taken together, these data showed that the Bilogistic model is able to fit lifespan data and distinguish the biphasic properties of the data. Unlike other models which assumed monophasic dynamics (Stroustrup et al., 2016, Petrascheck and Miller, 2017, Pletcher et al., 2000, Weibull, 1951, Gompertz, 1825), this model separated lifespan into 2 subpopulations (short- or long-lived) and calculated the effect of temperature on both the death rates and the median survival of each groups.

3.4.2 Analysis of lifespan models by goodness of fit test

As the 5-parameter Bilogistic model is able to fit biphasic lifespan data it was then compared to other published models and the number of parameters were reduced to test whether it was possible to simplify the model. Many existing lifespan models contain 2 to 4 parameters (Gompertz, 1825, Weibull, 1951, Wilson, 1994, Whiting and Buchanan, 1993, Makeham, 1860), but other proposed models can have up to 10 parameters (de Beer et al., 2017, Siler, 1979). The following simplifications were considered to reduce the model to 4 parameters: a single death rate (where k_1 is equal to k_2), a fixed f to be either 0.5 (equal weight of phases) or 0 (a single phase). Further simplifications were made to reduce the parameters to 3: a fixed f to 0.5 *and* k_1 equal to k_2 so phases had equal weighting and a single death rate, or a fixed f to an average of previously calculated f's *and* k_1 equal to k_2. The Bilogistic model and an assortment of commonly used lifespan models (see Methods, Equations 3-8) were fitted to the data from *C. elegans* maintained at 20°C (the standard culture temperature; Figures 3.2a-i). Visual inspection of representative experimental data indicates that the full model is able to accurately fit the data points well and clearly suggests the existence of two phases. In many of the other models there were systematic deviations in the fittings and therefore many did not capture the biphasic nature of the survival curve (see Figure 3.2d-i).

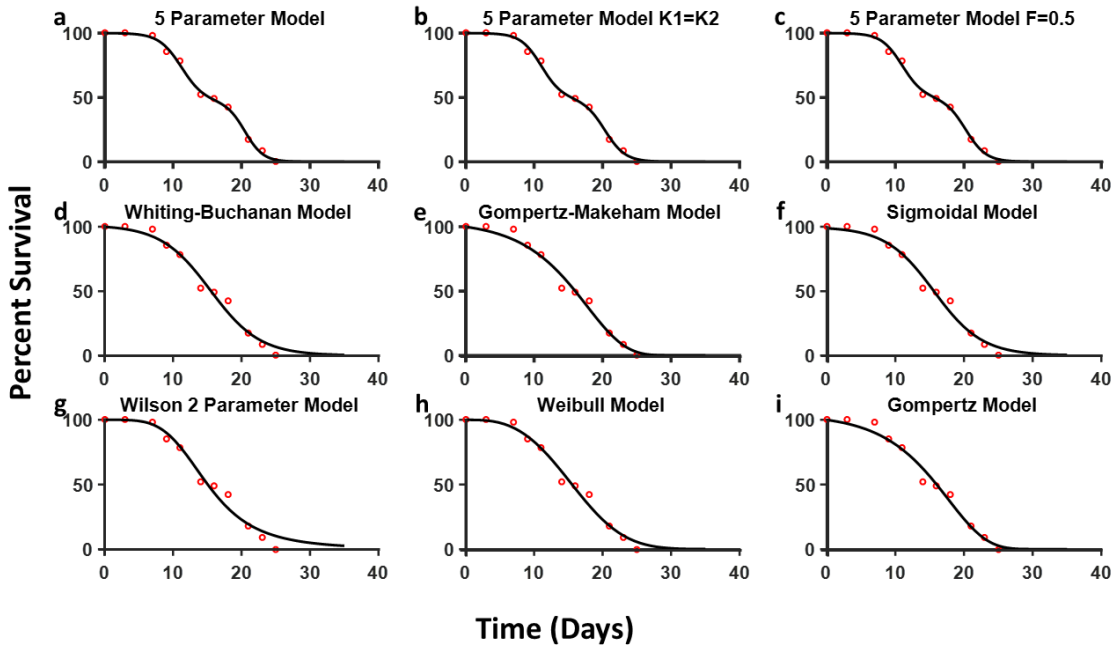

Figure 3.2: Fitting of a representative lifespan curve by different models. **(a-i)** Representative lifespan curve of N2 worms maintained at 20°C was fitted with a panel of lifespan models. Reducing the number of parameters in our Bilogistic model results in poorer fit of the data.

In order to confirm or reject this observation and to compare the goodness of fit of the parametric models, the residual differences between actual experimental lifespan data points and fitted model curves for each data set were calculated. Residual differences for each realisation in a data set was collated and underwent a data binning procedure by days to smooth data. In the *C. elegans* data, residuals were grouped into bins of 2, 3 or 4 days and plotted (Figures 3.3a-i). The Bilogistic model shows the smallest residual error with minimal systematic deviations in all bins (Figure 3.3a-i) when compared to the other models (Figure 3.4), indicating that it is the most complete fit fully able to capture biphasic lifespan data. The two 3 parameter variants of the Bilogistic model was also fitted to lifespan data (Figure 3.5 a, b) and residuals were collated and binned into groups of 2, 3 or 4 days to smooth data (Figure 3.5 c, d). These two simplified variants were compared to the 5-parameter Bilogistic model and show a greater residual error (bin 3) indicating that the simplified models are unable to capture biphasic lifespan data (Figure 3.5 e, f). Similar residual analysis was conducted at 15°C, 25°C

and 30°C which all show similar findings that the 5-parameter Bilogistic model shows the smallest residual error (Figures 3.6, 3.7, 3.8).

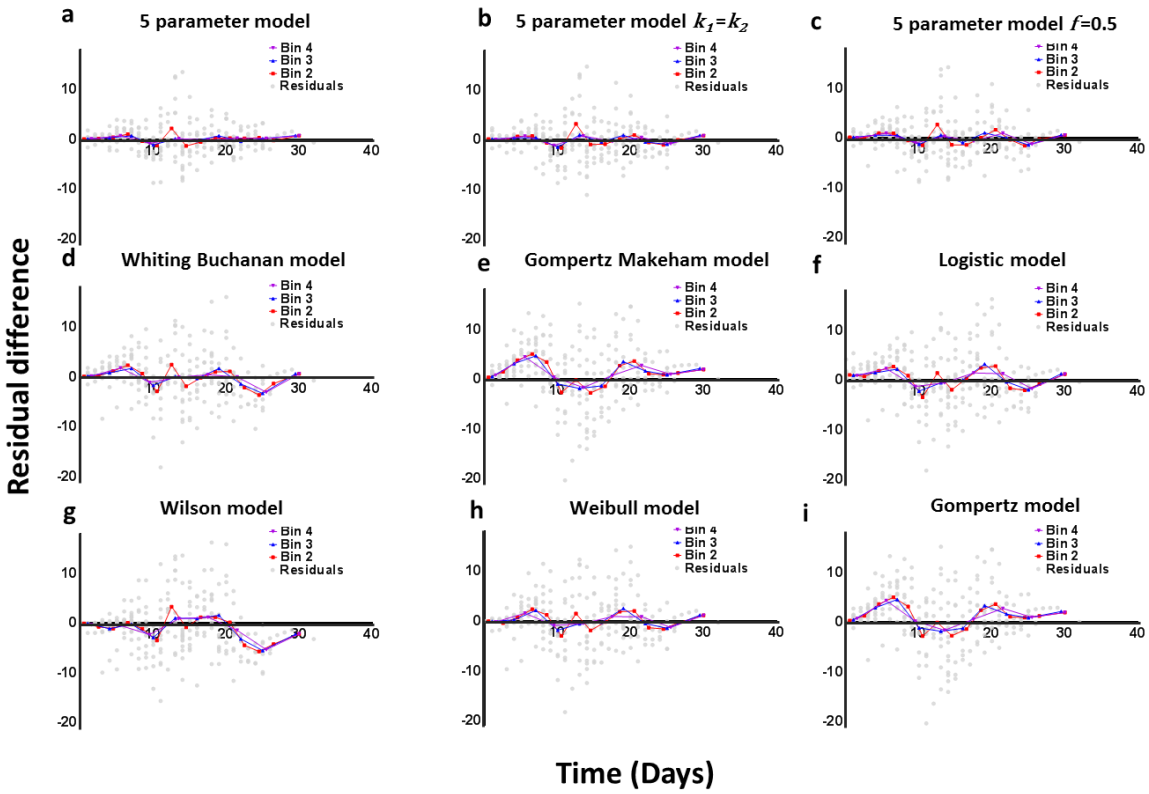

Figure 3.3: Analysis of lifespan models by residual difference analysis. **(a-i)** The residual differences between the experimental data and the fitted curve from individual models were calculated (grey dots) and data was grouped into bins of 2, 3, or 4 days (red, blue and purple lines respectively). Smaller residual differences indicate better fit. Data is from 15 replicate experiments.

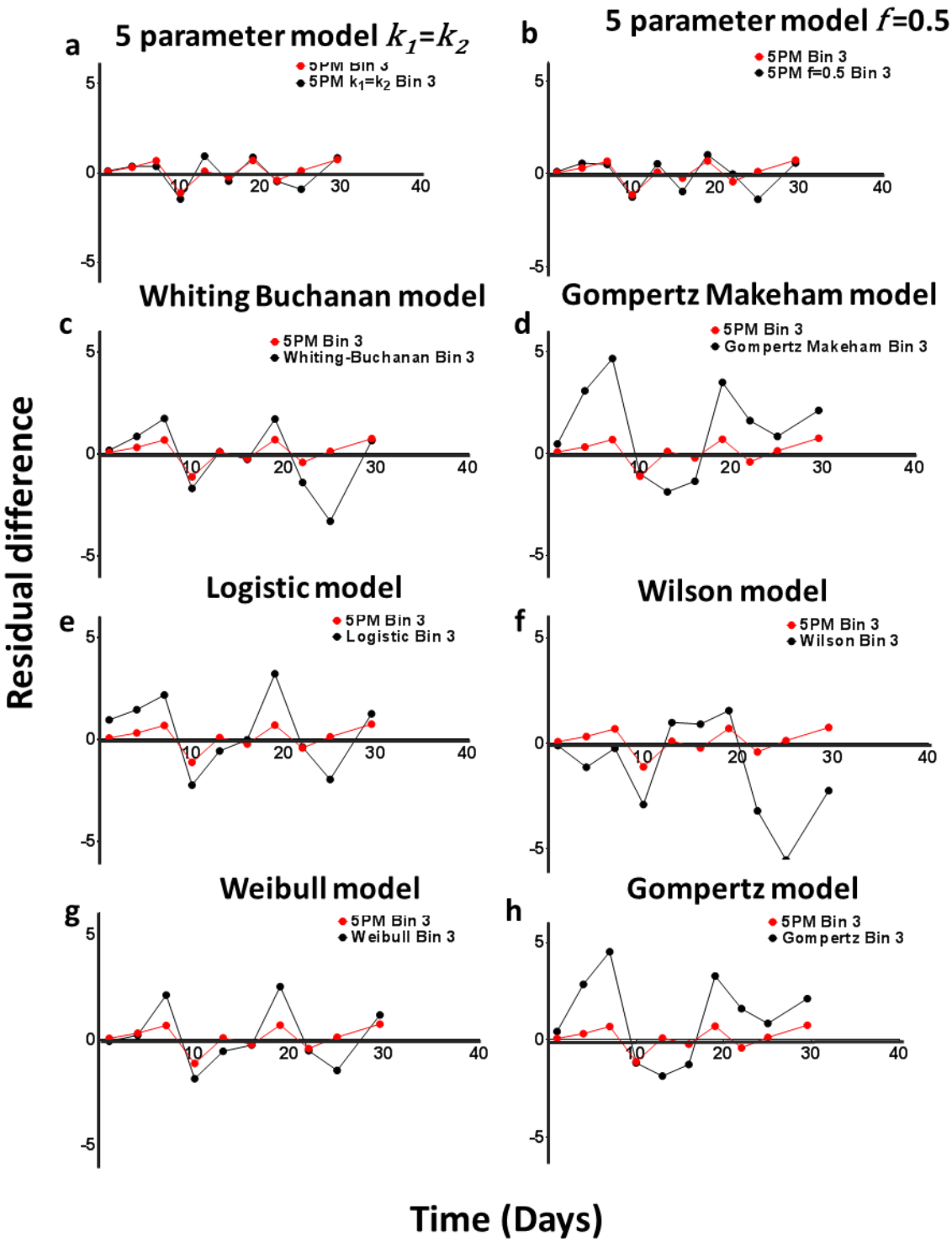

Figure 3.4: Comparison of Bilogistic model against other lifespan models. **(a-h)** Residual difference analysis of the Bilogistic model (red) against either simplified variants or other lifespan models (black). Binning was set to 3 days. Smaller residual differences indicate better fit. Data is from 15 replicate experiments.

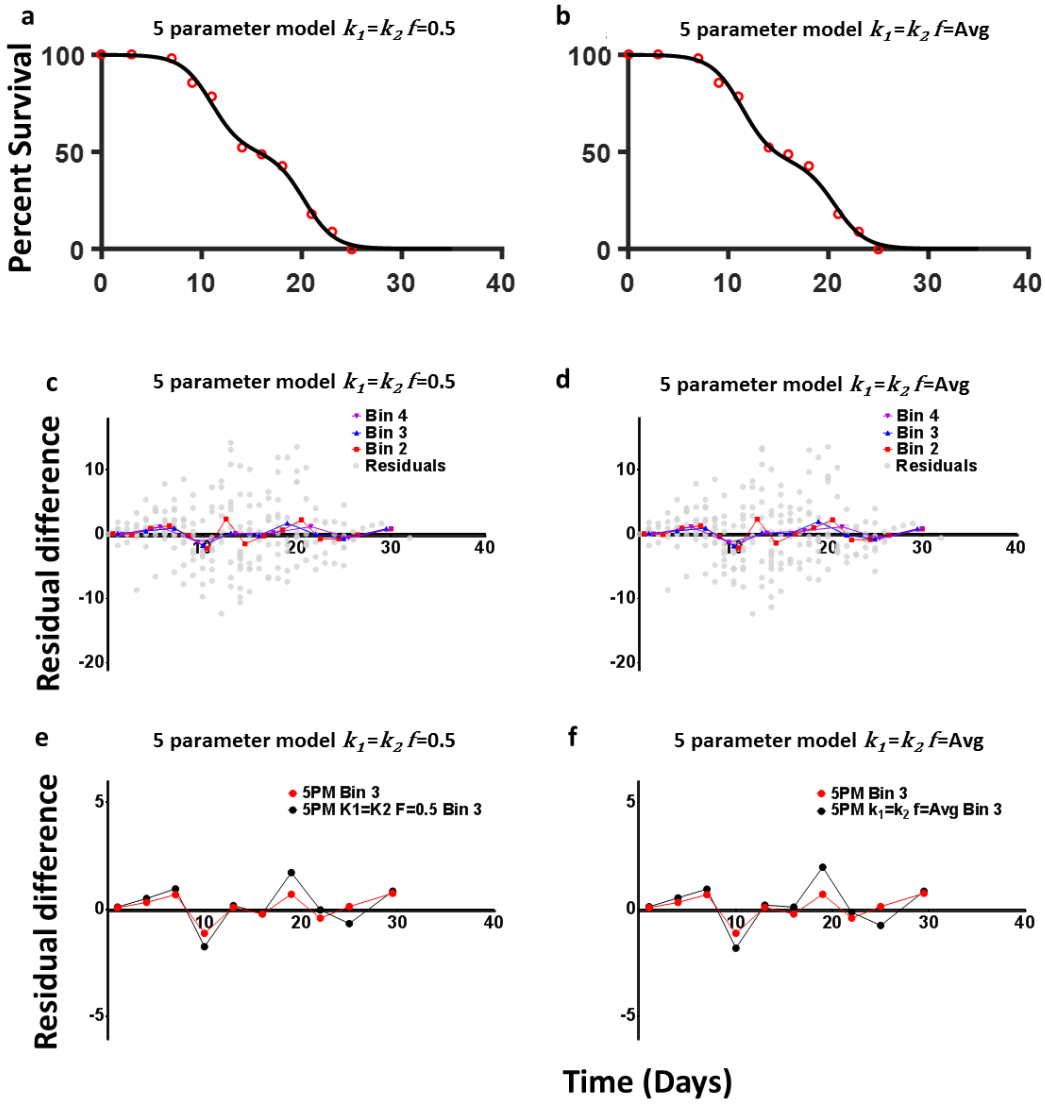

Figure 3.5: Analysis of variants of Bilogistic model. **(a, b)** Representative lifespan of *C. elegans* worms maintained at 20°C were fitted with the Bilogistic model where either k_1=k_2 and f=0.5 **(a)** or k_1=k_2 and f=Avg **(b)**. **(c, d)** Residual differences between the experimental data and the fitted curve from each model were calculated (grey dots) and data was grouped into bins of 2, 3, or 4 days (red, blue and purple lines respectively). **(e, f)** Comparison of the residual differences from Bilogistic model (red) against either simplified variants (black). Binning was set to 3 days. Smaller residual differences indicate better fit. Data is from 15 replicate experiments.

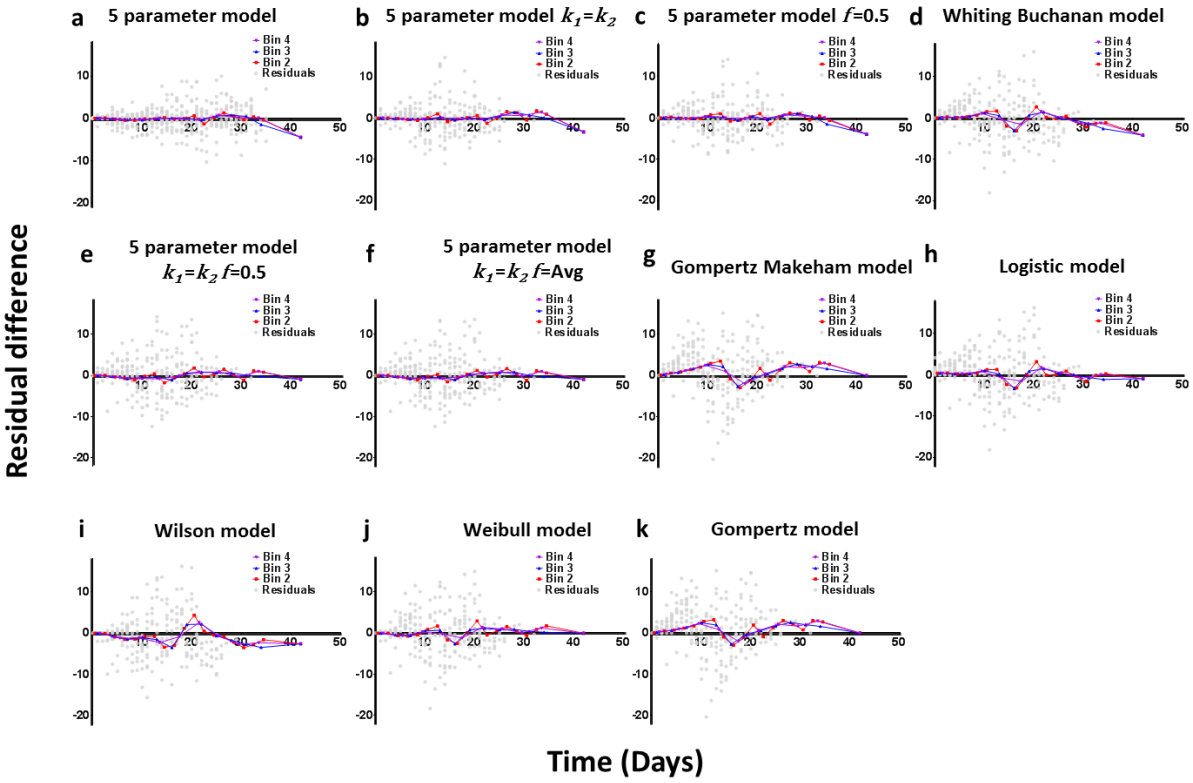

Figure 3.6: Analysis of lifespan models by residual difference analysis in *C. elegans* maintained at 15°C. The residual differences between the experimental data and the fitted curve from individual models were calculated (grey dots) and data was grouped into bins of 2, 3, or 4 days (red, blue and purple lines respectively). Smaller residual differences indicate better fit. Data is from 20 replicate experiments.

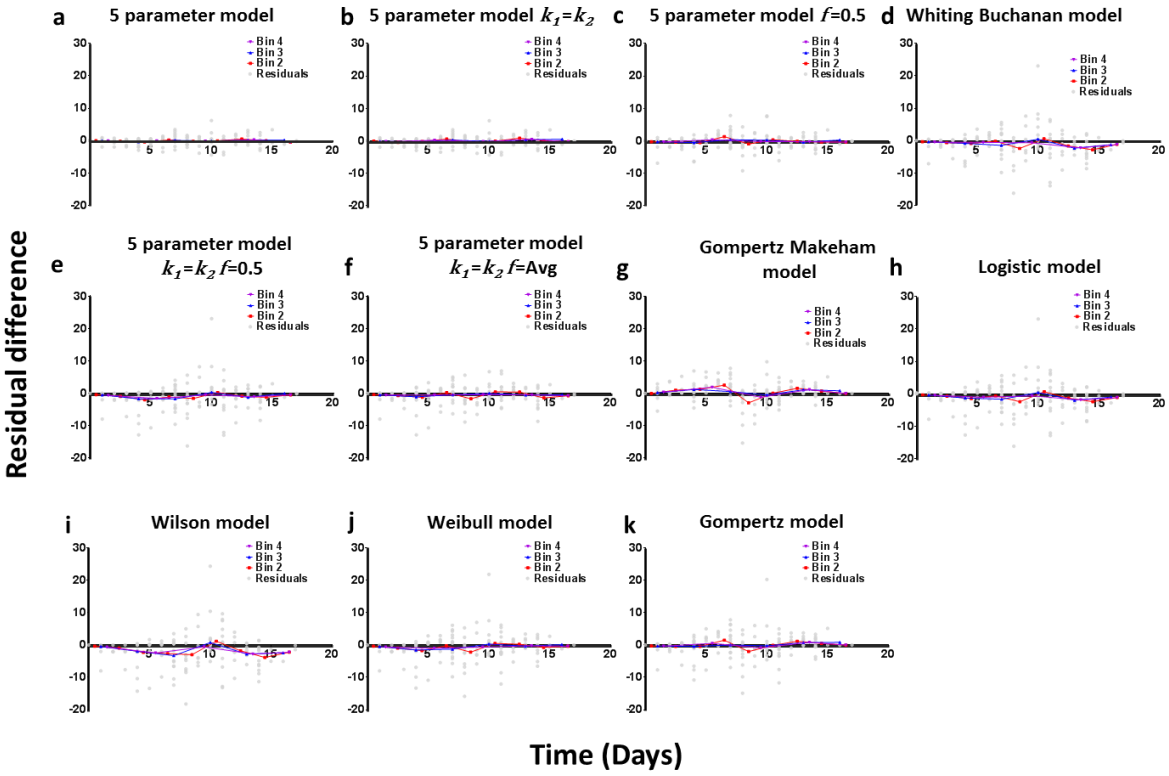

Figure 3.7: Analysis of lifespan models by residual difference analysis in *C. elegans* maintained at 25°C. The residual differences between the experimental data and the fitted curve from individual models were calculated (grey dots) and data was grouped into bins of 2, 3, or 4 days (red, blue and purple lines respectively). Smaller residual differences indicate better fit. Data is from 14 replicate experiments.

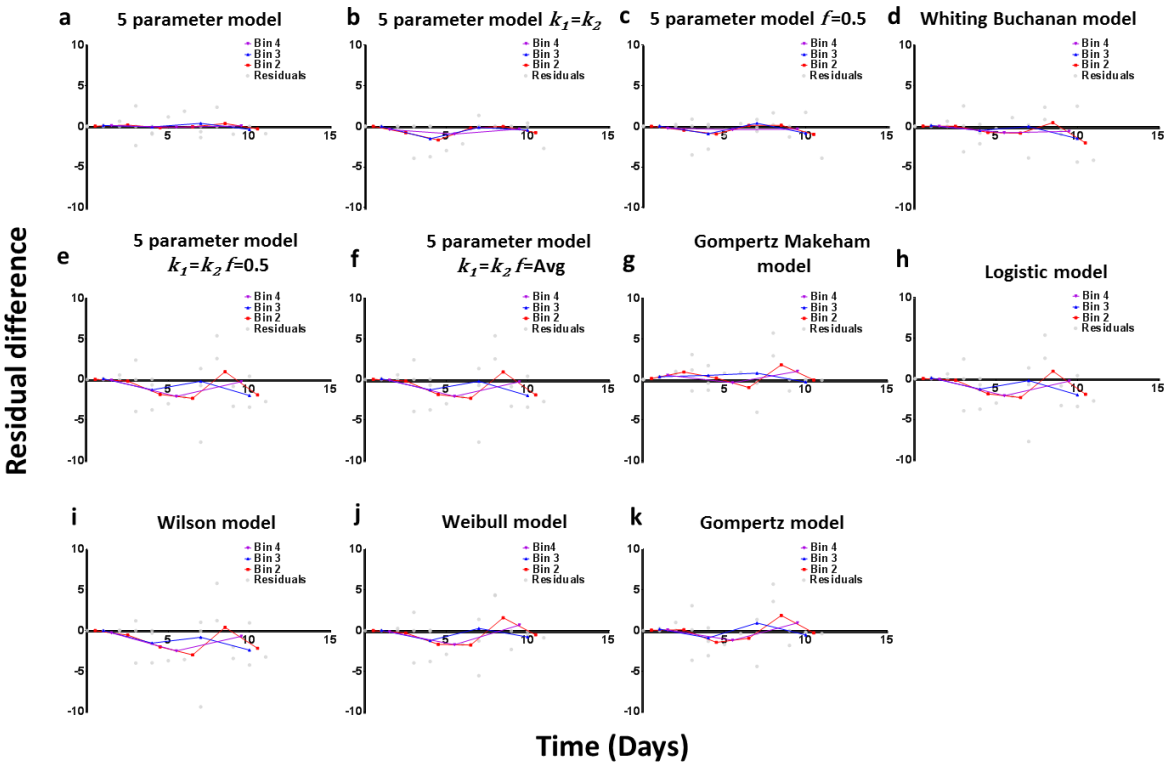

Figure 3.8: Analysis of lifespan models by residual difference analysis in *C. elegans* maintained at 30 °C. The residual differences between the experimental data and the fitted curve from individual models were calculated (grey dots) and data was grouped into bins of 2, 3, or 4 days (red, blue and purple lines respectively). Smaller residual differences indicate better fit. Data is from 3 replicate experiments.

For a more quantitative measure, the RMSE was also calculated for each model fitted curve. This type of analysis took into account the varying number of parameters present in each model (by applying greater penalties to models with more parameters) and therefore represented an unbiased model performance (Chai and Draxler, 2014). Using the lifespan data of *C. elegans* maintained at 20°C, the Bilogistic model showed significantly lower RMSE values compared to existing models (Figure 3.9). Similarly, significantly lower RMSE values using data from worms maintained at 15°C, 25°C and 30°C (Figure 3.10) were observed. Thus, the unbiased analysis of RMSE showed that the Bilogistic model is significantly better at fitting lifespan curves of *C. elegans* across different temperatures.

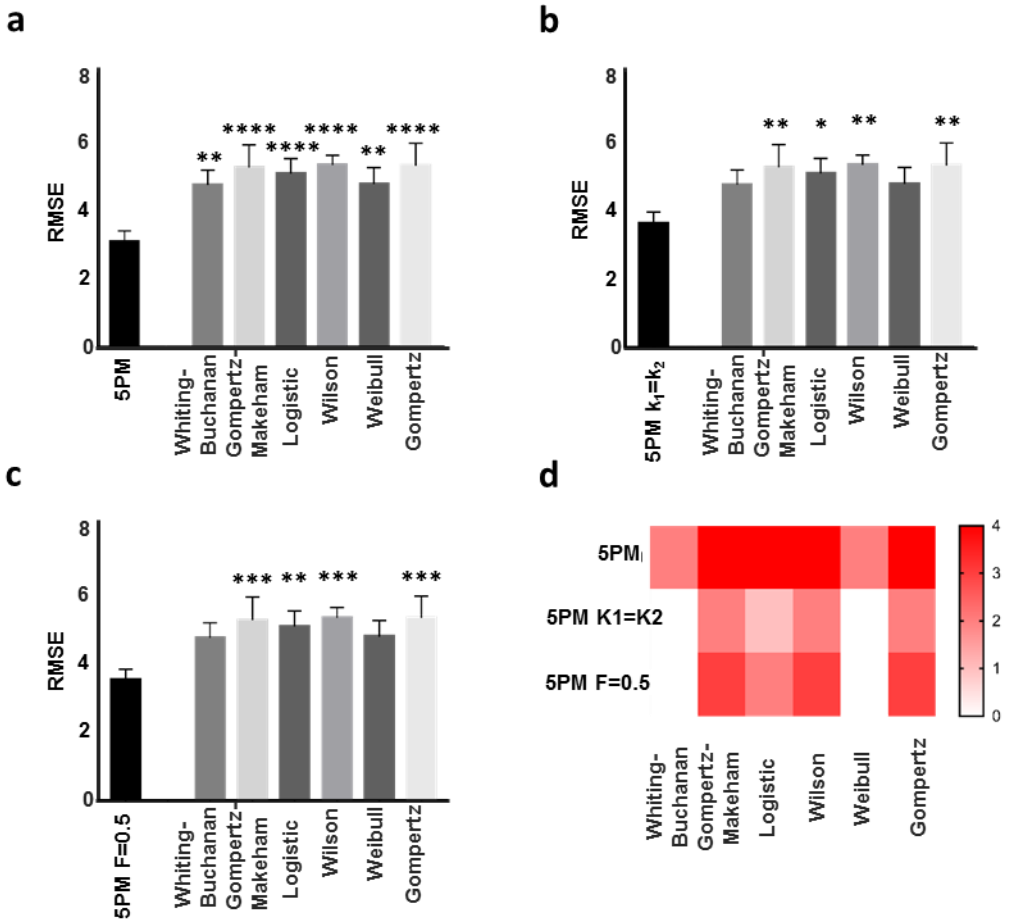

Figure 3.9: Analysis of goodness of fit by root mean square error (RMSE). The RMSE for each lifespan models was compared to either the Bilogistic model **(a)** or to variants where k1=k2 **(b)** or f=0 **(c)**. Lower values of RMSE indicate better fit. **(d)** Significance comparison for the Bilogistic model and variants against other lifespan models. The scale represents the *p-value* statistical significance (from no significance (0) to **** (4)). Data is shown as RMSE ± SEM, n=15. * $p<0.05$, ** $p<0.01$***, $p<0.001$, and **** $p<0.0001$.

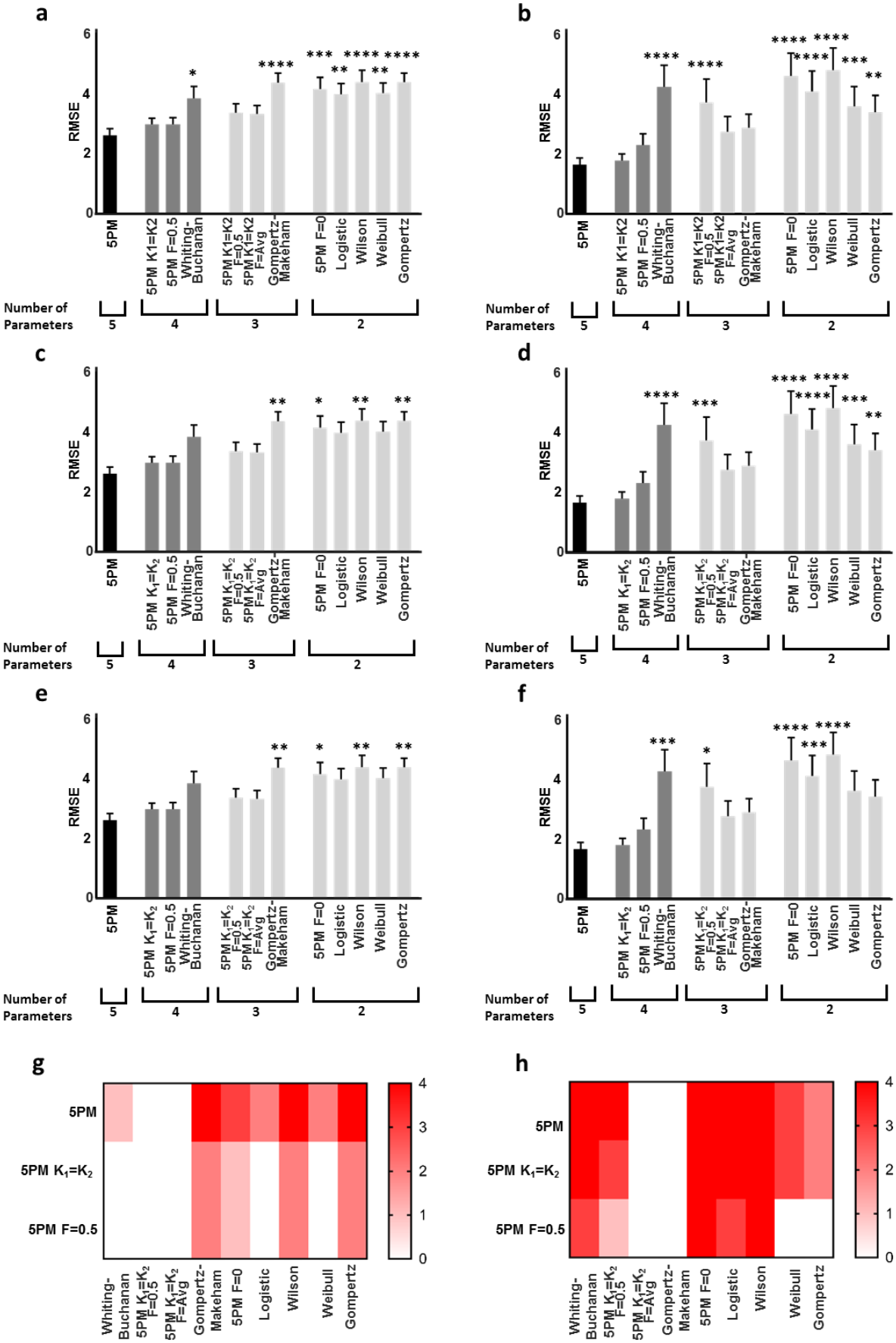
a
b
c
d
e
f
RMSE
0
2
4
6
5PM
5PM K1=K2
5PM F=0.5
Whiting-Buchanan
5PM K1=K2 F=0.5
5PM K1=K2 F=Avg
Gompertz-Makeham
5PM F=0
Logistic
Wilson
Weibull
Gompertz
5PM K1=K2
5PM F=0.5
5PM K1=K2 F=0.5
5PM K1=K2 F=Avg
5PM F=0
Number of Parameters
5
4
3
2
g
h
5PM
5PM K1=K2
5PM F=0.5
0
1
2
3
4

Figure 3.10: Goodness of fit testing for *C. elegans* at 15°C and 25°C**.** The root mean square error (RMSE) was calculated from model fitting of lifespan data of *C. elegans* maintained at either 15°C (**a, c, e, f;** n=20) or 25°C (**b, d, f, h;** n=14), and compared to either the Bilogistic model **(a)** or to variants where k_1=k_2 **(b)** or f=0 **(c)**. Smaller values of RMSE indicate better fit. **(g, h)** Significance comparison for the Bilogistic model and variants against other lifespan models. The scale represents the p-value statistical significance (from no significance (0) to **** (4)). Data is shown as RMSE ± SEM.* p<0.05, ** p<0.01, ***p<0.001, and ****p<0.0001.

3.4.3 Conserved effects of *daf-16/FOXO* deletion on lifespan

As the model had only been tested on wild type (N2 worms) alternative conditions were investigated. As genetics play a major role in lifespan it was tested whether the model could be applied to measure the effects of genetic manipulations on lifespan. The *daf-16*(*mu86*) mutation where worms are lacking DAF-16 (FOXO ortholog in nematodes) which is known to play a critical role in regulating lifespan (Kenyon et al., 1993) was considered. As expected, this resulted in a significantly shorter lifespan (Figure 3.11a), which could be fitted with the Bilogistic model (Figure 3.11b). The hazard showed that the loss of DAF-16 affected both phases of the survival curve (Figure 3.11c, d), primarily due the convergence of both phases (t_2; Figure 3.11e) which is the result of an increased rate of death of the 2nd subpopulation (k_2; Figure 3.11f). As sharp drops in a lifespan curve correspond to many death events in a short time and hence few data points, all parameter values derived from fitting procedures have to be assessed individually and with caution.

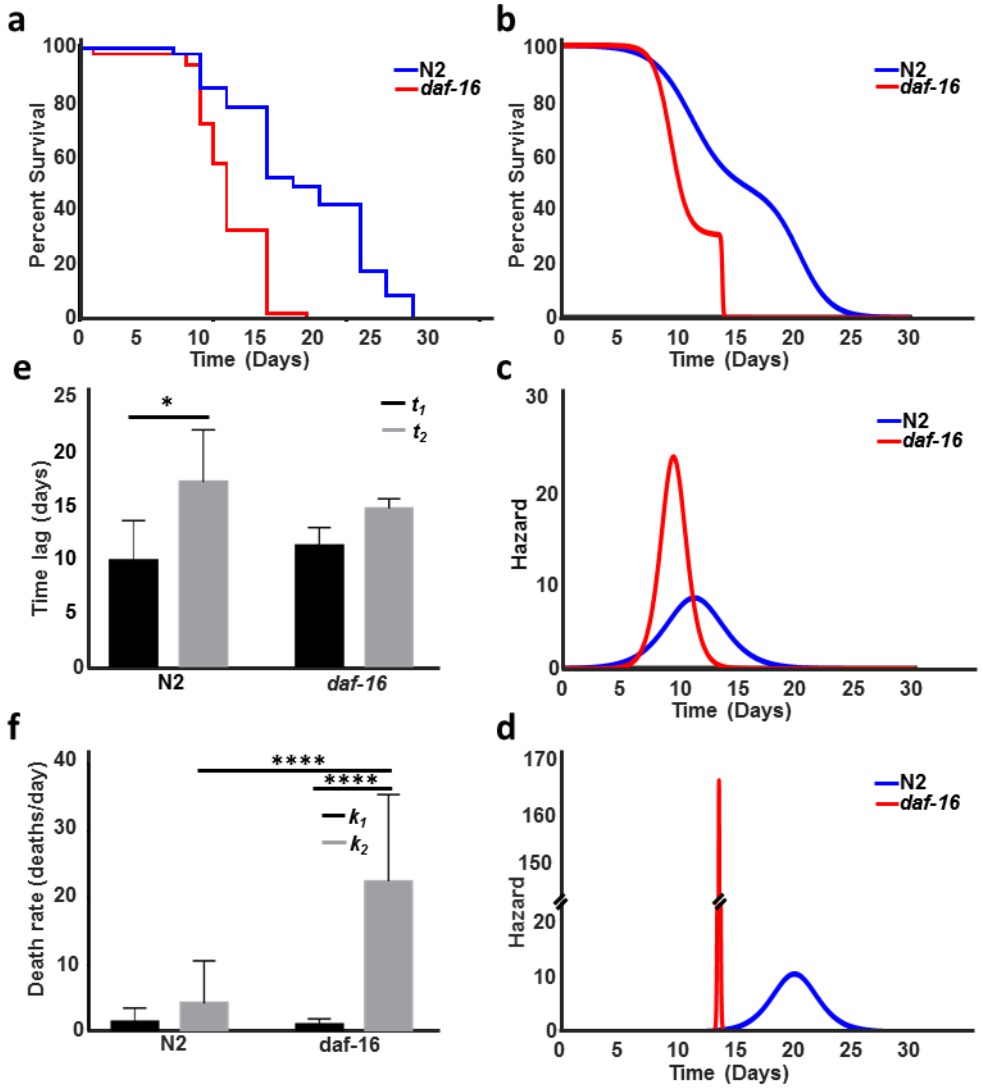

Figure 3.11: *daf-16(mu86)* deletion in *C. elegans* shortens lifespan by increasing rate of death in second phase. **(a)** Representative lifespan curves of N2 and *daf-16(mu86)* worms maintained at 20°C and **(b)** fitted with the Bilogistic model. The strong dip for the mutants corresponds to only few data points and the fitting has to be interpreted with caution. **(c, d)** Comparison of 1st (**c**) and 2nd (**d**) phases of lifespan curves of N2 and *daf-16(mu86)* worms, obtained from 1st order differentiation of fitted curves. **(e, f)** Quantification of parameters estimated for lifespan curves of N2 (n=9) and *daf-16(mu86)* (n=5) mutant worms. Data is shown as mean ± SEM. *p<0.05 and ****p<0.0001.

It was hypothesised that the effects of FOXO loss-of-function on lifespan are conserved in other organisms. To test this, the lifespans of *Drosophila melanogaster* lacking FOXO (*dfoxo*Δ), which also have a shorter lifespan than their control (w^{Dah}) (Slack et al., 2011) (Figure 3.12a) was analysed (Figures 3.12b). The effects of *dfoxo* deletion in *Drosophila* mirrored the findings from the *daf-16*(*mu86*) worms as a higher hazard in both 1st and 2nd phases in *dfoxo*Δ flies (Figure 3.12c, d), with an earlier median survival for the 2nd phase (Figure 3.12e) due to

the observed increased 2nd phase death rate (k_2, Figure 3.12f). Additionally the fitted data and residuals from drosophila were analysed indicating that the Bilogistic model has the lowest residual error indicating a better fit in both w^{Dah} and *dfoxo*Δ mutants Figure (3.13 and 3.14).

Taken together, the Bilogistic model is able to fit and detect the effects of nematode *daf-16(mu86)* and *Drosophila dfoxo*Δ mutation on lifespan. Importantly, the Bilogistic model found that *daf-16/FOXO* mutations resulted in similar changes in the lifespan curves in both organisms; The longer-lived subgroup in the mutant population started dying earlier and faster.

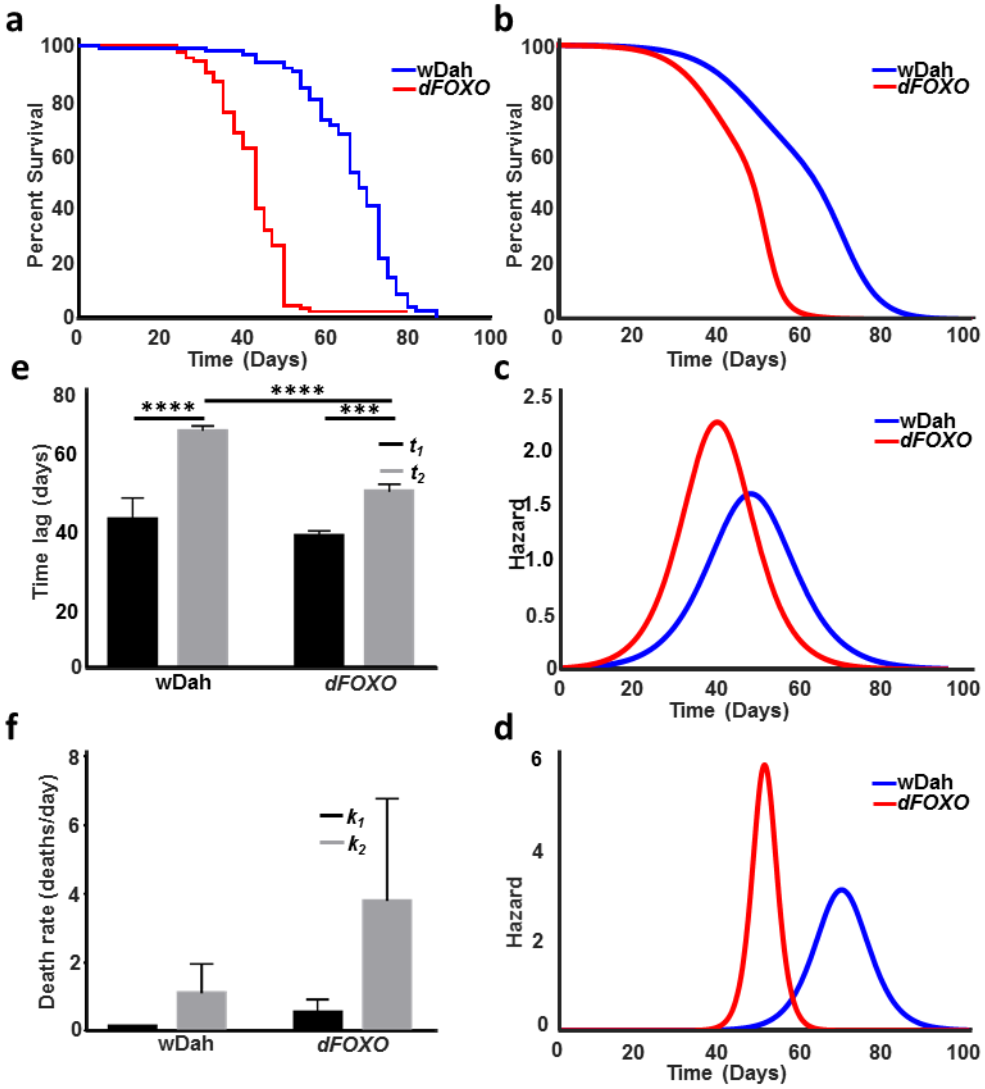

Figure 3.12: Mutation of *dFOXO* in *D. melanogaster* shortens lifespan by increasing rate of death in second phase**. (a)** Representative lifespan curves of wild type (w^{Dah}) and FOXO mutant (dfoxoΔ) flies and **(b)** fitted with the Bilogistic model. **(c, d)** Comparison of 1st **(c)** and 2nd **(d)** phases of lifespan curves of w^{Dah} and dfoxoΔ flies, obtained from 1st order differentiation of fitted curves. **(e, f)** Quantification of parameters estimated for lifespan curves of w^{Dah} and dfoxoΔ flies. Experimental data shown **(a)** was collected by Cathy Slack. Data is shown as mean ± SEM, n=10. *p<0.05, **p< 0.01, ***p< 0.001, and **** p<0.0001.

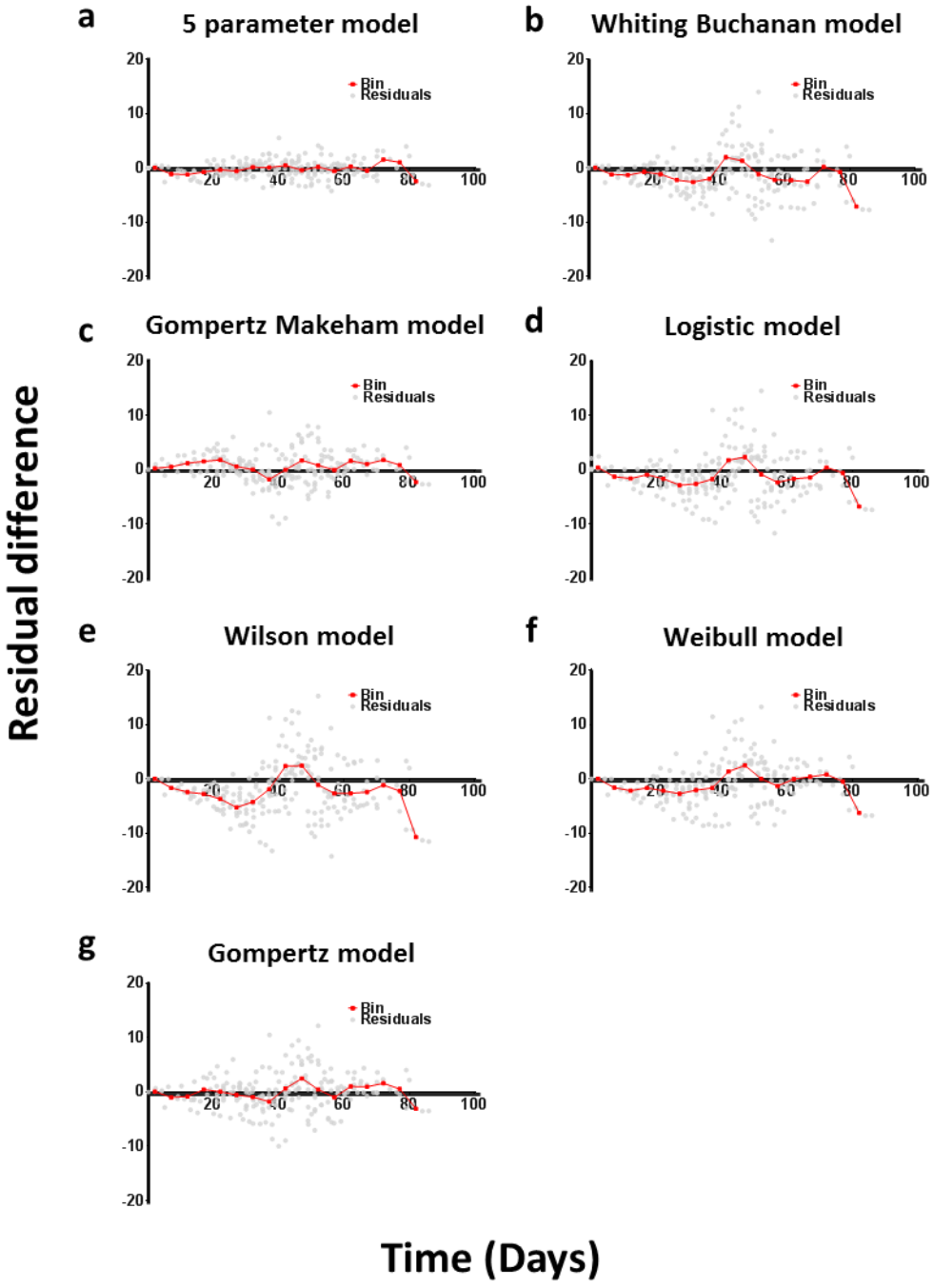

Figure 3.13: Analysis of lifespan models by residual difference analysis in w^{Dah} drosophila**.** Residual differences between the experimental data and the fitted curve from each model were calculated (grey dots) and data was grouped into bins of 5 days (red line). Smaller residual differences indicate better fit. Data for w^{Dah} drosophila **(a-g)** is from 10 replicate experiments.

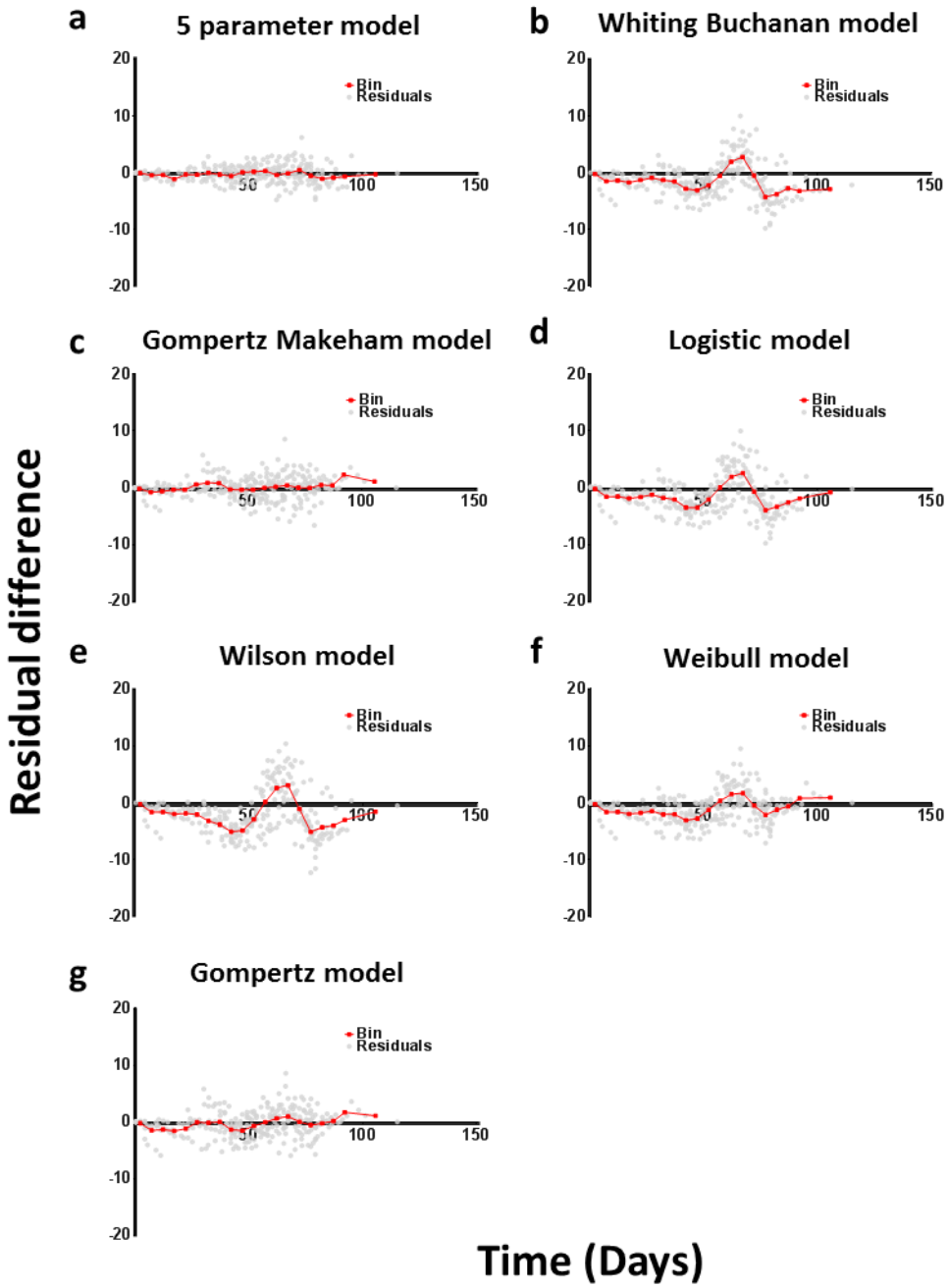

Figure 3.14: Analysis of lifespan models by residual difference analysis in dFOXOΔ drosophila. Residual differences between the experimental data and the fitted curve from each model were calculated (grey dots) and data was grouped into bins of 5 days (red line). Smaller residual differences indicate better fit. Data for dFOXOΔ drosophila **(a-g)** is from 10 replicate experiments.

3.4.4 Modelling type-2 survivorship in honey bees

Having modelled type-1 survival curves for the worms and flies, type-2 survivorship pattern (Demetrius, 1978) as observed in hived bees were tested to see if they could be modelled by analysing the lifespan of honey bees (*Apis mellifera carnica*) maintained in either hived or caged colonies (Figure 3.15a) (Sakagami and Fukuda, 1968, Woyciechowski and Moron, 2009). Additionally hived and caged bees show differences in survival and were investigated to see if the Bilogistic model is capable of identifying differences between the two. The log-rank test could not reliably distinguish differences in the survival of the two populations. Of the 4 replicates, 2 did not show significantly differences, the 3rd dataset showed significant differences between the two conditions at $p<0.05$, and the final dataset at $p<0.001$. However, by using the Bilogistic model to fit the data for both hived and caged bees, statistical comparison using all 4 replicates can be made (Figures 3.15b). A higher hazard for hived bees in the 1st phase was observed (Figure 3.15c) whilst most caged bees died in the 2nd phase (Figure 3.15d). Analysis of the model parameters between hived and caged bees showed a delayed median survival for the 1st phase (t_1) for caged bees (Figure 3.15e) and a reversal of the 1st and 2nd phase death rates (k_1 v k_2; Figure 3.15f) presumably due to absence of external hazards such as predators and weather conditions (Woyciechowski and Moron, 2009). Once again the Bilogistic model shows a superior fitting to lifespan data compared to other models in both hived and caged bees (Figure 3.16, 3.17).

These results therefore showed that the Bilogistic model detected biphasic behaviour in type-2 survivorship data from hived bees, and caging the bees reduced the numbers in the short-lived group.

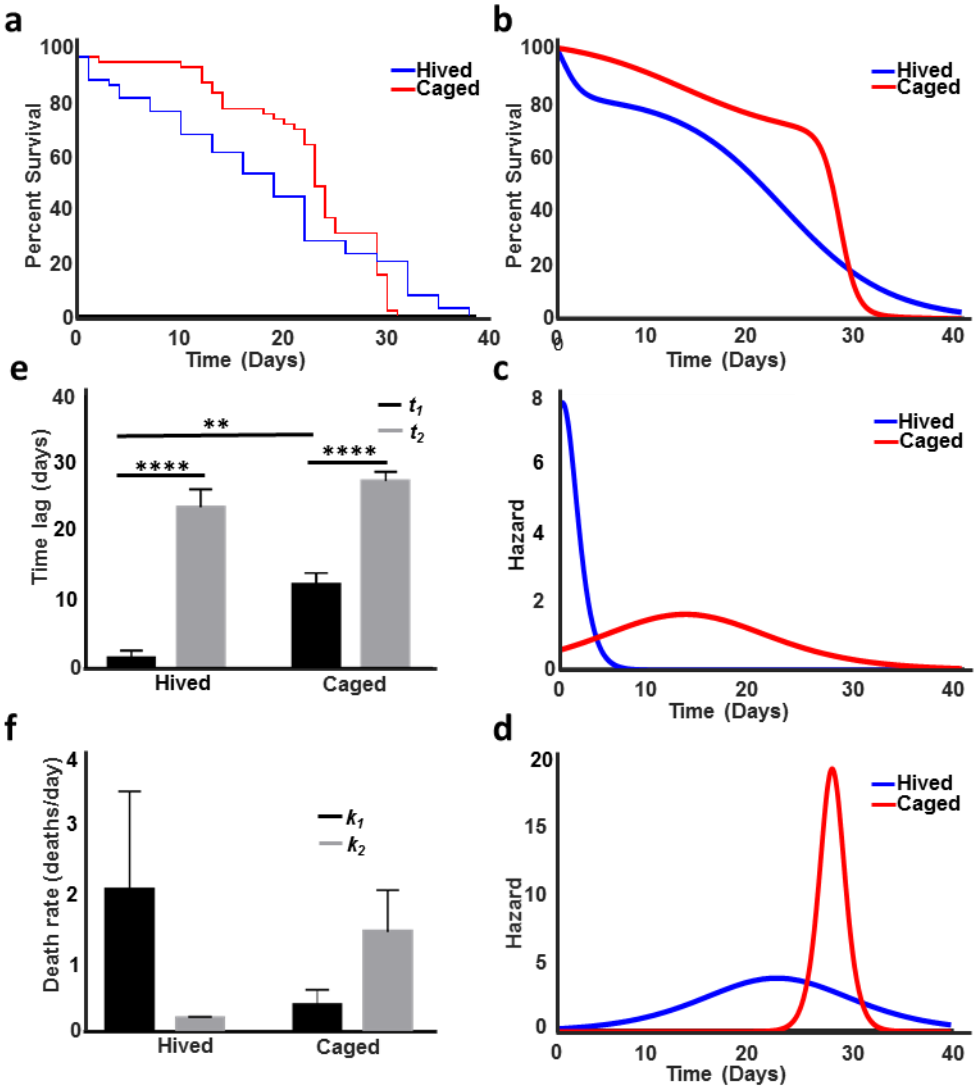

Figure 3.15: Caged carniolan honeybees (*A. mellifera carnica*) display increased lifespan compared to hived bees due to increased 1st phase survival. **(a)** Representative lifespan curves of caged and hived honeybees and **(b)** fitted with the Bilogistic model. **(c, d)** Comparison of 1st **(c)** and 2nd **(d)** phases of lifespan curves of caged and hived honeybees, obtained from 1st order differentiation of fitted curves. **(e, f)** Quantification of parameters estimated for lifespan curves of caged and hived honeybees. Experimental data shown **(a)** was collected by Karolina Kuszewska and Michał Woyciechowski. Data is shown as mean ± SEM, n=4. *p<0.05, **p< 0.01, and ****p< 0.0001.

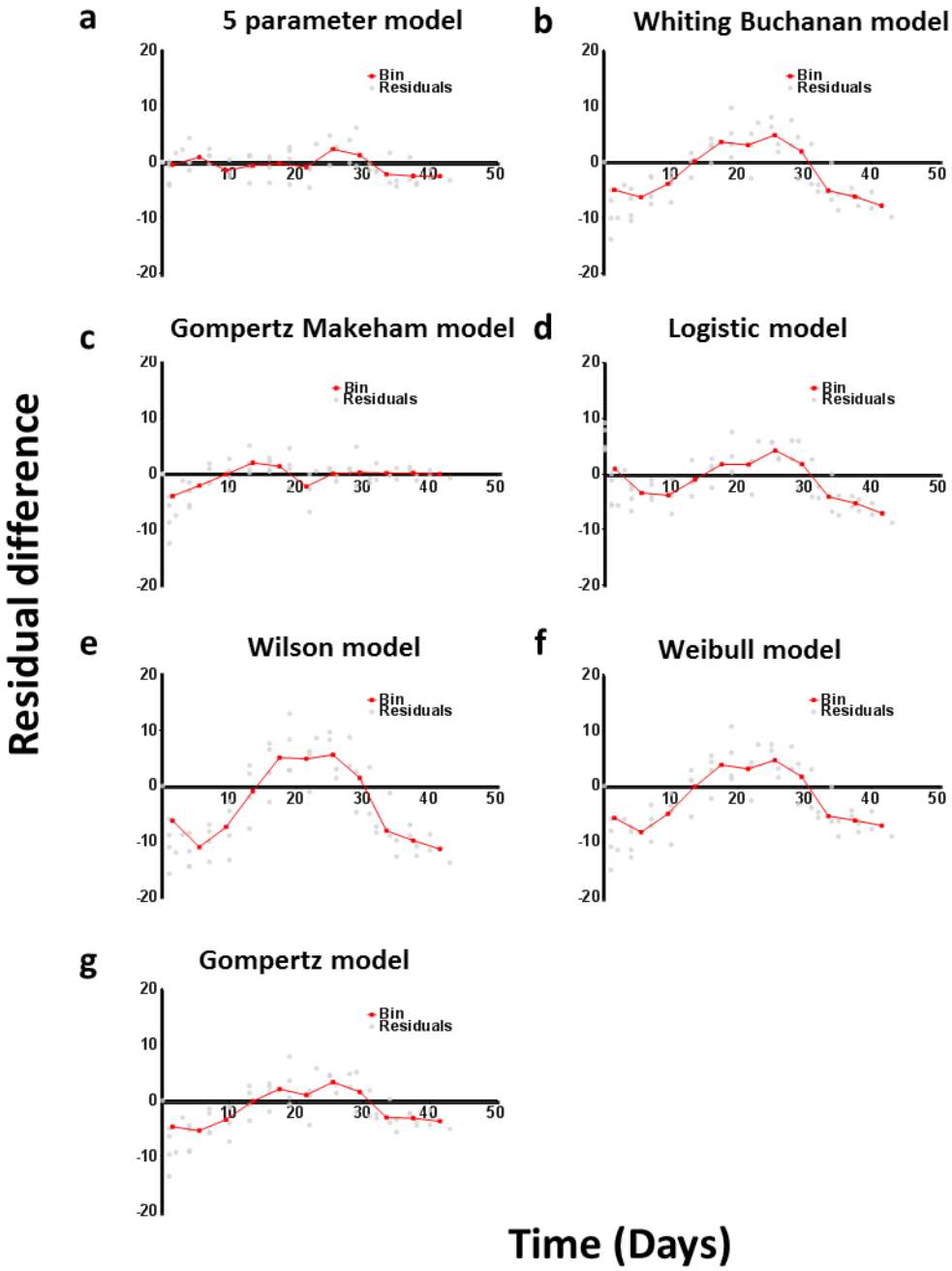

Figure 3.16: Analysis of lifespan models by residual difference analysis in hived bees. Residual differences between the experimental data and the fitted curve from each model were calculated (grey dots) and data was grouped into bins of 4 days (red line). Smaller residual differences indicate better fit. Data for hived bees **(a-g)** is from 4 replicate experiments.

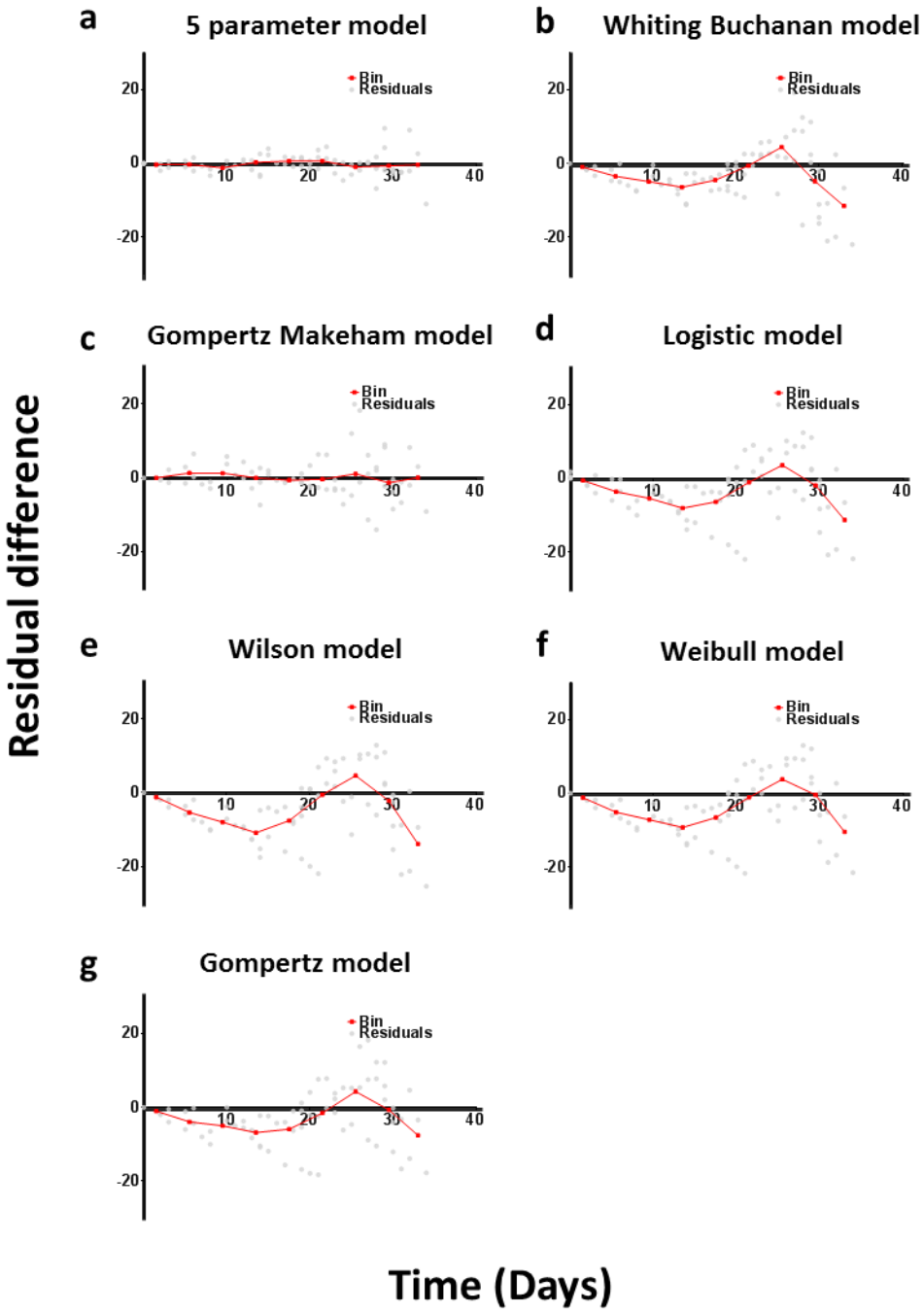

Figure 3.17: Analysis of lifespan models by residual difference analysis in caged bees**.** Residual differences between the experimental data and the fitted curve from each model were calculated (grey dots) and data was grouped into bins of 4 days (red line). Smaller residual differences indicate better fit. Data for caged bees **(a-g)** is from 4 replicate experiments.

3.4.5 Application to mammalian lifespan

Importantly it was assessed whether the model could be used for investigating mammalian lifespan data. In particular, survival data from one of the most common animal models, the mouse, kindly provided by the National Institute for Aging (NIA) Interventions Testing Program (ITP) was examined (Miller et al., 2014). Rapamycin treatment was shown to result in a significant extension of lifespan in both male and female UM-HET3 mice (Miller et al., 2014) (Figure 3.18a). The Bilogistic model could fit the data well (Figures 3.18b) and could allow for statistical comparison of all the replicates to be conducted. The Bilogistic model revealed that the onset of the 1st phase is sexually dimorphic, as in males but not in females, rapamycin delayed the onset of the 1st phase (Figure 3.18c, compare blue control and green rapamycin lines, Figure 3.18e). In both sexes, rapamycin delayed the onset of the 2nd phase (Figure 3.18d, e). Thus, in females, rapamycin emphasised the biphasic nature of their survival data (Figure 3.18e). Additionally, there is an earlier 1st phase median survival in control males than control female mice a further indication of sexual dimorphism (Figure 3.18e). Rapamycin therefore appeared to exert its effects on lifespan via alterations to the time-lag phases rather than through changes to the death rates (Figure 3.18f). In agreement with fitting of lifespan data from other model organisms once again the Bilogistic model is able to fit lifespan data better than other model as the residual error in all four groups is lowest with the Bilogistic model (Figure 3.19, 3.20, 3.21, 3.22).

The Bilogistic model was thus able to fit mouse lifespan data as biphasic dynamics and is likely to fit other mammalian lifespan data. The parameter analysis suggests that rapamycin delays the onset of the death but not the rate of death

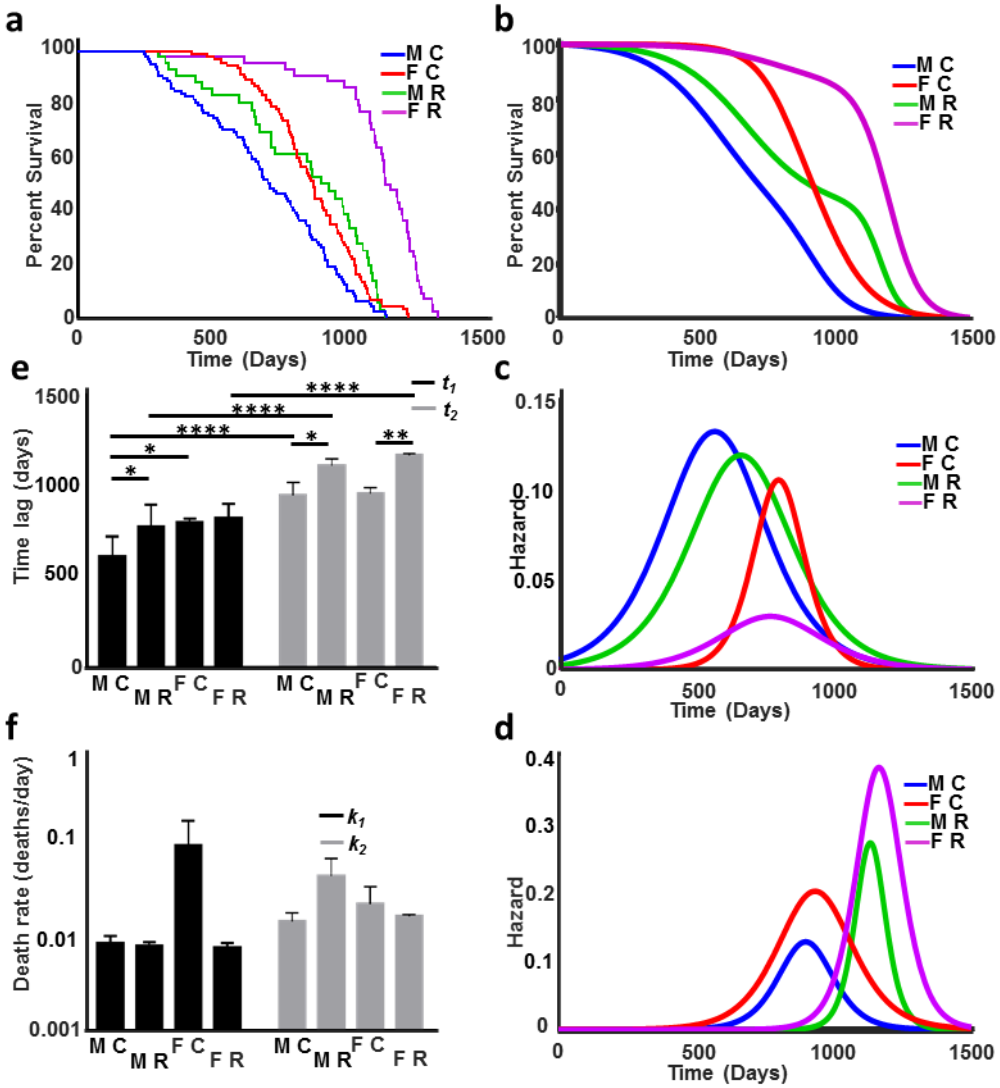

Figure 3.18: Rapamycin differentially increases lifespan in male and female UM-HET3 mice (*M. musculus*). **(a)** Representative lifespan curves of male and female UM-HET3 mice treated with and without rapamycin (42ppm; mg/kg) and **(b)** fitted with the Bilogistic model. **(c, d)** Comparison of 1st **(c)** and 2nd **(d)** phases of lifespan curves of male and female mice treated with and without rapamycin, obtained from 1st order differentiation of fitted curves. **(e-f)** Quantification of parameters estimated for lifespan curves of male and female mice treated with and without rapamycin. (MC= Male control, FC= Female control, MR= Male rapamycin treated, FR= Female rapamycin treated). Experimental data shown **(a)** was provided by the National Institute on Aging (NIA) Interventions Testing Program (ITP). Data is shown as mean ± SEM, n=3. *p< 0.05, **p< 0.01, and ****p< 0.0001.

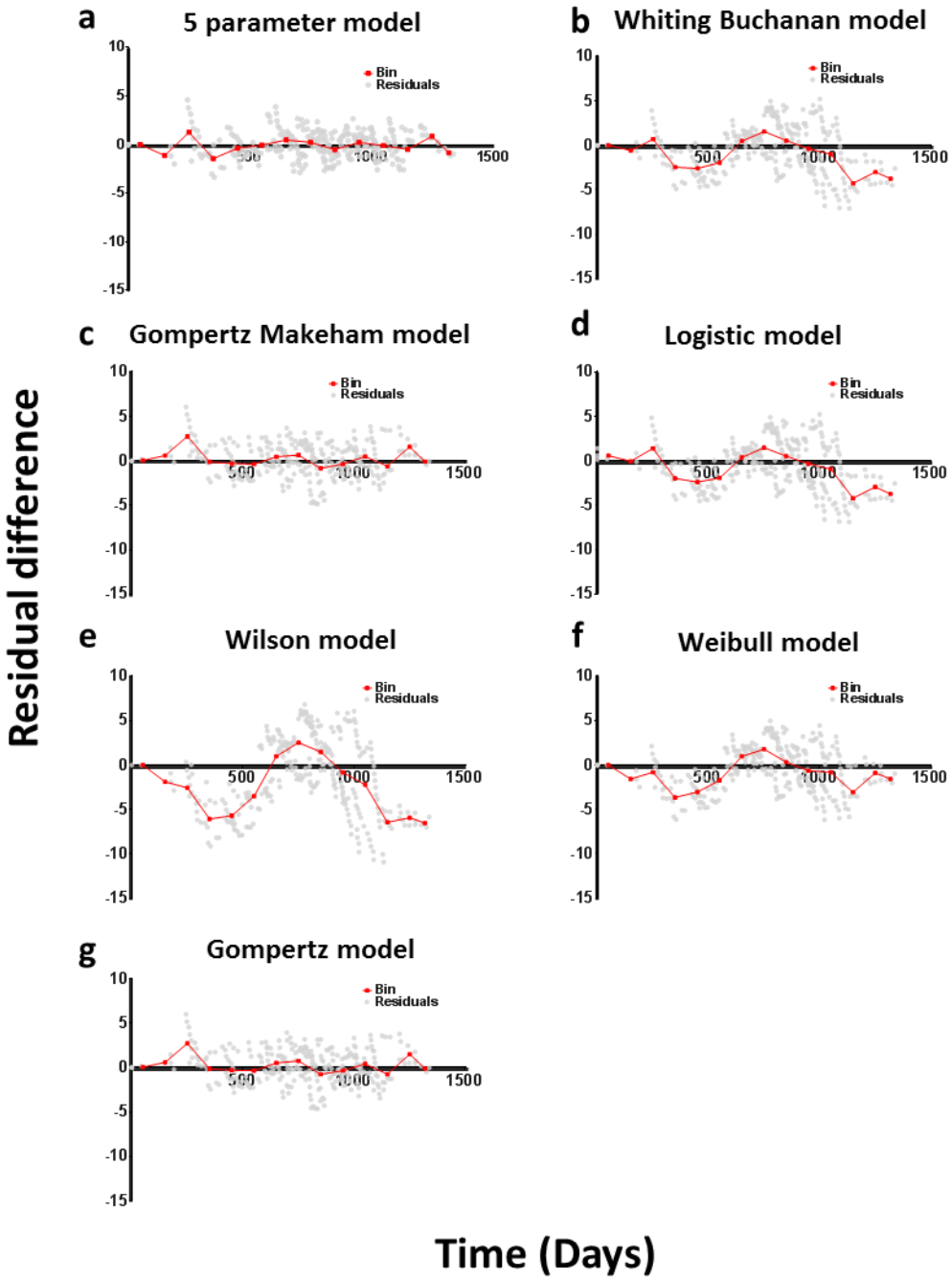

Figure 3.19: Analysis of lifespan models by residual difference analysis in male mice. Residual differences between the experimental data and the fitted curve from each model were calculated (grey dots) and data was grouped into bins of 100 days (red line). Smaller residual differences indicate better fit. Data for male mice **(a-g)** is from 3 replicate experiments.

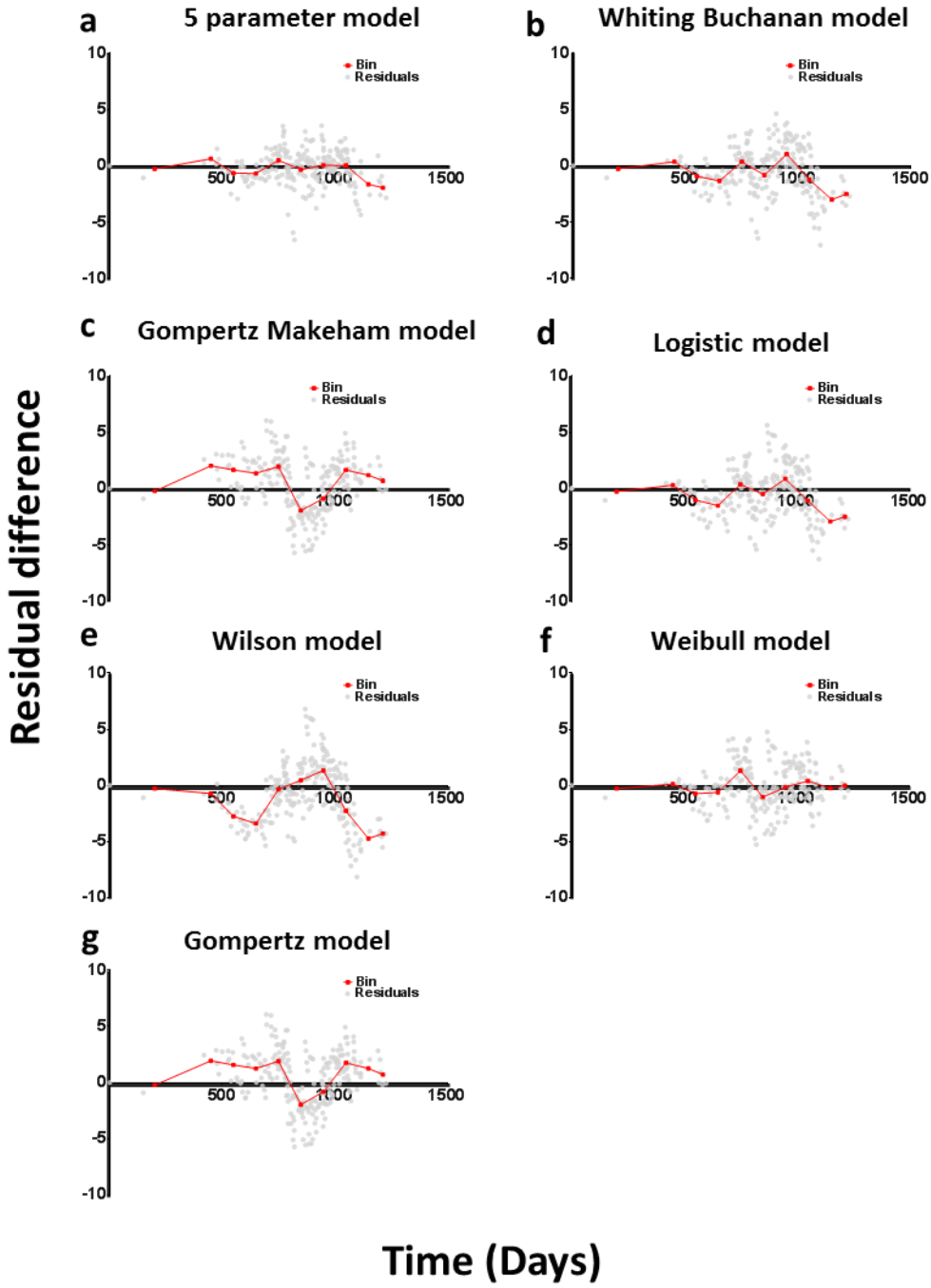

Figure 3.20: Analysis of lifespan models by residual difference analysis in female mice. Residual differences between the experimental data and the fitted curve from each model were calculated (grey dots) and data was grouped into bins of 100 days (red line). Smaller residual differences indicate better fit. Data for female mice **(a-g)** is from 3 replicate experiments.

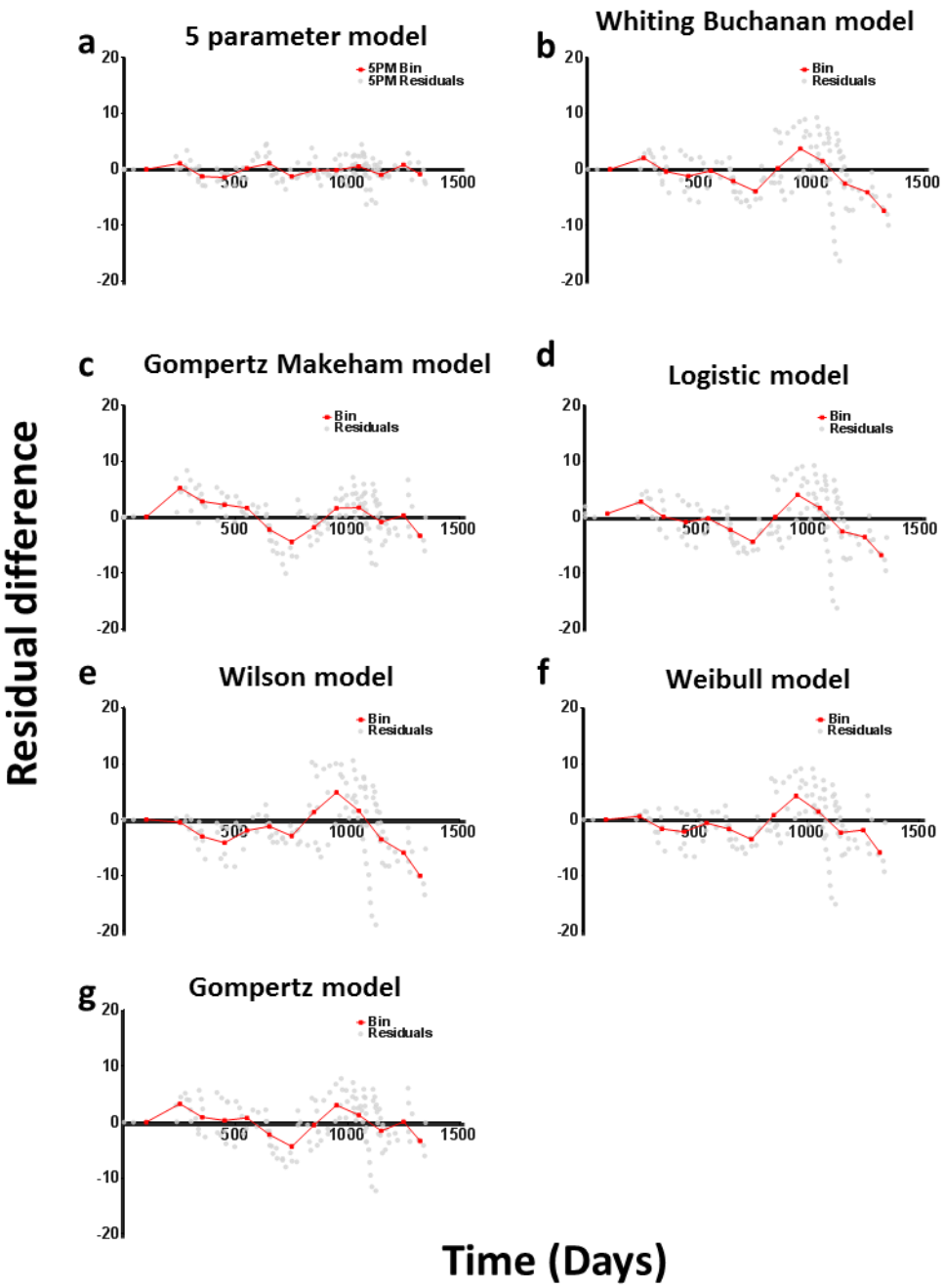

Figure 3.21: Analysis of lifespan models by residual difference analysis in rapamycin treated male mice**.** Residual differences between the experimental data and the fitted curve from each model were calculated (grey dots) and data was grouped into bins of 100 days (red line). Smaller residual differences indicate better fit. Data for male mice **(a-g)** is from 3 replicate experiments.

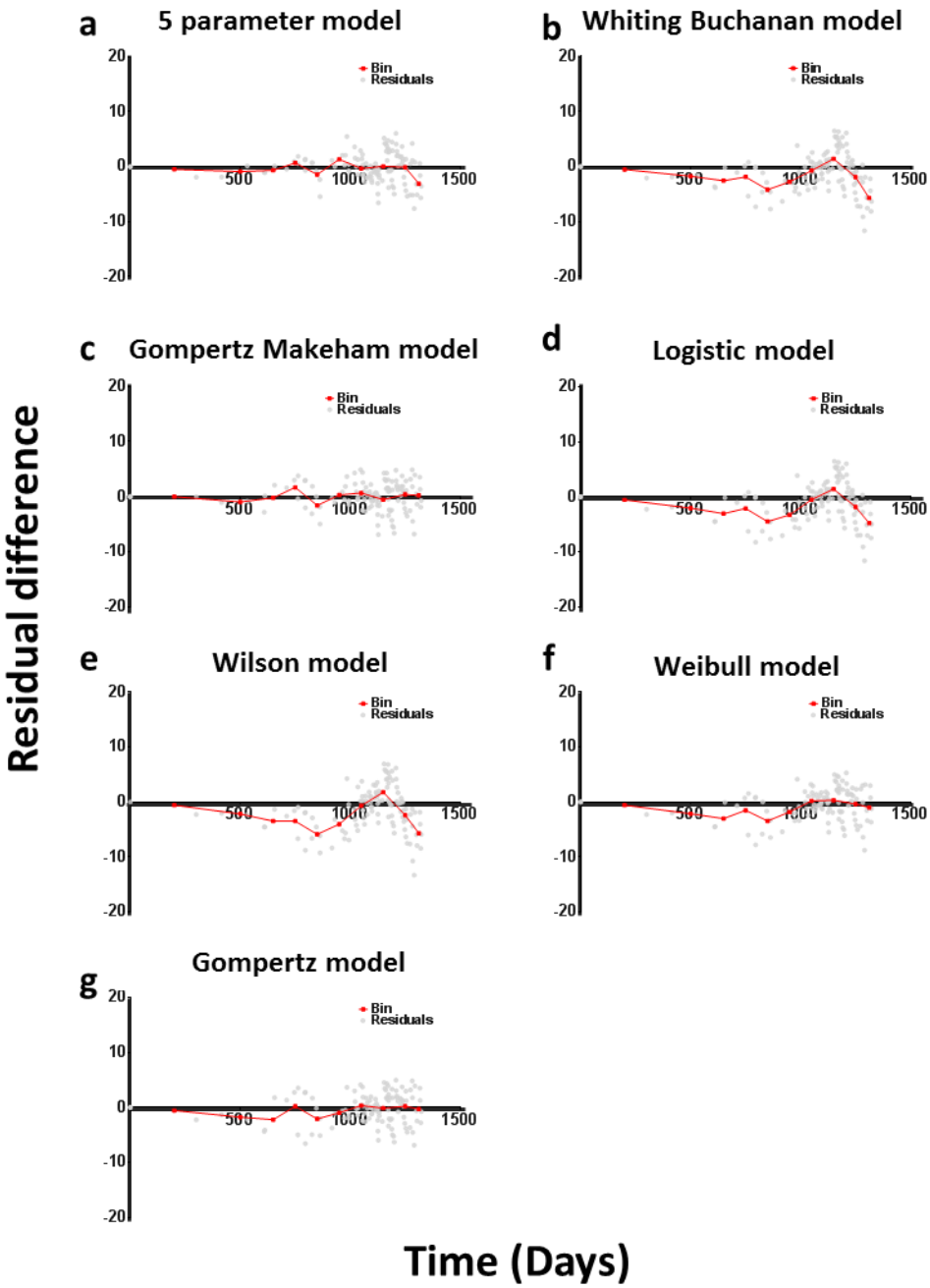

Figure 3.22: Analysis of lifespan models by residual difference analysis in rapamycin treated female mice. Residual differences between the experimental data and the fitted curve from each model were calculated (grey dots) and data was grouped into bins of 100 days (red line). Smaller residual differences indicate better fit. Data for female mice **(a-g)** is from 3 replicate experiments.

3.5 Discussion

This chapter has focused on introducing a novel 5-parameter Bilogistic model which is capable of fitting biphasic lifespan data. Additionally, this Bilogistic model was compared against a number of existing models and reduced versions of the Bilogistic model with fewer parameters. Furthermore, the Bilogistic model was used to model lifespan in a number of different animal models. In these animal models, lifespan modifiers such as genetic, pharmacological and environmental factors were quantitatively measured whilst taking into account multiple replicates.

Lifespan and survival are the results of a wide range of complex interactions within and amongst individual organisms, which makes discerning the effects of lifespan modifiers a challenging task. The log-rank test coupled to the Kaplan-Meier estimator works as a basic statistical test (Kaplan and Meier, 1958), comparing two curves and indicating whether they are statistically significantly different. With this testing methodology, there are two principal problems. The first lies in testing biological replicates as they often do not consistently show the same magnitude of effects. It is good experimental practice to observe similar results before reaching a conclusion and it is also good practice to compare the average of a control group to the average of a test group. Unfortunately, it is not possible to average different (Kaplan-Meier) lifespan curves due to differences in time of death. The second problem is due to the log-rank test not providing any further insight into where the difference lies i.e. the rate of death or the time of death.

Parametric models such as Gompertz and Weibull have previously been used to analyse and interpret such data (Lawless, 2014). By nature of using only two parameters, these models propose that lifespan follows a monophasic gradient (Vaupel et al., 1994) or shifts the lifespan curves along the time axis (Stroustrup et al., 2016). However, this assumes a monophasic lifespan with a uniform distribution throughout the lifespan, which is clearly not the case in many instances, furthermore biphasic dynamics can be more pronounced depending on experimental conditions or animal strains (Lucanic et al., 2017, Zhang et al., 2016). Note that the asymmetric shape of the Gompertz (and Gompertz-Makeham) curves can be referred to

as a biphasic, but this does not capture the dynamics described here as there is not an explicit exponential age-dependent component. These models also lack flexibility on the timing of biphasic dynamics and therefore fail to capture biphasic dynamics which are expressed during earlier or midway through the lifespan curves.

The experimental data clearly displays biphasic dynamics in certain conditions (e.g. *C. elegans* wild type (N2 strain) at 20°C, *daf-16*(*mu86*)). Furthermore, it has recently been reported that analysis of the pharynx of *C. elegans* corpses revealed two distinct death types which could be separated as occurring at an early and late phase (Zhang et al., 2016, Zhao et al., 2017). Thus, the timing of these phases seems to correlate well with this death phases shown by the Bilogistic model. Clearly the shape of the lifespan curve can reveal important clues to the action of lifespan modifiers. For example, both high temperature and loss of *daf-16/dfoxoΔ* increase the death rate in the 2nd phase in both worms and flies, suggesting that, in both organisms, the initiating events for death occur in the 1st phase. Rapamycin acts via delaying the onset of death in male but not female mice and has no effect on the rate of death. However, the death rate of bees is dependent on the level of external hazards, which is quite different for free flying and caged bees. The safe environment of the cages decreases the 1st phase death rate but at the same time it increases the 2nd phase death rate, most likely due to the fact that the bees are unable to leave the cage to carry out their dangerous foraging. Although the experimental organisms are isogenic, lifespan analysis shows that sub-populations of short- and long-lived individuals exist. The present analysis does not reveal the mechanisms behind the observed biphasic dynamics, although the wide range of lifespan modifiers may suggest a poly-mechanistic explanation. As the animal models are not closely related phylogenetically, this points towards a general mechanism operating on populations rather than on a specific conserved trait. It can only be speculated that the first phase corresponds to the growth and maturation of the organism (c.f. adolescence and adulthood) and the second phase to the post-maturation and the start of senescence.

As the shape of survival distribution is important (Wrycza et al., 2015), it is therefore crucial that parametric models capture the data as accurately as possible without smoothing important

aspects. Building on current parametric analysis, this study proposes a novel biphasic model which is able to model lifespan data in a variety of organisms commonly used for ageing research. The experimental data and residual differences for the Bilogistic model, its variants and several previously characterised parametric models have been carefully analysed. For each animal model used, i.e. worms, flies, bees and mice, the Bilogistic model performs better in fitting lifespan data compared to other models. By comparing it to simplified variants of the Bilogistic model it assesses the possibility that by using 5 parameters the model is overfitting the data. In some cases, lifespan modifiers do not significantly affect the weighting between the two phases (*f*; Table 3.1), suggesting one parameter can be removed by fixing *f* to 0.5. However, at least for the data sets studied, taking less than 5 parameters still weakens the general model's ability to fit the experimental data, particularly in individual cases. The model can be interpreted as an extension of a simple logistic model and a modification of the Whiting-Buchanan model (Whiting and Buchanan, 1993) with two instead of one time lag phase. A generalization to a triphasic model would be straightforward but is beyond the scope of this thesis.

As typical for survival models using logistic functions, it has not been derived from first principles, but is justified *a posteriori* due to its high predictive capacity. The results here agree with previous findings that logistic fittings provide better results than Gompertz-Makeham or Weibull fittings (Vanfleteren et al., 1998, Yashin et al., 2000), although the differences become clearly significant only for the full Bilogistic model. While five parameters might seem two too many, equations with up to 8 and 10 parameters have also been suggested (Siler, 1983, Heligman and Pollard, 2012). Based on goodness of fit testing and residual analysis, it is proposed that the full 5-parameter Bilogistic model is the preferred model to fit the majority of experimental lifespan data, although a reduced variant may be sufficient to fit other experimental data.

Table 3.1: *f* values for every experimental replicates performed. The organism and condition are labelled in the first and second row respectively.

	C. elegans						*Drosophila*		Bees		Mouse			
Replicate	N2 15°C	N2 20°C	N2 25°C	N2 30°C	N2	*daf-16*	w^{Dah}	dFOXO	Hived	Caged	Male Control	Male Rapamycin	Female Control	Female Rapamycin
1	0.8112	0.5318	0.5963	0.1803	0.5318	0.8976	0.1024	0.8027	0.1495	0.1761	0.2045	0.5962	0.2649	0.5764
2	0.5341	0.1088	0.7313	0.9334	0.1088	0.651	0.478	0.341	0.1378	0.4367	0.7431	0.8179	0.0447	0.1119
3	0.1216	0.1535	0.2138	0.38	0.1535	0.6965	0.579	0.863	0.2194	0.4108	0.6584	0.5838	0.8852	0.1494
4	0.647	0.7738	0.8425		0.7738	0.3215	0.417	0.9004	0.4102	0.2546				
5	0.4506	0.8034	0.4704		0.8034	0.2234	0.479	0.8578						
6	0.153	0.8236	0.2862		0.8236		0.04811	0.3577						
7	0.8524	0.8381	0.2784		0.8381		0.5299	0.3672						
8	0.3224	0.7923	0.1669		0.7923		0.1747	0.4125						
9	0.494	0.5501	0.1308		0.5501		0.796	0.5382						
10	0.8387	0.4171	0.3442				0.1287	0.514						
11	0.8533	0.0272	0.0946											
12	0.3089	0.3384	0.4338											
13	0.9284	0.6318	0.1593											
14	0.5625	0.4659	0.305											
15	0.5524	0.6418												
16	0.9503													
17	0.9271													
18	0.3958													
19	0.3296													
20	0.2539													
Average	0.56436	0.526509	0.360964	0.4979	0.59727	0.558	0.373281	0.59545	0.22923	0.31955	0.535333	0.665967	0.398267	0.279233
Median	0.54325	0.5501	0.2956	0.38	0.7738	0.651	0.4475	0.5261	0.18445	0.3327	0.6584	0.5962	0.2649	0.1494
N	20	15	14	3	9	5	10	10	4	4	3	3	3	3
Std Dev	0.27246	0.271595	0.228948	0.390148	0.28787	0.278859	0.246748	0.234072	0.12591	0.12496	0.289623	0.131724	0.435833	0.258036

Furthermore, the Bilogistic model is preferred to traditional methods as it allows statistical comparison of experimental replicates, an important analytical step which is lacking in many lifespan experiments. Unfortunately, in an increasing number of studies lifespan assays are only conducted in duplicate, with no statistical analysis of the replicates therefore resulting in weaker evidence which leads to the possibility of mistaken conclusions. In this study, a relatively large number of replicates has been used for each animal model. Backed up with the ability of this model allowing for a statistical analysis of the parameters, it provides confidence in the survival curves thus opening up the possibility to get insights into the mechanisms of action of the lifespan modifiers. Additionally, this model can be used to fit experimental lifespan data by easily inserting it in to commonly used statistical analysis programs such as GraphPad Prism and XLfit and programming languages such as MATLAB and R. Parameters from the curve fitting can then be grouped and statistically analysed. While other parametric and non-parametric models beyond Kaplan-Meier exist, their uptake by life scientists has been poor.

3.5.1 Future work

It is thought that this study will compel other researchers to use parametric modelling on their lifespan data making it a more prevalent approach. In addition to this this novel Bilogistic model has the potential to be useful in other fields of study. Many areas of research collect time to event data for example investigating bacterial or tumour growths and this model may provide an insight into the dynamics over time. Furthermore, application of this Bilogistic model to the lifespan of other model organisms will ascertain the possibility of universal lifespan properties across different species.

3.6 Conclusions

In conclusion, this chapter proposes a new parametric model for analysing lifespan assays. Having shown it is able to fit experimental data from a variety of animal models such as worms, flies, bees and mice, all of which exhibit biphasic dynamics and having carefully considered the danger of overfitting the experimental data residual difference analysis and goodness of fit tests show that the Bilogistic model offers a better fit than existing models. Finally, analysis of the parameters from curve fitting enables comparison of lifespan assays both within similar groups and among different experimental conditions and clearly offers an improvement on detecting the timing and magnitude to which lifespan modifiers are affecting survival. This novel Bilogistic model is therefore expected to facilitate the rational analysis of lifespan modifiers, e.g. through genetic analysis of long vs short lived sub-populations (Tissenbaum, 2012, Zhao et al., 2017), and improve understanding of their mechanisms of action.

Chapter 4.0: Modelling thermal intervention in *C. elegans*

4.1 Preface

Ageing research has focused on identifying lifespan modifiers and the extent to which they modify lifespan. A bigger challenge lies in investigating the dynamic effect of interventions which act to modify lifespan, such as genetic switches, environmental conditions and pharmacological treatment. In this section, the effects of switching temperatures (thermal intervention) from low to high and vice-versa on lifespan are investigated. Two predictive models, (which use the novel 5-parameter Bilogistic model) are proposed to model the effects of thermal intervention and are based upon either chronological age or biological age. Using average lifespan as a measure, the biological model is observed to better represent the experimental data from *C. elegans* subjected to thermal intervention. Additionally, the models predict critical time points for intervention such as the last possible time point for thermal intervention to affect lifespan and also time points at which it is too late for intervention to affect lifespan. Finally, further investigation is conducted into the temperature sensitive TRPA-1 channel protein in thermal determination of lifespan and lifespan intervention.

4.2 Introduction

4.2.1 The ageing complexity

Over the last few centuries, the lifespan of humans has increased resulting in a greater number of elderly people in the population. This is due to the sharp increase in improved standards of living, improved healthcare systems, advancement in biomedical and biotechnologies and lifestyle changes leading to a healthier lifestyle and genetic differences which collectively play a role to extend lifespan. This results in an increased prevalence of a number of ageing-related diseases which is plaguing the elderly and is driving up the cost of healthcare (Bansal et al., 2015).

4.2.2 Chronological age as a measure of ageing

Over the past few decades, lifespan or chronological age has been used as a surrogate measurement for the ageing process (Klass, 1977). Lifespan is clearly defined as a measurement of an organism's survival over time. This definition allows for easy measurement which is conducted by simple survival assays. Although extremely easy to conduct, there are positive and negative qualities in its ability to act as a measure of ageing. The chronological age of an individual is a measurement of lifespan. However, as a measure of ageing it is less meaningful due to intra individual variation. Population studies and the measurement of average lifespan of a population to generate survival curves are more useful and accurate measures of ageing.

4.2.3 Biological age as an alternative measure of ageing

Biological age is an alternative measure of the ageing process. Unlike chronological age which measures the time passed since birth, biological age is calculated from multiple different parameters which act as biomarkers of an organism's bodily function and its deterioration over time. Greater deterioration of the bodily functions which these biomarkers characterise result in a higher biological age. However, measurement of biological age is difficult because there is not a single direct measure. Biomarkers can be either lifestyle factors

or biomedical factors which can be investigated individually or collectively as a population to give a measure of biological age. However, these single tests of biomarkers show high inter- and intra- individual variability, making it difficult to extrapolate from a population, particularly when investigating treatments or intervention (Levine et al., 2018, Kato et al., 2006).

4.2.3.1 Healthspan

Healthspan is a measure linked to biological age but does not have a single universally accepted definition. Therefore, a standardised measure must be implemented before it can be widely used to act as a surrogate measure of ageing. One definition is that healthspan is a measure of the disease free or healthy time period of an individual's lifespan (Kaeberlein, 2018). Healthspan is characterised by a number of measures which identify if an individual is in a healthy state. Different studies measure a number of different parameters making it difficult to measure all of them and also difficult to standardise the measurements (Bansal et al., 2015). Coincidentally (or not) improvements to healthspan result in an increase in lifespan (Richardson et al., 2016).

4.2.3.2 Frailty Index and lifespan

Frailty index is another measure which determines the health status of an individual by looking at an index of health biomarkers and calculating healthy and frail (in deficit) proportions (Searle et al., 2008). Lifespan studies are able to provide data at various time points in which there is a proportion of the population that is in deficit (dead) and the remaining population which is alive and not in deficit. This assumption has been studied and found that the frailty index in humans and mice is a predictor of mortality (Rockwood et al., 2017, Goggins et al., 2005).

4.2.4 Importance of timing of intervention

Lifestyle change or pharmacological interventions are often implemented to prevent diseases so that individuals age more resiliently and healthily resulting in an improved healthspan (or reduced frailty) and a 'younger' biological age. The timing of these interventions is also

extremely important and it is reasonable to assume that the success of the intervention will only occur within a time window in which the internal mechanism is susceptible to change.

When investigating the effects of intervention both biological age and chronological age are important factors. However, as chronological age measurements have a single measure and can be conducted more easily than biological age they should be used first as a basic measure of intervention testing. Then, they should be verified and further analysed mathematically by parametric analysis to gain maximum information on the effects of intervention on a population (see chapter 3). Similarly, investigations can also be carried out to identify and understand the effect of different interventions on lifespan and also how the timing of the intervention affects the lifespan of the population.

4.2.5 The role of temperature on lifespan

There are many external environmental stimuli which can act as an intervention to extend lifespan such as diet, environment and pharmacological agents (Harrison et al., 2009, Wu et al., 2009). Environmental temperature is another main factor which influences lifespan, particularly in *C. elegans.*

The inverse relationship between lifespan and temperatures is well known and preserved across many organisms. It has been shown that a reduction in temperature results in an increased lifespan of many poikilotherms such as worms, flies and fish (Klass, 1977, Loeb and Northrop, 1916, Liu and Walford, 1966). Similarly, in the homeothermic mouse, it has been shown that a reduction in core body temperature results in an increased lifespan (Conti, 2008).

It has previously been hypothesised that the increase in lifespan is due to a reduction in chemical thermodynamic reaction rates (Shaw and Bercaw, 1962). This suggests a passive mechanism by which lifespan is extended and is in agreement with the rate of living theory (Pearl, 1928). However, it is highly unlikely to be the only mechanism by which lifespan extension occurs. It has been proposed that a more active physiological mechanism must exist which acts to control lifespan changes that is seen by altering the temperature (Conti,

2008). Naturally a genetic approach has been taken to investigate the mechanism by which temperature regulated lifespan extension occurs (Lee and Kenyon, 2009, Xiao et al., 2013, Miller et al., 2017).

One such proposed mechanism of temperature regulated lifespan extension is the somatosensory voltage dependent non-selective cation channel TRPA-1 (Transient Receptor potential ankyrin 1) which is expressed in many organisms including *C. elegans* and humans. TRPA-1 channels open in response to cool temperatures and act to target the master regulator of lifespan DAF-16 (the FOXO3 analogue) (Xiao et al., 2013). *Daf-16* is a transcription factor with over 3000 gene targets which act to extend lifespan, and investigations on its targets and mechanism of action is ongoing by many groups (Tepper et al., 2013). This role TRPA-1 has on regulating DAF-16 makes it an attractive target for investigating temperature-based lifespan extension.

4.2.6 Thermal intervention

One simple methodology of investigating temperature intervention is to look at differences between high and low temperature which act as a proxy for 'detrimental' and 'favourable' growth conditions. Worms can be grown and switched between these conditions at different time points in their life to see effects of intervention upon their lifespan and to identify critical time points at which intervention provides a beneficial effect on lifespan. Thermal intervention has been studied to an extent previously. One study (Zhang et al., 2015) exposed worms to normal growth temperatures (20°C) from eggs and switched the worms to either a high (25°C) or low (15°C) temperature at each larval stage and then back to the normal growth temperature (20°C) at adulthood. They found that growth at a low (15°C) temperature during developmental stages and transferring worms to normal temperature (20°C) at adulthood results in a reduction in lifespan, but developmental growth at a high temperature (25°C) and then switching to normal temperatures (20°C) at adulthood leads to an increase in lifespan. They also found L1 and L2 stages were critical for the worm in determining longevity and also that *trpa-1* was important in cold dependent lifespan extension (Zhang et al., 2015, Xiao et al., 2013).

Another study (Henderson et al., 2018) found similar results having conducted similar experiments whereby they exposed worms to high (25°C) or low (15°C) temperatures during development stages and switched to the opposite temperature at adulthood. They conclude that lifespan changes are dependent on redox levels with longer lived worms having fewer oxidants and short-lived worms having higher oxidant levels. Additionally they suggest this lifespan extension is due to increased *prdx-2* expression levels and the reduction in lifespan is due to reduced *prdx-2* levels (Henderson et al., 2018).

Another study (Wu et al., 2009) conducted similar experiments but focused on how lowering temperature or calorie restriction changes mortality. Mortality was analysed by using the Gompertz equation and investigating the differences in parameters α (Initial mortality) and β (rate of increase in mortality). They found there to be a delay of one day before changes in temperature changed mortality trajectory. Additionally, a change in mortality was seen when going from a high (25°C) temperature to a low temperature (16°C) when compared to 25°C but not 16°C. When switching from a low (16°C) temperature to a high (25°C) temperature an increase in mortality compared to 16°C is seen, but there is no difference in the increase in rate of mortality. They conclude by saying prior conditions are important in determining initial mortality rates but the current conditions determine future mortality rates (Wu et al., 2009).

These experiments show the importance of early developmental conditions which appear to play a role in determining the lifespan of worms. Therefore, the timing of the intervention is extremely important in determining the lifespan of these worms. Further to this, it would be useful to determine critical time points post-development as once adulthood has been reached conditions can change and influence lifespan.

Conducting these experiments to accurately identify critical time points is time consuming due to the number of lifespan assays and intervention times at which experiments can be conducted. Therefore, it would be beneficial to create a model which would accurately replicate the effects of intervention, which can then be tested against select experimental data for accuracy.

4.2.7 Aims and Objectives

This chapter aims to:

1) Develop predictive models which are able to use two initial survival curves from different conditions and combine them at different intervention times to generate theoretical curves representative of the different intervention times.
    a. Develop a predictive model based on chronological switching time.
    b. Develop a predictive model based on chronological switching time and survival proportions.
2) Compare the theoretical data from the two predictive models to experimental lifespan data from *C. elegans.*
3) Identify critical time points from theoretical and experimental data, at which predictions can be made regarding:
    a. The minimum time required to be spent in the favourable condition to gain full benefits of this condition.
    b. The minimum time required to be spent in the favourable condition to get any benefit from this compared to those who spend all their life in the detrimental condition.
    c. The maximum time spent in the detrimental condition before it is too late to gain any benefit from the favourable condition.

4.3 Materials and Methods

4.3.1 *C. elegans* lifespan assay

The *C. elegans* strains N2 (wild isolate), and *trpa-1*(*ok999*) were maintained on solid nematode growth media (NGM) plates supplemented with nystatin (10 µg/ml; Sigma) and seeded with *E. coli* OP50 strain at 20°C unless stated otherwise.

NGM plates used for lifespan assays were additionally supplemented with FuDR (50µM). Lifespan assays were conducted on a synchronised population of 50 L4 stage worms on fresh NGM FuDR plates as previously mentioned (section 2.2).

4.3.1.1 Temperature Intervention

In temperature intervention studies, *C. elegans* (L4 stage) were incubated at either at an initial temperature of either 15°C (favourable) or 25°C (detrimental) for a period of their lifetime and then incubated at the alternative temperature (25°C or 15°C) for the remaining length of their lifetime. N2 and *trpa-1(ok999)* strains were used in intervention experiments as multiple different time points were selected as intervention times at which the worms are switched between the two temperatures. Switching from 15°C to 25°C took place on days 5, 10, 13, 16 and 20, and switching from 25°C to 15°C took place on days 1, 3, 5, 8 and 12. Additionally switches which took place on day 0 was classified as being at the second temperature for their entire adult lifetime. Switches which took place on days 35 and 16 for 15°C and 25°C respectively are those which have not been switched and remained at the initial temperature for their entire adult lifetime (until death) (Figure 4.1).

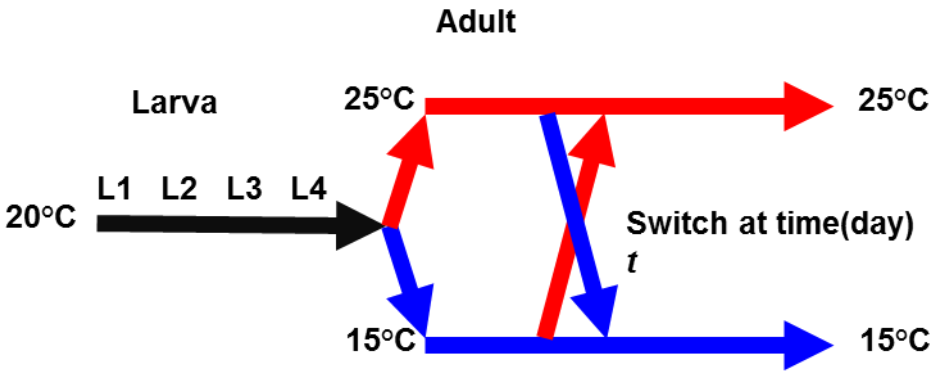

Figure 4.1: Temperature intervention timeline: Worms are synchronised and grown at 20°C until L4 stage and then transferred to 15°C or 25°C. At a given time *t* they are then switched to the opposite temperature (25°C or 15°C) until death.

4.3.2 Survival curve analysis

Kaplan-Meier survival curves were constructed by inputting events occurring at given time points into GraphPad Prism 7. Survival proportions at each time point were calculated and the novel 5-parameter Bilogistic model was used for fitting lifespan data (Equation 1). The *f* parameter splits the curve into two phases giving a weighting to each phase. There are two death rates (k_1 and k_2) and two time parameters t_1 and t_2, representing the median survival for each phase.

$$N(t) = N_0 \left[f \frac{1 + e^{-k_1 t_1}}{1 + e^{k_1 (t - t_1)}} + (1 - f) \frac{1 + e^{-k_2 t_2}}{1 + e^{k_2 (t - t_2)}} \right]$$

Equation 1: The 5-parameter Bilogistic model

4.3.3 Average lifetime and Median Survival

Average lifetime was calculated by finding the average time of death for a population (Sum of when worms die divided by the total number of worms that die). Average lifetime can be calculated for a whole population for their entire lifespan or for the worms remaining post intervention. This is equal to the integral of the survival curve. The median survival of a population is the time point at which 50% of a population is remaining.

4.3.4 Curve fitting

Non-linear regression models which were based on logistic functions were used to fit curves to the survival proportions. The MATLAB (MathWorks) Curve fitting toolbox (R2016a, v9.0.0.370719) and sfit objects were used to fit data using a non-linear least squared fit method (Trust-Region algorithm) to estimate parameters. When fitting the survival data, other settings were kept to default: Robust=Off, DiffMinChange=0.00000001, DiffMaxChange=0.1, MaxFunEvals=600, MaxIter=400, TolFun=0.000001, TolX=0.000001.

4.3.4.1 Average lifetime statistical analysis

After average lifetime values were obtained statistical analysis was conducted. GraphPad Prism was used to perform an ordinary one-way Analysis of Variance (ANOVA), with all groups compared to one another (non-repeated measure). In conjunction to this ANOVA, Tukey's multiple comparison test was also conducted. Statistical *p*-values $p<0.05$, $p<0.01$, $p<0.001$ and $p<0.0001$ shows a statistically significant difference between groups and is indicated in the figures.

4.3.5 Lifespan predictions from 2 models

MATLAB was used to create scripts (Appendix 8.2-8.5) which allowed the generation of switched survival curves for temperature switches from 15°C to 25°C and 25°C to 15°C for any time point based upon an initial data set of worms grown throughout their lifetime at either 15°C or 25°C. Generated survival curves follow the path of worms in the first condition (either 15°C or 25°C) and at the switch time follows the survival curve path of worms in the second condition. This can be done in two ways. The first is the chronological model (Appendix 8.2 & 8.3) which is able to make predictions based upon chronological age which refers to the time in days that the worm has been an adult (since day 0). The second is the biological model which is based upon biological age (Appendix 8.4 & 8.5) and the percentage alive and therefore assumes that at a given percentage alive from a population, worms have the same biological age.

Chronological age follows the path of the initial temperature and at any time point is able to switch to the other temperature but to account for the difference in survival proportions (percent alive) at the given switch time the second survival curve is rescaled so that the survival curve becomes continuous. To rescale the second temperature survival curve, a ratio of the survival proportions (percent alive) of the first condition over the survival proportions (percent alive) of the second condition is taken and incorporated to scale down the survival curve of the second condition so that the curve is continuous from pre-switch to post-switch (Figure 4.3a).

Biological age is based upon the survival proportion of a population which follows the path of the initial temperature and then switches to the second temperature but takes into account the survival proportions (percent alive) of the first condition. The post switch curves start at the survival proportion at the point where the first condition survival curve ends at the switch time point and continues onwards from the point at which the survival proportions is equal (rather than from the start of the curve). The post switch survival curve is shifted so that the survival proportions match at the same switch time point (Figure 4.4a).

Computer generated switched survival curves from either model can then be compared to experimental data and differences can be identified. This can be done by calculating the integral (which equates to the average lifetime of the survival curves) and compare the computer generated and experimental data sets.

4.4 Results

A temperature-based effect upon lifespan of *C. elegans* is observed in both wild type (N2) and *trpa-1(ok999)* mutant worms. The lower temperature and more favourable condition of 15°C results in a longer lifespan compared to the higher temperature and unfavourable condition of 25°C which results in a shorter lifespan. In wild type worms, the average lifespan is ~20 days at 15°C but ~10 days at 25°C (Figure 4.2).

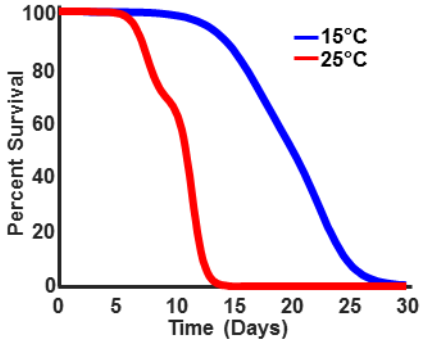

Figure 4.2: Fitted survival curves of wild type (N2) *C. elegans* at 15°C and 25°C. Data for 15°C (n=27 trials), data for 25°C (n=20 trials).

4.4.1 Predictive modelling of lifespan

Two models have been developed to predict the effect of lifespan intervention. In this study, 2 temperatures (15°C and 25°C) are investigated by switching wild type and mutant worms between the temperatures at different time points.

4.4.1.1 Chronological Model

Firstly, a chronological model is considered, which only takes into account the time the temperature switch occurred (Figure 4.3a).

The chronological model predicts that switching from a favourable condition of 15°C to a less favourable condition of 25°C leads to a reduction in lifespan. Additionally, the time at which this switching occurs is important. i.e. the earlier the switch from 15°C to 25°C the shorter the lifespan (Figure 4.3b).

Switching from the less favourable temperature of 25°C to the more favourable condition of 15°C extends the lifespan. Again, the timing of the switch is important in determining the lifespan of worms: earlier switches from 25°C to 15°C predicts longer lifespans due to the greater proportion of time spent at 15°C than 25°C (Figure 4.3c).

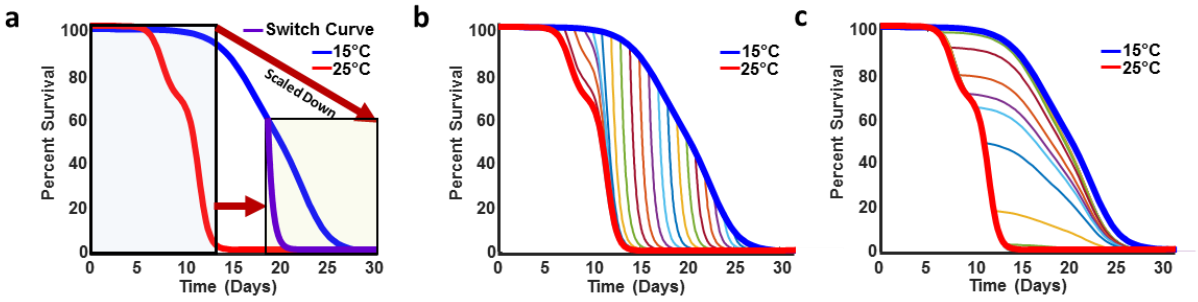

Figure 4.3: The chronological model **(a)** Chronological model showing the 25°C (red) curve scaled down (curve in grey box scaled down to yellow box) at the switch time to match the survival proportions of the 15°C (blue) curve. The switched curve is shown in purple. **(b)** Predictions for the chronological model when switching from 15°C to 25°C. **(c)** Predictions of the chronological model when switching from 25°C to 15°C Colours indicate stepwise change in intervention time (day by day).

4.4.1.2 Biological Model

An alternative model to predict the effect of intervention on survival curves is a model that takes into account both the chronological time point of switching and the survival proportion of the worms which are undergoing the switch (Figure 4.4a). When switching from 15°C to 25°C, the biological model shows similar predictions to the chronological model, although, the predicted lifespans more closely resemble the initial condition (Figure 4.4b). Additionally, the relationship between lifespan and the time of switching is predicted to be more linear compared to the chronological model. When switching from 25°C to 15°C, the biological model shows that the relationship between lifespan and switch time is not linear as many different switch times overlap (Figure 4.4c).

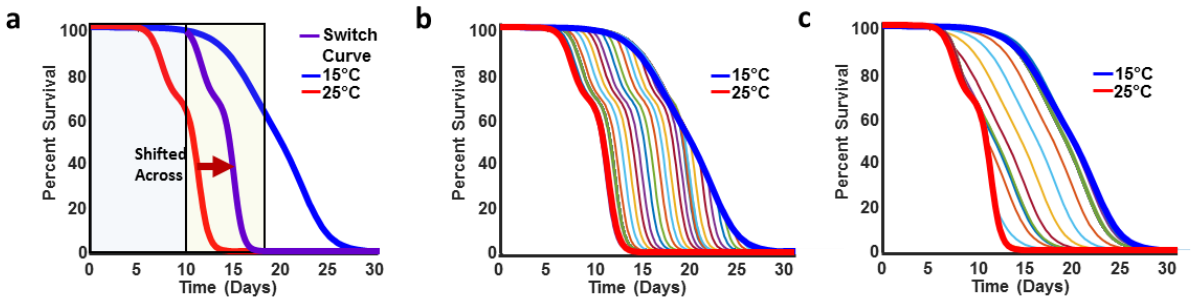

Figure 4.4: The biological model **(a)** Biological model showing the 25°C (red) curve shifted across (curve in grey box shifted across to yellow box) at the switch time to match survival proportions of the 15°C (blue) curve. The switched curve is shown in purple. **(b)** Predictions for the biological model when switching from 15°C to 25°C. **(c)** Predictions of the biological model when switching from 25°C to 15°C. Colours indicate stepwise change in intervention time (day by day)

4.4.1.3 The effect of thermal intervention on average lifespan

Having conducted thermal intervention experiments on *C. elegans* at 5 different time points, a relationship curve to show the experimental effect of thermal intervention upon average lifespan was generated. Initially the experimental data supports the theory that worms which have undergone thermal intervention generate hybrid survival curves of the two conditions which they are in.

Comparing the experimental survival curves with the chronological model computer generated curves for both 15°C to 25°C (Figure 4.5a-e) and 25°C to 15°C (Figure 4.6a-e) and also the biological model computer generated curves for both 15°C to 25°C (Figure 4.7a-e) and 25°C to 15°C (Figure 4.8a-e) show that, in more cases the biological model is closer at modelling the experimental curves more accurately than the chronological model.

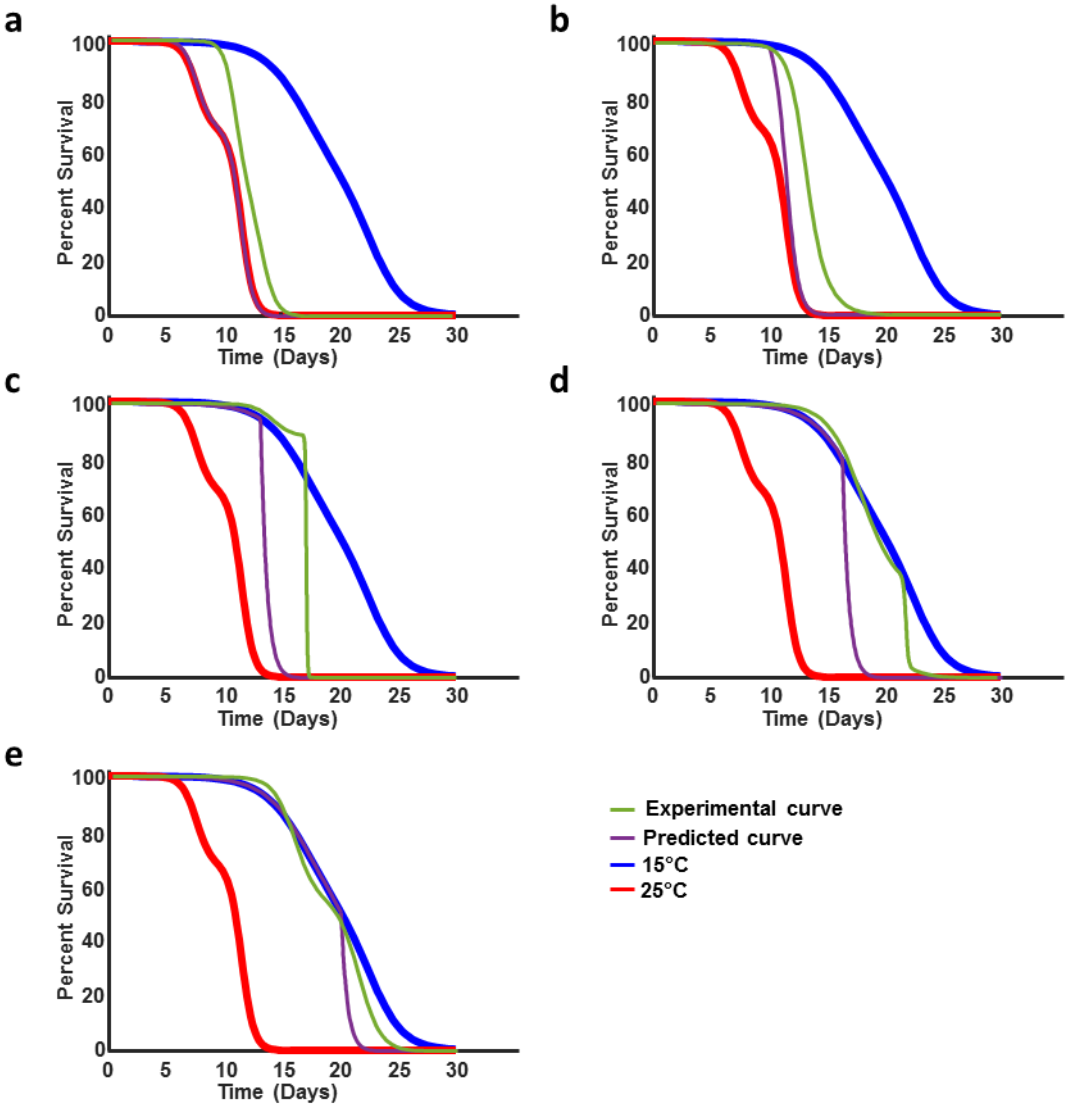

Figure 4.5: Chronological model predictions and experimental data for 15°C to 25°C. Switch days **(a)** 5, **(b)** 10, **(c)** 13, **(d)** 16 and **(e)** 20. Experimental data for switch day 5 (n=3), 10 (n=3), 13 (n=3), 16 (n=4), 20 (n=3)

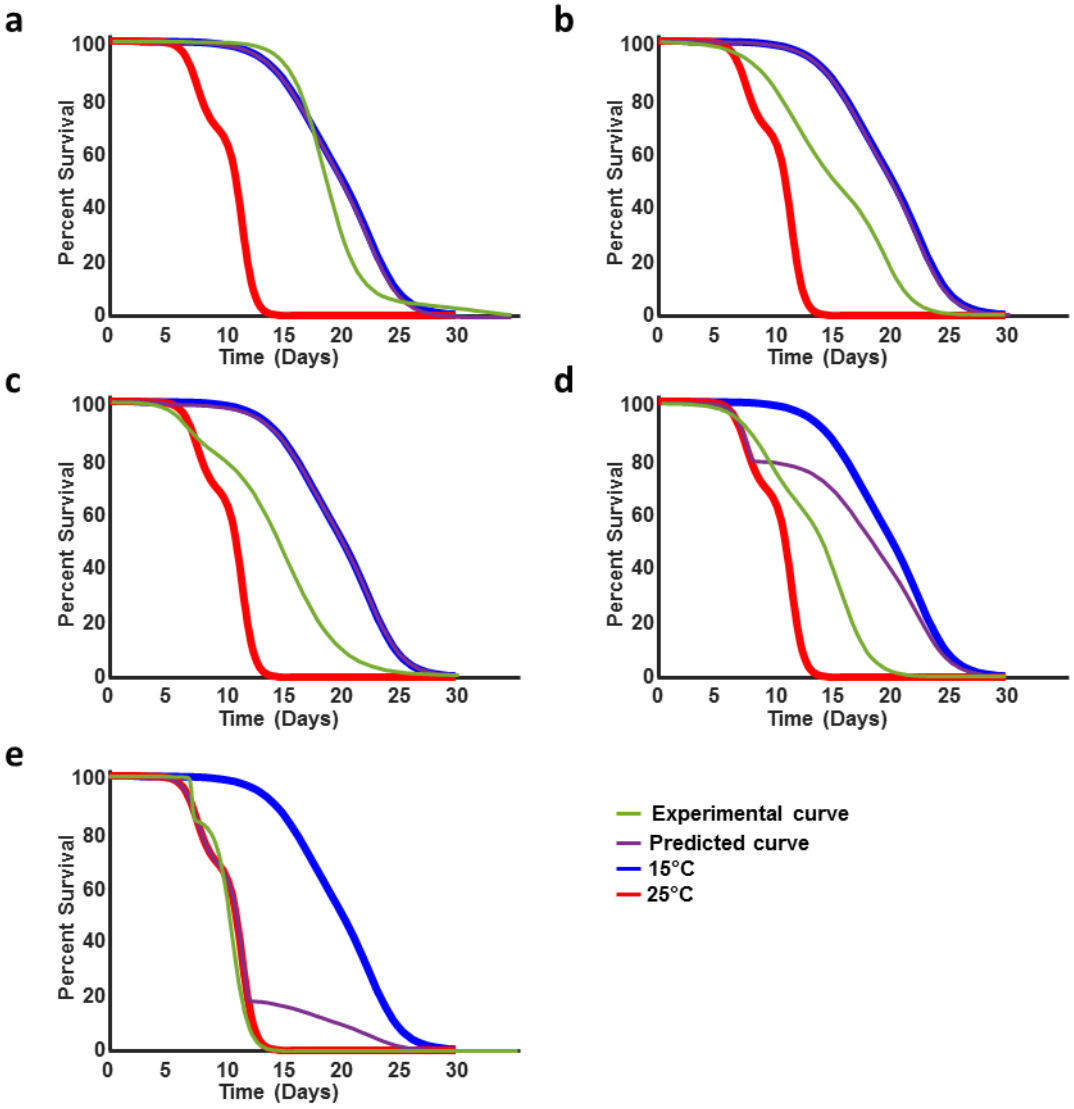

Figure 4.6: Chronological model predictions and experimental data for 25°C to 15°C. Switch days **(a)** 1, **(b)** 3, **(c)** 5, **(d)** 8 and **(e)** 12. Experimental data for switch day 1 (n=3), 3 (n=3), 5 (n=3), 8 (n=4), 12 (n=3)

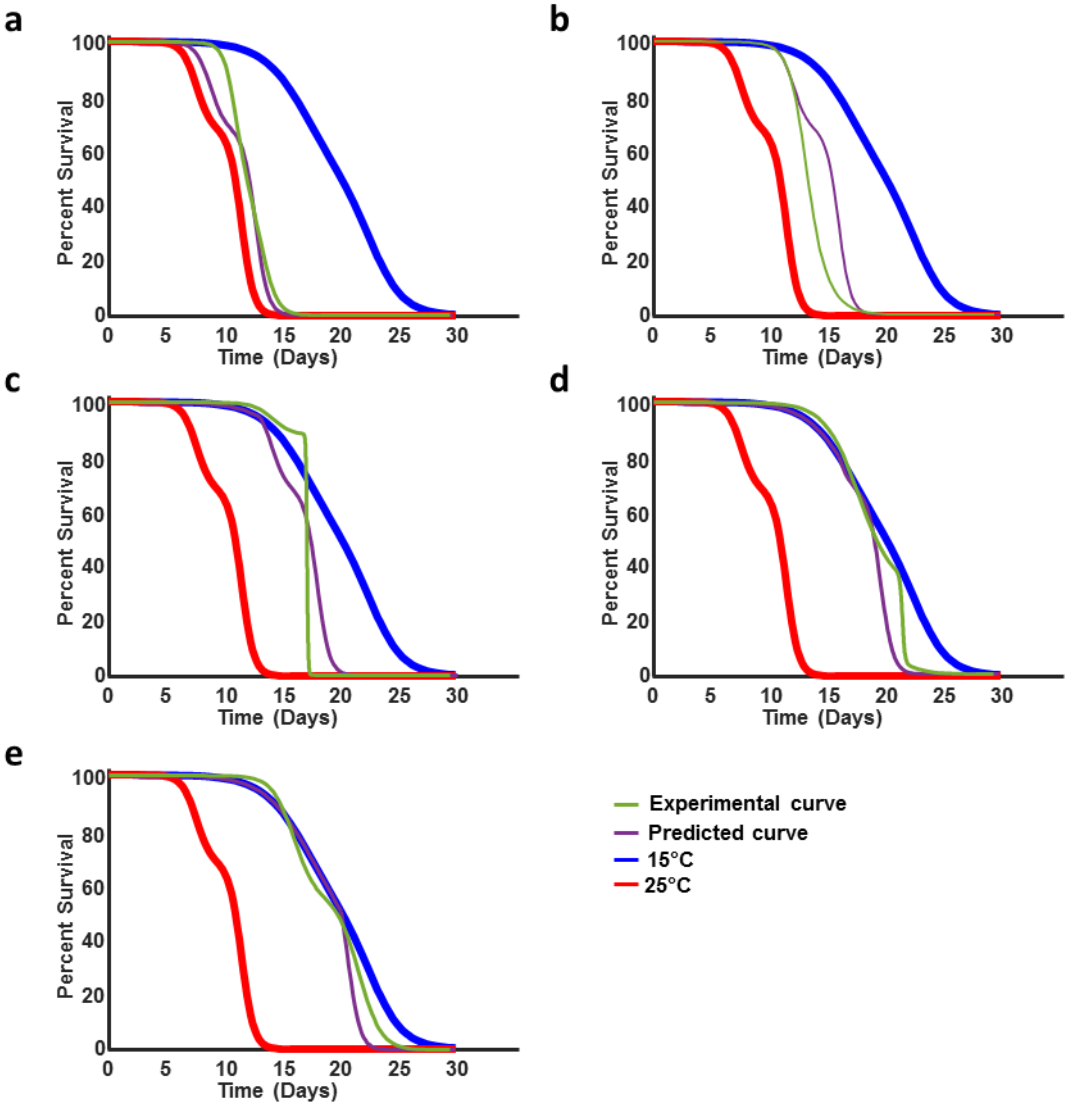

Figure 4.7: Biological model predictions and experimental data for 15°C to 25°C. Switch days **(a)** 5, **(b)** 10, **(c)** 13, **(d)** 16 and **(e)** 20. Experimental data for switch day 5 (n=3), 10 (n=3), 13 (n=3), 16 (n=4), 20 (n=3)

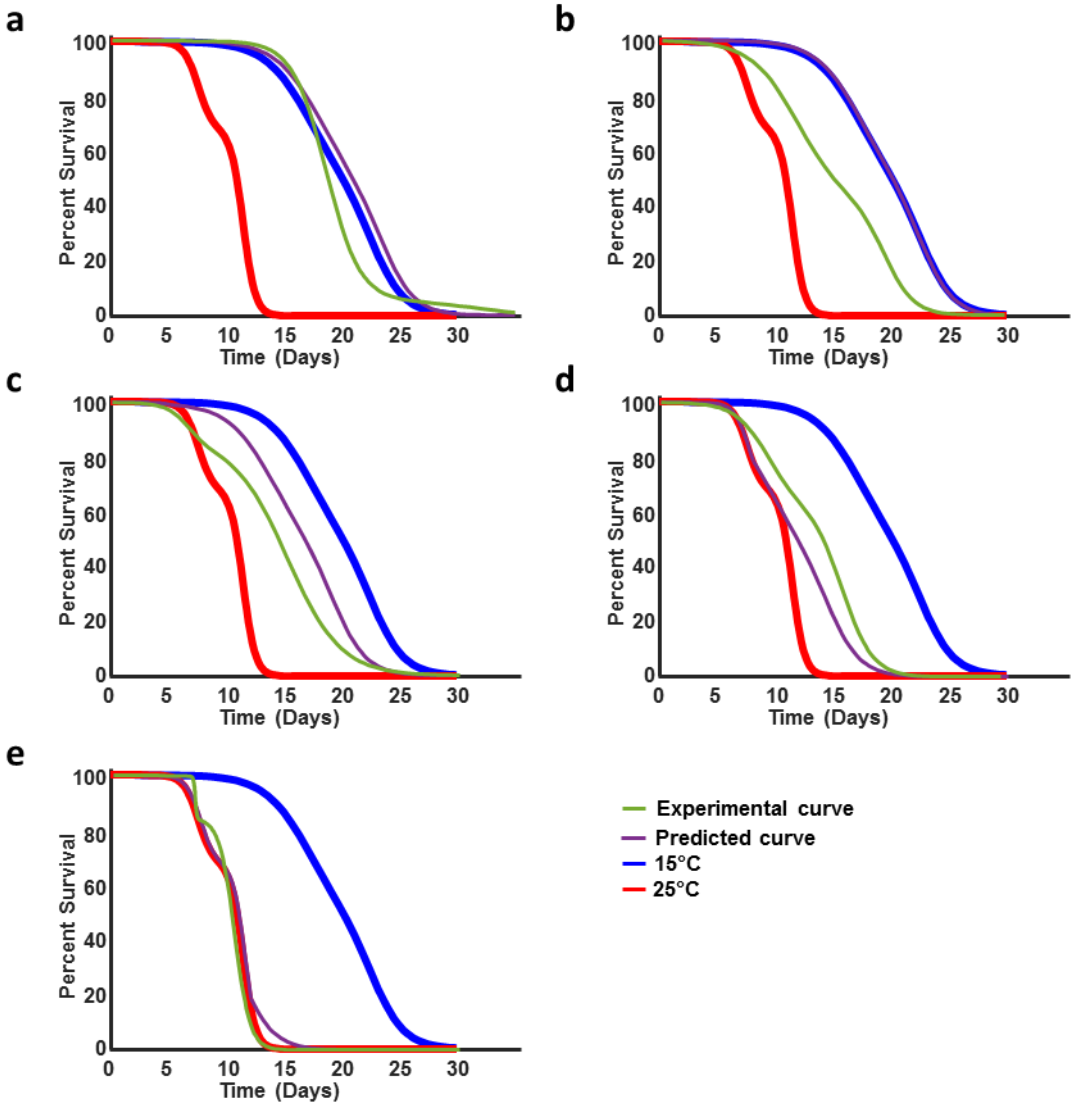

Figure 4.8: Biological model predictions and experimental data for 25°C to 15°C. Switch days **(a)** 1, **(b)** 3, **(c)** 5, **(d)** 8 and **(e)** 12. Experimental data for switch day 1 (n=3), 3 (n=3), 5 (n=3), 8 (n=4), 12 (n=3)

Additionally, the relationship between average lifespan and thermal intervention times of the two predicted relationships from the models shows that the biological model prediction is a more accurate model of thermal intervention compared to the chronological model (Figure 4.9).

Experimentally, the thermal intervention from 15°C to 25°C results in an increase in lifespan with later intervention times. From this a critical time point of 13 days can be identified, as spending a minimum of 13 days is required to gain a benefit from the favourable conditions of 15°C, to spend any longer than this is not detrimental to the lifespan of the worm but also

does not provide any significant extra benefit. Similarly, if only 10 days (or less) are spent at the favourable condition than a significant reduction in average lifespan is seen (Figure 4.9a). This is important as it shows that there is an irreversible time point beyond which the intervention is unable to make a difference. Additionally, it shows that before this time, lifespan can be altered to an extent but the later the intervention occurs the less impact it has.

Investigating interventions from 25°C to 15°C uncovers several critical time points. A critical time point of 3 days is identified as spending longer than 3 days at the unfavourable condition of 25°C shows an irreversible reduction in average lifespan compared to those not experiencing the unfavourable condition at 15°C. Additionally, spending longer than 8 days in the unfavourable conditions will result in an irreversible reduction in lifespan to the point where there is no significant difference to those that have spent their entire lifespan in the unfavourable condition (Figure 4.9b). This means that, after 8 days it is too late for any chance of recovery by intervention (switching to the favourable condition of 15°C). Again, this indicates that the timing of the intervention is extremely important and that leaving a beneficial intervention too late will have no effect.

For the 15°C to 25°C thermal intervention, the biological model is much more accurate in predicting the effect of the temporal thermal intervention compared to the chronological model. The biological model has a similar average lifespan at most time points of switching with few deviations at the extreme ends (when switching occurs very early or very late in the lifespan of the worm; Figure 4.9a). Overall however, it is a good predictor unlike the chronological model which appears to be consistently underestimating the average lifespan of the worms undergoing thermal intervention, with an average difference between experimental results and predicted data from the chronological model of 4 days and biological model is within a 1-day difference (Figure 4.9a).

With the opposite thermal intervention (from 25°C to 15°C), similar results are seen. The biological model is observed to be a more accurate predictor of thermal intervention compared to the chronological model and can differ slightly by a few days compared to the experimental data. Once again, the chronological model overestimates average lifespan,

although in this case it is less clear due to greater variations depending on the intervention time. The biological model is closer although it initially overestimates the average lifespan and at later intervention times it underestimates the average lifespan by a 2 day margin (Figure 4.9b).

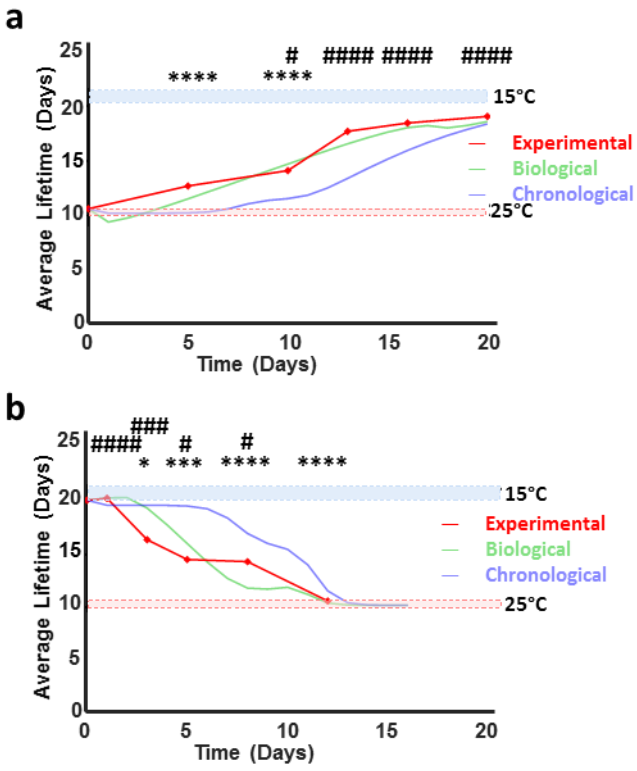

Figure 4.9: Comparison of predicted average lifespan of wild type *C. elegans* by chronological model and biological model with experimental data. **(a)**15°C to 25°C. **(b)** 25°C to 15°C. One-way ANOVA with Tukey's multiple comparison test. *shows statistical comparison to 15°C, # shows statistical comparison to 25°C. ****p<0.0001, ***p<0.001, *p<0.05, ####p<0.0001, #p<0.05.

4.4.2 The role of TRPA-1 in temperature regulation of lifespan

The *trpa-1(ok999)* mutant shows varying results when the same methodology is applied. The temperature dependent lifespan reduction due to the *trpa-1* mutation is not seen in this investigation as a similar lifespan to wild type is seen in both cases. The average lifespan for *trpa-1* mutants is ~21 days at 15°C and ~11 days at 25°C (Figure 4.10). However, there are varied effects the intervention has on lifespan. Neither the chronological model (Figure 4.11a, b), nor biological model (Figure 4.11c, d) are entirely suitable models to predict how

intervention affects the survival of *trpa-1(ok999)* mutants (Figure 4.12, 4.13, 4.14, 4.15). However, a general increase in average lifespan of *trpa-1(ok999)* mutants is observed compared to wild type worms but it is not significant to suggest that TRPA-1 may play a part in temperature-based regulation of lifespan (Figure 4.9a, b and 4.16a, b).

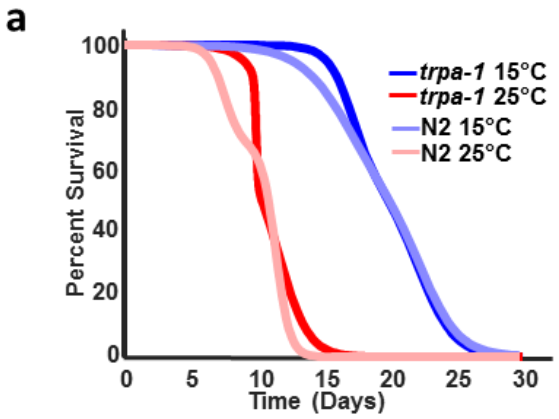

Figure 4.10: Fitted survival curves of *trpa-1(ok999) C. elegans* at 15°C (dark blue) and 25°C (dark red) compared to N2 at 15°C (light blue) and 25°C (light red). Data for *trpa-1* 15°C (n=12 trials), data for *trpa-1* 25°C (n=7 trials). Data for N2 15°C (n=27 trials), data for N2 25°C (n=20 trials).

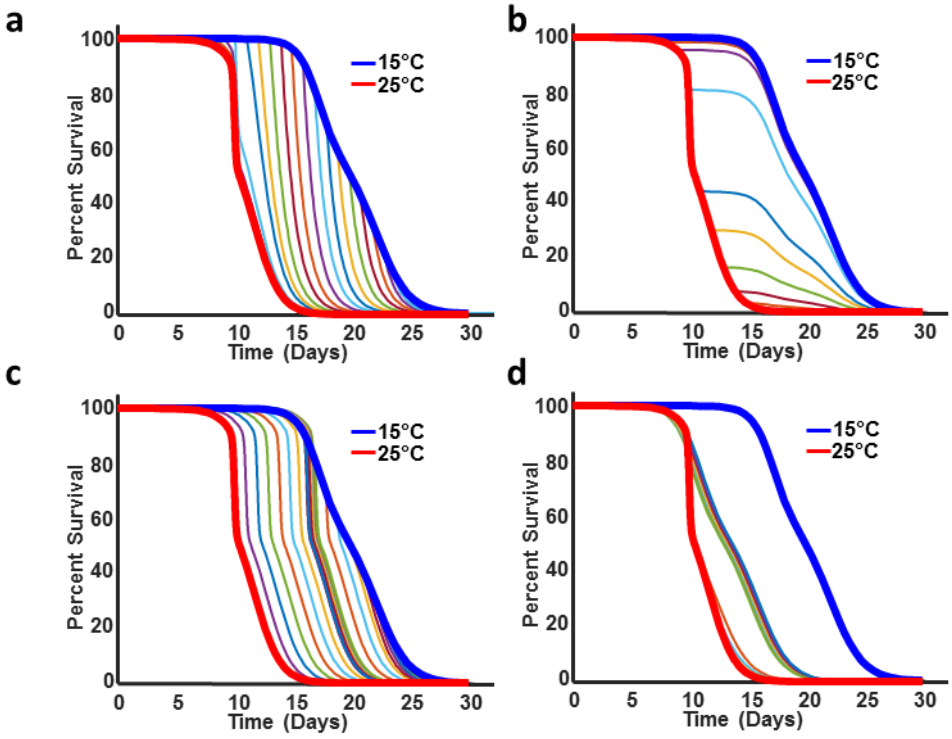

Figure 4.11: *trpa-1(ok999)* survival predictions **(a)** Predictions for the chronological model when switching from 15°C to 25°C. **(b)** Predictions of the chronological model when switching from 25°C to 15°C. **(c)** Predictions for the biological model when switching from 15°C to 25°C. **(d)** Predictions of the biological model when switching from 25°C to 15°C.

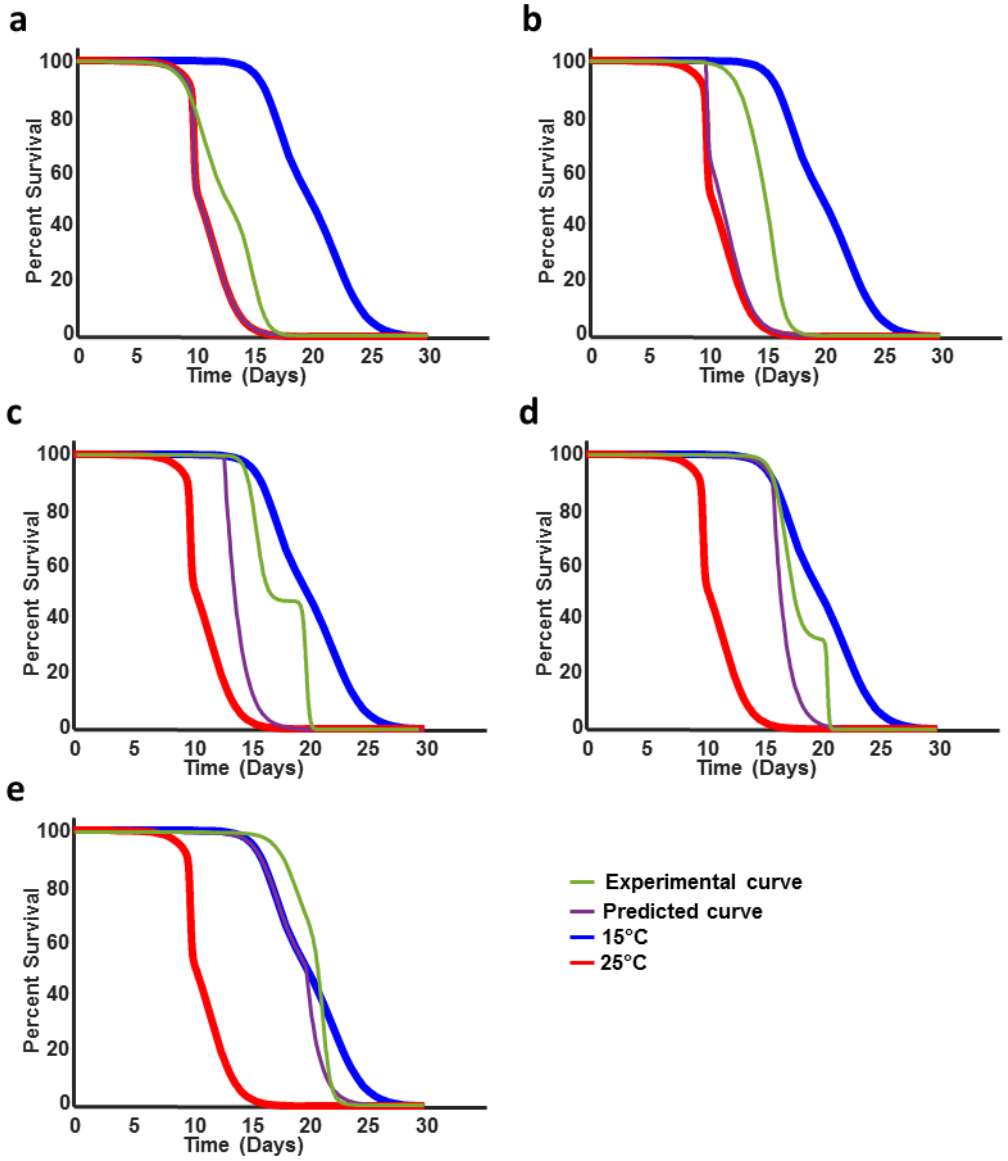

Figure 4.12: *trpa-1(ok999)* chronological model predictions and experimental data for 15°C to 25°C. Switch days **(a)** 5, **(b)** 10, **(c)** 13, **(d)** 16 and **(e)** 20. Experimental data for switch day 5 (n=3), 10 (n=3), 13 (n=3), 16 (n=3), 20 (n=3)

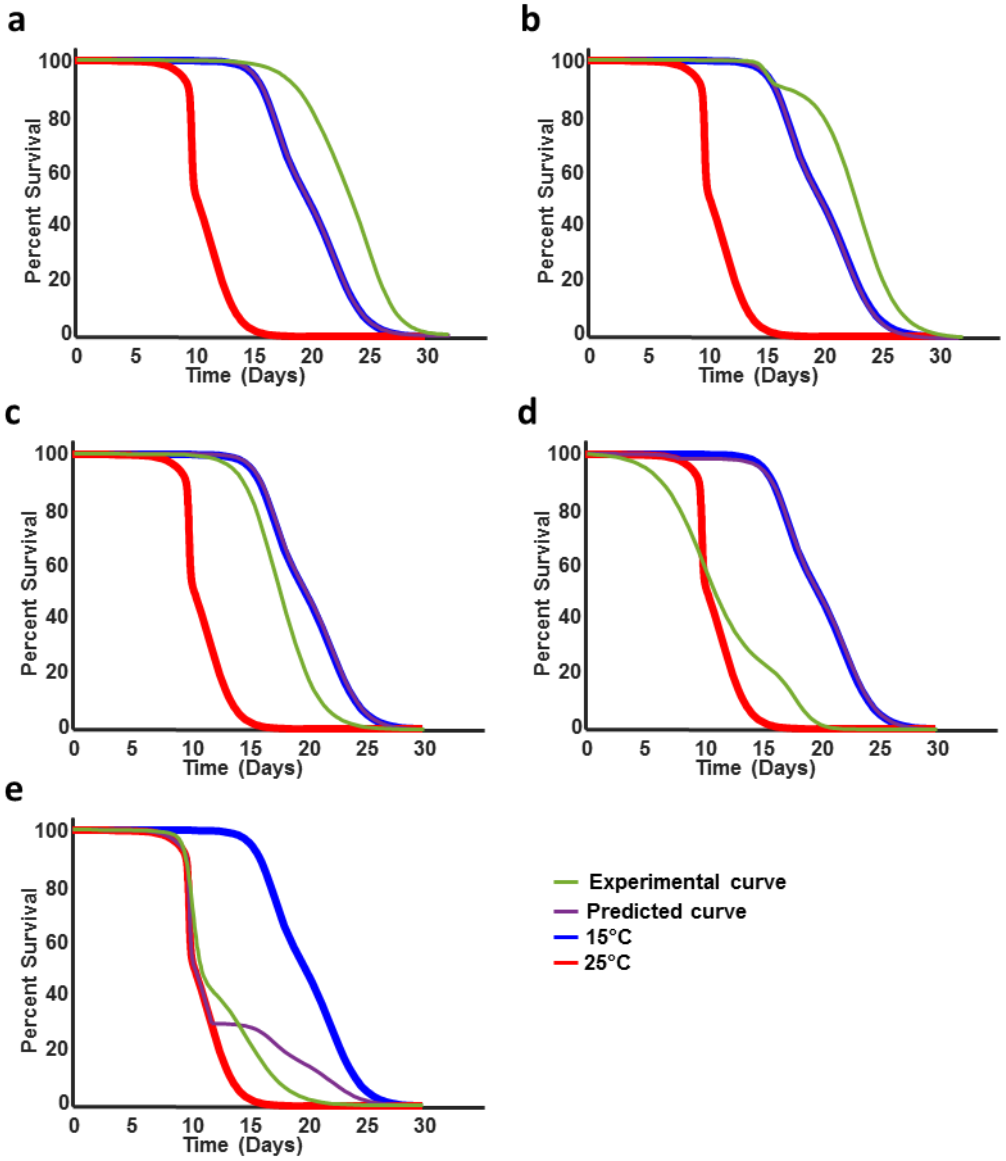

Figure 4.13: *trpa-1(ok999)* chronological model predictions and experimental data for 25°C to 15°C. Switch days **(a)** 1, **(b)** 3, **(c)** 5, **(d)** 8 and **(e)** 12. Experimental data for switch day 1 (n=3), 3 (n=3), 5 (n=3), 8 (n=3), 12 (n=3)

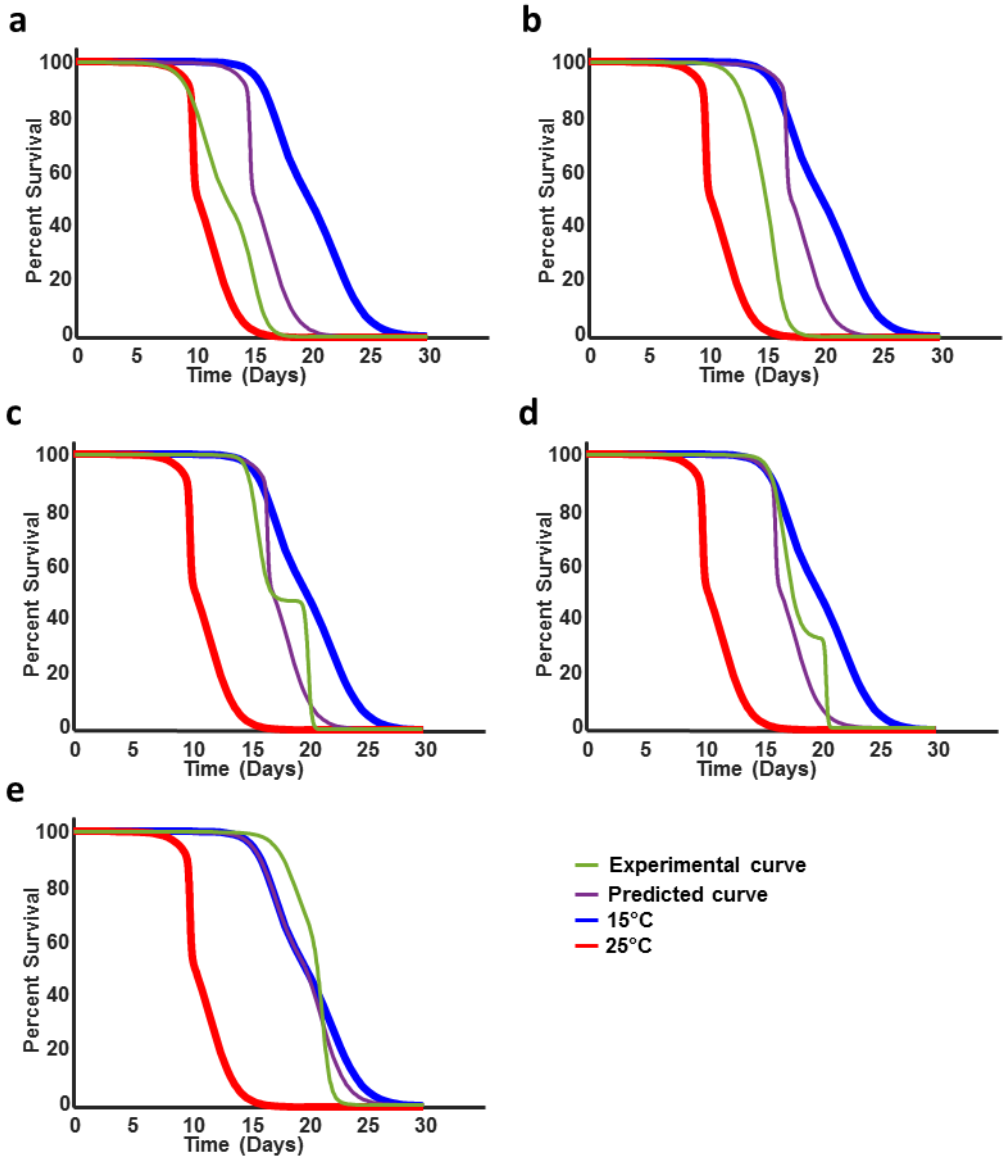

Figure 4.14: *trpa-1(ok999)* biological model predictions and experimental data for 15°C to 25°C. Switch days **(a)** 5, **(b)** 10, **(c)** 13, **(d)** 16 and **(e)** 20. Experimental data for switch day 5 (n=3), 10 (n=3), 13 (n=3), 16 (n=3), 20 (n=3)

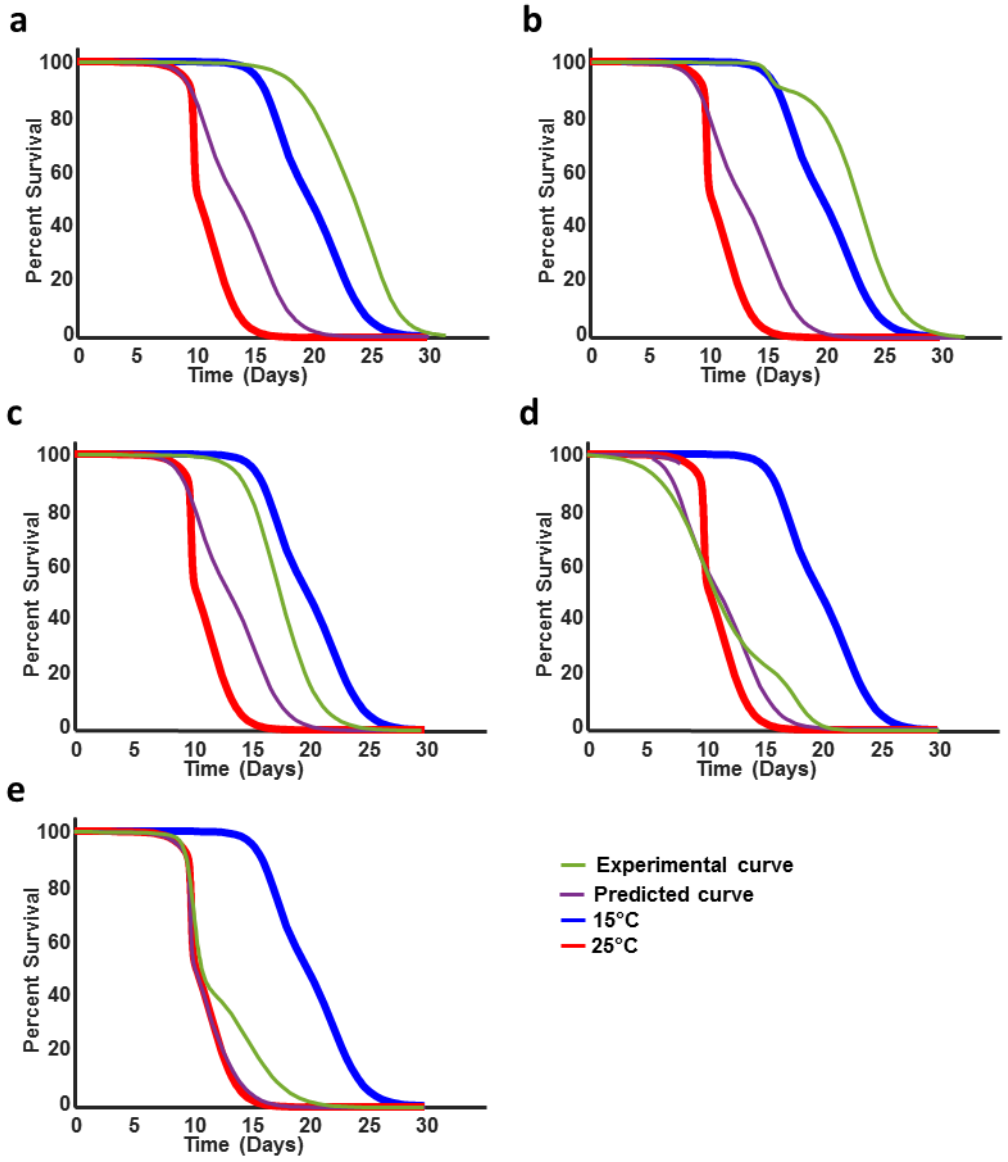

Figure 4.15: *trpa-1(ok999)* biological model predictions and experimental data for 25°C to 15°C. Switch days **(a)** 1, **(b)** 3, **(c)** 5, **(d)** 8 and **(e)** 12. Experimental data for switch day 1 (n=3), 3 (n=3), 5 (n=3), 8 (n=3), 12 (n=3)

The *trpa-1(ok999)* mutant has an impaired overall ability to adapt from both 15°C to 25°C or from 25°C to 15°C as the average lifespan is closer to the 25°C worms compared to wild type (Figure 4.9a, b and 4.16a, b). However, *trpa-1(ok999)* mutants switching from 25°C to 15°C in the early switch stages (days 1 and 3) show a slight but not significant increase in average lifespan compared to those which have spent their entire lifespan at 15°C.

Neither the chronological or biological models are able to predict this effect but instead demonstrate that the average lifespan remains constant for most of the lifespan intervention times and does not change until later lifespan intervention times (Figure 4.11).

As for the switch from 15°C to 25°C similar trends between the actual data and the experimental model are observed although there can be differences in the average lifespan. The biological model shows fairly accurate average lifespan predictions with improved accuracy to experimental data in later switch times. During the early stages of lifespan intervention, the biological model overestimates the average lifespan (Figure 4.16b).

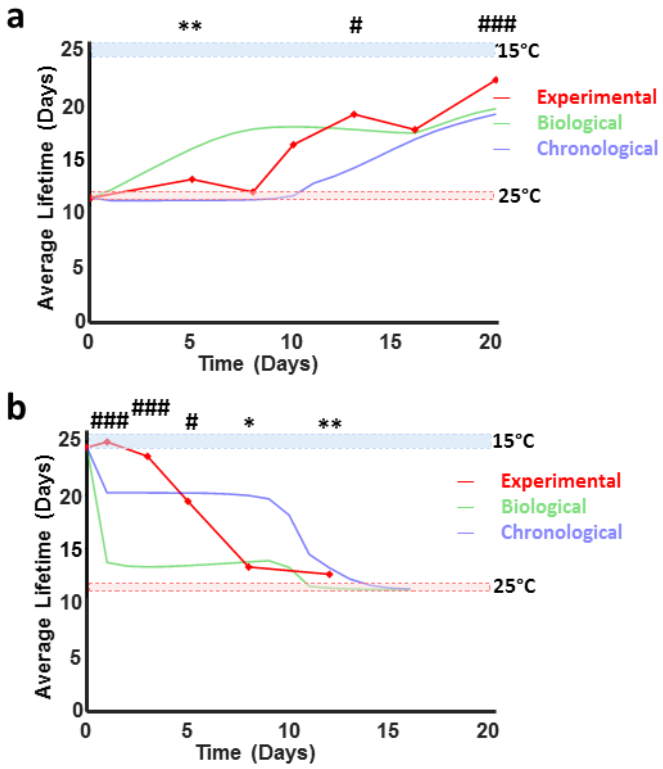

Figure 4.16: Comparison of predicted average lifespan of *trpa-1(ok999)* mutants by chronological model and biological model with experimental data. **(a)** 25°C to 15°C. **(b)**15°C to 25°C. One-way ANOVA with Tukey's multiple comparison test. *shows statistical comparison to 15°C, # shows statistical comparison to 25°C. **p<0.01, *p<0.05, ###p<0.001, #p<0.05.

4.5 Discussion

Overall, this study shows that the lifespan of wild type worms which have undergone thermal intervention can be predicted with two different models. The first is a chronological model based on the time which has passed from the start of the experiment and the second is a biological model which is based on the survival proportions of worms at the given switch time. Between the two models developed, the biological model is a better predictor of lifespan intervention compared to the chronological model. This suggests that when investigating lifespan, it is not only important to analyse lifespan based upon their chronological age but to also take in to account the survival proportion of worms throughout their lifespan as it is an important indicator of how the worms are ageing. Both models show that the predictions more closely resemble the condition at which a longer time is spent. Additionally, our findings show that the early lifespan is crucial and that changes at the early stage can have lasting consequences later on in life, which is in agreement with previous studies (Zhang et al., 2015, Henderson et al., 2018). Both the chronological and biological models are unable to accurately model intervention of *trpa-1* mutants. This is likely due to the loss TRPA-1 affecting normal lifespan dynamics and impairing the worms ability to adapt to changing temperature. In wild type worms the ability to adapt is not impaired and so normal lifespan dynamics can be accurately predicted.

This model can be applied to many other intervention types such as genetic, dietary, pharmacological and environmental. For example, when investigating the role of a gene, the gene can be active or inactive, and the activation of this gene may occur differentially throughout the lifespan of the organism. Therefore, this methodology can be used to investigate how genetic activity or intervention can alter lifespan over time by comparing different intervention times throughout the organism lifespan.

Dietary intervention is another commonly studied area and can be investigated fairly easily by looking at different diets (e.g. high fat diet vs calorie restriction) and predicting the effect dietary intervention at different time points has on lifespan.

In this study the effect of thermal intervention on lifespan was investigated but further to this, other environmental factors such as oxygen levels (normoxia vs hypoxia vs hyperoxia) or other stress causing factors can be investigated.

Pharmacological intervention is currently a major area of research and these models are extremely beneficial to investigators (for example those in the interventions testing programme) looking to screen the effect of drugs on lifespan. It would allow predictions of when is the best time for a drug to be given to extend lifespan. Furthermore, this can be potentially extrapolated to other species too, importantly those which have a much longer lifespan such as flies, rodents and even fish. Also, in higher order species in which surgical operations are conducted, these can be classed as an intervention.

Although useful, the models predictions for different interventions must be interpreted with caution as in some cases where normal lifespan dynamics are severely affected the ability to predict lifespan is impaired. The different intervention types must be conducted to identify the universality of the models. What is also understood from this methodology is that it is of utmost importance that the original data sets are of high quality and are accurate, and therefore this stresses the importance of replication and reproducibility of data.

4.5.1 Critical time points

Another important output of this methodology is the critical time points. In this study, the critical time points show that the later the intervention occurs the less impact it has upon lifespan. This is in agreement with existing advice on intervention (for example early diagnosis result in a better prognosis). Additionally, the effect of intervention is highly dependent on the initial conditions. As such poor initial conditions would result in an increased death rate and a faster reduction in survival proportions, resulting in a smaller possibility of the intervention having an effect.

Specifically, in poor initial conditions (e.g. high temperatures), the effect of intervention is biphasic as lifespan increases then decreases with later switch time. This is likely due to the

worm developing a tolerance or stress resistance factors at a young age therefore making the worm more resilient with an improved ability to adapt in changing conditions.

This effect is not seen in interventions which begin in beneficial initial conditions and later switches to the detrimental conditions. This is probably because there is minimal stress in early development due to the condition and therefore minimal development of resistance. Furthermore, switching to detrimental conditions later on in life has greater consequences as the worms are more aged and also have a reduced capability to adapt to the detrimental condition and therefore the detrimental switching has a greater impact upon lifespan. Therefore, our results indicate that being in detrimental conditions later in life with no previous exposure results in a shorter average lifetime compared to spending the same amount of time early on in the lifetime. This further signifies the importance of not only the duration of the intervention but also the timing of it.

4.5.2 The role of TRPA-1 in *C. elegans* lifespan

The role of TRPA-1 as a temperature regulator in *C. elegans* has previously been investigated with data showing that TRPA-1 acts to extend lifespan in cooler temperature but not at warmer temperatures. This result was unable to be replicated as a similar lifespan to wild type is seen at both 15°C and 25°C. Although differences in lifespan between wild type and *trpa-1(ok999)* mutants is not expected at 25°C, differences are expected to be seen at 15°C. Although the data is not statistically significant it does show a temperature sensitive role. However this does not replicate what has previously been reported but in fact shows the opposite effect as at low temperatures the *trpa-1(ok999)* mutants have an extended lifespan meaning TRPA-1 acts to reduce lifespan. At high temperatures a similar effect is seen although at an even lesser magnitude. This is unexpected, particularly as it has previously been suggested that *trpa-1* is a cold temperature sensor which is activated in a noxious cold environment (i.e. 15°C) and normally functions to extend lifespan.

However, our results are in agreement with another study which suggest TRPA-1 may not necessarily be a noxious cold sensitive regulator in *C. elegans*. The temperature range by

which TRPA-1 sensitivity occurs could be different to what has previously been suggested (Xiao et al., 2013, Miller et al., 2017). It is proposed that although it is temperature sensitive, TRPA-1 functionality in *C. elegans* is still to be explored and its effect upon lifespan is still to be determined.

The increase in average lifespan of *trpa-1(ok999)* worms which have spent early lifespan in detrimental conditions is in agreement with previous studies which shows that the growth temperature at developmental stages is important (Xiao et al., 2013, Henderson et al., 2018). These results show that this idea can be extended from the developmental stages to the first 3 days of lifespan which are important for development and lifespan regulation later on in life. Additionally, this shows that the TRPA-1 ion channel plays an important role particularly early on in the lifespan of worms which have grown at 25°C and switched to 15°C as *trpa-1(ok999)* mutant worms have a significantly higher average lifespan at day 3 compared to wild type worms, suggesting that exposure to high temperatures early on may act to reduce lifespan by signalling via TRPA-1.

The *trpa-1(ok999)* mutants were not able to be modelled by either of the two predictive models as the lifespan predictions for interventions from 25°C to 15°C were shown to be constant in many cases. This is likely due to the effect of intervention on lifespan changes predicted by the model, amounting to the lifespan reduction that is due to the additional time in the detrimental temperature, therefore counteracting one another resulting in an average lifespan which does not change over the most part of the lifespan. Another explanation is that the intervention survival curve predictions by the models is heavily dependent on (and can be skewed by) the shape of the curve for the initial data of the worms grown in a single condition (15°C or 25°C). Indeed, the intervention from 25°C to 15°C is not well described by either model due to the relatively long period early on in the lifespan where worms do not die and so the survival proportions remain at 100% leading to an overestimation of lifespan. When they do die, there is an initial sudden decrease in survival proportions followed by a secondary shallower decrease in which both the 15°C and 25°C curves have a similar gradient. Thus,

this results in a clustering of predicted survival curves, leading to similar average lifespans regardless of the theoretical switch time (Figure 4.11d).

4.5.3 Future work

Having shown that temperature intervention has a dynamic affect upon lifespan of *C. elegans* and that many factors are involved, much is still left to be investigated beyond this chapter. It is still important to fully determine the role of TRPA-1 in *C. elegans* and the extent to which this ion channel influences nociception and thermoception. Further to this, it is important to see whether and to what extent this channel acts to alter lifespan. Additionally, other factors must be considered, for example the AFD neurons involvement with cyclic GMP ion channels activity in thermoregulation (Lee and Kenyon, 2009, Land and Rubin, 2017). It is also possible for there to be crosstalk between multiple different factors which react to variations in temperature.

Although important, temperature is not the only intervention which has life changing consequences. Other interventions play an equally critical role and it is important to understand how these interventions act to alter lifespan with time. Here two models are proposed which can be used as an initial point for investigating the effect of these interventions. With minimal data input required, a substantial amount of data can be obtained which provides insight into lifespan effects of different interventions.

4.6 Conclusion

This study proposes a chronological and a biological model for predicting lifespan interventions and the timing of the intervention. Also identified are critical time points in the *C. elegans* lifespan, these include time points at which lifespan is pre-determined and time points at which interventions are too late and so result in minimal effects. Additionally, this study shows that TRPA-1 does play a small role in temperature-based lifespan regulation, although not to the extent by which it has previously been reported and that TRPA-1 activity is differentially regulated with time.

Chapter 5.0: Interaction between HIF-1 and TRPA-1 signalling pathways and its effect on *C. elegans* lifespan

5.1 Preface

The purpose of this chapter is to use the Bilogistic model to investigate signalling between the hypoxia inducible factor 1 (HIF-1) (hypoxia) signalling pathway and the transient receptor potential ankyrin 1 (TRPA-1) (temperature) signalling pathway and the roles they play in regulating lifespan. Previous studies have implied some interaction between HIF-1 and TRPA-1. To investigate this, the *C. elegans* lifespan was explored under different temperatures and oxygen concentrations to identify the interaction between the HIF-1 hypoxia and TRPA-1 temperature signalling pathways. Additionally, the effect of TRPA-1 activation by the agonist carvacrol on HIF-1 activity was measured in mammalian cells. Furthermore, worms were treated with carvacrol to investigate whether the effect observed in mammalian cells were conserved in worms and could be applied to a whole model organism and to further provide insight into how this affects lifespan.

5.2 Introduction

5.2.1 Environment and lifespan

The lifespan of an organism is influenced by a number of internal and external factors. Internal factors include control by genetic regulators and external factors include environment and lifestyle choices. Temperature and oxygen concentrations are two key environmental factors which are known to influence lifespan.

5.2.1.1 Temperature and TRPA-1

In many organisms, temperature plays a conserved role in regulating lifespan. At high temperatures lifespan is reduced and vice-versa (Conti, 2008). Passive and active mechanisms of action which alter the lifespan have previously been described (section 1.4) (Keil et al., 2015). A number of active mechanisms involving temperature controlled genetic regulation of lifespan have been proposed. One such mechanism is the TRPA-1 signalling pathway previously identified to be stimulated by noxious cold stimuli and which extends lifespan in *C. elegans* (Xiao et al., 2013). TRPA-1 is thought to target DAF-16 (FOXO ortholog) via the calcium-sensitive PKC-2 and the kinase SGK-1 in *C. elegans* which is a known pathway involved in lifespan regulation. This indicates the TRPA-1 signalling pathway as an attractive target to investigate how temperature affects lifespan. In addition to noxious cold stimulation, the TRPA-1 cation channel can also be activated by pain stimulations or pharmacological agents such as the monoterpene carvacrol (Hasan et al., 2017).

5.2.1.2 Hypoxia and HIF-1

Oxygen is another important environmental factor which has a more varied effect upon lifespan and is also reported to be species dependent. High levels of oxygen are not known to have an effect on *C. elegans* lifespan but has been reported to negatively affect rodents and drosophila (Pitt et al., 2014). Low oxygen levels have varied effects upon lifespan and as previously described signal via the HIF-1 pathway (section 1.5.4). In flies some studies have shown that hypoxia extends lifespan whereas others report a reduction instead (Rascón and Harrison, 2010, Vigne et al., 2009). In *C. elegans,* hypoxia has been found to extend lifespan

and is also reported to act via the HIF-1 signalling pathway (Leiser et al., 2013). However, there is some variation in these studies due to differences in the methodology and individual definitions of hypoxia used. Most studies define hypoxia to be in a range of 0.5-2% oxygen concentration but other studies have a more extreme definition of hypoxia which is closer to anoxia (<0.1%) and can result in a lifespan reduction (Schieber and Chandel, 2014, Kitazume et al., 2018, Leiser et al., 2013, Fawcett et al., 2012, Mehta et al., 2009, Honda et al., 1993). This study defines hypoxia as 1% oxygen concentration.

Hypoxia leads to a number of cellular changes which are controlled by different signalling pathways. The primary signalling pathway which responds to hypoxia is the HIF-1 signalling pathway. In a normoxic environment HIF-1 is hydroxylated by the prolyl hydroxylase EGL-9 which is then targeted by von Hippel-Lindau 1 (VHL-1) for ubiquitination. Once ubiquitinated HIF-1 is targeted for degradation. Hypoxia prevents this degradation and allows HIF-1 to stabilise and function as a transcription factor. Therefore EGL-9 and VHL-1 act as regulators of HIF-1 function and signalling and prevent HIF-1 from binding to hypoxia response elements (HRE) which controls transcriptional activity of target genes (Epstein et al., 2001, Shen et al., 2005).

The function of HIF-1 as a transcription factor has been previously investigated, more so in mammalian systems (as the orthologue HIF-1α) compared to model organisms. HIF-1α has been reported to have a role in many different physiological mechanisms such as angiogenesis, erythropoiesis, cell proliferation, cell survival, proteolysis glucose metabolism and pH regulation. In *C. elegans,* it has been speculated to act as a key factor in the mechanism behind lifespan control (Dengler et al., 2014, Pitt et al., 2014). A deletion of *hif-1* extends the lifespan of *C. elegans,* suggesting that HIF-1 normally acts to shorten lifespan. However, overexpression of *hif-1* also leads to lifespan extension, suggesting a different pathway (Pitt et al., 2014, Mehta et al., 2009, Leiser and Kaeberlein, 2010, Zhang et al., 2009). Due to the uncertainty of the HIF-1 regulation of *C. elegans* longevity, it is important that further investigations are conducted to determine its role.

5.2.2 Interaction between HIF-1 hypoxia and TRPA-1 temperature signalling pathways

Oxygen concentration and temperature are two distinct environmental influencers which have been reported to act via their distinct pathways. However, a number of studies have shown that these pathways could be linked. The main physiological function linking these pathways is in inflammatory signalling where TRPA1 acts to signal pain and HIF-1 acts to induce immune functions. (Hatano et al., 2012, Nagarajan et al., 2017). Lifespan control in *C. elegans* also links these two pathways albeit by different stimuli (Leiser and Kaeberlein, 2010, Xiao et al., 2013). It is therefore reasonable to assume that there is some interaction between the TRPA-1 pathway and the HIF-1 pathway. Indeed, previous studies have shown that in mammalian cells HIF-1α is required for the signalling from NF-κb to induce TRPA1. This study also reports that pharmacological stabilisation of HIF-1 by desferroxamine increases mRNA levels of *TRPA1* (Hatano et al., 2012).

In addition to this TRPA-1 is also a target of the prolyl hydroxylases (which also target HIF-1) and in hypoxia it allows sensitisation of TRPA-1 activity and could possibly act to influence lifespan (So et al., 2016).

Further linking these signalling pathways together is the report that HIF-1 activity in *C. elegans* is temperature dependent. At higher temperatures (25°C) *hif-1(ia4)* mutant worms have an extended lifespan but at low temperatures (15°C) this effect is not seen (Leiser et al., 2011).

From these studies it is clear that the TRPA-1 temperature sensing pathway and the HIF-1 hypoxia signalling pathway have a close relationship and may be linked. Therefore, in the context of lifespan regulation, the interaction between these pathways can be further explored by investigating the actions of HIF-1 and TRPA-1 signalling pathway elements in *C. elegans*.

5.2.3 Aims and Objectives

The roles of the different components in the TRPA-1 temperature and HIF-1 hypoxia signalling pathways can be investigated, and their effect on lifespan can be measured and analysed by mathematical analysis to provide more data upon how these factors affect lifespan. The relationship between HIF-1 and TRPA-1 specifically can be further investigated in mammalian cells to identify cross talk between pathways and specific roles of pathway components. This can be applied to *C. elegans* to see how worms react to activation of pathways by environmental changes or pharmacological treatment.

The specific objectives are to measure and analyse lifespan of different *C. elegans* mutants (of both pathways) in normoxic and hypoxic conditions to investigate the effect on lifespan by using the Bilogistic model. This study will also measure the effect that TRPA1 activation has on HIF-1 levels in human mammalian cells and the effect it has upon *C. elegans* lifespan. Activation of the different factors will be conducted by environmental and pharmacological activation to identify their effect on lifespan of wild type and mutant worms.

5.3 Methods

5.3.1 *C. elegans* lifespan assays

The *C. elegans* strains N2 (wild isolate), and *daf-16(mu86)*, *hif-1(ia4)*, *trpa-1(ok999)*, *egl-9(sa307)* and *egl-9(n586)* were acquired from the Caenorhabditis genetics center (CGC), University of Minnesota. *C. elegans* were maintained at 20°C on solid NGM media supplemented with nystatin (10μg/ml) and seeded with OP50 *E. coli* unless otherwise stated. A synchronised population of worms using alkaline hypochlorite treatment were generated for lifespan assays which were conducted on solid NGM plates additionally supplemented with FuDR (50μM). 50 or more L4 stage synchronised worms were transferred to fresh NGM plates containing FuDR and were further transferred to new plates weekly or more frequently if OP50 had depleted or if there were unwanted bacterial or fungal contamination. Day 0 is the first day of adulthood and the beginning of the lifespan assay and worms were measured almost daily for events such as death or censorship.

5.3.2 *C. elegans* lifespan assays from digital recordings

In hypoxic environments, *C. elegans* lifespan assays were conducted by digital recording using flatbed photo scanners. Oxygen and temperature was regulated by placing scanners in chambers with controlled oxygen levels (1%) and the temperature (20°C) was regulated using a climate control system in the room. The Epson Perfection V800 Photo Scanner was used to scan NGM plates and take images of the plates. Once images were acquired plates were analysed manually by comparing images from different time points, if worms had moved position then they were classified as alive, had they not moved they were classified as dead. Additionally, worms missing (crawled off the plate) were classified as censored along with worms which were seen to have had internal hatching of eggs (bagging), bacterial or fungal contamination, vulval protrusion and rupturing.

5.3.3 Carvacrol dose response

Worms were treated with carvacrol at varying concentrations. NGM plates used for lifespan assays were supplemented with 0mM, 50mM, 200mM and 500mM of carvacrol. At the beginning (day 0) of the lifespan assays worms were transferred to carvacrol plates and were maintained until completion of the lifespan assay.

5.3.4 Curve fitting and statistical analysis of parameters

Kaplan-Meier survival curves were constructed in GraphPad Prism 7. Survival proportions were calculated and the MATLAB (MathWorks) Curve fitting toolbox (R2016a, v9.0.0.370719) and sfit objects were used to fit the novel 5-parameter Bilogistic model (Chapter 3) was used to fit lifespan data (Equation 1).

$$N(t) = N_0 \left[f \frac{1 + e^{-k_1 t_1}}{1 + e^{k_1 (t - t_1)}} + (1 - f) \frac{1 + e^{-k_2 t_2}}{1 + e^{k_2 (t - t_2)}} \right]$$

Equation 1: The 5-parameter Bilogistic model

Fitting of data was conducted by using a non-linear least squared fit method (Trust-Region algorithm) to estimate parameters. When fitting the survival data, other settings were kept to default: Robust=Off, DiffMinChange=0.00000001, DiffMaxChange=0.1, MaxFunEvals=600, MaxIter=400, TolFun=0.000001, TolX=0.000001.

After parameters were obtained, GraphPad Prism was used to perform an ordinary two-way Analysis of Variance (ANOVA), with all groups compared to one another (non-repeated measure). In conjunction to this ANOVA, Tukey's multiple comparison test was also conducted. Statistical *p*-values $p<0.05$, $p<0.01$, $p<0.001$ and $p<0.0001$ shows a statistically significant difference between groups and is indicated in the figures.

5.3.5 Plasmid cloning

Plasmids used were pHRE-MP-GLuc HIF responsive plasmid DNA (Cavadas and Cheong, 2014) and pcDNA3.1/neo(+)-human TRPA1 plasmid DNA (Hatano et al., 2012). Plasmids

were transformed into mammalian cells using the heat shock method and purified using the Pureyield Plasmid Midiprep System (A2492; Promega).

5.3.6 Mammalian cell growth and maintenance

HEK-293 and HepG2 cell lines were cultured in DMEM (41966-029; Gibco Life Technologies) and RPMI-1640 (R8758) respectively supplemented with 10% Foetal Bovine Serum (FBS) and 5% Penicillin-Streptomycin.

When cells reached 70-80% confluency they were passaged using Trypsin-EDTA solution (T4174) and re-seeded into new flasks at the desired concentration. Growth media was replaced every 72 hours until cells required further passage. Cells were maintained in a CO_2 incubator at 37°C in an atmosphere of 5% CO_2/ 95% air.

When adherent HepG2 cells reached 70-80% confluence they were passaged and were seeded in a 24 well plate with 500μl of media per well. Cells were maintained at 37°C in 5% CO_2/ 95% air for 24 hours.

5.3.7 Transient Transfection

A calcium phosphate co-precipitation method (Chen, 2012) was used for transient transfection of seeded cells. After the transfection solution (Table 2.2) was added, cells were incubated at 37°C in 5% CO_2/95% air for 48 hours.

5.3.8 Cell treatments

24 hours post transfection growth media was replaced with fresh media and then treated using a number of different conditions. Treatment of cells lasted 24 hours. Cells were exposed to hypoxic conditions (1% O_2, 94% N_2, 5% CO_2) in a hypoxia O_2 Control InVitro Glove Box (Coy laboratories) and the fresh growth media was pre-exposed to hypoxia for at least 16 hours before application to cells. Additionally, carvacrol was used at varying doses of 5μM, 20μM, 50μM, 200μM and 500μM to treat cells.

5.3.9 Gaussia Luciferase assay

The pHRE-MP-GLuc HIF plasmid construct was used to measure HIF activity in mammalian cells (Figure 2.5). Conditioned media was collected 24 hours post-treatment and was read on a SpectraMax Gemini EM Microplate Reader (Molecular Devices) at the ambient temperature. The SoftMax Pro Software (v5.0) was used to configure the plate reading settings: Top read, Luminescence, Emission: Lm1 461nm, Reads/Well: 6 (Figure 2.6).

5.3.10 Statistical analysis

Average (relative) luminescence for individual treatments in the Gaussia Luciferase assay was calculated (±SEM) using GraphPad. An Ordinary One-Way ANOVA with Tukey's multiple comparisons test was used to compare individual treatments in the Gaussia Luciferase assay. Statistical *p*-values $p<0.05$, $p<0.01$, $p<0.001$ and $p<0.0001$ shows a statistically significant difference between groups and is indicated in the figures.

5.4 Results

5.4.1 *C. elegans* in normoxia at 20°C

Using the 5-parameter Bilogistic model, specific differences in the lifespan of *C. elegans* worms under different temperature and oxygen condition were identified. Furthermore, the role of signalling factors in these two pathways and their impact upon lifespan provide insight into how temperature and oxygen regulate lifespan.

In normoxic conditions at normal (20°C) growth temperature both TRPA-1 and DAF-16 have a shortened lifespan compared to N2 wild type worms (Figure 5.1). Parametric analysis shows that, only DAF-16 worms have a significantly higher late phase death rate (Figure 5.1c). Neither mutation appears to affect the *f* parameter nor the early time phase and although not statistically significant the late time phases are lower in both mutants compared to wild type (Figure 5.1b, d). Surprisingly, mutations to the factors in the hypoxia pathway do not show a significant change on lifespan as both *hif-1(ia4)* and *egl-9(sa307)* mutants tend to show similar lifespan and parameters as wild type worms (Figure 5.2a, b, c, d).

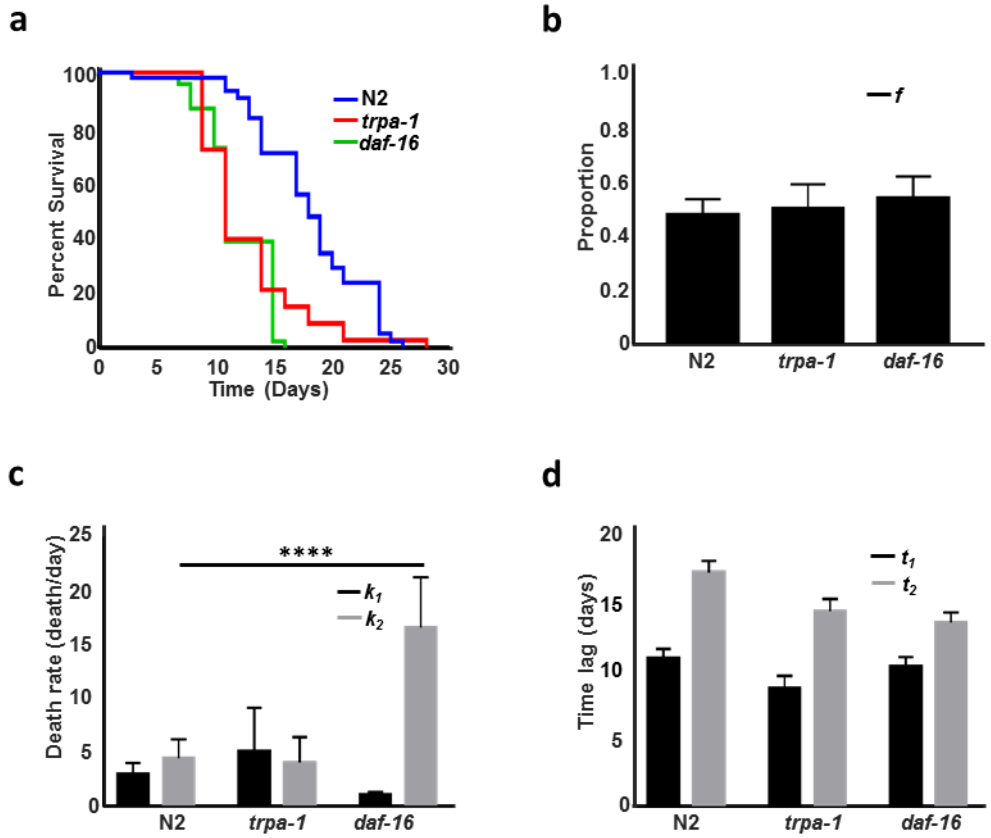

Figure 5.1: Lifespan and parameters of wild type (N2), *trpa-1(ok999)* mutant and *daf-16(mu86)* mutant worms in normoxia grown at 20°C. **(a)** representative survival curves, **(b)** *f* parameters, **(c)** early (*k1*) and late (*k2*) phase death rate and **(d)** early (*t1*) and late (*t2*) time phases. N2 (n=21), *trpa-1(ok999)* (n=8), *daf-16(mu86)* (n=8) Data is shown as mean ± SEM. **** $p<0.0001$.

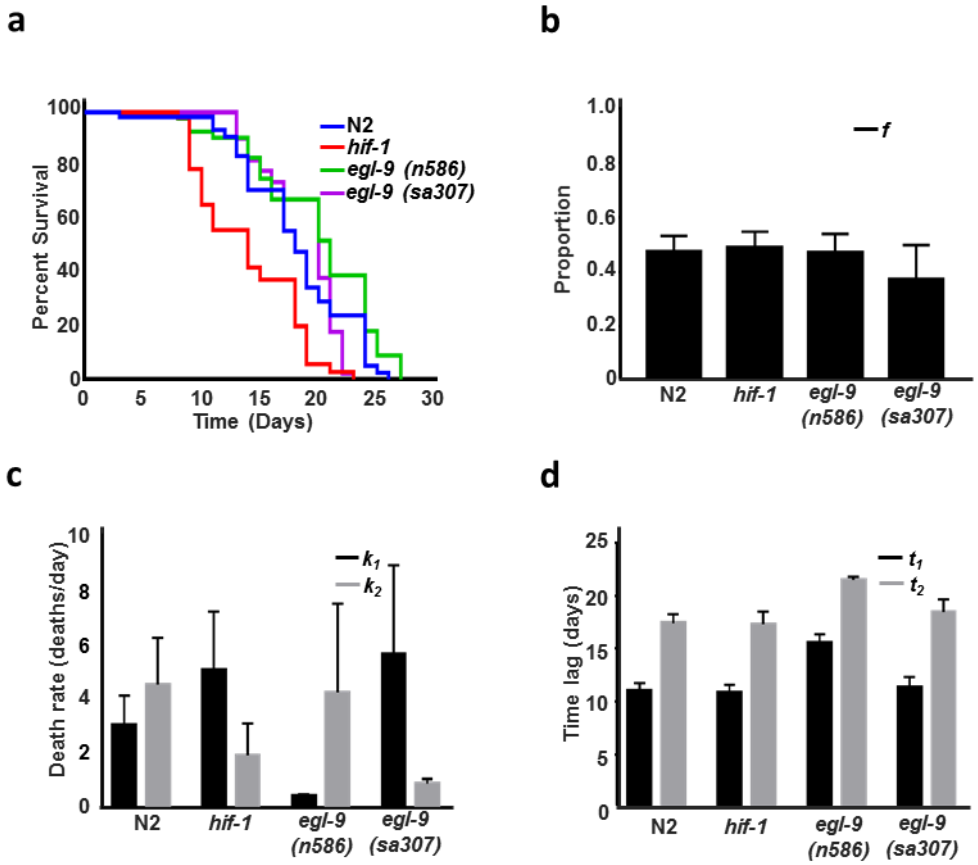

Figure 5.2: Lifespan and parameters of wild type (N2), *hif-1(ia4)* mutant and *egl-9 (n586)* and *egl-9 (sa307)* mutant worms in normoxia grown at 20°C. **(a)** representative survival curves, **(b)** *f* parameters, **(c)** early (*k1*) and late (*k2*) phase death rate and **(d)** early (*t1*) and late (*t2*) time phases. N2 (n=21), *hif-1(ia4)* (n=11), *egl-9(n586)* (n=6), *egl-9(sa307)* (n=6) Data is shown as mean ± SEM.

5.4.2 *C. elegans* in normoxia at 15°C

As shown previously (section 3.4) when lowering the temperature from 20°C to 15°C, an extension in lifespan in wild type worms and all mutant worms except the *hif-1(ia4)* mutants is observed (Figures 5.1, 5.2, 5.3 and 5.4). Lowering the temperature results in an extension of both time phases in wild type worms and *trpa-1(ok999)* mutants (Figures 5.1 and 5.3). *daf-16(mu86)* mutants show a decrease in the early phase death rate at the lower temperature while *egl-9(sa307)* shows an increase in the late time phase (Figures 5.2, and 5.4).

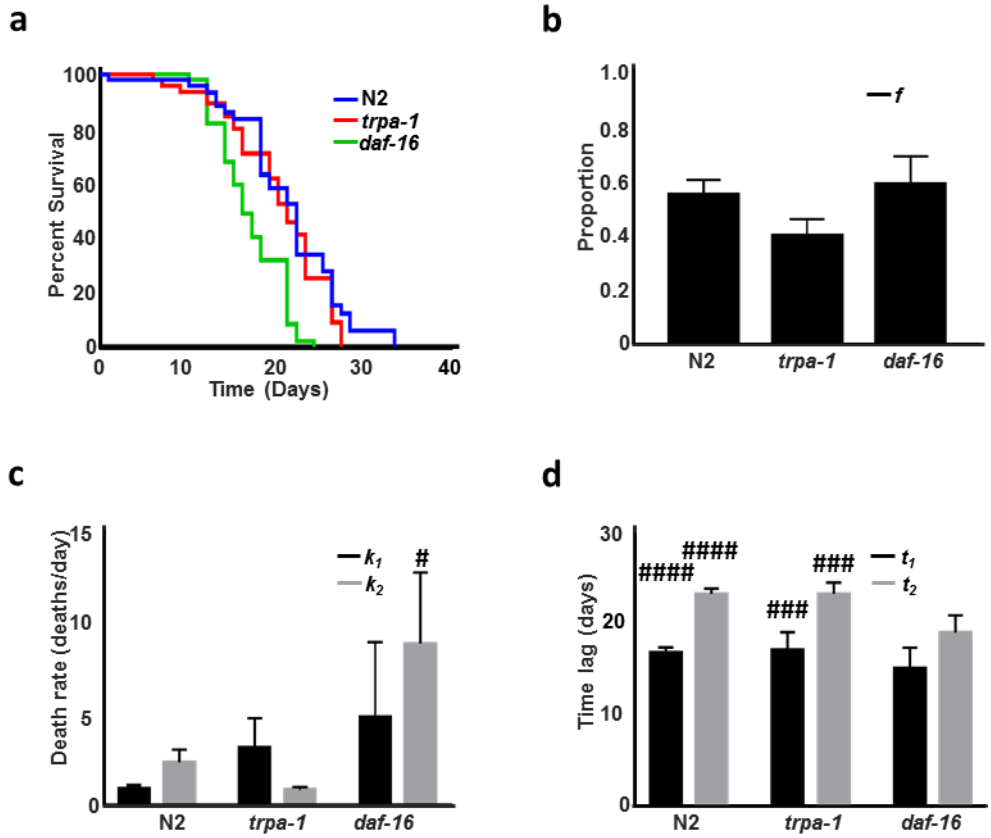

Figure 5.3: Lifespan and parameters of wild type (N2), *trpa-1(ok999)* mutant and *daf-16(mu86)* mutant worms in normoxia grown at 15°C. **(a)** representative survival curves, **(b)** *f* parameters, **(c)** early (*k1*) and late (*k2*) phase death rate and **(d)** early (*t1*) and late (*t2*) time phases. N2 (n=27), *trpa-1(ok999)* (n=12), *daf-16(mu86)* (n=5) Data is shown as mean ± SEM. # shows statistical comparison to 20°C. #### $p<0.0001$, ###$p<0.001$, #$p<0.05$.

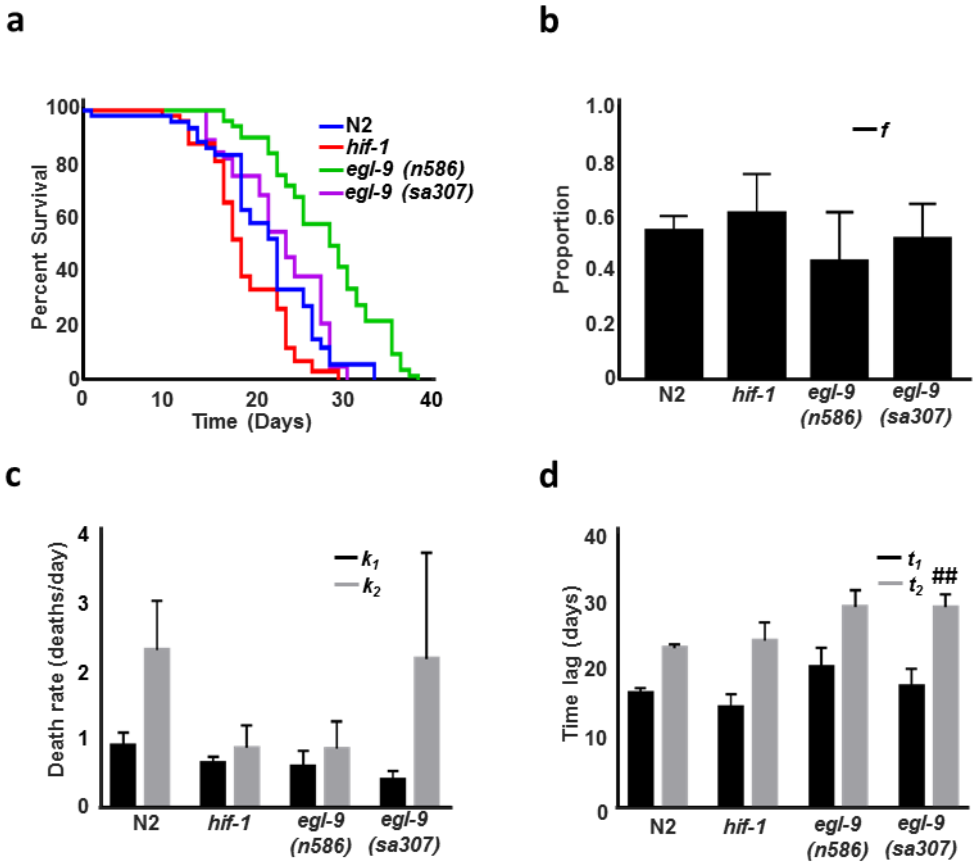

Figure 5.4: Lifespan and parameters of wild type (N2), *hif-1(ia4)* mutant and *egl-9 (n586)* and *egl-9 (sa307)* mutant worms in normoxia grown at 15°C. **(a)** representative survival curves, **(b)** *f* parameters, **(c)** early (*k1*) and late (*k2*) phase death rate and **(d)** early (*t1*) and late (*t2*) time phases. N2 (n=27), *hif-1(ia4)* (n=5), *egl-9(n586)* (n=3), *egl-9(sa307)* (n=3) Data is shown as mean ± SEM. # shows statistical comparison to 20°C. ##p<0.01.

5.4.3 Effect of hypoxia on *C. elegans*

In addition to temperature affecting lifespan, changes in oxygen levels also alter the lifespan of *C. elegans* (Figure 5.5). Although some lifespan extension is observed particularly in the later stage of life, hypoxia does not show statistically significant changes to parameters in both wild type worms and *hif-1(ia4)* mutants for the data gathered in our experiments (Figure 5.5a). However, *trpa-1(ok999)* mutants show similar overall lifespan changes as wild type worms in response to hypoxia, but the *trpa-1(ok999)* mutants report a significant difference in death rates compared to normoxic conditions. In *trpa-1(ok999)* mutants, hypoxia leads to a decrease in early phase death rate and an increase in late phase death rate, resulting in a slightly extended lifespan (Figure 5.5c). Mutants can also be compared to wild type to identify

the role the protein plays. There is no significant difference between wild type and *hif-1(ia4)* mutants. However, *trpa-1(ok999)* mutants show an increase in late phase death rate. Although *trpa-1(ok999)* mutants begin to live longer than wild type, they die more quickly in the late phase compared to wild type and thus die at similar times (Figure 5.5c). In wild type worms grown in hypoxic conditions, early phase death rate is significantly higher compared to late phase death rate and similar results are seen in *hif-1(ia4)* mutants but in *trpa-1(ok999)* mutants this is not seen as the late phase death rate increases (Figure 5.5c).

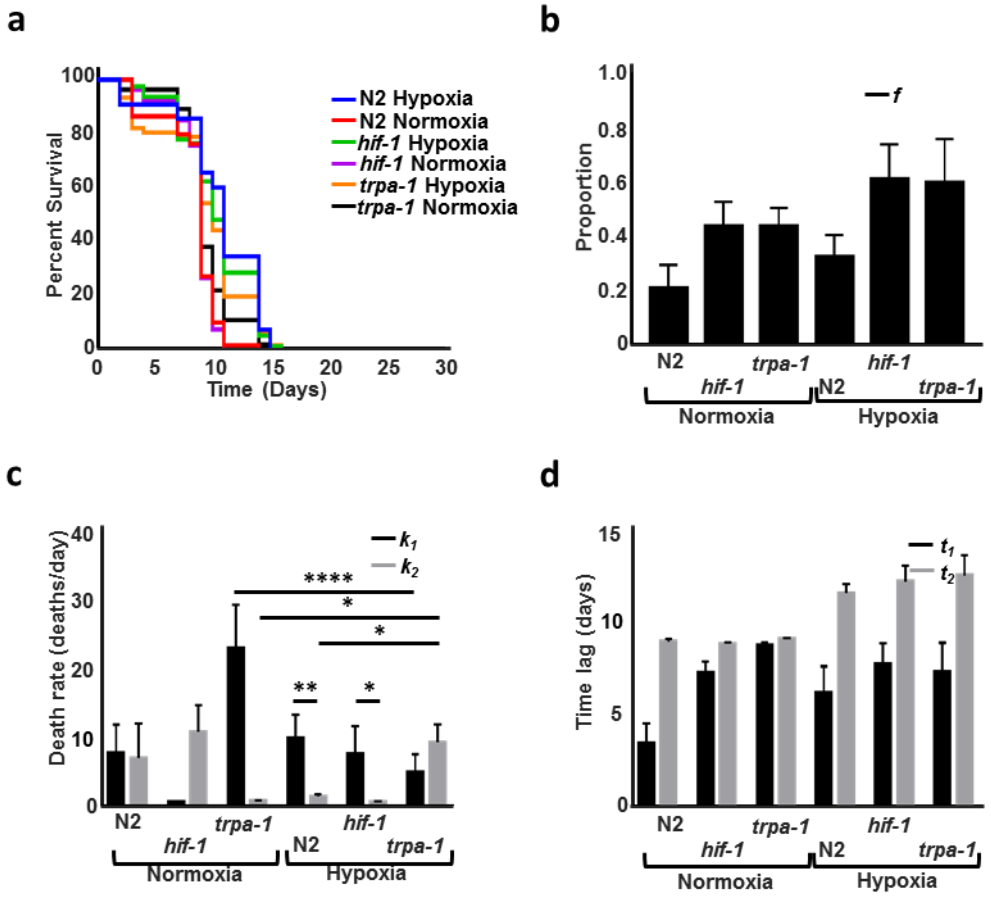

Figure 5.5: Lifespan and parameters of wild type (N2), *hif-1(ia4)* mutants and *trpa-1(ok999)* mutants in normoxia and hypoxia at 20°C using digital lifespan assays. **(a)** representative survival curves, **(b)** *f* parameters, **(c)** early (*k1*) and late (*k2*) phase death rate and **(d)** early (*t1*) and late (*t2*) time phases. N2 hypoxia (n=6), N2 Hypoxia (n=3), *hif-1(ia4)* hypoxia (n=6), *hif-1(ia4)* normoxia (n=3), *trpa-1(ok999)* hypoxia (n=6), *trpa-1(ok999)* normoxia (n=3). Data is shown as mean ± SEM. ****p<0.0001, **p<0.01, *p<0.05.

5.4.4 Manual vs digital lifespan assays

As manual lifespan assays cannot be conducted easily in hypoxic conditions alternative methods to manual measurements were implemented. However, it is important to identify if the change in methodology has any affect upon lifespan by comparing manual counting method for lifespan assays against the digital lifespan assay which used flatbed scanners. The lifespan curves appear to show that lifespan is lower when conducted by digital lifespan assays, and possible reasons why this may occur will be discussed later. Wild type worms do not show statistically significant differences in parameters if conducted by either by manual lifespan assays or digital lifespan assays (Figure 5.6). However other mutants (*hif-1(ia4)* and *trpa-1(ok999))* show a shorter overall lifespan and therefore any comparison between manual and digital lifespan assays must be made carefully (Figure 5.7 and 5.8). *Hif-1(ia4)* mutants show an increase in later phase death rate and a lower late time phase in digital lifespan assays compared to manual lifespan assays (Figure 5.7). Similarly, *trpa-1(ok999)* mutants show an increase in early phase death rate in digital lifespan assays.

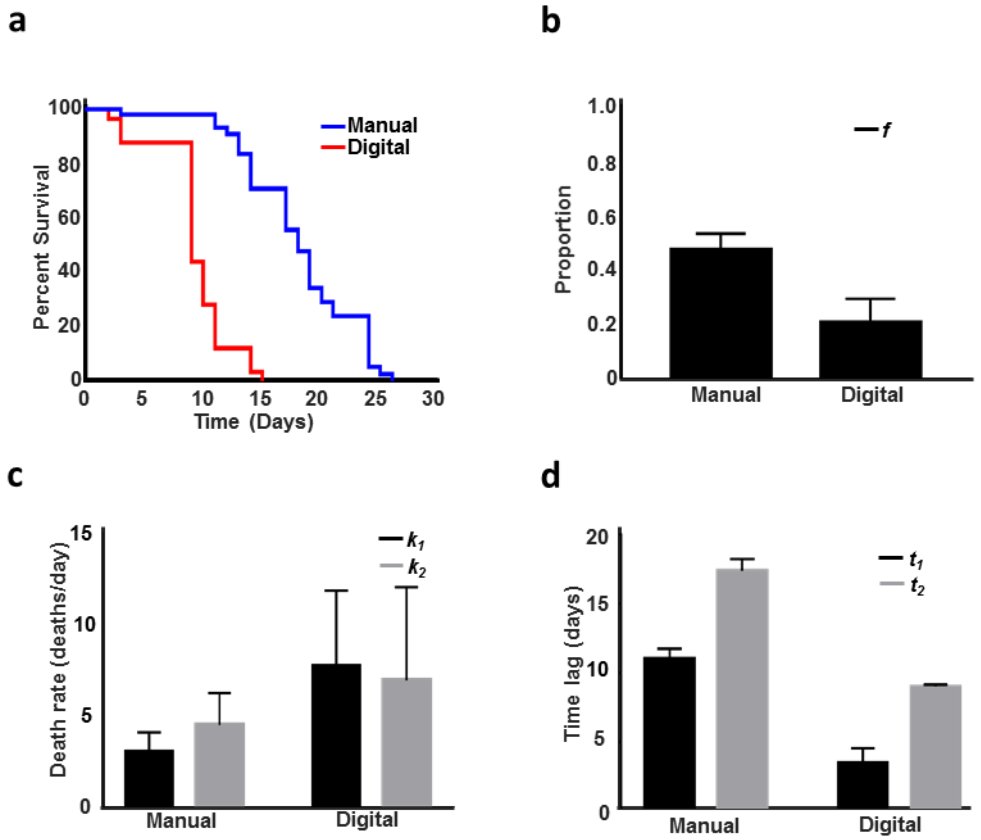

Figure 5.6: Lifespan and parameters of wildtype (N2) worms comparing manual lifespan assay and digital lifespan assay conducted at 20°C in normoxia. **(a)** representative survival curves, **(b)** *f* parameters, **(c)** early (*k1*) and late (*k2*) phase death rate and **(d)** early (*t1*) and late (*t2*) time phases. Manual (n=21), Digital (n=3). Data is shown as mean ± SEM.

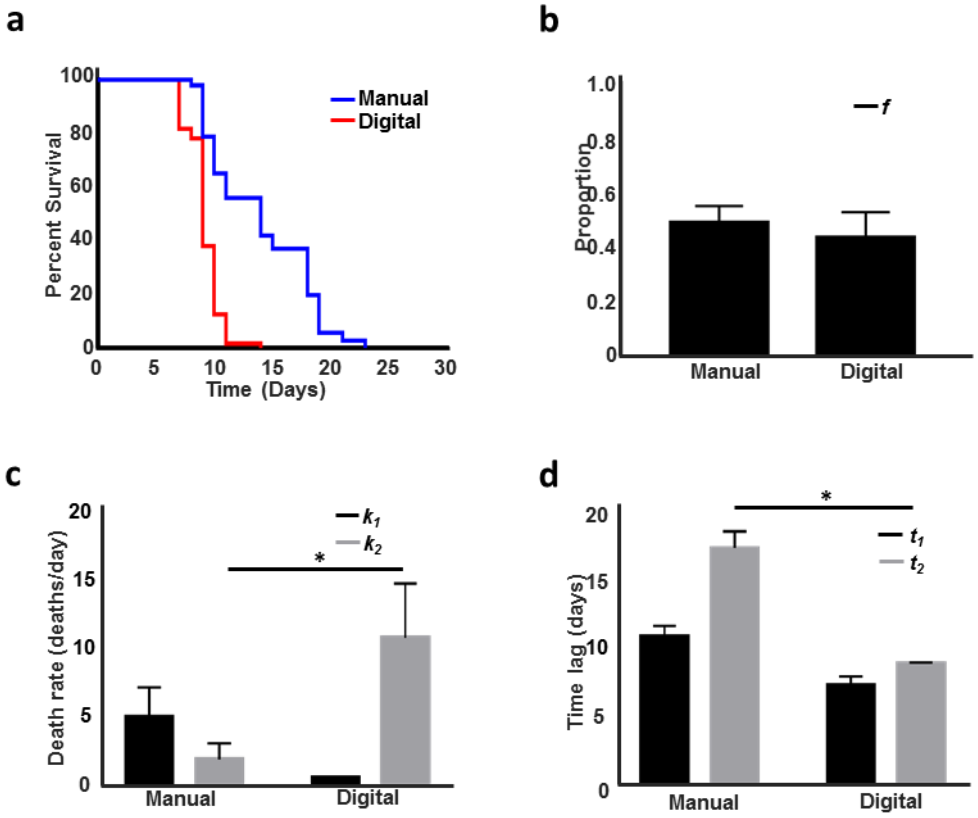

Figure 5.7: Lifespan and parameters of *hif-1(ia4)* mutants comparing manual lifespan assay and digital lifespan assay conducted at 20°C in normoxia. **(a)** representative survival curves, **(b)** *f* parameters, **(c)** early (*k1*) and late (*k2*) phase death rate and **(d)** early (*t1*) and late (*t2*) time phases. Manual (n=11), Digital (n=3). Data is shown as mean ± SEM. *p<0.05

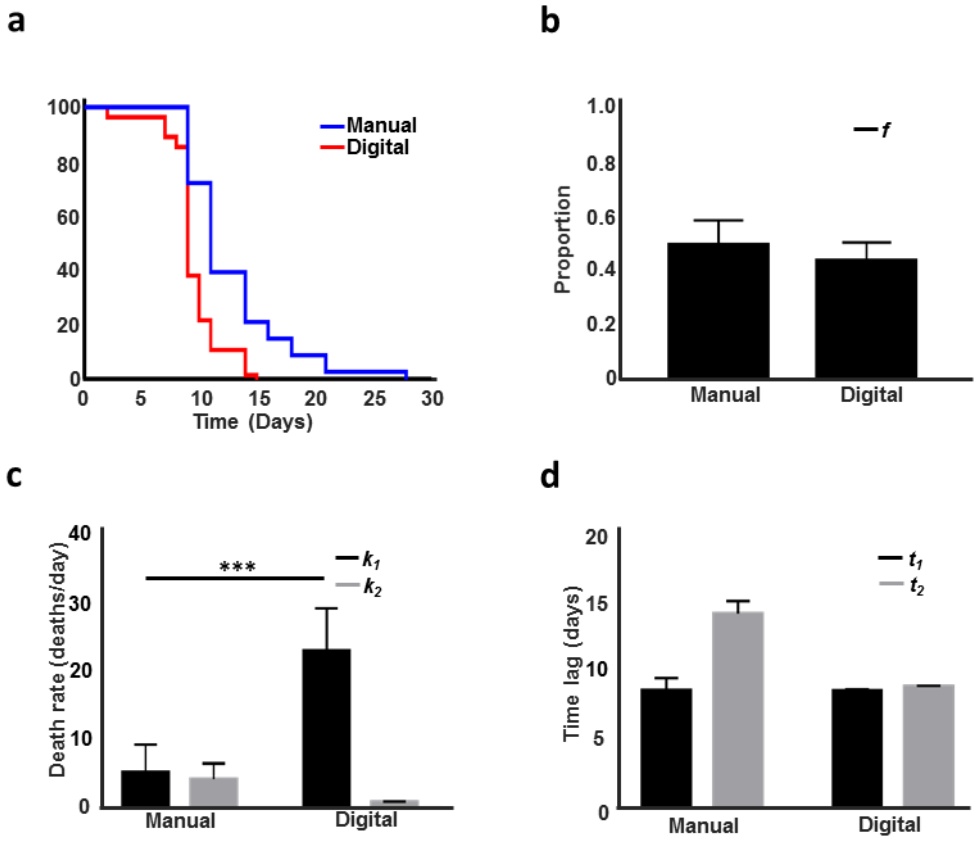

Figure 5.8: Lifespan and parameters of *trpa-1(ok999)* mutants comparing manual lifespan assay and digital lifespan assay conducted at 20°C in normoxia. **(a)** representative survival curves, **(b)** *f* parameters, **(c)** early (*k1*) and late (*k2*) phase death rate and **(d)** early (*t1*) and late (*t2*) time phases. Manual (n=8), Digital (n=3). Data is shown as mean ± SEM. ****p*<0.001

5.4.5 Carvacrol dose response on mammalian cells

TRPA-1 has been shown to play an important role in lifespan therefore its mechanism of action was further investigated in mammalian cells. Hypoxic treatment of HEK-293 and HepG2 cells increased HIF activity (Figure 5.9a and b). Overexpressing TRPA-1 and adding carvacrol to cells results in a significant reduction in HIF activity with a minimum concentration of 50μM of carvacrol required to significantly reduce HIF levels (Figure 5.9c and d). This is observed in both HEK-293 and HepG2 cells. The growth and morphology of cells appears to be unaffected by carvacrol as there is a similar level of growth and the cell morphology does not appear to change between control and treated cells (Figure 5.9e i & ii and f i & ii).

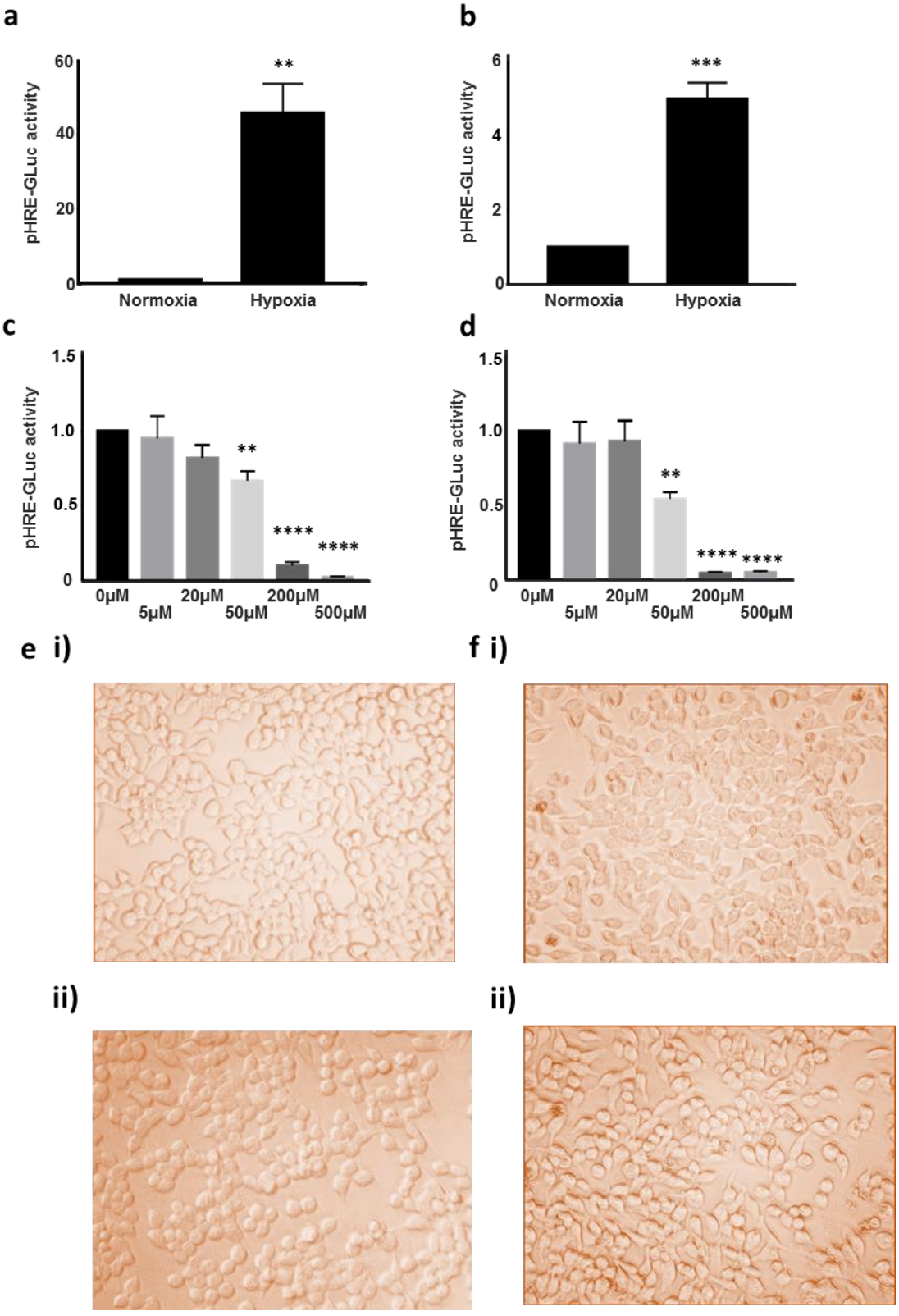

Figure 5.9: The effect of hypoxia and carvacrol on HIF-1 in mammalian cells. Hypoxia leads to an increase in HIF activity in both **(a)** HEK293 and **b)** HepG2 cells. Treatment with carvacrol decreases HIF activity in both **(c)** HEK293 and **(d)** HepG2 cells. In both cell lines cell growth and morphology appears to be similar for both **(e i** and **f i)** 0μM (control) and **(e ii** and **f ii)** 50μM. HEK293 Normoxia(n=5) HEK293 Hypoxia (n=5), HepG2 Normoxia(n=5) HepG2 Hypoxia (n=5).HEK293 D/R (n=9) HepG2 D/R (n=6). Data is shown as mean ± SEM. ****p<0.0001, ***p<0.001, **p<0.01.

5.4.6 Carvacrol dose-response on *C. elegans* in normoxia and hypoxia

C. elegans dose-response to carvacrol shows relatively few differences in worm lifespan. In most cases, addition of carvacrol appears to reduce the lifespan of *C. elegans* (Figures 5.10a-5.16a). Although there are some differences in parameters when treated with carvacrol, there does not appear to be consistent effects on lifespan.

In wild type worms carvacrol reduces lifespan and causes the phases to merge as normally without carvacrol there is a significant difference between early and late death time phases, yet with increasing carvacrol dosage this significant difference between the time phases is lost. (Figure 5.10 c and d). In hypoxic conditions, this is not observed, rather there are differences in death rates as early phase death rate is significantly higher compared to late phase death rate (Figure 5.14). With the addition of carvacrol this effect is reduced due to a slight decrease in early phase death rate and a slight increase in late phase death rate (Figure 5.14c).

Carvacrol has a similar effect on *hif-1(ia4)* mutants as in wild type worms as with carvacrol treatment phases merge together and there is a reduction in lifespan. However, in hypoxia this is not observed as time phases are already not significantly different to one another (Figure 5.11d and 5.15d).

Generally, *trpa-1(ok999)* mutants show similar overall lifespan with or without carvacrol (Figure 5.12 and 5.16). In normoxia, 200mM of carvacrol leads to a significantly higher death rate in the early phase compared to late phase (Figure 5.12c). In hypoxia the opposite is observed with the early phase death rate significantly lower than the late phase death rate (Figure 5.16c). At 200mM of carvacrol hypoxia results in a significant increase in the late phase death rate, which is also significantly higher than the other concentrations of carvacrol (Figure 5.16).

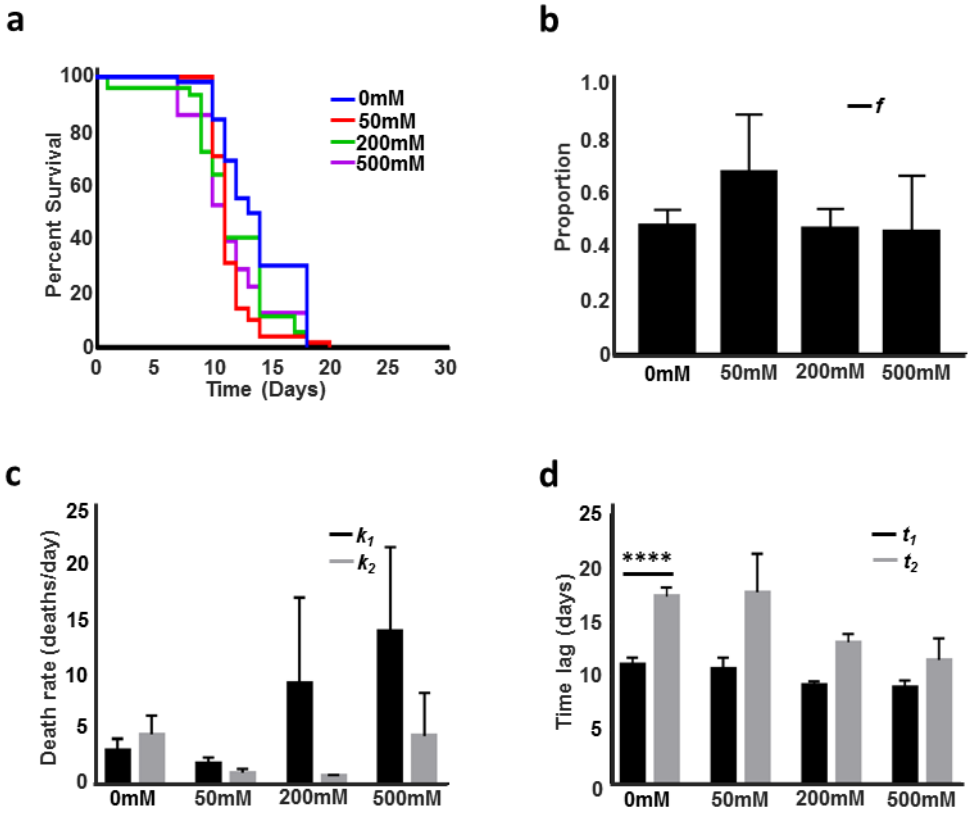

Figure 5.10: Lifespan and parameters of wild type (N2) *C. elegans* in normoxia treated with carvacrol (0mM control, 50mM, 200mM and 500mM). **(a)** representative survival curves, **(b)** *f* parameters, **(c)** early (*k1*) and late (*k2*) phase death rate and **(d)** early (*t1*) and late (*t2*) time phases. Carvacrol D/R (n=3). Data is shown as mean ± SEM. ****p<0.0001

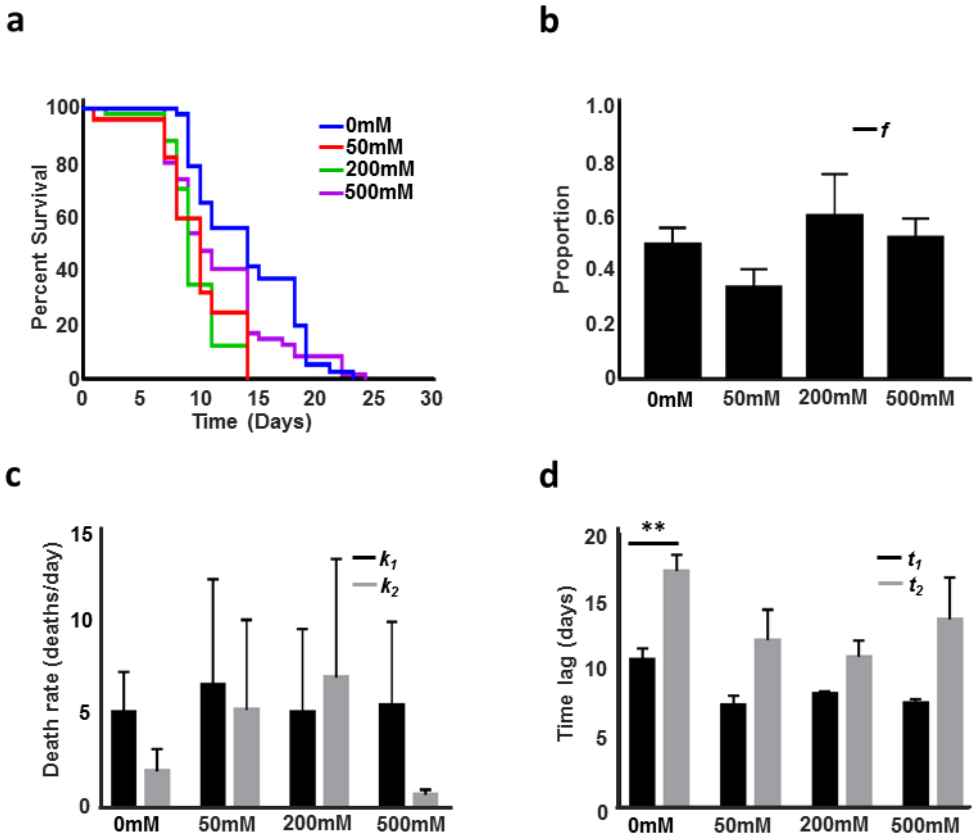

Figure 5.11: Lifespan and parameters of *hif-1(ia4)* mutants in normoxia treated with carvacrol (0mM/control, 50mM, 200mM and 500mM). **(a)** representative survival curves, **(b)** *f* parameters, **(c)** early (*k1*) and late (*k2*) phase death rate and **(d)** early (*t1*) and late (*t2*) time phases. Carvacrol D/R (n=3). Data is shown as mean ± SEM. ***p*<0.01

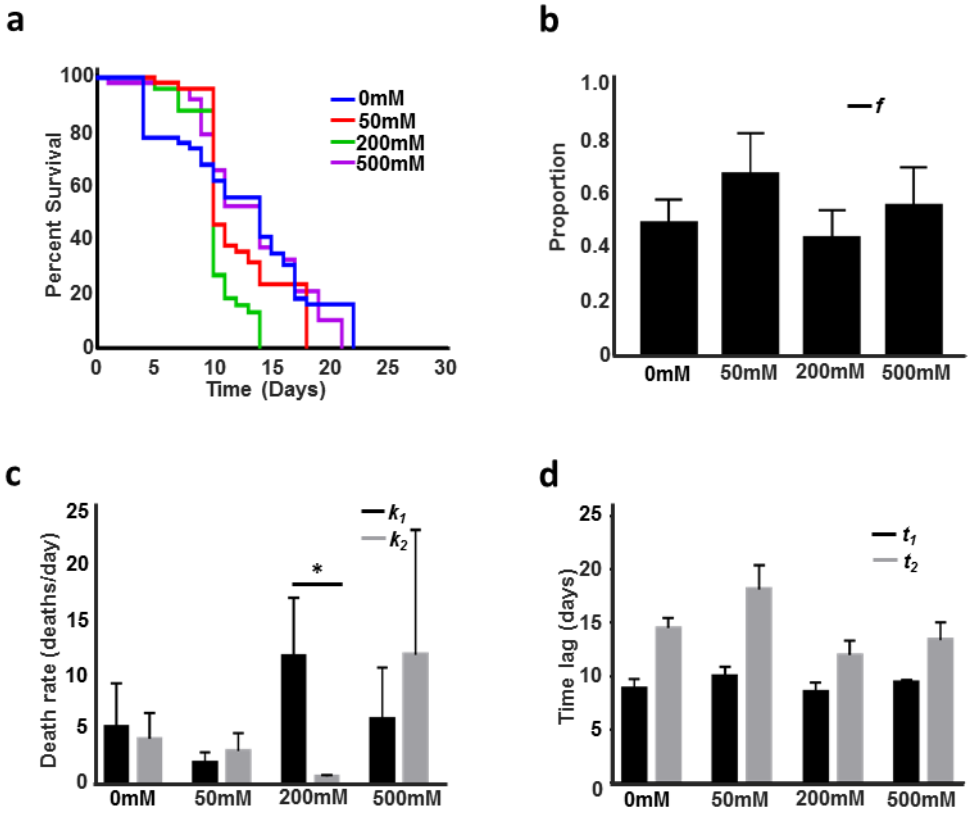

Figure 5.12: Lifespan and parameters of *trpa-1(ok999)* mutants in normoxia treated with carvacrol (0mM/control, 50mM, 200mM and 500mM). **(a)** representative survival curves, **(b)** *f* parameters, **(c)** early (*k1*) and late (*k2*) phase death rate and **(d)** early (*t1*) and late (*t2*) time phases. Carvacrol D/R (n=3). Data is shown as mean ± SEM. *p<0.05.

Carvacrol treatment of *daf-16(mu86)* mutants also shows differences in lifespan with a general decrease in lifespan at increasing concentrations (Figure 5.13a). In particular the late phase death rate is significantly higher with the increasing concentration of carvacrol. However, there is an unexpected decrease again at the highest dose of 500mM, which is indicative of phases merging (Figure 5.13c). Additionally, as previously shown (section 3.4.3), *daf-16(mu86)* mutants have a significantly higher late phase death rate in normoxic conditions compared to wild type. With increasing carvacrol concentrations, the difference between the late phase death rates increases except for treatment with 500mM (Figure 5.13).

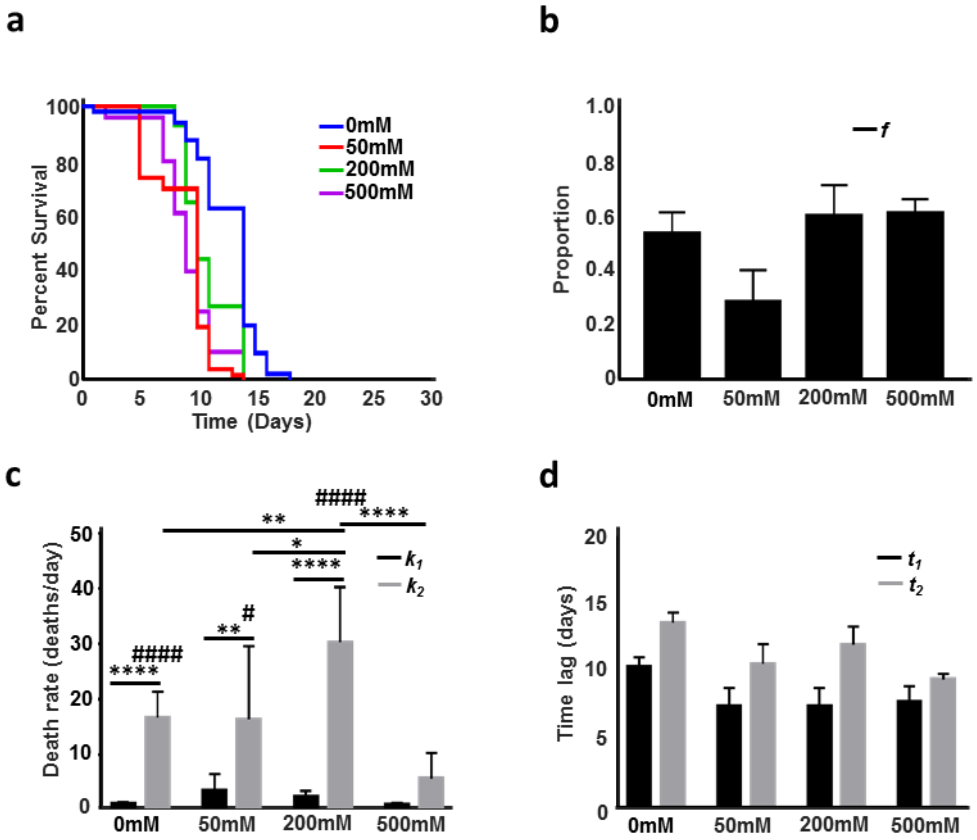

Figure 5.13: Lifespan and parameters of *daf-16(mu86)* mutants in normoxia treated with carvacrol (0mM/control, 50mM, 200mM and 500mM). **(a)** representative survival curves, **(b)** *f* parameters, **(c)** early (*k1*) and late (*k2*) phase death rate and **(d)** early (*t1*) and late (*t2*) time phases. Carvacrol D/R (n=3) *shows statistical comparison to other doses, # shows statistical comparison to WT. Data is shown as mean ± SEM. ****p<0.0001, **p<0.01, *p<0.05. ####p<0.0001

There is no significant difference between wild type worms and *hif-1(ia4)* mutants treated with carvacrol (Figure 5.10, 5.11, 5.14 and 5.15). However, a difference is observed between wild type and *trpa-1(ok999)* mutants in hypoxic conditions (Figure 5.14 and 5.16). There is a sharp increase in late phase death rate in *trpa-1(ok999)* mutants subjected to hypoxia (Figure 5.16c).

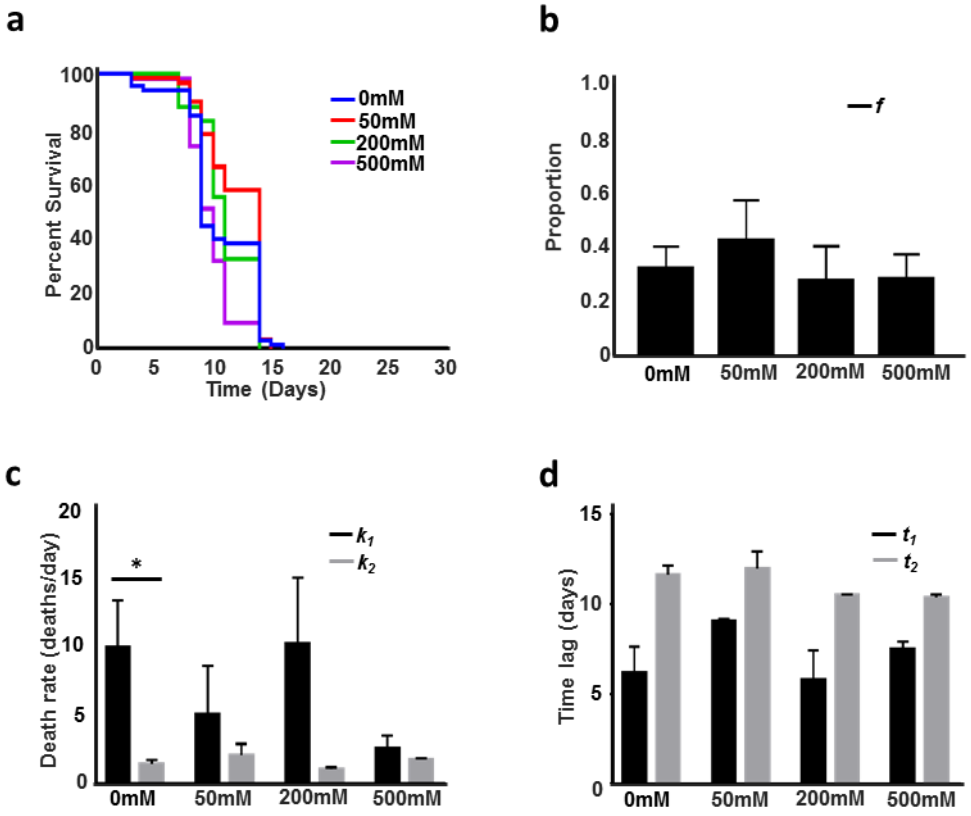

Figure 5.14: Lifespan and parameters of wild type (N2) *C. elegans* in hypoxia treated with carvacrol (0mM/control, 50mM, 200mM and 500mM). **(a)** representative survival curves, **(b)** *f* parameters, **(c)** early (*k1*) and late (*k2*) phase death rate and **(d)** early (*t1*) and late (*t2*) time phases. Carvacrol D/R (n=3). Data is shown as mean ± SEM. *p<0.05

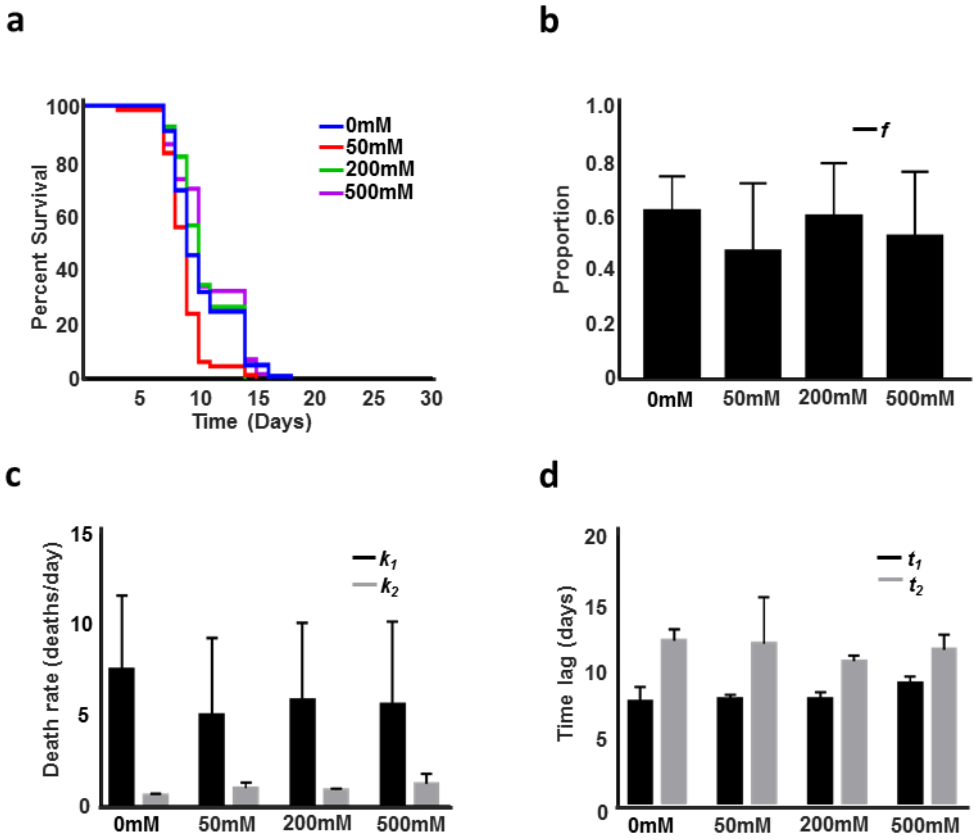

Figure 5.15: Lifespan and parameters of *hif-1(ia4)* mutants in hypoxia treated with carvacrol (0mM/control, 50mM, 200mM and 500mM). **(a)** representative survival curves, **(b)** *f* parameters, **(c)** early (*k1*) and late (*k2*) phase death rate and **(d)** early (*t1*) and late (*t2*) time phases. Carvacrol D/R (n=3). Data is shown as mean ± SEM.

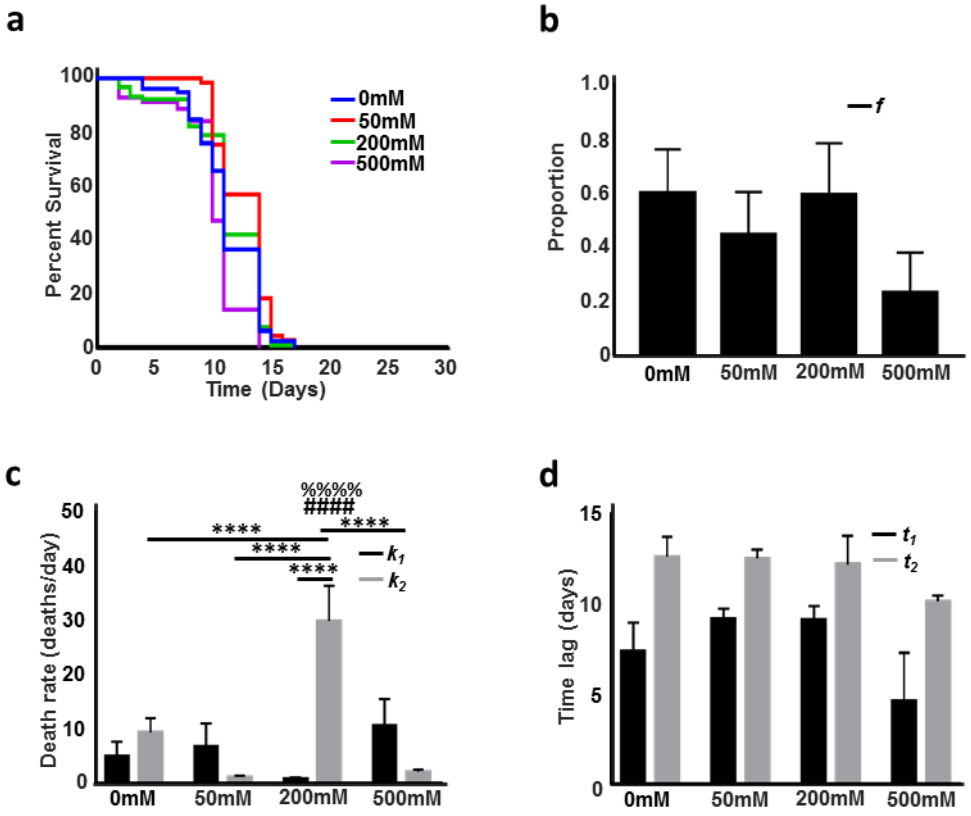

Figure 5.16: Lifespan and parameters of *trpa*-1*(ok999)* mutants in hypoxia treated with carvacrol (0mM/control, 50mM, 200mM and 500mM). **(a)** representative survival curves, **(b)** *f* parameters, **(c)** early (*k1*) and late (*k2*) phase death rate and **(d)** early (*t1*) and late (*t2*) time phases. Carvacrol D/R (n=3) *shows statistical comparison to other doses, # shows statistical comparison to WT in hypoxia, % shows statistical comparison to *trpa-1(ok999)* mutants in normoxia. Data is shown as mean ± SEM. ****p<0.0001, ####p<0.0001, %%%%p<0.0001.

5.5 Discussion

This chapter has focused on investigating the role of different factors suggested to be important in hypoxia and temperature signalling which also acts to regulate lifespan. Mutant *C. elegans* worms were subjected to different lifespan modifiers such as different temperatures and oxygen concentrations and pharmacological agents. By using the Bilogistic model, differences in early and late phase death rates and time phases were identified, quantified and compared. Additionally, the interaction between the hypoxia and temperature pathways were investigated in both mammalian cells and *C. elegans* by treatment with carvacrol to activate TRPA-1. A dose-response was conducted which allowed quantitative measurement of HIF levels in the mammalian cells and identification of parameter changes in worms.

It was expected that in normal conditions (i.e. normoxia and 20°C) mutations would alter the lifespan of worms. However only a few differences in lifespan of worms were observed. Although lifespan appears to change, it is only in *daf-16(mu86)* mutants in which significant differences in lifespan parameters is seen in particular the later phase death rate. Other mutants do not necessarily show differences in lifespan as differences may only occur in specific temperature or oxygen conditions.

As has previously been shown a reduction in temperature extends the lifespan of wild type worms (Klass, 1977). Temperature has a more varied effect on mutant worms depending on the mutation and the degree of temperature change. In most mutants used, except for *hif-1(ia4)* mutants and the egl-9 (n586) mutants, the reduction in temperature results in an extension in the late phase time phase or a decrease in the late phase death rate. An explanation for the absence of effect in *hif-1(ia4)* and *egl-9(n586)* mutants could be that they may have a temperature sensitive role. However, this also shows that not all mutations have the same effect as the two different *egl-9* mutations (*egl-9(n586)* and *egl-9(sa307)*) do not produce the overall same effect on lifespan. This is due to the *egl-9(n586)* mutation being a substitution and the *egl-9(sa307)* mutation is a 243 base pair deletion, so that there may still be some activity in the *egl-9(n586)* mutation.

In hypoxic conditions, there is a general but not always significant increase in lifespan. In wild type worms a significant increase in lifespan is not observed but this may be due to the low number of realisations (n=3). The general increase in lifespan follows similar trends as previous studies in hypoxia, however, due to the differences in methodologies there still remain difficulties in comparing studies (Leiser et al., 2013). Additionally, the lifespan and parameters of *hif-1(ia4)* mutants are not changed in hypoxic conditions which is also supported by a previous study (Leiser et al., 2013). The *trpa-1(ok999)* mutants have a more varied response to hypoxia as in hypoxic conditions, *trpa-1(ok999)* mutants show a decrease in early phase lifespan and an increase in late phase lifespan suggesting that hypoxia results in worms dying slowly in early lifespan but more quickly in later lifespan. Additionally, comparison with wild type worms in hypoxia shows an increase in late phase death rate of *trpa-1(ok999)* mutants. Our data suggests that *trpa-1* is affected by hypoxia with a reduction in lifespan regulation. The sensitisation of *trpa-1* by hypoxia has previously been reported in mice (So et al., 2016).

The measured differences between wild type and mutant worms are dependent on the method of lifespan measurement. It is observed that measurement using the scanner reduces lifespan in all cases; an explanation for this is that on the surface of the scanner the heat generated on the glass may affect lifespan. Another explanation is the light generated from the scanners whilst taking scans. Although it has previously been stated that the light from the scanners only show small differences in lifespan further research into the effect of visible light shows that this may not be the case as worm lifespan shows sensitivity to visible light radiation (Stroustrup et al., 2013, De Magalhaes Filho et al., 2018). Although this methodology of digital recordings of lifespan in hypoxia is not fully optimised it does provide a more complete solution than other hypoxic measurement of lifespan. This methodology allows multiple plates of worm to be observed and recorded whilst in completely hypoxic conditions for the entirety of their lifespan.

Primarily the *in vitro* investigation in mammalian cells allowed the interaction between HIF and TRPA-1 to be identified. It is known that TRPA-1 is activated by carvacrol leading to

calcium entry and signalling (Hasan et al., 2017). Additionally, it is known that HIF activity increases in hypoxic conditions. This short study expands on these findings and shows that increasing carvacrol concentrations reduces HIF activity in both HEK293 and HEPG2 cell with a minimum effective dose of 50μM. We conclude from our mammalian cell studies that carvacrol affects TRPA-1 signalling and HIF activity and therefore would be an ideal pharmacological agent to treat worms with to further investigate how the HIF-1 and TRPA-1 signalling pathways regulate lifespan and additionally show if this signalling link is applicable to *C. elegans*. Although interactions from PHDs/HIFs to TRPA-1 have been identified we report the first plausible interaction from TRPA-1 to HIF-1 (Hatano et al., 2012, Nagarajan et al., 2017). Additionally, it has been extensively reported that other Ca^{2+} channels (TRPC and TRPM) regulate HIF-1 (mRNA levels, translation, stabilisation and translocation) activity (Azimi, 2018). This supports our findings that TRPA-1 acts to regulate HIF activity in mammalian cells.

The carvacrol dose response treatment on *C. elegans* has varied effect between the different mutants, conditions and concentrations used. Worms are able to survive in the presence of carvacrol, although previous studies have shown that carvacrol has nematocidal effects with 100% mortality within 24 hours (Lei et al., 2010, Yu, 2000). Again, the difference in the results is likely due to differences in methodology, as the previous study used worms in a liquid culture with a growth temperature between 22°C and 25°C which may be detrimental to the worms. However, as our study did not find nematocidal activity from carvacrol, and thus it was used to investigate its effect upon different mutants (Lei et al., 2010, Yu, 2000). Another possibility as to why carvacrol does not have a consistent effect in its dose-response is that in our study carvacrol was added to the melted NGM agar before pouring in to plates but other studies apply carvacrol on top of the agar. This may possibly account for different effects of carvacrol. In wild type and most other mutants, there is a small reduction in lifespan but in *trpa-1(ok999)* mutants, more specific changes have been identified. In these mutants, differences are observed at 200mM in both hypoxia and normoxia, however, there is much variation among replicates. From the lifespan curves however, it is clear that in normoxia and at all doses of carvacrol used lifespan is mostly similar and suggests that carvacrol does not

have a defined effect. In *trpa-1(ok999)* mutants this is expected because there is no TRPA-1 for carvacrol to act upon. But in wild type and other mutants, this lack of effect suggests that carvacrol is not necessarily acting upon TRPA-1. This can be explained by the differences between TRPA-1 homology in humans and *C. elegans*. It has been reported that there is only a 41% similarity between human and *C. elegans* TRPA-1, and this may be why carvacrol may not act upon *C. elegans* TRPA-1 in the same way as it acts upon human TRPA-1 (Kindt et al., 2007). Overall, carvacrol does not display a consistent effect on the different worm lifespans making it difficult to assess how as a chemical activator of TRPA-1 it could influence lifespan by targeting other components of either pathway. However, the results shown are based upon 3 replicates and analysed and shown in a similar manner as to previous chapters for consistency, further experimental realisations may allow for more consistent results.

5.5.1 Future work

Having shown a number of changes in lifespan (and parameters from the novel 5-parameter Bilogistic model) of multiple different mutant worms in response to temperature and hypoxia, it is important to investigate these factors mechanistically. By measuring gene expression, protein expression or activity of the different factors in response to the different conditions and pharmacological treatment, it would provide a more detailed picture on the relationship between the factors. Once again this can be done in the different mutants and also at different time points throughout the worms lifespan to identify the relationship dynamics in the ageing worm. Additionally, further investigation could be conducted specifically to investigate the relationship between TRPA-1 and HIF-1. For example, in mammalian cells the calcium currents could be investigated to measure TRPA-1 ion channel opening and further signal transduction which may affect HIF-1. Alternative approaches to activate TRPA-1 can be considered to determine the relationship between the two pathways.

Additionally, this study utilises scanners to carry out digital lifespan assays and to maintain a record of worm lifespan. Ideally this methodology would need to be improved to reduce the number of variables which may affect worm lifespan so to reduce differences between manual lifespan assays and digital lifespan assays.

5.6 Conclusion

This study investigates the lifespan of *C. elegans* in relation to temperature and hypoxia signalling. Genetic mutations, temperature changes and oxygen levels and treatment with pharmacological agents all effect the lifespan of *C. elegans*. Specific changes in lifespan parameters have provided an insight into whether early or late phase of worms are affected and also the magnitude of effect which take place. A relationship between TRPA-1 and HIF has also been established in mammalian cells but our data suggests that this pathway is not applicable to *C. elegans.* Finally, a pilot methodology for measurement of worm lifespan in continuous hypoxia has been introduced. These studies are expected to facilitate the understanding of how hypoxia and temperature affect lifespan and how the two pathways interact with one another.

Chapter 6.0: General Discussion

6.1 Discussion

Two phases of lifespan have been described in *C. elegans* in a number of different studies (Zhao et al., 2017, Hahm et al., 2015, Zhang et al., 2016). The majority of studies analysing lifespan generally use non-parametric analysis methods which provide limited conclusions. Relatively few studies use parametric lifespan analysis and those that do tend to use monophasic parametric models which by construction are incapable of modelling two phases of lifespan. The initial objective of generating a parametric model capable of modelling biphasic lifespan was achieved and has been shown to provide a more meaningful interpretation of data than existing non-parametric and parametric models as early and late lifespan death rates and time phases can be defined. Furthermore, due to the superior fitting with the Bilogistic model this confirms that lifespan in *C. elegans* can be biphasic. Additionally, this novel Bilogistic model has been shown to accurately fit lifespan data from not only worms but also from other species such as flies, bees and mice. In *C. elegans,* the Bilogistic model is able to fit different mutants and temperature conditions in which the effect of these changes on the parameters can be identified.

Interventions are important in altering lifespan. To be able to predict the effect of interventions would be beneficial as it would provide information on the optimum time point for intervention. In *C. elegans* one of the easiest interventions is to change the temperature. An initial objective of generating two predictive models capable of modelling intervention data was achieved by using the Bilogistic model. The two predictive models were shown to predict the effect of switching the temperature between high detrimental conditions and low favourable conditions which were compared to experimental data. However, the predictive model based on chronological age is not entirely capable of predicting the effect of temperature intervention but by incorporating biological age the predictions improve as the predicted average lifespan is closer to experimental average lifespan. This suggests that at a given time the chronological age is less important than the survival proportions as high survival proportion are more indicative of a healthier population compared to those with a lower survival proportion. An additional important output from this intervention investigation is the identification of critical

time points which indicate time points at which the average lifespan is pre-determined and time points at which interventions are too late and so result in minimal effects. Generally, the more time spent in favourable conditions results in a higher average lifespan. This suggests that time spent in favourable conditions must be prolonged for as long as possible and time spent in detrimental conditions should be avoided to gain maximum benefit. Additionally, many early environmental conditions have lasting effects later on in lifespan. For example, early detrimental conditions may act as a stressor which the worm is capable of adapting to and by introducing a favourable intervention it can lead to further lifespan extension compared to if the early detrimental condition was not experienced. This is supported by reports which look at intervention in developmental stages of worms and show similar findings on the importance of the larval stage (Zhang et al., 2015). TRPA-1 based lifespan extension in response to low temperatures compared to wild type was not seen as previously reported (Xiao et al., 2013). Although, our findings do suggest that TRPA-1 is more sensitive to low temperatures compared to high temperatures. Additionally, *trpa-1(ok999)* mutants show an impaired ability to adapt to interventions (both high to low and low to high temperatures). This suggests that TRPA-1 does play a role in detecting temperature and regulating lifespan in *C. elegans* however other factors which respond to temperature cannot be ruled out. Overall this suggests that TRPA-1 may not actively act to increase average lifespan or that the temperature range at which it does act may be outside the range investigated. Generally TRPA-1 as a cold sensor has been a much debated topic and a more detailed investigation into its function and response to temperature would need to be conducted (Caspani and Heppenstall, 2009). Both of the predicted models presented can be applied to a range of different intervention types, however the prediction accuracy is dependent on the initial input data used by the model.

In addition to TRPA-1, a number of other factors reported to be involved in the temperature and hypoxia signalling pathways were investigated. *Daf-16(mu86)* mutants show that the increase in late phase death rate is what reduces lifespan. Furthermore, by reducing temperature there is an increase in lifespan in most mutants which is considered to be due to changes in late phase death rate and time phases. In hypoxic conditions *trpa-1(ok999)*

mutants die more quickly earlier but more slowly later suggesting that in hypoxia *trpa-1* normally acts to prevent earlier death but also may play a role in promoting death later on. This links well to previous reports in which TRPA-1 is regulated by hypoxia, and the effect of this regulation may have an impact upon lifespan (Takahashi et al., 2011). In mammalian cells, the link between HIF and TRPA-1 was investigated and shown that pharmacological activation of TRPA-1 by carvacrol acts to reduce HIF activity and may act via calcium signalling (Hasan et al., 2017). Worms treated with carvacrol to activate TRPA-1 show greater levels of survival than that which has previously been reported (Lei et al., 2010). Generally, the lifespan of carvacrol treated worms is lower than non-treated, however this effect on lifespan is generally not significant or consistent. This may be due to carvacrol not specifically targeting TRPA-1 in *C. elegans* or that there may be erratic activation of TRPA-1 by the compound resulting in varied effects. Worms which were treated with carvacrol and additionally grown in a hypoxic environment did not provide conclusive data into identifying the effect of both TRPA-1 and HIF-1 activation. Another explanation for the varied effects of carvacrol in these studies is that the carvacrol is added to molten NGM agar and so may not have a direct impact on the worms. The chemical activation of TRPA-1 did not show any significant consistent change to lifespan and does not appear to affect HIF-1 in the same way that was seen in mammalian cells and so the interaction is not yet pertinent to *C. elegans*.

Overall the Bilogistic model has provided a way to collate and analyse lifespan data to identify the proportion of worms that die in the early and late phase of lifespan and from the parameter values changes to early and late phase death rate or time phases can be identified (Figure 6.1). By using this method to investigate the TRPA-1 and HIF-1 signalling pathways this model has provided further insight into the role played on lifespan and when these factors are important, yet the exact role played by the individual factors is yet to be determined.

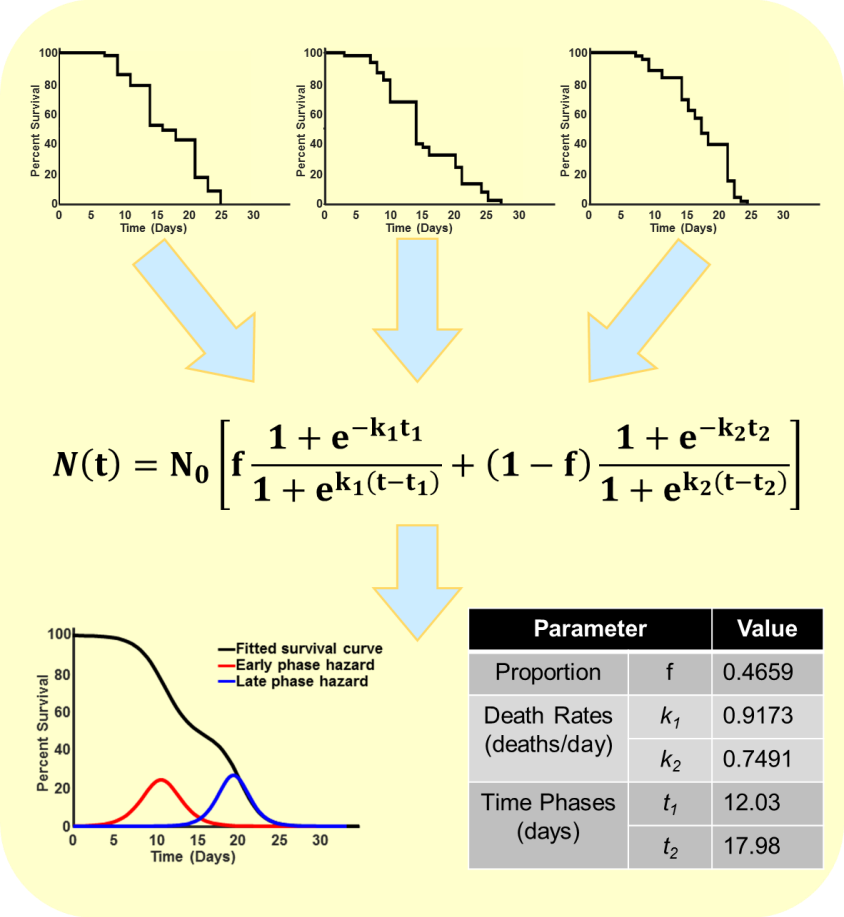

Parameter		Value
Proportion	f	0.4659
Death Rates (deaths/day)	k_1	0.9173
	k_2	0.7491
Time Phases (days)	t_1	12.03
	t_2	17.98

Figure 6.1: The Bilogistic model; a novel mathematical model which can be used to collate and analyse lifespan data outputting 5 parameter values defining early and late phases.

6.1.1 Future Work

For future investigations into lifespan, we propose that the Bilogistic model is used to analyse lifespan data to gain maximum information. As the Bilogistic model has been identified as a superior model for fitting *C. elegans* lifespan data it could still be compared to a number of other proposed models. Additionally, the Bilogistic model can be applied to a range of other time to event data sets for example survival of other animals, tumour growth, bacterial growth or inactivation or even to applications outside of biology such as investigation of component failure in engineering.

The biphasic nature of lifespan is an important area to be studied further, particularly as biphasic dynamics are seen in a range of organisms. It would be important to identify (transcriptional and translational) universal mechanisms which result in biphasic lifespan.

Furthermore, lifespan, genetic, molecular and physiological measurements can be conducted relatively easily and quickly in worms compared to other organisms.

In future investigations on the effects of intervention on lifespan, different interventions could be used for example environmental interventions such as hypoxia or pharmacological interventions to identify critical time points at which each intervention is important. The biological and chronological models can also be applied and tested against these different interventions and can be used to generate lifespan predictions. Temperature interventions can also be investigated further in more detail, with a range of different temperatures or more time points can be considered to further characterise the role of TRPA-1. However other factors which are temperature sensitive such as the AFD neurons must also be studied to identify differential regulation of lifespan in response to temperature.

The interaction between the HIF-1 and TRPA-1 signalling pathways also need to be investigated further. In mammalian cells, additional studies could be conducted to identify the specific signalling pathway from TRPA-1 to HIF-1 for example by investigating TRPA-1 ion channel function and signal transduction. In *C. elegans* alternative methods could be used to investigate the role of the different factors regulating lifespan, for example using RNAi to inhibit gene expression or to overexpress genes with different output measures such as gene or protein expression. Furthermore, alternative approaches to activation of HIF-1 and TRPA-1 could be conducted to identify relationship changes.

6.2 Conclusion

This thesis proposes a Bilogistic model used to model the lifespan of *C. elegans* and other species in a range of conditions. It shows an improved methodology to investigate lifespan by providing more specific outcomes and the ability to be used for predictive modelling of interventions. Additionally, this thesis describes the roles played by factors involved in hypoxia and temperature signalling and proposes a link between TRPA-1 and HIF-1. It can be confirmed that the specific objectives have been met:

- A novel mathematical model capable of modelling biphasic lifespan data has been generated. Additionally with this model we are able to confirm that *C. elegans* can display biphasic lifespan. Comparison of this novel model with other existing models with RMSE and residual analysis shows that the novel Bilogistic model provides a more versatile and superior fitting capability and that this model is applicable to flies bees and mice.
- Two predictive models were designed to predict the effect of temperature interventions on lifespan. The biological model provides better predictions of intervention compared to the chronological model in wild type worms. A number of critical time points in both wild type and *trpa-1(ok999)* mutants were identified showing time points at which changes to average lifespan occur.
- The Bilogistic model was used to identify parameter changes in response to mutations, temperature and oxygen changes. Additionally in mammalian cells it has identified that TRPA-1 activation results in a reduction of HIF activity. This link has not been shown to be applicable to *C. elegans*.

Overall this thesis has used mathematical modelling techniques effectively to investigate how TRPA-1 and HIF-1 signalling regulate lifespan.

Chapter 7.0: List of References

ADEN, D., FOGEL, A., PLOTKIN, S., DAMJANOV, I. & KNOWLES, B. 1980. Controlled synthesis of HBsAG in a differentiated human liver carcinoma-derived cell line.

AMRIT, F. R., RATNAPPAN, R., KEITH, S. A. & GHAZI, A. 2014. The C. elegans lifespan assay toolkit. Methods, 68, 465-75.

ANDERSEN, E. C., GERKE, J. P., SHAPIRO, J. A., CRISSMAN, J. R., GHOSH, R., BLOOM, J. S., FELIX, M. A. & KRUGLYAK, L. 2012. Chromosome-scale selective sweeps shape Caenorhabditis elegans genomic diversity. Nat Genet, 44, 285-90.

ANDERSON, J. L., MORRAN, L. T. & PHILLIPS, P. C. 2010. Outcrossing and the maintenance of males within C. elegans populations. J Hered, 101 Suppl 1, S62-74.

ARGENTINO, D. P., DOMINICI, F. P., MUNOZ, M. C., AL-REGAIEY, K., BARTKE, A. & TURYN, D. 2005. Effects of long-term caloric restriction on glucose homeostasis and on the first steps of the insulin signaling system in skeletal muscle of normal and Ames dwarf (Prop1df/Prop1df) mice. Exp Gerontol, 40, 27-35.

ARRHENIUS, S. 1889. Über die Dissociationswärme und den Einfluss der Temperatur auf den Dissociationsgrad der Elektrolyte. Zeitschrift für Physikalische Chemie.

AZIMI, I. 2018. The interplay between HIF-1 and calcium signalling in cancer. Int J Biochem Cell Biol, 97, 73-77.

BAKKER, W. J., HARRIS, I. S. & MAK, T. W. 2007. FOXO3a is activated in response to hypoxic stress and inhibits HIF1-induced apoptosis via regulation of CITED2. Mol Cell, 28, 941-53.

BANSAL, A., ZHU, L. J., YEN, K. & TISSENBAUM, H. A. 2015. Uncoupling lifespan and healthspan in Caenorhabditis elegans longevity mutants. Proc Natl Acad Sci U S A, 112, E277-86.

BASS, T. M., GRANDISON, R. C., WONG, R., MARTINEZ, P., PARTRIDGE, L. & PIPER, M. D. 2007. Optimization of dietary restriction protocols in Drosophila. J Gerontol A Biol Sci Med Sci, 62, 1071-81.

BLAXTER, M. 2011. Nematodes: the worm and its relatives. PLoS Biol, 9, e1001050.

BODKIN, N. L., ALEXANDER, T. M., ORTMEYER, H. K., JOHNSON, E. & HANSEN, B. C. 2003. Mortality and morbidity in laboratory-maintained Rhesus monkeys and effects of long-term dietary restriction. The Journals of Gerontology Series A: Biological Sciences and Medical Sciences, 58, B212-B219.

BONSALL, M. B. 2006. Longevity and ageing: appraising the evolutionary consequences of growing old. Philos Trans R Soc Lond B Biol Sci, 361, 119-35.

BRADBURN, M. J., CLARK, T. G., LOVE, S. B. & ALTMAN, D. G. 2003. Survival analysis part II: multivariate data analysis--an introduction to concepts and methods. British journal of cancer, 89, 431-436.

BROWN, S. T., KELLY, K. F., DANIEL, J. M. & NURSE, C. A. 2009. Hypoxia inducible factor (HIF)-2 alpha is required for the development of the catecholaminergic phenotype of sympathoadrenal cells. J Neurochem, 110, 622-30.

BUGNARD, F., DUCROT, C. & CALAVAS, D. 1994. Advantages and inconveniences of the Cox model compared with the logistic model: application to a study of risk factors of nursing cow infertility. Vet Res, 25, 134-9.

BURKLE, A., MORENO-VILLANUEVA, M., BERNHARD, J., BLASCO, M., ZONDAG, G., HOEIJMAKERS, J., TOUSSAINT, O., GRUBECK-LOEBENSTEIN, B., MOCCHEGIANI, E., COLLINO, S., GONOS, E., SIKORA, E., GRADINARU, D., DOLLE, M., SALMON, M., KRISTENSEN, P., GRIFFITHS, H., LIBERT, C., GRUNE, T., BREUSING, N., SIMM, A., FRANCESCHI, C., CAPRI, M., TALBOT, D., CAIAFA, P., FRIGUET, B., SLAGBOOM, P., HERVONEN, A., HURME, M. & ASPINALL, R. 2015. MARK-AGE biomarkers of ageing. Mechanisms of Ageing and Development, 151, 2-12.

CASPANI, O. & HEPPENSTALL, P. A. 2009. TRPA1 and cold transduction: an unresolved issue? The Journal of general physiology, 133, 245-249.

CAVADAS, M. A. & CHEONG, A. 2014. Monitoring of transcriptional dynamics of HIF and NFκB activities. Methods Mol Biol, 1098, 97-105.

CHAI, T. & DRAXLER, R. R. 2014. Root mean square error (RMSE) or mean absolute error (MAE)? - Arguments against avoiding RMSE in the literature. Geoscientific Model Development, 7, 1247-1250.

CHANG, A. J., CHRONIS, N., KAROW, D. S., MARLETTA, M. A. & BARGMANN, C. I. 2006. A distributed chemosensory circuit for oxygen preference in C. elegans. PLoS Biol, 4, e274.

CHAUDHARI, S. N. & KIPREOS, E. T. 2018. The Energy Maintenance Theory of Aging: Maintaining Energy Metabolism to Allow Longevity. Bioessays, 40, e1800005.

CHEN, J. 2015. The evolutionary divergence of TRPA1 channel: heat-sensitive, cold-sensitive and temperature-insensitive. Temperature (Austin), 2, 158-9.

CHEN, J., KANG, D., XU, J., LAKE, M., HOGAN, J. O., SUN, C., WALTER, K., YAO, B. & KIM, D. 2013. Species differences and molecular determinant of TRPA1 cold sensitivity. Nat Commun, 4, 2501.

CHEN, Y. 2012. Calcium Phosphate Transfection of Eukaryotic Cells. Bio-protocol, 2, e86.

CHEUNG, B. H., ARELLANO-CARBAJAL, F., RYBICKI, I. & DE BONO, M. 2004. Soluble guanylate cyclases act in neurons exposed to the body fluid to promote C. elegans aggregation behavior. Curr Biol, 14, 1105-11.

COATES, J. C. & DE BONO, M. 2002. Antagonistic pathways in neurons exposed to body fluid regulate social feeding in Caenorhabditis elegans. Nature, 419, 925-9.

COHEN, H. Y., MILLER, C., BITTERMAN, K. J., WALL, N. R., HEKKING, B., KESSLER, B., HOWITZ, K. T., GOROSPE, M., DE CABO, R. & SINCLAIR, D. A. 2004. Calorie restriction promotes mammalian cell survival by inducing the SIRT1 deacetylase. Science, 305, 390-2.

COLLETT, D. 2015. Modelling Survival Data in Medical Research, Third Edition, CRC Press.

COLMAN, R. J., BEASLEY, T. M., KEMNITZ, J. W., JOHNSON, S. C., WEINDRUCH, R. & ANDERSON, R. M. 2014. Caloric restriction reduces age-related and all-cause mortality in rhesus monkeys. Nat Commun, 5, 3557.

CONTI, B. 2008. Considerations on temperature, longevity and aging. Cell Mol Life Sci, 65, 1626-30.

CORSI, A. K., WIGHTMAN, B. & CHALFIE, M. 2015. A Transparent Window into Biology: A Primer on Caenorhabditis elegans. Genetics, 200, 387-407.

COX, D. R. 1972. Regression Models and Life-Tables. Journal of the Royal Statistical Society. Series B (Methodological), 34, 187-220.

CRIMMINS, E. M. 2015. Lifespan and Healthspan: Past, Present, and Promise. The Gerontologist, 55, 901-911.

CULETTO, E. & SATTELLE, D. B. 2000. A role for Caenorhabditis elegans in understanding the function and interactions of human disease genes. Human Molecular Genetics, 9, 869-877.

CYPSER, J. R., TEDESCO, P. & JOHNSON, T. E. 2006. Hormesis and aging in Caenorhabditis elegans. Exp Gerontol, 41, 935-9.

DANOVARO, R., DELL'ANNO, A., PUSCEDDU, A., GAMBI, C., HEINER, I. & KRISTENSEN, R. M. 2010. The first metazoa living in permanently anoxic conditions. BMC Biol, 8, 30.

DAWE, A. S., SMITH, B., THOMAS, D. W., GREEDY, S., VASIC, N., GREGORY, A., LOADER, B. & DE POMERAI, D. I. 2006. A small temperature rise may contribute towards the apparent induction by microwaves of heat-shock gene expression in the nematode Caenorhabditis Elegans. Bioelectromagnetics, 27, 88-97.

DE BEER, J., BARDOUTSOS, A. & JANSSEN, F. 2017. Maximum human lifespan may increase to 125 years. Nature, 546, E16-E20.

DE MAGALHAES FILHO, C. D., HENRIQUEZ, B., SEAH, N. E., EVANS, R. M., LAPIERRE, L. R. & DILLIN, A. 2018. Visible light reduces C. elegans longevity. Nat Commun, 9, 927.

DEEVEY, E. S. 1947. Life Tables for Natural Populations of Animals. The Quarterly Review of Biology, 22, 283-314.

DEMETRIUS, L. 1978. Adaptive value, entropy and survivorship curves. Nature, 275, 213-4.

DENGLER, V. L., GALBRAITH, M. & ESPINOSA, J. M. 2014. Transcriptional regulation by hypoxia inducible factors. Critical reviews in biochemistry and molecular biology, 49, 1-15.

DILLIN, A., GOTTSCHLING, D. E. & NYSTROM, T. 2014. The good and the bad of being connected: the integrons of aging. Curr Opin Cell Biol, 26, 107-12.

DUFFY, P. H., FEUERS, R. J. & HART, R. W. 1990. Effect of Chronic Caloric Restriction on the Circadian Regulation of Physiological and Behavioral Variables in Old Male B6C3F1 Mice. Chronobiology International, 7, 291-303.

DÄTWYLER, C. & STUCKI, T. 2011. Parametric survival models.

EPSTEIN, A. C., GLEADLE, J. M., MCNEILL, L. A., HEWITSON, K. S., O'ROURKE, J., MOLE, D. R., MUKHERJI, M., METZEN, E., WILSON, M. I., DHANDA, A., TIAN, Y. M., MASSON, N., HAMILTON, D. L., JAAKKOLA, P., BARSTEAD, R., HODGKIN, J., MAXWELL, P. H., PUGH, C. W., SCHOFIELD, C. J. & RATCLIFFE, P. J. 2001. C. elegans EGL-9 and mammalian homologs define a family of dioxygenases that regulate HIF by prolyl hydroxylation. Cell, 107, 43-54.

EWALD, C. Y., HOURIHAN, J. M., BLAND, M. S., OBIEGLO, C., KATIC, I., MORONETTI MAZZEO, L. E., ALCEDO, J., BLACKWELL, T. K. & HYNES, N. E. 2017. NADPH oxidase-mediated redox signaling promotes oxidative stress resistance and longevity through. Elife, 6.

FAWCETT, E. M., HORSMAN, J. W. & MILLER, D. L. 2012. Creating defined gaseous environments to study the effects of hypoxia on C. elegans. J Vis Exp, e4088.

FELIX, M. A. & BRAENDLE, C. 2010. The natural history of Caenorhabditis elegans. Curr Biol, 20, R965-9.

FLATT, T. 2012. A new definition of aging? Front Genet, 3, 148.

FREITAS, A. A. & DE MAGALHAES, J. P. 2011. A review and appraisal of the DNA damage theory of ageing. Mutat Res, 728, 12-22.

FRIEDMAN, D. B. & JOHNSON, T. E. 1988. A mutation in the age-1 gene in Caenorhabditis elegans lengthens life and reduces hermaphrodite fertility. Genetics, 118, 75-86.

GEMS, D. & RIDDLE, D. L. 2000. Genetic, behavioral and environmental determinants of male longevity in Caenorhabditis elegans. Genetics, 154, 1597-610.

GENCODE VERSION 29, G. 2019. GENCODE - Statistics.

GENSLER, H. L. & BERNSTEIN, H. 1981. DNA damage as the primary cause of aging. The Quarterly review of biology, 56, 279-303.

GIACCIA, A. J. 2013. HIF-2: the missing link between obesity and cardiomyopathy. J Am Heart Assoc, 2, e000710.

GOEL, M. K., KHANNA, P. & KISHORE, J. 2010. Understanding survival analysis: Kaplan-Meier estimate. Int J Ayurveda Res, 1, 274-8.

GOGGINS, W. B., WOO, J., SHAM, A. & HO, S. C. 2005. Frailty index as a measure of biological age in a Chinese population. J Gerontol A Biol Sci Med Sci, 60, 1046-51.

GOMPERTZ, B. 1825. On the Nature of the Function Expressive of the Law of Human Mortality, and on a New Mode of Determining the Value of Life Contingencies. Philosophical Transactions of the Royal Society of London, 115, 513-583.

GRAHAM, F. L., SMILEY, J., RUSSELL, W. C. & NAIRN, R. 1977. Characteristics of a Human Cell Line Transformed by DNA from Human Adenovirus Type 5. Journal of General Virology, 36, 59-72.

GRAY, J. M., KAROW, D. S., LU, H., CHANG, A. J., CHANG, J. S., ELLIS, R. E., MARLETTA, M. A. & BARGMANN, C. I. 2004. Oxygen sensation and social feeding mediated by a C. elegans guanylate cyclase homologue. Nature, 430, 317-22.

GU, Y. Z., MORAN, S. M., HOGENESCH, J. B., WARTMAN, L. & BRADFIELD, C. A. 2018. Molecular characterization and chromosomal localization of a third alpha-class hypoxia inducible factor subunit, HIF3alpha. Gene expression, 7, 205-213.

HAHM, J.-H., KIM, S., DILORETO, R., SHI, C., LEE, S.-J. V., MURPHY, C. T. & NAM, H. G. 2015. C. elegans maximum velocity correlates with healthspan and is maintained in worms with an insulin receptor mutation. Nature Communications, 6, 8919.

HARMAN, D. 1956. Aging: a theory based on free radical and radiation chemistry. J Gerontol, 11, 298-300.

HARMAN, D. 2006. Free radical theory of aging: an update: increasing the functional life span. Ann N Y Acad Sci, 1067, 10-21.

HARRISON, D. E., STRONG, R., SHARP, Z. D., NELSON, J. F., ASTLE, C. M., FLURKEY, K., NADON, N. L., WILKINSON, J. E., FRENKEL, K., CARTER, C. S., PAHOR, M., JAVORS, M. A., FERNANDEZ, E. & MILLER, R. A. 2009. Rapamycin fed late in life extends lifespan in genetically heterogeneous mice. Nature, 460, 392-5.

HASAN, R., LEESON-PAYNE, A. T., JAGGAR, J. H. & ZHANG, X. 2017. Calmodulin is responsible for Ca. Sci Rep, 7, 45098.

HATANO, N., ITOH, Y., SUZUKI, H., MURAKI, Y., HAYASHI, H., ONOZAKI, K., WOOD, I. C., BEECH, D. J. & MURAKI, K. 2012. Hypoxia-inducible factor-1α (HIF1α) switches on transient receptor potential ankyrin repeat 1 (TRPA1) gene expression via a hypoxia response element-like motif to modulate cytokine release. J Biol Chem, 287, 31962-72.

HELIGMAN, L. & POLLARD, J. H. 2012. The age pattern of mortality. Journal of the Institute of Actuaries, 107, 49-80.

HENDERSON, D., HUEBNER, C., MARKOWITZ, M., TAUBE, N., HARVANEK, Z. M., JAKOB, U. & KNOEFLER, D. 2018. Do developmental temperatures affect redox level and lifespan in C. elegans through upregulation of peroxiredoxin? Redox Biol, 14, 386-390.

HESP, K., SMANT, G. & KAMMENGA, J. E. 2015. Caenorhabditis elegans DAF-16/FOXO transcription factor and its mammalian homologs associate with age-related disease. Exp Gerontol, 72, 1-7.

HILLIER, L. W., COULSON, A., MURRAY, J. I., BAO, Z., SULSTON, J. E. & WATERSTON, R. H. 2005. Genomics in C. elegans: so many genes, such a little worm. Genome Res, 15, 1651-60.

HONDA, S., ISHII, N., SUZUKI, K. & MATSUO, M. 1993. Oxygen-dependent perturbation of life span and aging rate in the nematode. J Gerontol, 48, B57-61.

HOUTHOOFD, K., JOHNSON, T. E. & VANFLETEREN, J. R. 2005. Dietary restriction in the nematode Caenorhabditis elegans. J Gerontol A Biol Sci Med Sci, 60, 1125-31.

HOWELL, N. J. & TENNANT, D. A. 2014. The role of HIFs in ischemia-reperfusion injury. Hypoxia (Auckl), 2, 107-115.

HU, P. J. 2007. Dauer. WormBook: the online review of C. elegans biology, 1-19.

HYUN, M., LEE, J., LEE, K., MAY, A., BOHR, V. A. & AHN, B. 2008. Longevity and resistance to stress correlate with DNA repair capacity in Caenorhabditis elegans. Nucleic Acids Res, 36, 1380-9.

JAMIESON, D. 1989. Oxygen toxicity and reactive oxygen metabolites in mammals. Free Radical Biology and Medicine, 7, 87-108.

JIANG, H., GUO, R. & POWELL-COFFMAN, J. A. 2001. The Caenorhabditis elegans hif-1 gene encodes a bHLH-PAS protein that is required for adaptation to hypoxia. Proc Natl Acad Sci U S A, 98, 7916-21.

JIANG, J. C., JARUGA, E., REPNEVSKAYA, M. V. & JAZWINSKI, S. M. 2000. An intervention resembling caloric restriction prolongs life span and retards aging in yeast. FASEB J, 14, 2135-7.

JOHNSON, T. E., MITCHELL, D. H., KLINE, S., KEMAL, R. & FOY, J. 1984. Arresting development arrests aging in the nematode Caenorhabditis elegans. Mechanisms of ageing and development, 28, 23-40.

KAEBERLEIN, M. 2018. How healthy is the healthspan concept? Geroscience, 40, 361-364.

KALETTA, T. & HENGARTNER, M. O. 2006. Finding function in novel targets: C. elegans as a model organism. Nat Rev Drug Discov, 5, 387-98.

KANE, A. E., HILMER, S. N., MACH, J., MITCHELL, S. J., DE CABO, R. & HOWLETT, S. E. 2016. Animal models of frailty: current applications in clinical research. Clinical interventions in aging, 11, 1519-1529.

KAPLAN, E. L. & MEIER, P. 1958. Nonparametric Estimation from Incomplete Observations. Journal of the American Statistical Association, 53, 457-481.

KATO, I., REN, J., HEILBRUN, L. K. & DJURIC, Z. 2006. Intra- and inter-individual variability in measurements of biomarkers for oxidative damage in vivo: Nutrition and Breast Health Study. Biomarkers, 11, 143-52.

KEIL, G., CUMMINGS, E. & DE MAGALHÃES, J. P. 2015. Being cool: how body temperature influences ageing and longevity. Biogerontology, 16, 383-97.

KENYON, C., CHANG, J., GENSCH, E., RUDNER, A. & TABTIANG, R. 1993. A C-Elegans Mutant That Lives Twice as Long as Wild-Type. Nature, 366, 461-464.

KENYON, C. J. 2010. The genetics of ageing. Nature, 464, 504-12.

KIMBLE, J. & HIRSH, D. 1979. The postembryonic cell lineages of the hermaphrodite and male gonads in Caenorhabditis elegans*1.

KINDT, K. S., VISWANATH, V., MACPHERSON, L., QUAST, K., HU, H., PATAPOUTIAN, A. & SCHAFER, W. R. 2007. Caenorhabditis elegans TRPA-1 functions in mechanosensation. Nat Neurosci, 10, 568-77.

KIRKWOOD, T. B., FEDER, M., FINCH, C. E., FRANCESCHI, C., GLOBERSON, A., KLINGENBERG, C. P., LAMARCO, K., OMHOLT, S. & WESTENDORP, R. G. 2005. What accounts for the wide variation in life span of genetically identical organisms reared in a constant environment? Mech Ageing Dev, 126, 439-43.

KITAZUME, H., DAYI, M., TANAKA, R. & KIKUCHI, T. 2018. Assessment of the behaviour and survival of nematodes under low oxygen concentrations. PLoS One, 13, e0197122.

KLASS, M. R. 1977. Aging in the nematode Caenorhabditis elegans: major biological and environmental factors influencing life span. Mechanisms of ageing and development, 6, 413-429.

KOBAYASHI, S., YAMASHITA, T., OHNEDA, K., NAGANO, M., KIMURA, K., NAKAI, H., POELLINGER, L. & OHNEDA, O. 2015. Hypoxia-inducible factor-3α promotes angiogenic activity of pulmonary endothelial cells by repressing the expression of the VE-cadherin gene. Genes Cells, 20, 224-41.

KOJIMA, G., ILIFFE, S. & WALTERS, K. 2018. Frailty index as a predictor of mortality: a systematic review and meta-analysis. Age Ageing, 47, 193-200.

KULKARNI, A. & WILSON, D. M., 3RD 2008. The involvement of DNA-damage and -repair defects in neurological dysfunction. Am J Hum Genet, 82, 539-66.

KUSZEWSKA, K., MILLER, K., ROJEK, W. & WOYCIECHOWSKI, M. In preparation. Reproductive potential of honeybee workers predicts their longevity.

KWON, E. S., NARASIMHAN, S. D., YEN, K. & TISSENBAUM, H. A. 2010. A new DAF-16 isoform regulates longevity. Nature, 466, 498-502.

LAND, M. & RUBIN, C. S. 2017. A Calcium- and Diacylglycerol-Stimulated Protein Kinase C (PKC), Caenorhabditis elegans PKC-2, Links Thermal Signals to Learned Behavior by Acting in Sensory Neurons and Intestinal Cells. Mol Cell Biol, 37.

LARA, J., COOPER, R., NISSAN, J., GINTY, A. T., KHAW, K. T., DEARY, I. J., LORD, J. M., KUH, D. & MATHERS, J. C. 2015. A proposed panel of biomarkers of healthy ageing. BMC Med, 13, 222.

LAWLESS, J. F. 2014. Parametric Models in Survival Analysis. Wiley StatsRef: Statistics Reference Online. John Wiley & Sons, Ltd.

LEE, S. J. & KENYON, C. 2009. Regulation of the longevity response to temperature by thermosensory neurons in Caenorhabditis elegans. Curr Biol, 19, 715-22.

LEI, J., LESER, M. & ENAN, E. 2010. Nematicidal activity of two monoterpenoids and SER-2 tyramine receptor of Caenorhabditis elegans. Biochem Pharmacol, 79, 1062-71.

LEISER, S. F., BEGUN, A. & KAEBERLEIN, M. 2011. HIF-1 modulates longevity and healthspan in a temperature-dependent manner. Aging Cell, 10, 318-26.

LEISER, S. F., FLETCHER, M., BEGUN, A. & KAEBERLEIN, M. 2013. Life-span extension from hypoxia in Caenorhabditis elegans requires both HIF-1 and DAF-16 and is antagonized by SKN-1. J Gerontol A Biol Sci Med Sci, 68, 1135-44.

LEISER, S. F. & KAEBERLEIN, M. 2010. The hypoxia-inducible factor HIF-1 functions as both a positive and negative modulator of aging. Biol Chem, 391, 1131-7.

LENART, P. & BIENERTOVA-VASKA, J. 2017. Keeping up with the Red Queen: the pace of aging as an adaptation. Biogerontology, 18, 693-709.

LEVINE, M. E., LU, A. T., QUACH, A., CHEN, B. H., ASSIMES, T. L., BANDINELLI, S., HOU, L., BACCARELLI, A. A., STEWART, J. D., LI, Y., WHITSEL, E. A., WILSON, J. G., REINER, A. P., AVIV, A., LOHMAN, K., LIU, Y., FERRUCCI, L. & HORVATH, S. 2018. An epigenetic biomarker of aging for lifespan and healthspan. Aging (Albany NY), 10, 573-591.

LIN, K., DORMAN, J. B., RODAN, A. & KENYON, C. 1997. daf-16: An HNF-3/forkhead family member that can function to double the life-span of Caenorhabditis elegans. Science, 278, 1319-22.

LIN, K., HSIN, H., LIBINA, N. & KENYON, C. 2001. Regulation of the Caenorhabditis elegans longevity protein DAF-16 by insulin/IGF-1 and germline signaling. Nat Genet, 28, 139-45.

LIU, R. K. & WALFORD, R. L. 1966. Increased Growth and Life-span with Lowered Ambient Temperature in the Annual Fish, Cynolebias adloffi. Nature, 212, 1277.

LIU, T. & CAI, D. 2013. Counterbalance between BAG and URX neurons via guanylate cyclases controls lifespan homeostasis in C. elegans. The EMBO journal, 32, 1529-1542.

LOEB, J. & NORTHROP, J. H. 1916. Is There a Temperature Coefficient for the Duration of Life? Proc Natl Acad Sci U S A, 2, 456-7.

LUCANIC, M., PLUMMER, W. T., CHEN, E., HARKE, J., FOULGER, A. C., ONKEN, B., COLEMAN-HULBERT, A. L., DUMAS, K. J., GUO, S., JOHNSON, E., BHAUMIK, D., XUE, J., CRIST, A. B., PRESLEY, M. P., HARINATH, G., SEDORE, C. A., CHAMOLI, M., KAMAT, S., CHEN, M. K., ANGELI, S., CHANG, C., WILLIS, J. H., EDGAR, D., ROYAL, M. A., CHAO, E. A., PATEL, S., GARRETT, T., IBANEZ-VENTOSO, C., HOPE, J., KISH, J. L., GUO, M., LITHGOW, G. J., DRISCOLL, M. & PHILLIPS, P. C. 2017. Impact of genetic background and experimental reproducibility on identifying chemical compounds with robust longevity effects. Nat Commun, 8, 14256.

LÓPEZ-OTÍN, C., BLASCO, M. A., PARTRIDGE, L., SERRANO, M. & KROEMER, G. 2013. The hallmarks of aging. Cell, 153, 1194-217.

MAKEHAM, W. M. 1860. On the Law of Mortality and the Construction of Annuity Tables. The Assurance Magazine, and Journal of the Institute of Actuaries, 8, 301-310.

MANSFELD, J., URBAN, N., PRIEBE, S., GROTH, M., FRAHM, C., HARTMANN, N., GEBAUER, J., RAVICHANDRAN, M., DOMMASCHK, A., SCHMEISSER, S., KUHLOW, D., MONAJEMBASHI, S., BREMER-STRECK, S., HEMMERICH, P., KIEHNTOPF, M., ZAMBONI, N., ENGLERT, C., GUTHKE, R., KALETA, C., PLATZER, M., SUHNEL, J., WITTE, O. W., ZARSE, K. & RISTOW, M. 2015. Branched-chain amino acid catabolism is a conserved regulator of physiological ageing. Nat Commun, 6, 10043.

MARUSIC, M. 1996. Mathematical models of tumor growth.

MASSEY, F. J. 1951. The Kolmogorov-Smirnov Test for Goodness of Fit AU. Journal of the American Statistical Association, 46, 68-78.

MATHER, K. A., JORM, A. F., PARSLOW, R. A. & CHRISTENSEN, H. 2011. Is telomere length a biomarker of aging? A review. J Gerontol A Biol Sci Med Sci, 66, 202-13.

MATHEW, M. D., MATHEW, N. D. & EBERT, P. R. 2012. WormScan: a technique for high-throughput phenotypic analysis of Caenorhabditis elegans. PLoS One, 7, e33483.

MATTISON, J. A., COLMAN, R. J., BEASLEY, T. M., ALLISON, D. B., KEMNITZ, J. W., ROTH, G. S., INGRAM, D. K., WEINDRUCH, R., DE CABO, R. & ANDERSON, R. M. 2017. Caloric restriction improves health and survival of rhesus monkeys. Nat Commun, 8, 14063.

MAUPAS, E. 1900. Modes et formes de reproduction des nématodes.

MCCAY, C. M., CROWELL, M. F. & MAYNARD, L. A. 1935. The effect of retarded growth upon the length of life span and upon the ultimate body size one figure. The journal of Nutrition, 10, 63-79.

MEDAWAR, P. B. 1952. An Unsolved problem of biology : an inaugural lecture delivered at University College, London, 6 December, 1951.

MEHTA, R., STEINKRAUS, K. A., SUTPHIN, G. L., RAMOS, F. J., SHAMIEH, L. S., HUH, A., DAVIS, C., CHANDLER-BROWN, D. & KAEBERLEIN, M. 2009. Proteasomal regulation of the hypoxic response modulates aging in C. elegans. Science, 324, 1196-8.

MILLER, H., FLETCHER, M., PRIMITIVO, M., LEONARD, A., SUTPHIN, G. L., RINTALA, N., KAEBERLEIN, M. & LEISER, S. F. 2017. Genetic interaction with temperature is an important determinant of nematode longevity. Aging Cell, 16, 1425-1429.

MILLER, R. A., HARRISON, D. E., ASTLE, C. M., FERNANDEZ, E., FLURKEY, K., HAN, M., JAVORS, M. A., LI, X., NADON, N. L., NELSON, J. F., PLETCHER, S., SALMON, A. B., SHARP, Z. D., VAN ROEKEL, S., WINKLEMAN, L. & STRONG, R. 2014. Rapamycin-mediated lifespan increase in mice is dose and sex dependent and metabolically distinct from dietary restriction. Aging Cell, 13, 468-77.

MITCHELL, S. J., SCHEIBYE-KNUDSEN, M., LONGO, D. L. & DE CABO, R. 2015. Animal models of aging research: implications for human aging and age-related diseases. Annu Rev Anim Biosci, 3, 283-303.

MORI, I. & SASAKURA, H. 2009. Aging: shall we take the high road? Curr Biol, 19, R363-4.

MORLEY, J. F. & MORIMOTO, R. I. 2004. Regulation of longevity in Caenorhabditis elegans by heat shock factor and molecular chaperones. Mol Biol Cell, 15, 657-64.

NAGARAJAN, Y., RYCHKOV, G. Y. & PEET, D. J. 2017. Modulation of TRP Channel Activity by Hydroxylation and Its Therapeutic Potential. Pharmaceuticals (Basel, Switzerland), 10, 35.

NICCOLI, T. & PARTRIDGE, L. 2012. Ageing as a risk factor for disease. Curr Biol, 22, R741-52.

OLSHANSKY, S. J. 2018. From Lifespan to HealthspanFrom Lifespan to HealthspanFrom Lifespan to Healthspan. JAMA, 320, 1323-1324.

ONKEN, B. & DRISCOLL, M. 2010. Metformin induces a dietary restriction-like state and the oxidative stress response to extend C. elegans Healthspan via AMPK, LKB1, and SKN-1. PLoS One, 5, e8758.

PACKER, L. & FUEHR, K. 1977. Low oxygen concentration extends the lifespan of cultured human diploid cells. Nature, 267, 423-5.

PEARL, R. 1928. The Rate of Living, New York, Alfred A Knopf .Inc.

PETRASCHECK, M. & MILLER, D. 2017. Computational Analysis of Lifespan Experiment Reproducibility. bioRxiv.

PITT, J. N., LEISER, S. & KAEBERLEIN, M. 2014. Oxygen and Aging.

PLETCHER, S. D., KHAZAELI, A. A. & CURTSINGER, J. W. 2000. Why Do Life Spans Differ? Partitioning Mean Longevity Differences in Terms of Age-Specific Mortality Parameters. The Journals of Gerontology: Series A, 55, B381-B389.

RAICES, M., MARUYAMA, H., DILLIN, A. & KARLSEDER, J. 2005. Uncoupling of longevity and telomere length in C. elegans. PLoS Genet, 1, e30.

RAMOT, D., MACINNIS, B. L. & GOODMAN, M. B. 2008. Bidirectional temperature-sensing by a single thermosensory neuron in C. elegans. Nat Neurosci, 11, 908-15.

RASCÓN, B. & HARRISON, J. F. 2010. Lifespan and oxidative stress show a non-linear response to atmospheric oxygen in Drosophila. J Exp Biol, 213, 3441-8.

RATCLIFFE, P. J. 2007. HIF-1 and HIF-2: working alone or together in hypoxia? J Clin Invest, 117, 862-5.

REA, S. L., WU, D., CYPSER, J. R., VAUPEL, J. W. & JOHNSON, T. E. 2005. A stress-sensitive reporter predicts longevity in isogenic populations of Caenorhabditis elegans. Nat Genet, 37, 894-8.

REDMAN, L. M., MARTIN, C. K., WILLIAMSON, D. A. & RAVUSSIN, E. 2008. Effect of caloric restriction in non-obese humans on physiological, psychological and behavioral outcomes. Physiol Behav, 94, 643-8.

REZNICK, R. M., ZONG, H., LI, J., MORINO, K., MOORE, I. K., YU, H. J., LIU, Z. X., DONG, J., MUSTARD, K. J., HAWLEY, S. A., BEFROY, D., PYPAERT, M., HARDIE, D. G., YOUNG, L. H. & SHULMAN, G. I. 2007. Aging-associated reductions in AMP-activated protein kinase activity and mitochondrial biogenesis. Cell Metab, 5, 151-6.

RICHARDSON, A., FISCHER, K. E., SPEAKMAN, J. R., DE CABO, R., MITCHELL, S. J., PETERSON, C. A., RABINOVITCH, P., CHIAO, Y. A., TAFFET, G., MILLER, R. A., RENTERÍA, R. C., BOWER, J., INGRAM, D. K., LADIGES, W. C., IKENO, Y., SIERRA, F. & AUSTAD, S. N. 2016. Measures of Healthspan as Indices of Aging in Mice-A Recommendation. J Gerontol A Biol Sci Med Sci, 71, 427-30.

RIDDLE, D. L., BLUMENTHAL, T., MEYER, B. J. & PRIESS, J. R. 1997. Introduction to C. elegans - C. elegans II.

RISTOW, M. & SCHMEISSER, K. 2014. Mitohormesis: Promoting Health and Lifespan by Increased Levels of Reactive Oxygen Species (ROS). Dose Response, 12, 288-341.

RISTOW, M. & SCHMEISSER, S. 2011. Extending life span by increasing oxidative stress. Free Radic Biol Med, 51, 327-36.

ROCKWOOD, K., BLODGETT, J. M., THEOU, O., SUN, M. H., FERIDOONI, H. A., MITNITSKI, A., ROSE, R. A., GODIN, J., GREGSON, E. & HOWLETT, S. E. 2017. A Frailty Index Based On Deficit Accumulation Quantifies Mortality Risk in Humans and in Mice. Sci Rep, 7, 43068.

ROGERS, C., PERSSON, A., CHEUNG, B. & DE BONO, M. 2006. Behavioral motifs and neural pathways coordinating O2 responses and aggregation in C. elegans. Curr Biol, 16, 649-59.

ROLLINS, J. A., HOWARD, A. C., DOBBINS, S. K., WASHBURN, E. H. & ROGERS, A. N. 2017. Assessing Health Span in Caenorhabditis elegans: Lessons From Short-Lived Mutants. The journals of gerontology. Series A, Biological sciences and medical sciences, 72, 473-480.

SAKAGAMI, S. F. & FUKUDA, H. 1968. Life tables for worker honeybees. Researches on Population Ecology, 10, 127-139.

SALMINEN, A. & KAARNIRANTA, K. 2012. AMP-activated protein kinase (AMPK) controls the aging process via an integrated signaling network. Ageing Res Rev, 11, 230-41.

SAMMUT, M., COOK, S. J., NGUYEN, K. C. Q., FELTON, T., HALL, D. H., EMMONS, S. W., POOLE, R. J. & BARRIOS, A. 2015. Glia-derived neurons are required for sex-specific learning in C. elegans. Nature, 526, 385-390.

SCHIEBER, M. & CHANDEL, N. S. 2014. TOR signaling couples oxygen sensing to lifespan in C. elegans. Cell Rep, 9, 9-15.

SEARLE, S. D., MITNITSKI, A., GAHBAUER, E. A., GILL, T. M. & ROCKWOOD, K. 2008. A standard procedure for creating a frailty index. BMC Geriatr, 8, 24.

SEMENZA, G. L. 2009. Regulation of oxygen homeostasis by hypoxia-inducible factor 1. Physiology (Bethesda), 24, 97-106.

SHAMMAS, M. A. 2011. Telomeres, lifestyle, cancer, and aging. Curr Opin Clin Nutr Metab Care, 14, 28-34.

SHAW, R. F. & BERCAW, B. L. 1962. Temperature and life-span in poikilothermous animals. Nature, 196, 454-7.

SHEN, C., NETTLETON, D., JIANG, M., KIM, S. K. & POWELL-COFFMAN, J. A. 2005. Roles of the HIF-1 hypoxia-inducible factor during hypoxia response in Caenorhabditis elegans. J Biol Chem, 280, 20580-8.

SILER, W. 1979. Competing-Risk Model for Animal Mortality. Ecology, 60, 750-757.

SILER, W. 1983. Parameters of mortality in human populations with widely varying life spans. Statistics in Medicine, 2, 373-380.

SKERRATT, S. 2017. Recent Progress in the Discovery and Development of TRPA1 Modulators. Prog Med Chem, 56, 81-115.

SLACK, C., GIANNAKOU, M. E., FOLEY, A., GOSS, M. & PARTRIDGE, L. 2011. dFOXO-independent effects of reduced insulin-like signaling in Drosophila. Aging Cell, 10, 735-748.

SO, TOKUMARU, T., MIYAHARA, K. & OHSHIMA, Y. 2011. Control of lifespan by food bacteria, nutrient limitation and pathogenicity of food in C. elegans. Mech Ageing Dev, 132, 210-2.

SO, K., TEI, Y., ZHAO, M., MIYAKE, T., HIYAMA, H., SHIRAKAWA, H., IMAI, S., MORI, Y., NAKAGAWA, T., MATSUBARA, K. & KANEKO, S. 2016. Hypoxia-induced sensitisation of TRPA1 in painful dysesthesia evoked by transient hindlimb ischemia/reperfusion in mice. Sci Rep, 6, 23261.

SOHAL, R. S. & WEINDRUCH, R. 1996. Oxidative stress, caloric restriction, and aging. Science (New York, NY), 273, 59.

STROUSTRUP, N., ANTHONY, W. E., NASH, Z. M., GOWDA, V., GOMEZ, A., LOPEZ-MOYADO, I. F., APFELD, J. & FONTANA, W. 2016. The temporal scaling of Caenorhabditis elegans ageing. Nature, 530, 103-7.

STROUSTRUP, N., ULMSCHNEIDER, B. E., NASH, Z. M., LÓPEZ-MOYADO, I. F., APFELD, J. & FONTANA, W. 2013. The Caenorhabditis elegans Lifespan Machine. Nat Methods, 10, 665-70.

SULSTON, J. E. & HORVITZ, H. R. 1977. Sulston JE, Horvitz HR.. Post-embryonic cell lineages of the nematode, Caenorhabditis elegans. Dev Biol 56: 110-156.

SUN, X. J., CHEN, W. D. & WANG, Y. D. 2017. DAF-16/FOXO Transcription Factor in Aging and Longevity. Frontiers in Pharmacology, 8, 8.

SWINDELL, W. R. 2009. Accelerated failure time models provide a useful statistical framework for aging research. Experimental gerontology, 44, 190-200.

TAKAHASHI, N., KUWAKI, T., KIYONAKA, S., NUMATA, T., KOZAI, D., MIZUNO, Y., YAMAMOTO, S., NAITO, S., KNEVELS, E., CARMELIET, P., OGA, T., KANEKO, S., SUGA, S., NOKAMI, T., YOSHIDA, J. & MORI, Y. 2011. TRPA1 underlies a sensing mechanism for O2. Nat Chem Biol, 7, 701-11.

TANIMOTO, K., MAKINO, Y., PEREIRA, T. & POELLINGER, L. 2000. Mechanism of regulation of the hypoxia-inducible factor-1 alpha by the von Hippel-Lindau tumor suppressor protein. EMBO J, 19, 4298-309.

TAYLOR, R. C. 2016. Aging and the UPR(ER). Brain Res, 1648, 588-593.

TEPPER, R. G., ASHRAF, J., KALETSKY, R., KLEEMANN, G., MURPHY, C. T. & BUSSEMAKER, H. J. 2013. PQM-1 complements DAF-16 as a key transcriptional regulator of DAF-2-mediated development and longevity. Cell, 154, 676-690.

TIAN, H., MCKNIGHT, S. L. & RUSSELL, D. W. 1997. Endothelial PAS domain protein 1 (EPAS1), a transcription factor selectively expressed in endothelial cells. Genes & Development, 11, 72-82.

TISSENBAUM, H. A. 2012. Genetics, Life Span, Health Span, and the Aging Process in Caenorhabditis elegans. Journals of Gerontology Series a-Biological Sciences and Medical Sciences, 67, 503-510.

UNGVARI, Z., PARRADO-FERNANDEZ, C., CSISZAR, A. & DE CABO, R. 2008. Mechanisms underlying caloric restriction and lifespan regulation: implications for vascular aging. Circ Res, 102, 519-28.

VANFLETEREN, J. R. 1993. Oxidative stress and ageing in Caenorhabditis elegans. Biochem J, 292 (Pt 2), 605-8.

VANFLETEREN, J. R., DE VREESE, A. & BRAECKMAN, B. P. 1998. Two-parameter logistic and Weibull equations provide better fits to survival data from isogenic populations of Caenorhabditis elegans in axenic culture than does the Gompertz model. J Gerontol A Biol Sci Med Sci, 53, B393-403; discussion B404-8.

VAUPEL, J. W., JOHNSON, T. E. & LITHGOW, G. J. 1994. Rates of mortality in populations of Caenorhabditis elegans. Science, 266, 826; author reply 828.

VIGNE, P. & FRELIN, C. 2006. A low protein diet increases the hypoxic tolerance in Drosophila. PLoS One, 1, e56.

VIGNE, P., TAUC, M. & FRELIN, C. 2009. Strong dietary restrictions protect Drosophila against anoxia/reoxygenation injuries. PLoS One, 4, e5422.

WANG, G. L., JIANG, B. H., RUE, E. A. & SEMENZA, G. L. 1995. Hypoxia-inducible factor 1 is a basic-helix-loop-helix-PAS heterodimer regulated by cellular O2 tension. Proc Natl Acad Sci U S A, 92, 5510-4.

WANG, Q., ZHOU, F., XIE, W., ZHAO, X. & LIU, X. 2016. Research progress on aging mechanisms. Advances in Aging Research, 5, 49.

WANG, Z., STOLTZFUS, J., YOU, Y. J., RANJIT, N., TANG, H., XIE, Y., LOK, J. B., MANGELSDORF, D. J. & KLIEWER, S. A. 2015. The nuclear receptor DAF-12 regulates nutrient metabolism and reproductive growth in nematodes. PLoS Genet, 11, e1005027.

WEIBULL, W. 1951. A statistical distribution function of wide applicability. Journal of applied mechanics, 18, 293-297.

WEINDRUCH, R., WALFORD, R. L., FLIGIEL, S. & GUTHRIE, D. 1986. The retardation of aging in mice by dietary restriction: longevity, cancer, immunity and lifetime energy intake. J Nutr, 116, 641-54.

WHITING, R. C. & BUCHANAN, R. L. 1993. A Classification of Models in Predictive Microbiology - Reply. Food Microbiology, 10, 175-177.

WICKENS, A. P. 2001. Ageing and the free radical theory. Respiration physiology, 128, 379-391.

WILLIAMS, G. C. 1957. Pleiotropy, Natural Selection, and the Evolution of Senescence. Evolution, 11, 398-411.

WILSON, D. L. 1994. The Analysis of Survival (Mortality) Data - Fitting Gompertz, Weibull, and Logistic Functions. Mechanisms of Ageing and Development, 74, 15-33.

WOOD, W. B. 1988. The Nematode Caenorhabditis Elegans, Cold Spring Harbor Laboratory.

WOYCIECHOWSKI, M. & MORON, D. 2009. Life expectancy and onset of foraging in the honeybee (Apis mellifera). Insectes Sociaux, 56, 193-201.

WRYCZA, T. F., MISSOV, T. I. & BAUDISCH, A. 2015. Quantifying the shape of aging. PLoS One, 10, e0119163.

WS268, W. R. 2019. Wormbase release WS268 - WormBase : Nematode Information Resource [Online]. Available: http://www.wormbase.org/about/wormbase_release_WS261#0--10 [Accessed].

WU, D., REA, S. L., CYPSER, J. R. & JOHNSON, T. E. 2009. Mortality shifts in Caenorhabditis elegans: remembrance of conditions past. Aging Cell, 8, 666-75.

XIA, X., CHEN, W., MCDERMOTT, J. & HAN, J. J. 2017. Molecular and phenotypic biomarkers of aging. F1000Res, 6, 860.

XIAN, B., SHEN, J., CHEN, W., SUN, N., QIAO, N., JIANG, D., YU, T., MEN, Y., HAN, Z., PANG, Y., KAEBERLEIN, M., HUANG, Y. & HAN, J. D. 2013. WormFarm: a quantitative control and measurement device toward automated Caenorhabditis elegans aging analysis. Aging Cell, 12, 398-409.

XIAO, R., ZHANG, B., DONG, Y., GONG, J., XU, T., LIU, J. & XU, X. Z. 2013. A genetic program promotes C. elegans longevity at cold temperatures via a thermosensitive TRP channel. Cell, 152, 806-17.

XIONG, R., XIE, G., EDMONDSON, A. E. & SHEARD, M. A. 1999. A mathematical model for bacterial inactivation. Int J Food Microbiol, 46, 45-55.

XU, H., DELLING, M., JUN, J. C. & CLAPHAM, D. E. 2006. Oregano, thyme and clove-derived flavors and skin sensitizers activate specific TRP channels. Nat Neurosci, 9, 628-35.

YASHIN, A. Y., IACHINE, I. A. & BEGUN, A. S. 2000. Mortality modeling: A review. Mathematical Population Studies, 8, 305-332.

YEN, K., NARASIMHAN, S. D. & TISSENBAUM, H. A. 2011. DAF-16/Forkhead box O transcription factor: many paths to a single Fork(head) in the road. Antioxid Redox Signal, 14, 623-34.

YU, Q. 2000. Nematicidal Activity of Monoterpenoid Compounds against Economically Important Nematodes in Agriculture AU - Tsao, Rong. Journal of Essential Oil Research, 12, 350-354.

ZEVIAN, S. C. & YANOWITZ, J. L. 2014. Methodological considerations for heat shock of the nematode Caenorhabditis elegans. Methods, 68, 450-7.

ZHANG, B., XIAO, R., RONAN, E. A., HE, Y., HSU, A. L., LIU, J. & XU, X. Z. 2015. Environmental Temperature Differentially Modulates C. elegans Longevity through a Thermosensitive TRP Channel. Cell Rep, 11, 1414-24.

ZHANG, P., YAO, Q., LU, L., LI, Y., CHEN, P. J. & DUAN, C. 2014. Hypoxia-inducible factor 3 is an oxygen-dependent transcription activator and regulates a distinct transcriptional response to hypoxia. Cell Rep, 6, 1110-1121.

ZHANG, W. B., SINHA, D. B., PITTMAN, W. E., HVATUM, E., STROUSTRUP, N. & PINCUS, Z. 2016. Extended Twilight among Isogenic C. elegans Causes a Disproportionate Scaling between Lifespan and Health. Cell Syst, 3, 333-345.e4.

ZHANG, Y., SHAO, Z., ZHAI, Z., SHEN, C. & POWELL-COFFMAN, J. A. 2009. The HIF-1 hypoxia-inducible factor modulates lifespan in C. elegans. PLoS One, 4, e6348.

ZHAO, Y., GILLIAT, A. F., ZIEHM, M., TURMAINE, M., WANG, H., EZCURRA, M., YANG, C., PHILLIPS, G., MCBAY, D., ZHANG, W. B., PARTRIDGE, L., PINCUS, Z. & GEMS, D. 2017. Two forms of death in ageing Caenorhabditis elegans. Nature Communications, 8, 15458.

ZIMMER, M., GRAY, J., POKALA, N., CHANG, A., KAROW, D., MARLETTA, M., HUDSON, M., MORTON, D., CHRONIS, N. & BARGMANN, C. 2009. Neurons Detect Increases and Decreases in Oxygen Levels Using Distinct Guanylate Cyclases. Neuron, 61, 865-879.

Chapter 8.0: Appendix

8.1 Tables showing total dead, censored animals and number of trials

Table 8.1a: Experiments in Chapter 3.0

	Experiments in Chapter 3.0	Dead	Censored	n (Trials)
C. elegans	N2 15°C	711	330	20
	N2 20°C	564	189	15
	N2 25°C	557	143	14
	N2 30°C	144	6	3
	N2	338	115	9
	daf-16(mu86)	248	52	6
Drosophila	w^{Dah}	1038	90	10
	dFOXO	1047	34	10
Bees	Caged	400	0	4
	Hived	200	0	4
Mouse	Male Control	295	5	3
	Female Control	242	38	3
	Male Rapamycin	120	36	3
	Female Rapamycin	120	16	3

Table 8.1b: Experiments in Chapter 4.0

	Experiments in Chapter 4.0	Dead	Censored	n (Trials)
C. elegans	N2 15°C	1018	373	27
	N2 25°C	828	172	20
	N2 15°C - 25°C (Day 5)	137	13	3
	N2 15°C - 25°C (Day 10)	122	28	3
	N2 15°C - 25°C (Day 13)	145	5	3
	N2 15°C - 25°C (Day 16)	123	77	4
	N2 15°C - 25°C (Day 20)	112	38	3
	N2 25°C - 15°C (Day 1)	141	9	3
	N2 25°C - 15°C (Day 3)	138	12	3
	N2 25°C - 15°C (Day 5)	116	34	3
	N2 25°C - 15°C (Day 8)	131	69	4
	N2 25°C - 15°C (Day 12)	144	6	3
	trpa-1(ok999) 15°C	476	114	12
	trpa-1(ok999) 25°C	289	61	7
	trpa-1(ok999) 15°C - 25°C (Day 5)	122	28	3
	trpa-1(ok999) 15°C - 25°C (Day 10)	124	26	3
	trpa-1(ok999) 15°C - 25°C (Day 13)	129	21	3
	trpa-1(ok999) 15°C - 25°C (Day 16)	113	37	3
	trpa-1(ok999) 15°C - 25°C (Day 20)	136	14	3
	trpa-1(ok999) 25°C - 15°C (Day 1)	120	30	3
	trpa-1(ok999) 25°C - 15°C (Day 3)	134	16	3
	trpa-1(ok999) 25°C - 15°C (Day 5)	121	29	3
	trpa-1(ok999) 25°C - 15°C (Day 8)	114	36	3
	trpa-1(ok999) 25°C - 15°C (Day 12)	128	22	3

Table 8.1c: Experiments in Chapter 5.0

	Experiments in Chapter 5.0	Dead	Censored	n (Trials)
C. elegans	N2 20°C (Normoxia)	815	238	21
	trpa-1(ok999) 20°C (Normoxia)	328	64	8
	daf-16(mu86) 20°C (Normoxia)	341	59	8
	hif-1(ia4) 20°C (Normoxia)	445	112	11
	egl-9(sa307) 20°C (Normoxia)	242	58	6
	egl-9(n586) 20°C (Normoxia)	272	28	6
	N2 15°C (Normoxia)	1018	373	27
	trpa-1(ok999) 15°C (Normoxia)	476	114	12
	daf-16(mu86) 15°C (Normoxia)	223	27	5
	hif-1(ia4) 15°C (Normoxia)	209	49	5
	egl-9(sa307) 15°C (Normoxia)	122	28	3
	egl-9(n586) 15°C (Normoxia)	118	32	3
	N2 (Normoxia)	170	0	3
	N2 (Hypoxia)	358	0	6
	hif-1(ia4) (Normoxia)	163	0	3
	hif-1(ia4) (Hypoxia)	425	0	6
	trpa-1(ok999) (Normoxia)	165	0	3
	trpa-1(ok999) (Hypoxia)	405	0	6
	N2 0mM (Normoxia)	131	19	3
	N2 50mM (Normoxia)	129	21	3
	N2 200mM (Normoxia)	109	41	3
	N2 500mM (Normoxia)	131	19	3
	hif-1(ia4) 0mM (Normoxia)	131	19	3
	hif-1(ia4) 50mM (Normoxia)	128	22	3
	hif-1(ia4) 200mM (Normoxia)	136	14	3
	hif-1(ia4) 500mM (Normoxia)	144	6	3
	trpa-1(ok999) 0mM (Normoxia)	139	10	3
	trpa-1(ok999) 50mM (Normoxia)	138	12	3
	trpa-1(ok999) 200mM (Normoxia)	139	11	3
	trpa-1(ok999) 500mM (Normoxia)	134	16	3
	daf-16(mu86) 0mM (Normoxia)	139	11	3
	daf-16(mu86) 50mM (Normoxia)	133	17	3
	daf-16(mu86) 200mM (Normoxia)	122	28	3
	daf-16(mu86) 500mM (Normoxia)	147	3	3
	N2 0mM (Hypoxia)	186	0	3
	N2 50mM (Hypoxia)	168	0	3
	N2 200mM (Hypoxia)	185	0	3
	N2 500mM (Hypoxia)	165	0	3
	hif-1(ia4) 0mM (Hypoxia)	261	0	3
	hif-1(ia4) 50mM (Hypoxia)	208	0	3
	hif-1(ia4) 200mM (Hypoxia)	188	0	3
	hif-1(ia4) 500mM (Hypoxia)	192	0	3
	trpa-1(ok999) 0mM (Hypoxia)	229	0	3
	trpa-1(ok999) 50mM (Hypoxia)	227	0	3
	trpa-1(ok999) 200mM (Hypoxia)	235	0	3
	trpa-1(ok999) 500mM (Hypoxia)	189	0	3

8.2 MATLAB script for Chronological model for intervention from 15°C to 25°C

```
    clear all
%Median N2 35 (15C) 20  16  13  10  5   0 (25C)
        %n2 15 and 25 all realisations median
f=[0.5276   0.448682    0.68265 0.119627    0.6424  0.517
0.3246];
k1=[0.5199  1.0729  0.68545 1.1916  1.482   1.866   1.566116];
k2=[0.7094  1.062505    9.4775  20.5533 0.8518  1.497
1.881];
t1=[17.06   15.9109 17.715  14.1178 13.03   11.01   7.594];
t2=[22.71   21.5673 21.505  17.07   14  13.22   11.48];
 figure( 'Name', '15 vs 25');
N2_15MS=@(x)MSModel(x,f(1),k1(1),k2(1),t1(1),t2(1));
fplot((N2_15MS),[0,35,-1,105],'Linewidth',3);
hold on
N2_25MS=@(x)MSModel(x,f(7),k1(7),k2(7),t1(7),t2(7));
fplot((N2_25MS),[0,35,-1,105],'Linewidth',3);
hold on
xlim([0 35]);
ylim([0 105]);
Average_Lifetime=zeros(35,1);
    figure( 'Name', 'Tempswitch');
    for i=1:35 %day switch
a1=N2_15MS(i); %y value (percent alive) for given switch day
at N2_15
a2=N2_25MS(i); %y value (percent alive) for given switch day
at N2_25
t_avg_N215=
integral(@(x)MSModel(x,f(1),k1(1),k2(1),t1(1),t2(1)),0,i)/100;
%average lifetime (integral) of N2 15 from 0 to switch time
t_avg_N225=
integral(@(x)MSModel(x,f(7),k1(7),k2(7),t1(7),t2(7)),i,Inf)/10
0; %average lifetime (integral) of N2 25 from switch time to
end
a=a1/a2; %rescaling N2 25 to N2 15
t_avg=(t_avg_N215)+(a*(t_avg_N225)); %Average lifetime of N2
15 from 0 to switch time + rescaled N2 25 from switch time to
end
Average_Lifetime(i,1)=t_avg; %Generate average lifetime table
N2_25MSresc=@(x)a*MSModel(x,f(7),k1(7),k2(7),t1(7),t2(7));%
Post switch curve rescaled to switch day
fplot((N2_15MS),[0,i,-1,105],'Linewidth',3);% plot n2_15
hold on
fplot((N2_25MSresc),[i,35,-1,105],'Linewidth',3); %plot n2 25
post switch
hold on
xlim([0 35]);
ylim([0 105]);
hold on
    end
    title('Switch 15-25')
```

```
j= [20  16  13  10  5]; %days with actual data
for i=1:35 %day switch
    h=figure;
a1=N2_15MS(i); %y value (percent alive) for given switch day
at N2_15
a2=N2_25MS(i); %y value (percent alive) for given switch day
at N2_25
t_avg_N215=
integral(@(x)MSModel(x,f(1),k1(1),k2(1),t1(1),t2(1)),0,i)/100;
%average lifetime (integral) of N2 15 from 0 to switch time
t_avg_N225=
integral(@(x)MSModel(x,f(7),k1(7),k2(7),t1(7),t2(7)),i,Inf)/10
0; %average lifetime (integral) of N2 25 from switch time to
end
a=a1/a2;%rescaling N2 25 to N2 15
t_avg=(t_avg_N215)+(a*(t_avg_N225)); %Average lifetime of N2
15 from 0 to switch time + rescaled N2 25 from switch time to
end
Average_Lifetime(i,1)=t_avg; %Generate average lifetime table
N2_25MSresc=@(x)a*MSModel(x,f(7),k1(7),k2(7),t1(7),t2(7));
%Post switch curve rescaled to switch day
N2_15MS=@(x)MSModel(x,f(1),k1(1),k2(1),t1(1),t2(1));
fplot((N2_15MS),[0,35,-1,105],'Linewidth',3);% plot n2_15
hold on
N2_25MS=@(x)MSModel(x,f(7),k1(7),k2(7),t1(7),t2(7));
fplot((N2_25MS),[0,35,-1,105],'Linewidth',3);% plot n2_25
hold on
fplot((N2_15MS),[0,i,-1,105],'Linewidth',3); % plot n2_15 from
0 to switch time
hold on
fplot((N2_25MSresc),[i,35,-1,105],'Linewidth',3); %plot
switched 25 from switch time to end
hold on
if i==j(1) %if switch day is same as actual switch day 20
    N2_15MS20=@(x)MSModel(x,f(2),k1(2),k2(2),t1(2),t2(2));
fplot((N2_15MS20),[0,35,-1,105],'-o','Linewidth',3);
elseif i==j(2) %if switch day is same as actual switch day 16
     N2_15MS16=@(x)MSModel(x,f(3),k1(3),k2(3),t1(3),t2(3));
fplot((N2_15MS16),[0,35,-1,105],'-o','Linewidth',3);
elseif i==j(3) %if switch day is same as actual switch day 13
     N2_15MS13=@(x)MSModel(x,f(4),k1(4),k2(4),t1(4),t2(4));
fplot((N2_15MS13),[0,35,-1,105],'-o','Linewidth',3);
elseif i==j(4) %if switch day is same as actual switch day 10
     N2_15MS10=@(x)MSModel(x,f(5),k1(5),k2(5),t1(5),t2(5));
fplot((N2_15MS10),[0,35,-1,105],'-o','Linewidth',3);
elseif i==j(5) %if switch day is same as actual switch day 5
    N2_15MS5=@(x)MSModel(x,f(6),k1(6),k2(6),t1(6),t2(6));
fplot((N2_15MS5),[0,35,-1,105],'-o','Linewidth',3);
else
end
xlim([0 35]);
ylim([0 105]);
title(['Day ' num2str(i) ' Switch 15-25']);
hold on
```

```
 %saveas(h,sprintf('Day %d TempSwitch15_25.pdf',i));
end
openvar('Average_Lifetime');
```

8.3 MATLAB script for Chronological model for intervention from 25°C to 15°C

```
clear all
%Median N2  16(25C) 12  8   5   3   1   0(15C)
%n2 15 and 25 all realisations median
f=[0.3246   0.1533  0.37975 0.1395  0.5949  0.9479  0.5276];
k1=[1.566116    14.17   0.6985  1.141   0.4822  0.681845
0.5199];
k2=[1.881   1.492   0.7714  0.4329  0.7844  0.406   0.7094];
t1=[7.594   7.128   9.191   6.551   11.936  18.58892
17.06];
t2=[11.48   10.56   15.725  15.21   19.65917    31.69869
22.71];
 figure( 'Name', '25 vs 15');
N2_25MS=@(x)MSModel(x,f(1),k1(1),k2(1),t1(1),t2(1));
fplot((N2_25MS),[0,35,-1,105],'Linewidth',3);
hold on
N2_15MS=@(x)MSModel(x,f(7),k1(7),k2(7),t1(7),t2(7));
fplot((N2_15MS),[0,35,-1,105],'Linewidth',3);
hold on
xlim([0 35]);
ylim([0 105]);
Average_Lifetime=zeros(16,1);
    figure( 'Name', 'Tempswitch');
%collated figures
    for i=1:16
a1=N2_25MS(i);
a2=N2_15MS(i);
t_avg_N225=
integral(@(x)MSModel(x,f(1),k1(1),k2(1),t1(1),t2(1)),0,i)/100;
t_avg_N215=
integral(@(x)MSModel(x,f(7),k1(7),k2(7),t1(7),t2(7)),i,Inf)/10
0;
a=a1/a2;
t_avg=(t_avg_N225)+(a*(t_avg_N215));
Average_Lifetime(i,1)=t_avg;
N2_15MSresc=@(x)a*MSModel(x,f(7),k1(7),k2(7),t1(7),t2(7));
fplot((N2_25MS),[0,i,-1,105],'Linewidth',3);
hold on
fplot((N2_15MSresc),[i,35,-1,105],'Linewidth',3);
hold on
xlim([0 35]);
ylim([0 105]);
hold on
    end
        title('Switch 25-15')
%print('Tempswitch25_15', '-dpdf' );
%individual figures
j= [12  8   5   3   1];
for i=1:16
    %Tempswitch=char(i);
    h= figure;
    %( 'Name', Tempswitch(i,1));
```

```
a1=N2_25MS(i);
a2=N2_15MS(i);
t_avg_N225=
integral(@(x)MSModel(x,f(1),k1(1),k2(1),t1(1),t2(1)),0,i)/100;
t_avg_N215=
integral(@(x)MSModel(x,f(7),k1(7),k2(7),t1(7),t2(7)),i,Inf)/10
0;
a=a1/a2;
t_avg=(t_avg_N225)+(a*(t_avg_N215));
Average_Lifetime(i,1)=t_avg;
N2_15MSresc=@(x)a*MSModel(x,f(7),k1(7),k2(7),t1(7),t2(7));
N2_15MS=@(x)MSModel(x,f(7),k1(7),k2(7),t1(7),t2(7));
fplot((N2_15MS),[0,35,-1,105],'Linewidth',3);
hold on
N2_25MS=@(x)MSModel(x,f(1),k1(1),k2(1),t1(1),t2(1));
fplot((N2_25MS),[0,35,-1,105],'Linewidth',3);
hold on
fplot((N2_25MS),[0,i,-1,105],'Linewidth',3);
hold on
fplot((N2_15MSresc),[i,35,-1,105],'Linewidth',3);
hold on
if i==j(1)
    N2_15MS12=@(x)MSModel(x,f(2),k1(2),k2(2),t1(2),t2(2));
fplot((N2_15MS12),[0,35,-1,105],'Linewidth',3);
elseif i==j(2)
     N2_15MS8=@(x)MSModel(x,f(3),k1(3),k2(3),t1(3),t2(3));
fplot((N2_15MS8),[0,35,-1,105],'Linewidth',3);
elseif i==j(3)
     N2_15MS5=@(x)MSModel(x,f(4),k1(4),k2(4),t1(4),t2(4));
fplot((N2_15MS5),[0,35,-1,105],'Linewidth',3);
elseif i==j(4)
     N2_15MS3=@(x)MSModel(x,f(5),k1(5),k2(5),t1(5),t2(5));
fplot((N2_15MS3),[0,35,-1,105],'Linewidth',3);
elseif i==j(5)
    N2_15MS1=@(x)MSModel(x,f(6),k1(6),k2(6),t1(6),t2(6));
fplot((N2_15MS1),[0,35,-1,105],'Linewidth',3);
else
end
xlim([0 35]);
ylim([0 105]);
title(['Day ' num2str(i) ' Switch 25-15'])
hold on
%saveas(h,sprintf('Day %d TempSwitch25_15.pdf',i));
end
openvar('Average_Lifetime');
```

8.4 MATLAB script for Biological model for intervention from 15°C to 25°C

```
clear all
%Median N2 35 (15C) 20  16  13  10  5   0 (25C)
f=[0.5276   0.448682    0.68265 0.119627    0.6424  0.517
0.3246];
k1=[0.5199  1.0729  0.68545 1.1916  1.482   1.866   1.566116];
k2=[0.7094  1.062505    9.4775  20.5533 0.8518  1.497
1.881];
t1=[17.06   15.9109 17.715  14.1178 13.03   11.01   7.594];
t2=[22.71   21.5673 21.505  17.07   14  13.22   11.48];
 figure( 'Name', '15 vs 25');
N2_15MS=@(x)MSModel(x,f(1),k1(1),k2(1),t1(1),t2(1));
fplot((N2_15MS),[0,35,-1,105],'Linewidth',3);
hold on
N2_25MS=@(x)MSModel(x,f(7),k1(7),k2(7),t1(7),t2(7));
fplot((N2_25MS),[0,35,-1,105],'Linewidth',3);
hold on
xlim([0 35]);
ylim([0 105]);
Average_Lifetime=zeros(35,1);
    figure( 'Name', 'Tempswitch');
%collated figures
    for i=1:35
a1=N2_15MS(i);
a2=N2_25MS(i);
t_N2_at_yN215 =
fzero(@(x)MSModel(x,f(7),k1(7),k2(7),t1(7),t2(7))-a1, 50);
N215_tminusN225_t=(i-t_N2_at_yN215);
N2_switchedMS=@(x)MSModel(x-
N215_tminusN225_t,f(7),k1(7),k2(7),t1(7),t2(7));
fplot((N2_15MS),[0,35,-1,105],'Linewidth',3);
hold on
fplot((N2_25MS),[0,35,-1,105],'Linewidth',3);
hold on
fplot((N2_15MS),[0,i,-1,105],'Linewidth',3);
hold on
fplot((N2_switchedMS),[i,35,-1,105],'Linewidth',3);
hold on
xlim([0 35]);
ylim([0 105]);
t_avg_N215=
integral(@(x)MSModel(x,f(1),k1(1),k2(1),t1(1),t2(1)),0,i)/100;
%average lifetime (integral) of N2 15 from 0 to switch time
t_avg_N2_switchedMS= integral(N2_switchedMS,i,Inf)/100;
%average lifetime (integral) of N2 25 from switch time to end
t_avg=(t_avg_N215)+(t_avg_N2_switchedMS); %Average lifetime of
N2 15 from 0 to switch time + switched N2  from switch time to
end
Average_Lifetime(i,1)=t_avg; %Generate average lifetime table
    end
    title('Switch 15-25')
%print('Tempswitch15_25', '-dpdf' );
```

```
%individual figures
j= [20  16  13  10  5];
for i=1:35
    %Tempswitch=char(i);
    h=figure;
    %( 'Name', Tempswitch(i,1));
a1=N2_15MS(i);
a2=N2_25MS(i);
t_N2_at_yN215 =
fzero(@(x)MSModel(x,f(7),k1(7),k2(7),t1(7),t2(7))-a1, 50);
N215_tminusN225_t=(i-t_N2_at_yN215);
N2_switchedMS=@(x)MSModel(x-
N215_tminusN225_t,f(7),k1(7),k2(7),t1(7),t2(7));
fplot((N2_15MS),[0,35,-1,105],'Linewidth',3);
hold on
fplot((N2_25MS),[0,35,-1,105],'Linewidth',3);
hold on
fplot((N2_15MS),[0,i,-1,105],'Linewidth',3);
hold on
fplot((N2_switchedMS),[i,35,-1,105],'Linewidth',3);
hold on
xlim([0 35]);
ylim([0 105]);
if i==j(1)
    N2_15MS20=@(x)MSModel(x,f(2),k1(2),k2(2),t1(2),t2(2));
fplot((N2_15MS20),[0,35,-1,105],'-o','Linewidth',3);
elseif i==j(2)
     N2_15MS16=@(x)MSModel(x,f(3),k1(3),k2(3),t1(3),t2(3));
fplot((N2_15MS16),[0,35,-1,105],'-o','Linewidth',3);
elseif i==j(3)
     N2_15MS13=@(x)MSModel(x,f(4),k1(4),k2(4),t1(4),t2(4));
fplot((N2_15MS13),[0,35,-1,105],'-o','Linewidth',3);
elseif i==j(4)
     N2_15MS10=@(x)MSModel(x,f(5),k1(5),k2(5),t1(5),t2(5));
fplot((N2_15MS10),[0,35,-1,105],'-o','Linewidth',3);
elseif i==j(5)
    N2_15MS5=@(x)MSModel(x,f(6),k1(6),k2(6),t1(6),t2(6));
fplot((N2_15MS5),[0,35,-1,105],'-o','Linewidth',3);
else
end
xlim([0 35]);
ylim([0 105]);
title(['Day ' num2str(i) ' Switch 15-25']);
hold on
 %saveas(h,sprintf('Day %d TempSwitch15_25.pdf',i));
end
openvar('Average_Lifetime');
```

8.5 MATLAB script for Biological model for intervention from 25°C to 15°C

```
clear all
%Median N2  16(25C) 12  8   5   3   1   0(15C)
%n2 15 and 25 all realisations median
f=[0.3246   0.1533  0.37975 0.1395  0.5949  0.9479  0.5276];
k1=[1.566116    14.17   0.6985  1.141   0.4822  0.681845
0.5199];
k2=[1.881   1.492   0.7714  0.4329  0.7844  0.406   0.7094];
t1=[7.594   7.128   9.191   6.551   11.936  18.58892
17.06];
t2=[11.48   10.56   15.725  15.21   19.65917    31.69869
22.71];
 figure( 'Name', '25 vs 15');
N2_25MS=@(x)MSModel(x,f(1),k1(1),k2(1),t1(1),t2(1));
fplot((N2_25MS),[0,35,-1,105],'Linewidth',3);
hold on
N2_15MS=@(x)MSModel(x,f(7),k1(7),k2(7),t1(7),t2(7));
fplot((N2_15MS),[0,35,-1,105],'Linewidth',3);
hold on
xlim([0 35]);
ylim([0 105]);
Average_Lifetime=zeros(16,1);
    figure( 'Name', 'Tempswitch');
%collated figures
    for i=1:16
a1=N2_25MS(i);
a2=N2_15MS(i);
t_N2_at_yN225 =
fzero(@(x)MSModel(x,f(7),k1(7),k2(7),t1(7),t2(7))-a1, 50);
N225_tminusN215_t=(t_N2_at_yN225-i);
N2_switchedMS=@(x)MSModel(x+N225_tminusN215_t,f(7),k1(7),k2(7)
,t1(7),t2(7));
fplot((N2_15MS),[0,35,-1,105],'Linewidth',3);
hold on
fplot((N2_25MS),[0,35,-1,105],'Linewidth',3);
hold on
fplot((N2_25MS),[0,i,-1,105],'Linewidth',3);
hold on
fplot((N2_switchedMS),[i,35,-1,105],'Linewidth',3);
hold on
xlim([0 35]);
ylim([0 105]);
t_avg_N225=
integral(@(x)MSModel(x,f(1),k1(1),k2(1),t1(1),t2(1)),0,i)/100;
%average lifetime (integral) of N2 25 from 0 to switch time
t_avg_N2_switchedMS= integral(N2_switchedMS,i,Inf)/100;
%average lifetime (integral) of N2 Switch from switch time to
end
t_avg=(t_avg_N225)+(t_avg_N2_switchedMS); %Average lifetime of
N2 25 from 0 to switch time + N2 Switched from switch time to
end
Average_Lifetime(i,1)=t_avg; %Generate average lifetime table
```

```
    end
        title('Switch 25-15')
%print('Tempswitch25_15', '-dpdf' );
%individual figures
j= [12   8    5    3    1];
for i=1:16
   %to plot actual data with predictions
    %Tempswitch=char(i);
    h= figure;
    %('Name', Tempswitch(i,1));
a1=N2_25MS(i);
a2=N2_15MS(i);
t_N2_at_yN225 =
fzero(@(x)MSModel(x,f(7),k1(7),k2(7),t1(7),t2(7))-a1, 50);
N225_tminusN215_t=(t_N2_at_yN225-i);
N2_switchedMS=@(x)MSModel(x+N225_tminusN215_t,f(7),k1(7),k2(7)
,t1(7),t2(7));
fplot((N2_15MS),[0,35,-1,105],'Linewidth',3);
hold on
fplot((N2_25MS),[0,35,-1,105],'Linewidth',3);
hold on
fplot((N2_25MS),[0,i,-1,105],'Linewidth',3);
hold on
fplot((N2_switchedMS),[i,35,-1,105],'Linewidth',3);
hold on
xlim([0 35]);
ylim([0 105]);
if i==j(1)
    N2_15MS12=@(x)MSModel(x,f(2),k1(2),k2(2),t1(2),t2(2));
fplot((N2_15MS12),[0,35,-1,105],'Linewidth',3);
elseif i==j(2)
     N2_15MS8=@(x)MSModel(x,f(3),k1(3),k2(3),t1(3),t2(3));
fplot((N2_15MS8),[0,35,-1,105],'Linewidth',3);
elseif i==j(3)
     N2_15MS5=@(x)MSModel(x,f(4),k1(4),k2(4),t1(4),t2(4));
fplot((N2_15MS5),[0,35,-1,105],'Linewidth',3);
elseif i==j(4)
     N2_15MS3=@(x)MSModel(x,f(5),k1(5),k2(5),t1(5),t2(5));
fplot((N2_15MS3),[0,35,-1,105],'Linewidth',3);
elseif i==j(5)
    N2_15MS1=@(x)MSModel(x,f(6),k1(6),k2(6),t1(6),t2(6));
fplot((N2_15MS1),[0,35,-1,105],'Linewidth',3);
else
end
xlim([0 35]);
ylim([0 105]);
title(['Day ' num2str(i) ' Switch 25-15'])
hold on
%saveas(h,sprintf('Day %d TempSwitch25_15.pdf',i));
end
openvar('Average_Lifetime');
```